CUADERNOS de INVESTIGACIÓN GEOGRÁFICA

GEOGRAPHICAL RESEARCH LETTERS

Tomo 48 (1) 2022 ISSN: 1697-9540

UNIVERSIDAD DE LA RIOJA
LOGROÑO (ESPAÑA)

CUADERNOS DE INVESTIGACIÓN GEOGRÁFICA
GEOGRAPHICAL RESEARCH LETTERS

Cuadernos de Investigación Geográfica = Geographical Research Letters (ISSN: 0211-6820) is a scientific journal that publishes two issues per year. It includes papers on Physical Geography and other related environmental sciences (Hydrology, Ecology, Climatology). Interdisciplinary studies with Human Geography are also welcome. The peer review and publication of articles in *Cuadernos de Investigación Geográfica* is free of charge, in agreement with the policy of the journal of making accessible the advances in Physical Geography to the scientific community. All papers are subject to full peer review.

Since 2015 **Cuadernos de Investigación Geográfica = Geographical Research Letters** has been included in the Emerging Sources Citation Index (ESCI) of Clarivate Analytics, a new edition of the Web of Science, within the subject category of *Geography (Physical)*. The journal is also indexed in SCOPUS and SCIMAGO Journal & Country Rank within the subject categories of Geography, Planning and Development, Environmental Sciences, and Earth and Planetary Sciences.

Fotografía de portada/Cover photo: Dehesa extremeña (España) / Extremadura dehesa (Spain). Autor / Author: J. Arnáez)

CUADERNOS DE INVESTIGACIÓN GEOGRÁFICA
GEOGRAPHICAL RESEARCH LETTERS

ISSN 1697-9540

Tomo 48 (1) 2022

CONTENIDO / CONTENT

Cuadernos de Investigación Geográfica *Geographical Research Letters*	2022	Nº 48 (1)	pp. 3-21	EISSN 1697-9540

http://doi.org/10.18172/cig.5338

FLOOD PROCESSES AND MORPHOLOGICAL CHANGES IN AGGRADATIONAL EPHEMERAL RIVERS. RECONSTRUCTION OF THE OCTOBER 1957 FLOOD IN THE RAMBLA CASTELLARDA (SPAIN)

CARLES SANCHIS-IBOR[1*], JOSÉ LUIS IRANZO QUEVEDO[2], FRANCISCA SEGURA-BELTRAN[2]

[1]*Centro Valenciano de Estudios del Riego, Universitat Politècnica de València, España.*

[2]*Departament de Geografia, Universitat de València, España.*

ABSTRACT. During the latter half of the twentieth century, Mediterranean ephemeral rivers underwent a profound metamorphosis. Fluvial adjustment processes narrowed the channels, simplified their planform pattern and notably reduced sediment availability. Today, this makes it extremely difficult to analyse the behaviour of this type of river in former aggradational contexts, such as those seen at the middle part of the twentieth century. For this reason, this paper addresses a reconstruction and analysis of the 1957 flood that occurred in the Rambla Castellarda, a tributary of the Turia river. The research is based, among other sources, on a series of extraordinary, high-precision aerial photographs carried out a few weeks after the flood. These images make it possible to recreate the processes observed in this ephemeral river and map the post-event river forms. Results show the behaviour of a Mediterranean aggradational ephemeral stream, very different from the current processes, and allows a comparative reflection to be made about flood processes in different sedimentary contexts. The study reveals that in-channel agricultural activity was, together with floods, the most relevant factor conditioning the river channel adjustment trajectory in that sedimentary context. Finally, the analysis of the impact of the flood in the Tura river highlights the importance of overflows – and therefore the connection between channel–floodplain – both for in-channel processes and in the lamination of floods.

Procesos de crecida y cambios morfológicos en un río efímero agradacional. Reconstrucción de la riada de octubre de 1957 de la rambla Castellarda

RESUMEN. Durante la segunda mitad del siglo XX, los ríos efímeros mediterráneos han experimentado una profunda metamorfosis: han sufrido procesos de ajuste fluvial que han estrechado los cauces, han simplificado sus formas y han reducido notablemente la disponibilidad de sedimentos. Esto hace que sea extremadamente difícil analizar hoy el comportamiento de este tipo de ríos en contextos agradacionales previos, como el que tenían hasta la primera mitad del siglo XX. Por ello, este artículo aborda el análisis de la crecida de 1957 en la Rambla Castellarda, afluente del río Turia. La investigación se basa, entre otras fuentes, en una extraordinaria serie de fotografías aéreas de alta precisión llevadas a cabo pocas semanas después de la riada. Estas imágenes nos permiten reconstruir los procesos observados en este río efímero y cartografiar las formas del río post-evento. Los resultados muestran el comportamiento de un río efímero agradacional mediterráneo, muy diferente a los procesos actuales, y permiten hacer una reflexión comparativa sobre los procesos de inundación en diferentes contextos sedimentarios. El estudio revela que la actividad agrícola en el cauce fue, junto con las inundaciones, el factor más relevante que condicionó la trayectoria de ajuste del cauce del río en dicho contexto sedimentario. Finalmente, el análisis del impacto de la crecida del río Turia pone de relieve la importancia de los desbordamientos –y por tanto

de la conexión cauce-llano de inundación– tanto para los procesos en el cauce como en la laminación de las crecidas.

Keywords: Floods, ephemeral streams, aggradational processes, river forms, Rambla Castellarda.

Palabras clave: Inundaciones, ríos efímeros, procesos agradacionales, formas fluviales, Rambla Castellarda.

Received: 19 January 2022

Accepted: 3 April 2022

*Corresponding author: Carles Sanchis-Ibor. Centro Valenciano de Estudios del Riego, Universitat Politècnica de València, España (Spain). E-mail address: csanchis@hma.upv.es

1. Introduction

In the middle of the twentieth century, most of the intermittent rivers and ephemeral streams (IRES) of the Spanish Mediterranean basins had a wide channel with a braided pattern when crossing their floodplains and alluvial fans. This morphology was the response of the IRES to past climatic conditions and to a specific context of anthropic action (Hooke, 2006). On the one hand, in the transition between the nineteenth and twentieth centuries, the region had undergone the final pulses of the Little Ice Age (Barrera-Escoda and Llasat, 2015), a particularly humid period characterised by a frequent recurrence of floods (Benito *et al.,* 2008). These conditions, favourable to the mobilisation of sediments, occurred in some basins whose headwater areas featured scarce vegetation cover, due to pressures exerted by the rural population. Since the eighteenth century, overgrazing, the mass terracing of slopes, and the extraction of firewood or charcoal had significantly reduced the biomass (Beguería *et al.,* 2006). The slopes exported significant amounts of sediment, which formed large deposits of gravel on the riverbeds (Conesa, 1987; Segura-Beltran and Sanchis-Ibor, 2013; Conesa and Pérez, 2014; Calle *et al.,* 2017).

During the second half of the century, these conditions drastically changed. The rural exodus, the reduction of the cultivated and grazed area, and the reforestation policies contributed to a significant recovery of the vegetation in the mountainous areas. In addition, many river channels suffered intense gravel mining in-stream, and in many others sediment flow was interrupted by dikes and dams. Consequently, most Mediterranean IRES have undergone fluvial adjustment processes that have notably reduced sediment availability, have narrowed the channels and have simplified their pattern (from braided to single thread) (Liébault and Piégay, 2002; Surian, 2021). These processes and forms have been documented in the Iberian Peninsula (Batalla, 2003; Martín-Vide *et al.,* 2010; Beguería *et al.,* 2006; Rovira *et al.,* 2005; Martínez-Fernández *et al.,* 2016), France (Liébault *et al.,* 2005;) and the Italian Peninsula (Surian *et al.,* 2009; Scorpio *et al.,* 2015; Magliulo *et al.,* 2021).

As a result of these adjustment processes, the current river forms are radically different form the aggradational morphology they had at the middle of the twentieth century. For this reason, addressing the analysis of a flood that occurred in an IRES in 1957 gives us the opportunity to document and understand a phenomenon that cannot currently be observed. The reconstruction of the effects of this flood that occurred more than sixty years ago would be extremely difficult, since the post-event information is very limited, especially in ephemeral rivers and in floods that do not affect urban areas. However, in this case there is a series of photographs of exceptional quality, made expressly by the Spanish Company of Aerial Photogrammetric Works (CEFTA) a few weeks after the extraordinary flood occurred in the Turia river basin, which seriously affected the city of Valencia (Portugués *et al.,* 2016). In addition, the flood took

place a few months after the photographs of the 1956–57 flight of the United States Army (Series B) were taken, which portray the condition of the channel prior to the flood.

The objective of this work is to reconstruct the flood of 14 October 1957 in the Rambla Castellarda -a tributary of the Turia river- with two main aims: first, to document the processes that took place in that event and the resulting forms; and second, to reflect on the implications the changes that occurred in the riverbeds may have on current floods and in fluvial adjustment processes.

2. Study area. The Rambla Castellarda and the flood of 14 October 1957

The Rambla Castellarda is an IRES located in the Region of Valencia that is a tributary of the Turia river (Fig. 1 and 2). It has a basin of 447 km^2, between 112 and 1,568 m above sea level, and drains part of the south face of the Sierra de Javalambre and the Sierra de Andilla mountains. These predominantly calcareous reliefs are compartmentalised by small grabens filled with quaternary materials (Higueruelas, Alcublas, Oset and Artaj valleys), resulting from the different compression and distension phases that shaped the Iberian Range (Pérez Cueva, 1985). The transition between these mountains and the Turia river is established by a wide Pleistocene alluvial piedmont, only interrupted by some Mesozoic calcareous hills and by an outcrop of Miocene marls near the Turia river. Flash floods in ephemeral streams (Camarasa, 2021) are recurrent in this basin.

Between 12 and 14 October 1957, a storm swept most of the Valencia Region, causing a dramatic flood of the Turia river in the city of Valencia (Marco and Mateu, 2007; Portugués *et al.,* 2016). The storm was caused by a relatively typical atmospheric situation in the region: an atmospheric depression at high levels that coincides with a low-pressure cell anchored over the Gulf of Cádiz. It drove an E and SE flow over the Gulf of Valencia that was channelled through the Iberian reliefs and generated abundant rainfall. The hydrological analysis carried out after the event (Cánovas, 1958) and its recent review (Marco and Mateu, 2007; Puertes and Francés, 2016) have shown that the two peaks of the Turia hydrograph that ravaged the city of Valencia on 14 October were generated downstream of the last dam (Benagéber). The main precipitation nucleus was located over the Rambla Castellarda and Rambla Primera sub-basins (García and Carrasco, 1958; Armengot, 2002; Núñez and Riesco, 2007), causing flash floods.

The hydrological response of the Turia basin was conditioned by an episode of rainfall that had occurred in the first days of the month (Table 1), which had left the soils of the region close to saturation. Some days later, at the end of the afternoon on 13 October, moderate rainfall was recorded throughout the Rambla Castellarda basin, which increased in intensity after midnight, mainly in the middle and lower zones. In Andilla and Alcublas 100.5 and 167.5 mm were recorded on the 14th; while downstream, in Casinos and Llíria, 200 and 225 mm were recorded respectively (Table 1 and Fig. 1). The most intense precipitation took place in the surroundings of Villar del Arzobispo, whose rain gauge was overflowing at the time of the consultation; for this reason, the 235 mm recorded there during the 14th must be considered to be a lower value than that of the actual precipitation. According to García and Carrasco (1958), the water began to flow through the Rambla d'Artaix between 6:00 p.m. and 8:00 p.m. on the 13th, but the flood did not occur until the night of the 14th, reaching a first peak around at 4:00 in the morning, which decreased after 6:00. The rains continued after sunrise, and very heavy rainfall was recorded again between 8:00 a.m. and 2:00 p.m.

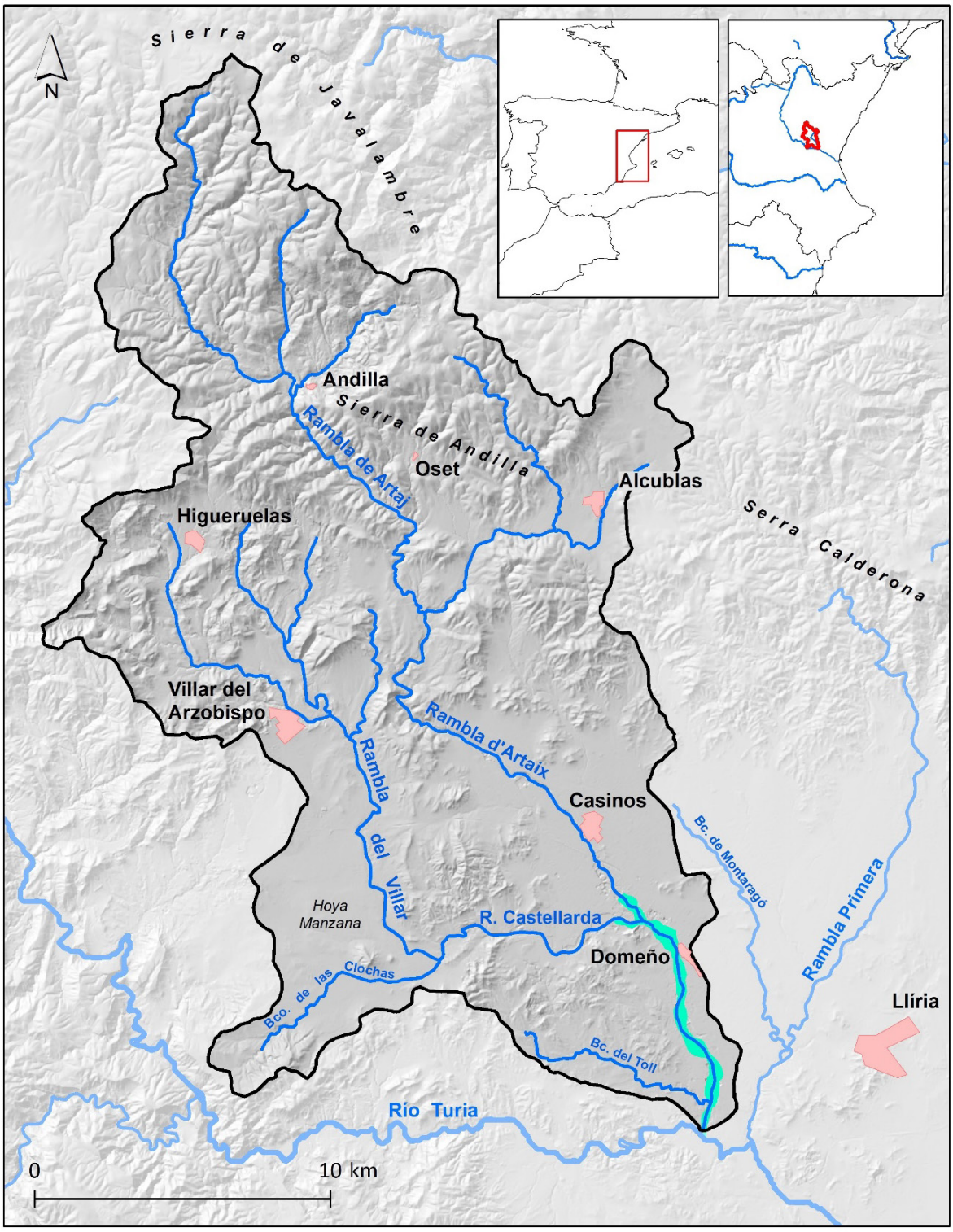

Figure 1. Rambla Castellarda basin and study area highlighted in turquoise.

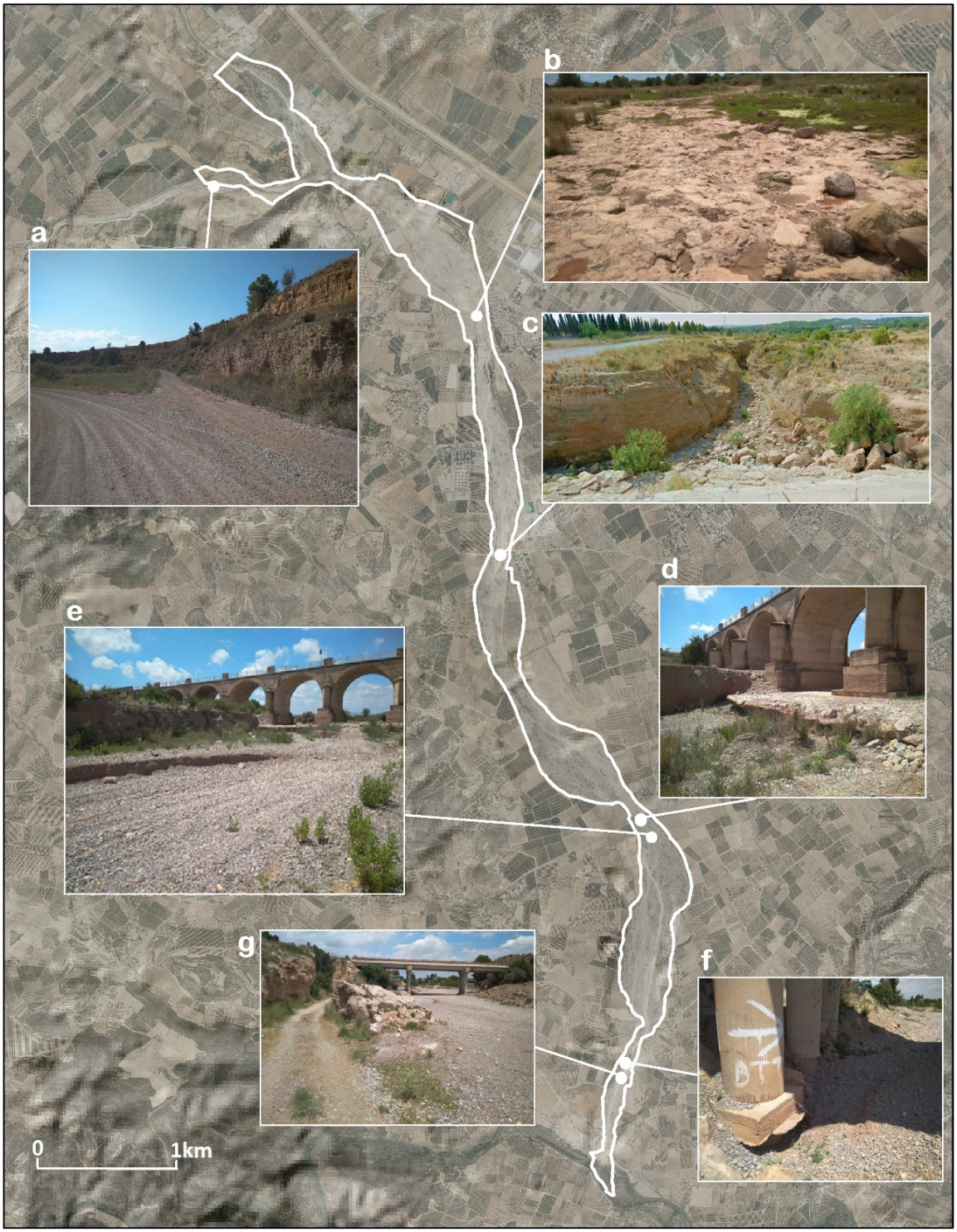

Figure 2. Study area and photographs taken in spring and autumn 2021, which show current processes, mainly as a result of the current sedimentary deficit: a) Rambla Castellarda converted into a road for gravel transport trucks; b) Exhumed crusts in the bed of the river next to the ford of Domeño; c) Fluvial incision next to the ford of Casas de Pablo; d) Undermining of the CV-376 bridge foundation; e) Microterraces generated by the recent incision downstream of the CV-376 bridge; f) Undermining of pillars under the CV-364 bridge; g) Rambla Castellarda at its narrowest section, downstream of the CV-364 bridge.

Table 1. Rainfall (mm) in different observatories of the Castellarda basin during the first fortnight of October. See Figure 1 for location.

	October 1957												
	Daily										Accumulated		
	1	2	3	4	5	….	12	13	14	15	From 1 to 5	From 12 to 15	From 1 to 15
Andilla		38.7	33.3	28.2	0.2		2	9.5	100.5	42	100.4	154	254.4
Alcublas	4.7	29.6	38.5	25			8.6	9.8	167.5	116.5	97.8	302.4	400.2
Villar del Arzobispo		43	27.5	38				18	235*	42	108.5	295*	403.5*
Casinos		47.5	14	26				11	200	15	87.5	226	313.5
Llíria		48	26	31				11	225	221	105	457	562
Llíria (HS)		55	26	30				10	175	195	111	380	491

* Villar del Arzobispo's figures for the 14th are considered to be an underrepresentation, since the rain gauge was overflowing when the observation was made. Source: Instituto Nacional de Meteorología (García and Carrasco, 1958)

Based on these records and the consultations made, García and Carrasco (1958) concluded that the flood at the Rambla Castellarda had a double peak – at dawn and noon on 14 October – that was slightly ahead of the peak in the city of Valencia. Puertes and Francés (2016) have refined this information using hydrological simulation techniques and have calculated a peak of 862.3 m^3/s for the first wave, which took place at 02:00 on the 14th, and a second peak of 940.2 m^3/s, which took place at 12:00 that same day. The contribution of this IRES and the adjoining Rambla Primera, with a combined flow of 2,159 m^3/s, exceeded the flow added by the Turia river at the confluence between these three channels during the second wave, which devastated the city of Valencia.

3. Materials and methods

The main source of information for this work has been the photographic series called *Itinerario del Turia* (IdT), made by the company CEFTA a few weeks after the flood, between November and December, according to Mateu *et al.* (2012). This series is made up of 238 negatives arranged in eight passes. They are 23.5 x 24 cm negatives, with a focal length of 210 and a scale of approximately 1:7,500, which allowed a pixel size of 0.16 m to be obtained after a precision scan. In total, 14 frames were used, which were georeferenced by introducing ten control points, with a mean residual error of less than 1 m in all images. The resolution of the IdT is notably higher than that presented by Series B, from the 1956–1957 flight made by the US Army. This series was performed at a scale of 1:33,000 and with a pixel size of 1.15 m, and it was consulted through the Web Map Service of the National Geographic Information Center (CNIG). Frame 260-032 from Series A by the US Army (1946) has also been used. To reduce its distortion, the frame has been cut into eight 1 m resolution images, which have been georeferenced using ten control points, with a mean residual error of 0.34 m. These images have been used for digitisation, but a wider image taken from the same frame has been reproduced in Figures 3 and 4.

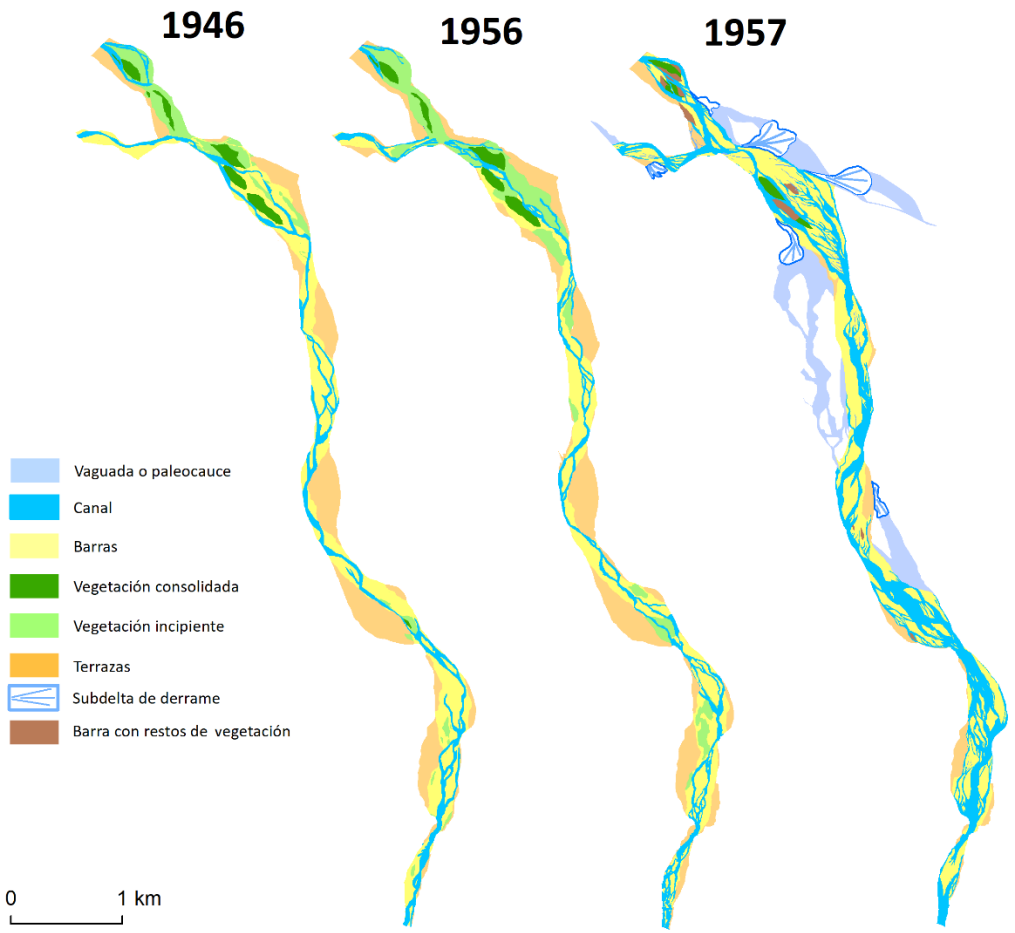

Figure 3. General view of the active channel forms in 1946, 1956 and 1957.

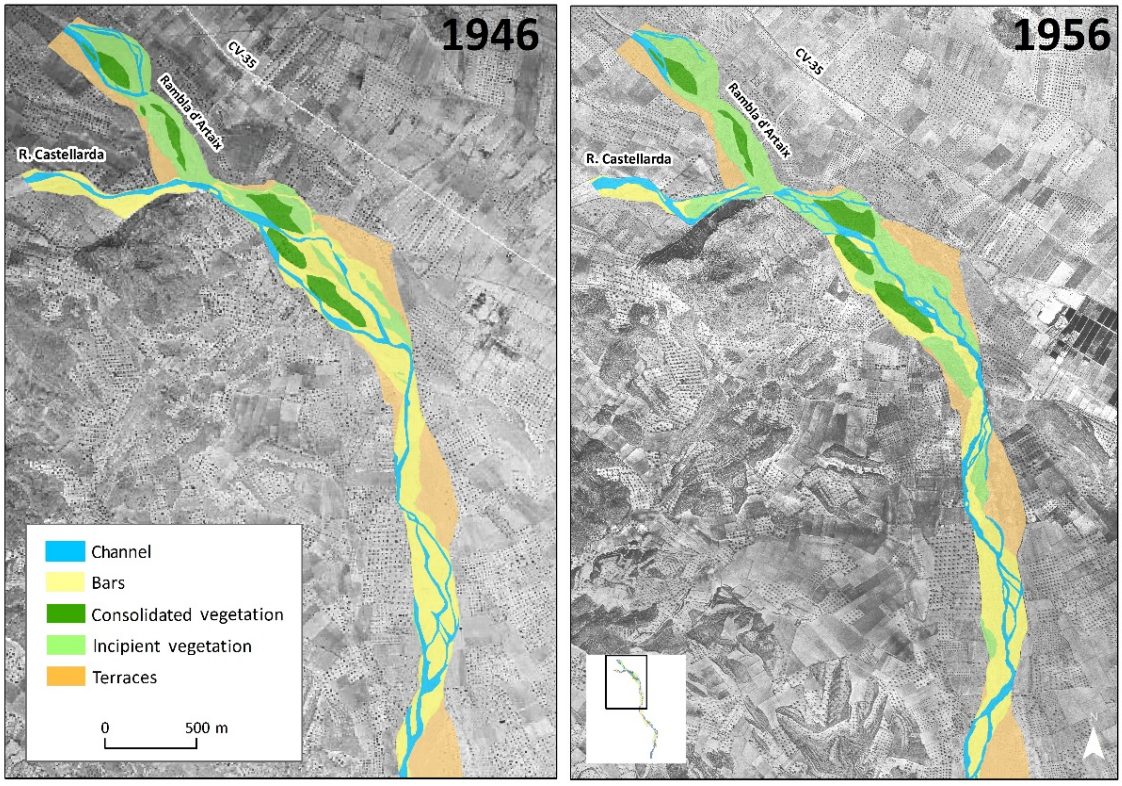

Figure 4. Active canal forms in the northern sector of the study area in 1946 and 1956.

For the analysis of flood and overflow processes and changes in fluvial forms, the study area has been photointerpreted and mapped before and after the 1957 flood. This cartography, prepared using ArcGIS v10.8 (Redlands, California), has been carried out over the entire area that shows evidence of water flow in the IdT images, both in the active channel and in the vegetated areas of the riverbed or on the alluvial fan. For the pre-flood situation, six features have been distinguished as polygons, according to the following criteria of classification:

- Channel: areas devoid of vegetation with evidence of water flow.
- Bars: sediment deposits devoid of vegetation.
- Incipient vegetation: stretches of channel, bars or islands covered by herbaceous vegetation and scattered shrubs or trees.
- Consolidated vegetation: stretches of channel, bars or islands covered by crops or shrub or tree vegetation.
- Terraces (active): sedimentary platforms attached to the banks of the channel and occupied by crops, separated by more or less pronounced escarpments from the body of the alluvial fan and the active channel.
- Alluvial fan: this category includes only those parts of the alluvial fan of the Rambla Castellarda through which the overflowing waters ran in the October 1957 flood. This has not been represented in the figures that represent the Rambla Castellarda before the flood, but its extent has been mapped and quantified in Table 2 to facilitate pre- and post-event map comparison.

Table 2. Area occupied by the forms identified in 1946, 1956 and after the October 1957 flood.

	1946		1956			1957	
	ha	%	ha	%		ha	%
Channels	32.6	9.2	35.5	10.0	Channels	115.1	32.6
					Main channel	*108.4*	
					Channels on bars	*6.7*	
Bars	100.5	28.5	76.9	21.8	Bars	112.7	31.9
					Medial bars	*15.3*	
					Lateral bars	*48.1*	
					Others bars	*49.3*	
Incipient vegetation	25.5	7.2	48.5	13.7	Incipient vegetation	0	0
Consolidated vegetation	11.8	3.4	12.1	3.5	Consolidated vegetation	5.0	1.4
					Flattened vegetation	5.5	1.5
Terraces	77.6	21.8	75.2	21.1	Terraces	21.7	6.1
Aluvial fan	104.7	29.9	104.6	29.9	Alluvial fan	0	0
					Crevasse splay deposits	24.8	7.0
					Overbank Flow channels	69.2	19.6
	352.8	100	352.8	100		352.8	100

Six other categories have been added for post-flood mapping, two of which are subcategories of the bars:

- Lateral bars: deposits devoid of vegetation attached to the outer margins of the Rambla Castellarda, on which parallel microchannels are recognised that drain the bar towards one of the margins of the active channel.
- Medial bars: spindle-shaped deposits devoid of vegetation, generally in a central position in the riverbed, characterised by the presence of a central channel in its upper part that progressively subdivides into an arborescent network of microchannels, followed by another network microchannels of drainage in its lower part.

The channels have been subdivided into two other types:

- Main channel: channels that divide bars and river islands.
- Channel on bar: channels that go up or drain medial and lateral bars. Only those that are wide enough to be digitised at a 1:2,000 scale have been mapped.

For vegetated areas, the inclusion of a new category has been necessary:

- Flattened vegetation: areas with stumps or degraded remains of crops or other forms of consolidated or incipient pre-event vegetation.

And, finally, two other categories have been distinguished for those areas of the alluvial fan affected by overflow processes:

- Crevasse splay deposits: semicircular or semielliptical accumulations on the alluvial fan at some overflow points.
- Overbank flow channels: swallow depressions of the alluvial fan through which the overflowing water of the Rambla Castellarda has circulated.

In addition, for the interpretation of the flood, the gullies formed in the fan have been identified and digitised as lines, regardless of whether they are associated with the flow of the Rambla Castellarda or that of the small tributaries or the runoff concentrated on the cultivated plots of the floodplain. Finally, the channel mobility index (CMI, Sanchis-Ibor *et al.,* 2019) has been calculated to estimate the shift of the river channels between the three aerial pictures used.

4. Results

4.1. The Rambla Castellarda forms before the 1957 flood

The aerial photographs taken in 1946 and 1956 show very similar forms (Table 2 and Fig. 3, 4 and 5), which define the pre-event situation. In those decades, the *rambla* (watercourse) had a wide channel, mainly covered by gravel bars, the active channel was only slightly incised, and the most significant direct human pressure was the agricultural use of the lateral microterraces.

The abundance of sediments is clearly perceived in the upper part of the study area, where the riverbed seems practically levelled with the alluvial fan, particularly on its left bank. Only a small cliff is observed on the banks of the Rambla Castellarda, where it narrows (downstream, bottom part of Fig. 4). This scarp progressively increases as the river approaches the confluence with the Turia river.

In both pre-event aerial pictures (1946 and 1956), the Rambla Castellarda presents more signs of recent activity than the Rambla de Artaix, since the former has a wide active channel, while the latter is completely covered by sparse vegetation, with some islands occupied by crops and denser vegetation (Figure 4). The Castellarda channel, narrow and winding, is continuous and seems to carry a little water in 1946, while that of Artaix is dry in both aerial pictures and vanishes before the confluence.

After the confluence, the active channel (bars and channels) has a high sinuosity, alternately leaving wide terraces on one side and the other, in a regular sequence (Fig. 4 and 5). As occurs in many IRES in this Mediterranean region, the number of simultaneous channels rarely exceeded three, so it was closer to a wandering than to a braided type river.

The active channel was wide, occupying 133.1 ha in 1946. Most of it featured large gravel bars (100.5 ha), while the channels extended over 32.6 ha. Ten years later, the active channel had slightly reduced, down to 112.4 ha, but the channels barely occupied 0.8% more than in 1956 – a fact that is irrelevant, given that the presence of water in the 1956 aerial pictures does not allow their area to be quantified with sufficient precision. Vegetation was scant in 1946: the bars covered by incipient vegetation extended over 25.5 ha of the rambla and 11.8 ha were occupied by islands with consolidated vegetation. In 1956, incipient vegetation almost doubled (48.5 ha), but consolidated vegetation remained practically stable (12.1 ha). The terraces, which also stabilised (77.6 in 1946 and 75.2 ha in 1956), were mostly parcelled up and planted, mainly with carob trees (Table 2).

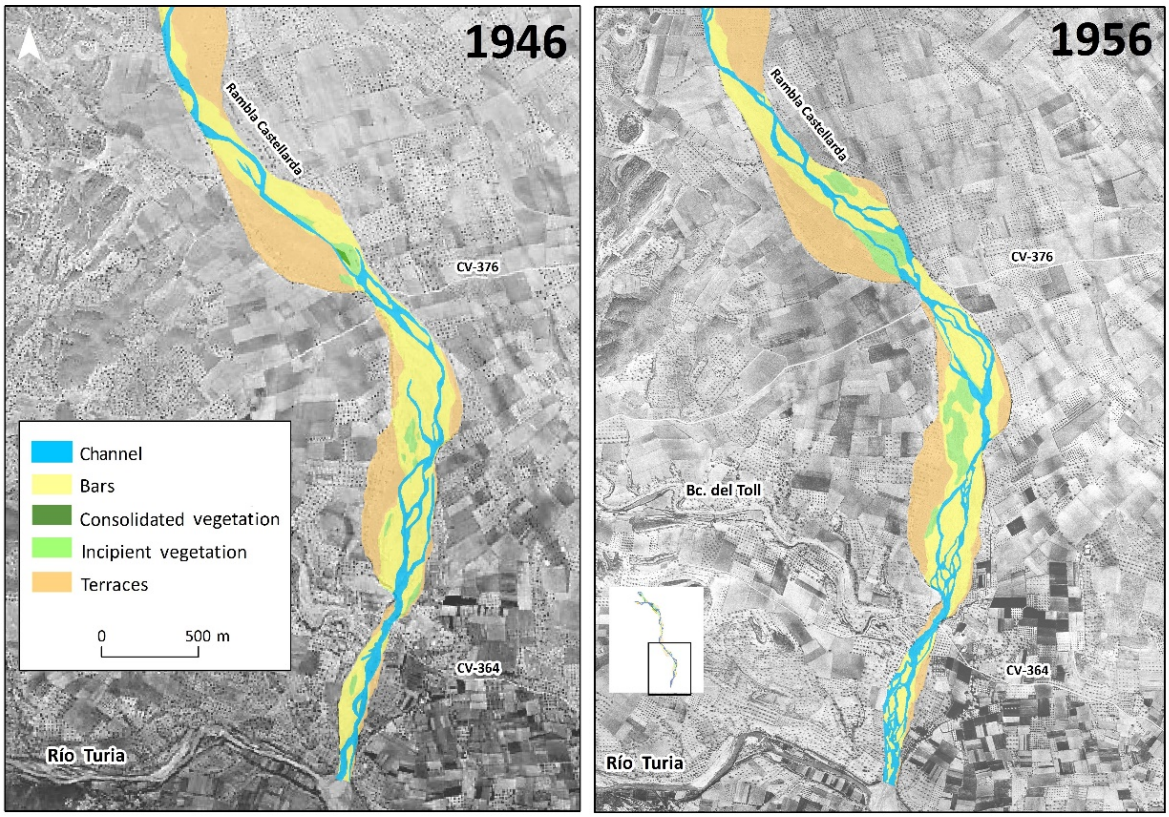

Figure 5. Active channel forms in the southern sector of the study area in 1946 and 1956.

Between 1946 and 1956, only one significant flood was registered, on 28 September 1949, which also dramatically affected the Turia river and the city of Valencia (Portugués, 2012; Portugués and Mateu, 2012). This event explains the change in the course of the channels, which presents high mobility, as shown by the CMI index (4.3) calculated between both dates. The channel shifted but maintained similar forms and significant changes have been detected in the margins of the active channel (Fig. 4 and 5). The bars and terraces maintained their position, almost with complete accuracy, from which we deduce that the flood was not extraordinary in the Rambla Castellarda. This also explains the abovementioned stability, in terms of area, of the consolidated vegetation and the terraces, and the lack of evidence of erosive or depositional processes in the river banks. The advance of the areas covered by incipient vegetation (+ 23%), which is produced at the expense of the bars (-23.6%), proves that no significant floods took place after the 1949 event, and the vegetation expanded in the zones closest to the deposits already vegetated in 1949.

4.2. The 1957 flood. Processes and forms

The flood processes of October 1957 were intense, went beyond the active corridor and radically changed the river morphology. The following lines and figures (Fig. 6 to 9) describe the observed processes and forms, from top to bottom of the study area.

In the upper sector, upstream the confluence with the Rambla de Artaix, the Rambla Castellarda formed a new medial bar (Fig. 6). On its southern shore, the waters overflowed the active channel, destroyed a plot covered with trees and formed a small crevasse splay deposit in the adjacent plots. The overflowing waters soon returned to the channel when colliding with the calcareous reliefs of the Cabeçó de l'Ermita. On the northern shore, the flood eroded the left bank, making the cliff recede 37 m, and followed its course in a straight line to merge with the Rambla de Artaix.

On the Rambla de Artaix, the flood reactivated a paleochannel and opened a new, deeper one, breaking in two a small terrace that had been cultivated since at least before the 1940s. To its left, it set the bank back by up to 37 m (Fig. 6). A first overflow took place along this margin, which formed a small crevasse splay deposit and the channel was divided again. Part of the flow ran through the alluvial fan to the east, and another part returned to the channel 200 m downstream.

At the confluence, the IdT photographs show how the Rambla Castellarda channel was partially perched above the channel excavated by the Rambla de Artaix, a fact that indicates that the peak of the Rambla de Artaix flood was somewhat later than the Rambla de la Castellarda or that it had a greater erosive capacity. The coincidence of two asynchronous peak flows had another very clear hydraulic effect. The flow from the Castellarda, supported by the Cabeçó de l'Ermita hill, contributed to diverting the waters of Artaix towards the opposite shore, overflowing and forming a large semi-circular splay deposit, with a radius greater than 300 m. In the shadow of the aforementioned hill, protected from the main flow, a bar was formed, attached to the right bank (Fig. 6).

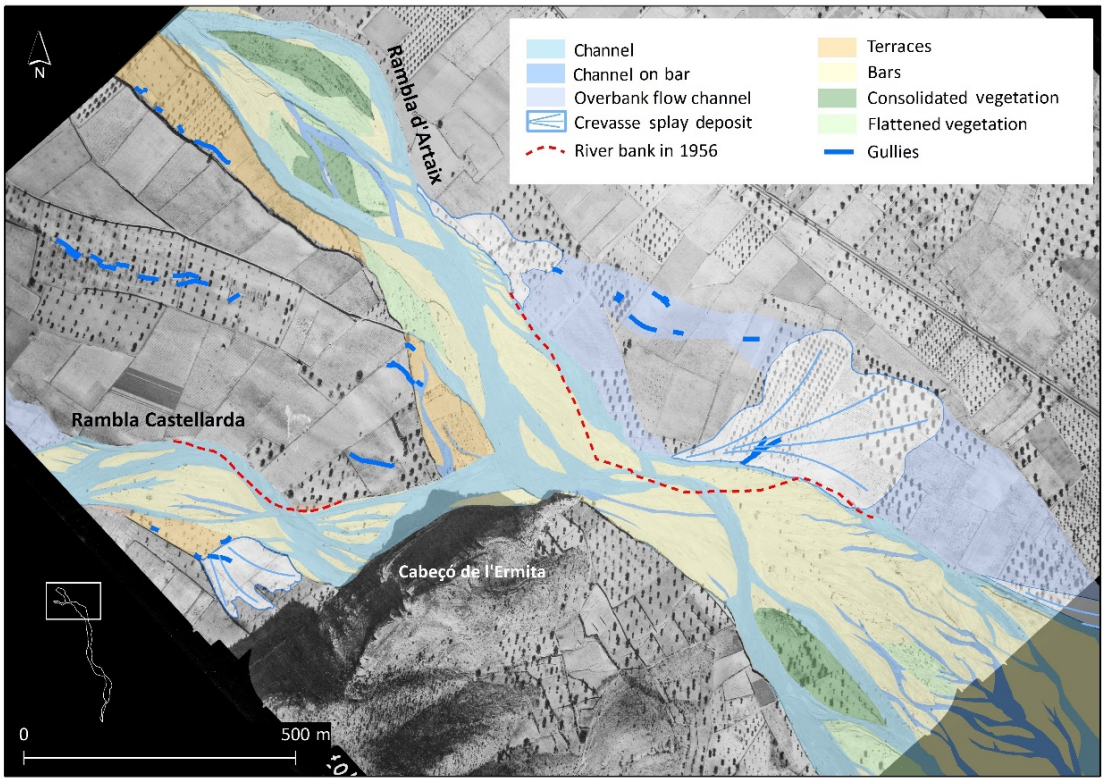

Figure 6. Confluence of the Artaix and Castellarda ramblas. Post-event forms in the first photograph of the IdT series.

Downstream of the confluence, the Rambla Castellarda had its least incised sections (Fig. 7). The sediments were practically levelled with the river margins. These conditions favoured the dispersion of the flow and the overflow on both banks during the October 1957 flood. The waters covered all this space, passing over some areas that had been transformed in agricultural plots decades previously. The flood also formed a large medial bar on the left and other smaller ones, on the main channel, on the right.

On the left bank, right at the ford of the Villar Road, a third overflow took place. The ford gave rise to another splay deposit, and the medieval road transported the waters along the alluvial fan. The overbank flow was captured by the Montaragó ravine, which followed a sinuous path and fell on the Rambla Primera, 3.5 km from its mouth in the Turia (Fig. 7). On the right bank, the overflow took place 500 m after the previous one, it also formed a splay deposit and flowed south, forming a diffluence. The area affected by this flow cannot be specified with precision, but, by following the gullies over the fields, it is possible to identify divergent and convergent flow lines, sometimes forced by the small Jurassic reliefs that emerge in the margin of the alluvial fan (Fig. 7). These calcareous hills finally forced the waters to return to the rambla, 2.2 km after having abandoned it. Previously, to its right, this flow had received lateral contributions from small ravines and gullies that eroded the cultivated plots. To its left, more overflowing streams from the Castellarda joined this current (Fig. 7). In its last 500 m, this overbank flow channel activated erosive processes, clearly seen in two confluent channels, wider than 40 m at various points, which had vertical banks and gullies (Fig. 7 and 8).

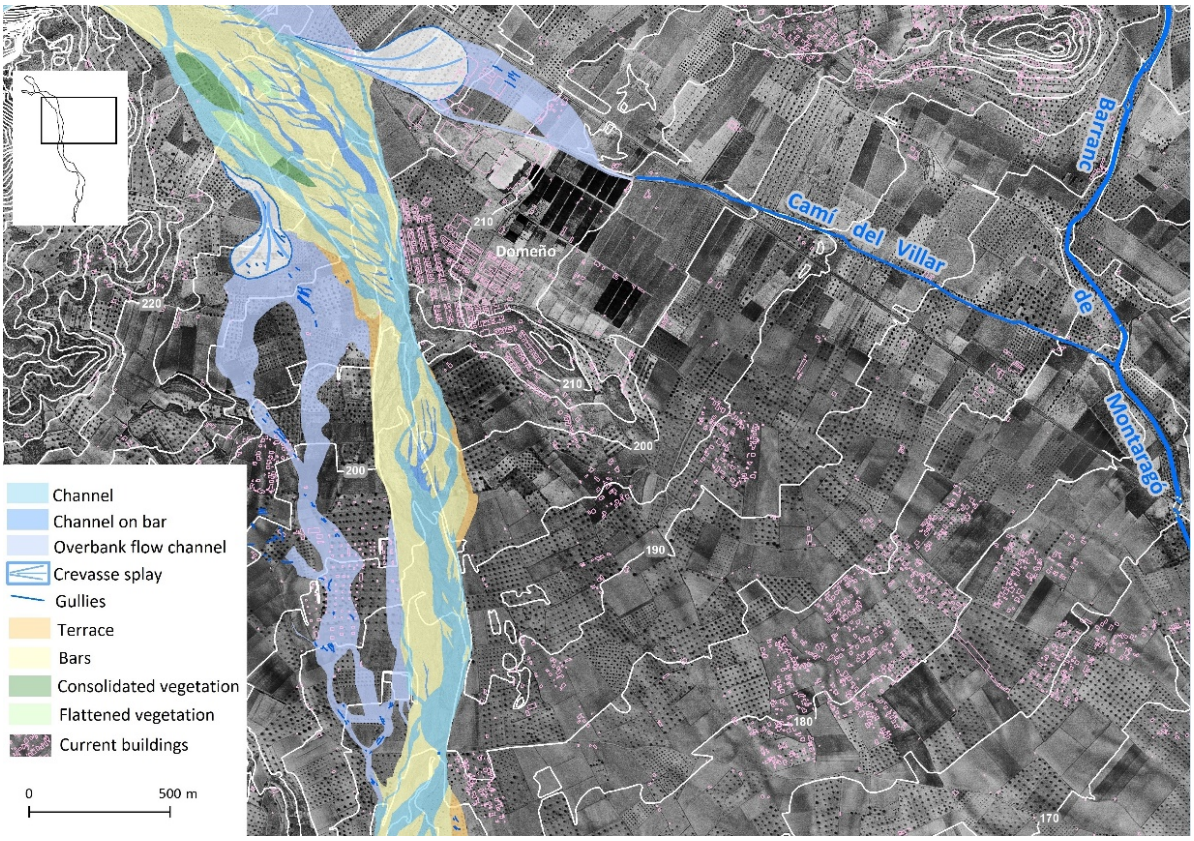

Figure 7. Forms of the Rambla Castellarda after the confluence with the Rambla de Artaix, in 1957. At the top, an overflow channel crosses the area where the industrial park of Domeño stands today and is captured by the ravine (barranc) of Montaragó. The contour lines show the convexity of the Castellarda alluvial fan, in its apical zone. The Rambla Castellarda crosses this sedimentary body and leaves, as evidenced by the contour lines and the humidity lines, various paleo-channels on the surface of the fan, one of which has been used as a road since the medieval period (Camí del Villar).

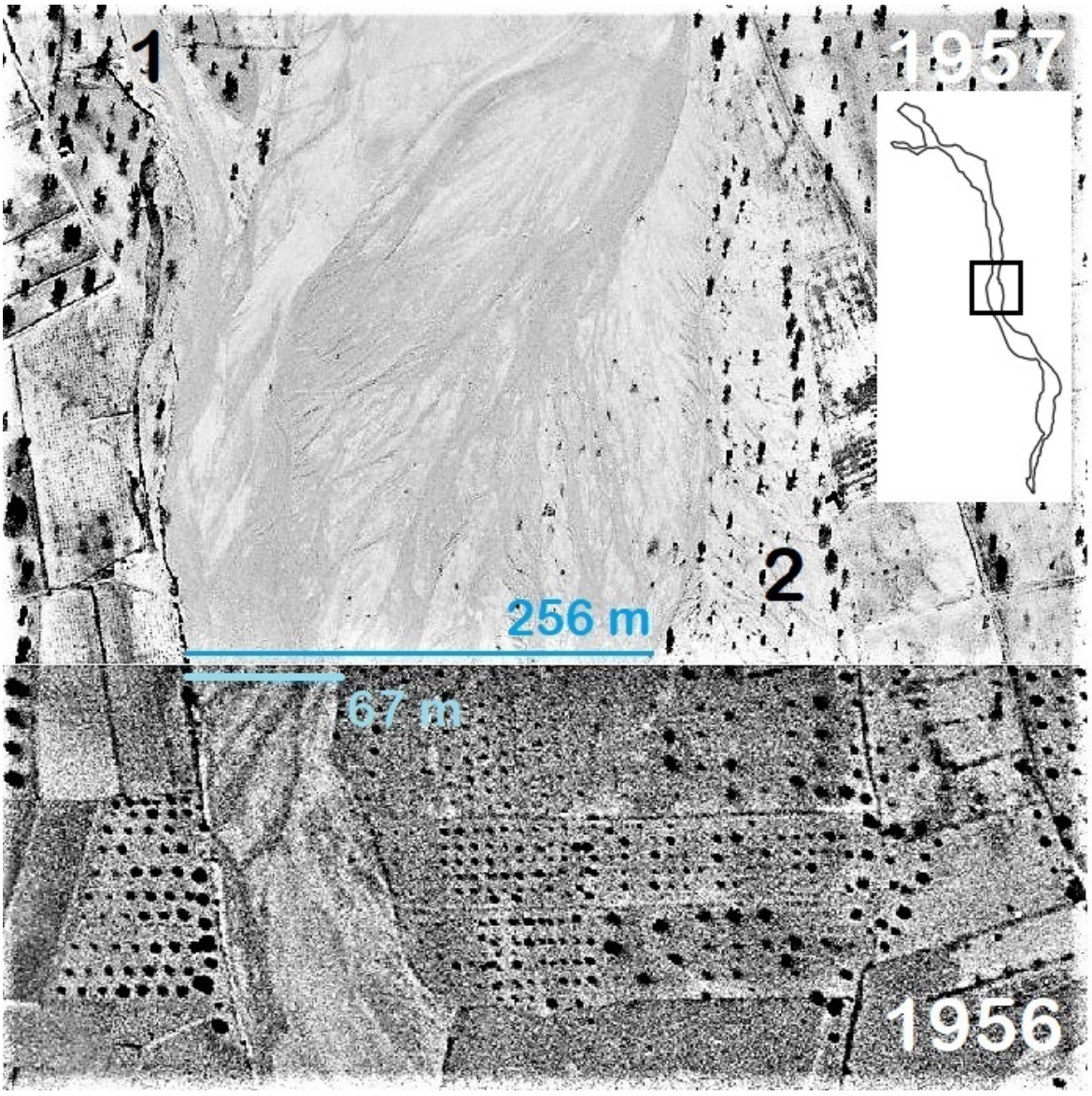

Figure 8. Comparison of pre- and post-event photographs. The contrast of the images has been increased to improve the perception of the printed version. Above, in the IdT image, a broad medial bar formed by the flood can be seen. In this image, at the top left, readers can see the channel excavated by the overbank flow channel that acted as a diffluence (1) and, to its right, (2) the overflow that occurs immediately downstream on the other bank. The blue lines represent the width of the active channel before and after the flood. Below, the image from 1956, with an active channel narrowed by rainfed crops.

The channel of Rambla Castellarda was unable to absorb all this return flow and overflowed again, this time on the opposite bank, starting right at the point where these waters joined the main current (Fig. 8 and 9). In this lateral overflow, the flood did not generate any deposit and presented two lines of flow: one that dissipated its flow through the alluvial fan and left a small splay deposit; and another that forked and converged, to return to the main channel 1.3 km downstream of the overflow point.

In this 4 km long section with various outflow and return flows (Fig. 7), all the spontaneous vegetation and crops located within the 1956 channel were washed away by the waters, but there are no signs of destruction or retreat of the banks. The channel had its lowest sinuosity in the first 2 km of this reach. It circulated contiguous to a large lateral bar and only formed a medial bar in the initial section, which was wider. Further down, there are two consecutive wider areas that had a more complex

morphology, probably conditioned by the change in section and the lateral discharge of flows, which gave rise to various lateral bars, ranging between 300 and 500 m in length, and two medial bars, with an uneven degree of development.

This pattern was repeated in the next reach of the Castellarda (Fig. 9), between the ford of the road CV-376 and the bridge of the CV-364, where the river is more incised, passing between vertical banks formed by silts, clays and cemented gravels. However, at the beginning of the narrow section used by the CV-364 bridge, the flow destroyed the left bank, which was lower than the right, and moved it 36 m from its former position. The road bridge, of which only the abutments remained, was also swept away, and 50 m of the access road to the bridge disappeared. Downstream, it also set back the left bank between 10 and 15 m, in a combination of the Venturi effect and the confluence of the Toll Ravine flow. This ravine also partially destroyed another bridge of the CV-364.

Downstream, in the last section of the rambla, the microchannels of the river clearly drew the network of convergence and divergence of flows typical of a large medial bar, which barely protruded from the adjacent channels, probably due to the intensity of the river flow in a narrow, straight and partially confined section. On the left bank, where the terraces gradually descend to the riverbed, the flood washed away several plots, expanding the active channel section up to 50 m. Finally, at the end of the study area, the waters of the Castellarda, together with those of the Turia, destroyed the Benaguasil irrigation canal and all the crops surrounding the confluence (Fig. 9).

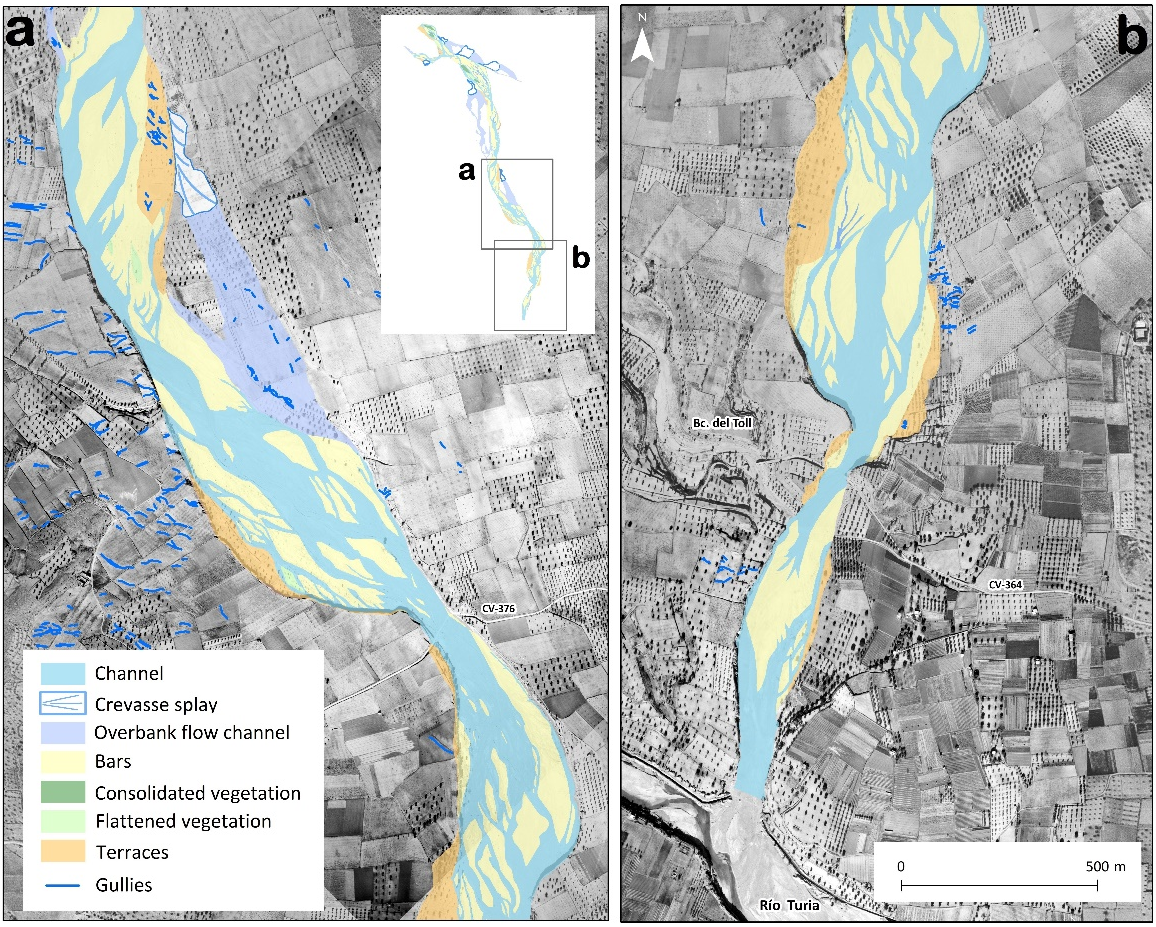

Figure 9. Rambla Castellarda forms after the 1957 event, in the two last reaches of the study area.

5. Discussion

5.1. The 1949 flood compared to the 1957 flood. Ordinary vs extraordinary events

The storm of 1949, despite having dreadful effects in the city of Valencia and other neighbouring basins (Portugués, 2012), had a much lesser impact in the Rambla Castellarda. First, between the images of 1946 and 1956, no displacements of the banks of the active corridor were observed. Second, and although the subsequent plant colonisation and the lower precision of the images may have impaired their observation, channels are scarcely detected on the bars. Finally, the terraces mostly conserved their size, position and crops. However, the canal shows high mobility (CMI = 4.3) between 1946 and 1956, which is just below that observed between the 1956 and 1957 images (CMI = 4.5). In short, despite the evident lower magnitude, the 1949 flood was able to significantly reshape the deepest part of the active canal, the one occupied by bars and canals, but had little influence on the external and higher part of the riverbed, occupied by rainfed crops.

The analysed images also make it possible to ascertain that, following the 1949 episode, there was a brief period of stability. Some vegetation colonised part of the bars, increasing from occupying 25 ha in 1946 to 50 ha ten years later. This short dry period was interrupted by the extraordinary flood of October 1957 which, as has been explained, swept away all these herbaceous communities and completely altered the forms of the active corridor. Therefore, the first flood impact was limited to the active channel, while the second affected the whole active corridor and created ephemeral external forms (crevasse splay deposits and overbank flow channels). This comparison enables the opportunity to adapt the classical quali-quantitative perception and classification of floods as ordinary, extraordinary, and catastrophic, used for paleo-flood reconstruction (Barrera-Escoda and Llasat, 2015) and partially based on the impact on infrastructures. From a river morphology perspective, it is probably more useful to link this classification on three levels to the three areas where significant geomorphic changes can be detected: the active channel, the active corridor and the floodplain.

5.2. The 1957 flood in light of the current sedimentary context

In the current context of sediment deficit, in-channel changes caused by floods are significantly different. The important development of bars observed in 1957, typical of an aggradational river, would be impossible in a flood at present. As observed on field (Fig. 2), the current scarcity of sediments in the active corridor (in this and other IRES in this region) does not allow the complete development of the bars, which are reduced to incipient lobes, with the appearance of erosive bars in compact sediments and outcrops of parent rock being frequent (Segura-Beltran and Sanchis-Ibor, 2011; Calle *et al.,* 2017).

Beyond the river banks, overflow processes are an essential dynamic function of ephemeral rivers, connecting the channel with the alluvial fan and other ecosystems (Ollero *et al.,* 2021), and also conditioning the hydraulics of the in-channel flood processes. In the Rambla Castellarda, the overflows undoubtedly played an important role in laminating the flood peak at the confluence with the Turia river. It is impossible, however, to estimate the amount of this effect. Most of the water spilled by the left bank returned to the channel, since in this bank the topography does not allow the dispersion of flows and returns them to the IRES, as has been seen in Figure 8. Its route through the alluvial fan should have slowed or slightly attenuated the impact of the flood. However, the water that came out on the left bank was dispersed by the Castellarda alluvial fan and a good part was drained by the Montaragó ravine, both of which undoubtedly reduced the flow of the rambla, since most of it did not return to the channel. They partially laminated the flood, but increased the contributions of the Rambla Primera on the Turia river; thus, overall, they cannot have had much effect on the flood peak that devastated the city of Valencia.

The flood of 1957 inundated some spaces that today feature intensive urban occupation. Although predominantly agricultural land use is maintained on the right bank, with the exception of

some scattered houses and a pyrotechnic factory, the new urban centre of Domeño was built on the left bank in 1967 (Fig. 7). It currently has an industrial park that occupies 16 ha and a scattering of leisure homes. The buildings of the polygon are located in the area that flooded, the waters conveyed by the old Villar road towards the Montaragó ravine during the October 1957 event. In fact, the road has recently been dismantled and replaced by an open-air channel that crosses the industrial estate and disappears downstream among the cultivated fields. However, none of these zones is considered a relevant dangerous area by the official flood mapping, neither have they been taken into account by the regional flood risk planning instruments (PATRICOVA) nor by the national system of flooding zones (SNCZI). This is not an oversight: the massive removal of gravel deposits for construction, and the erosion of the channel experienced in recent decades has incised the active channel to such an extent (lateral slopes between 4 and 10 m depending on the sector), so it is very unlikely that new overflows will occur in this area, at least while the current morphosedimentary conditions are maintained in the IRES. The incision, on the one hand, facilitates the protection of the alluvial fan urbanisation, and on the other, undermines the transversal infrastructures on the riverbed (Fig. 2 c, d and f).

5.3. Floods and adjustment processes: the paradox of the hydro-sedimentary connection

Large flash-floods establish a hydro-sedimentary connection between the river basin and the river channel, which is momentary but instrumental in the evolution of ephemeral rivers. This connexion generates a paradox in the adjustment trajectories of rivers. When sediment is abundant and increasingly available, floods stimulate aggradation and channel widening, boosting and accelerating the river adjustment trajectories to these conditions. However, in contexts of sediment starvation — for natural or human causes — floods temporally invert the predominant trends of channel narrowing and vegetation encroachment, so this brief hydrosedimentary connection slows down the inevitable adjustment trajectories (Croke *et al.,* 2013; Segura-Beltran and Sanchis-Ibor, 2013; Tuset *et al.,* 2015; Calle Navarro, 2019; Scorpio and Piègay, 2021).

The flood of the Rambla Castellarda in October 1957 stimulated erosional and sedimentary processes that clearly consolidated an aggradational river adjustment trajectory. The mobility of the materials was very high, devastating and occupying vegetated and cultivated lands. In some sections there was considerable erosion of the alluvial fan escarpments, whose banks were set back by up to 50 m. Flow circulated over the bars, causing a massive dissection and creating numerous microchannels (Fig. 6, 7 and 8). Channels notably widened, from 35.5 to 115.1 ha (Table 2). Of the 75 ha mapped as terraces in 1956, less than one third (21.7 ha) preserved their trees after the flood. Finally, the areas covered by incipient or consolidated vegetation, were reduced to only 5 ha, with a scant covering of trees that survived the flood or stumps and remnants of destroyed vegetation, whose subsequent viability cannot be verified.

As a whole, the active channel went from representing 31.6% of the mapped area in 1956 to occupying over 64.1% in 1957. Unfortunately, the lack of photographs after the IdT -there are no more images until 1967, when gravel mining was already destroying the riverbed- makes it impossible to know what proportion of this active channel was consolidated after the flood, and which part was shortly after revegetated or returned to cultivation. This hinders the complete interpretation of the river trajectory at the end of its aggradational period. Moreover, the active corridor (active channel + vegetated areas + terraces) barely expanded 11.8 ha after the flood, and the overflow channels and splay deposits did not alter the agricultural matrix.

Had this IRES, and others within the Spanish Mediterranean Region, achieved a steady state by the middle of the twentieth century? Or were they still going through an adjustment process to the consequences of the last stage of the Little Ice Age and the population peak of the rural areas? It is likely that more data is required to reach a conclusion. What this case and others covering the same period (Segura-Beltran and Sanchis-Ibor, 2013; Sanchis-Ibor *et al.,* 2017, 2019) demonstrate is that

spontaneous vegetation was not controlling or limiting channel widening in this region during the decades of 1940 and 1950. This vegetation, easily destroyed by ordinary and extraordinary floods and probably affected by in-channel grazing, did not find space to consolidate itself in the active corridor, and its geo-ecological niche was almost completely occupied by rainfed crops. During these two decades, farmers persisted in the transformation of the microterraces located within the active corridor, maintaining a continuous fight against floods, which is easily visible in the aerial pictures of this period.

6. Conclusions

The October 1957 flood was an extraordinary event, from both a paleo-flood historical perspective and in river geomorphologic terms; it devastated the entire active corridor and modified its forms. In contrast, the 1949 flood can be considered an ordinary event, whose impact was limited to the active channel. Despite their different magnitudes, both floods contributed, in different ways, to sustaining a path of fluvial adjustment to conditions of abundance and availability of sediment.

The three series of aerial pictures consulted are probably not conclusive enough to completely define the two last decades of this aggradational stage, but they are sufficiently valid to make some interesting considerations about this period. The analysis of the 1957 pre- and post-event has highlighted how, during the final years of this stage, in-channel agricultural activity was, together with floods, the most relevant factor conditioning the river channel adjustment trajectory. Both processes left no space in the rambla for spontaneous revegetation processes, which would not be predominant until the last decades of the twentieth century. The channel pattern changes of the Mediterranean ramblas during this aggradational stage are a socio-ecological process, in which some factors can be easily followed through aerial pictures, such as rainfed agriculture, but others that are doubtless important, such as in-channel grazing, require different methodological approaches.

The most recent and future floods have taken place or will take place in a context of sedimentary deficit, and consequently will define a different active corridor, adjusted to the new conditions of the basin and channel. In this sense, this study highlights the importance of overflows -and therefore the connection between channel–floodplain- both for in-channel processes and in the lamination of floods. This latter function, which was common in past decades, is currently problematic in many basins, due to the environmental changes that have occurred in river systems and the urbanisation processes of alluvial fans and floodplains. The lateral connection of the channel–floodplain/alluvial fan can be hindered under current conditions, as it adds elements of complexity to land planning. The processes of fluvial adjustment to changes induced naturally or through anthropic action have many facets, which are sometimes contradictory and which should be permanently analysed, since the fluvial dynamics and trajectories are changing.

Funding

This work has been funded by the research projects of the Ministry of Science and Innovation EPHIMED (CGL2017-86839-C3-1-R) and EPHIDREAMS (PID2020-116537RB-I00), both co-financed with European funds (FEDER).

Acknowledgements

To Joan F. Mateu Bellés, for the transfer of the IdT photographs, and to Irene Laborda Martínez, who made a first attempt to study this event almost a decade ago.

References

Armengot, R., 2002. *Las lluvias intensas en la Comunidad Valenciana*. Ministerio de Medio Ambiente, Instituto Nacional de Meteorología. Barcelona.

Barrera-Escoda, A., Llasat, M. 2015. Evolving flood patterns in a Mediterranean region 1301-2012 and climatic factors–the case of Catalonia. *Hydrology and Earth System Sciences* 191, 465-483. https://doi.org/10.5194/hess-19-465-2015

Batalla, R.J., 2003. Sediment deficit in rivers caused by dams and instream gravel mining. A review with examples from NE Spain. *Cuaternario y Geomorfología* 17(2), 79-91.

Beguería, S., López-Moreno, J.I., Gómez-Villar, A., Rubio, V., Lana-Renault, N., García-Ruiz, J.M., 2006. Fluvial adjustments to soil erosion and plant cover changes in the Central Spanish Pyrenees. *Geografiska Annaler: Series A, Physical Geography* 88(3), 177-186. https://www.jstor.org/stable/3878364

Benito, G., Thorndycraft, V.R., Rico, M., Sánchez-Moya, Y., Sopeña, A., 2008. Palaeoflood and floodplain records from Spain: Evidence for long-term climate variability and environmental changes. *Geomorphology* 1011-2, 68-77. http://doi.org/10.1016/j.geomorph.2008.05.020

Calle Navarro, M., 2019. *Morphosedimentary dynamics of ephemeral rivers affected by gravel mining: GIS mapping and geomorphic change detection*, PhD Thesis, Universidad Complutense de Madrid.

Calle, M., Alho, P., Benito, G., 2017. Channel dynamics and geomorphic resilience in an ephemeral Mediterranean river affected by gravel mining. *Geomorphology* 285, 333-346. http://hdl.handle.net/10261/155132

Camarasa-Belmonte, A.M., 2021. Flash-flooding of ephemeral streams in the context of climate change. *Cuadernos de Investigación Geográfica (Geographical Research Letters)* 47, 121-142. http://doi.org/10.18172/cig.4838

Cánovas, M., 1958. Avenidas motivadas por las lluvias extraordinarias de los días 13 y 14 de octubre de 1957. *Revista de Obras Públicas* 106, I 2914, 59-68.

Conesa García, C., 1987. Barras de grava en lechos de rambla del campo de Cartagena. *Papeles de Geografía* 12, 33-46.

Conesa García, C., Pérez Cutillas, P., 2014. Alteraciones geomorfológicas recientes en los sistemas fluviales mediterráneos de la Península Ibérica: Síntomas y problemas de incisión en los cauces. *Revista de Geografía Norte Grande* 59, 25-44.

Croke, J., Fryirs, K., Thompson, C., 2013. Channel–floodplain connectivity during an extreme flood event: implications for sediment erosion, deposition, and delivery. *Earth Surface Processes and Landforms* 38(12), 1444-1456. https://doi.org/10.1002/esp.3430

García, V. Carrasco, A., 1958. *Lluvias de intensidad y extensión extraordinarias causantes de las inundaciones de los días 13 y 14 de octubre de 1957, en las provincias de Valencia, Castellón y Alicante*. Ministerio del Aire, Servicio Meteorológico Nacional, Publicaciones Serie A (Memorias) nº 30, Madrid.

Hooke, J.M., 2006. Human impacts on fluvial systems in the Mediterranean región, *Geomorphology* 79 (3-4), 311-335. https://doi.org/10.1016/j.geomorph.2006.06.036

Liébault, F., Piégay, H., 2002. Causes of 20th century channel narrowing in mountain and piedmont rivers of Southeastern France. *Earth Surface and Landforms* 27, 425-444. https://doi.org/10.1002/esp.328

Liébault, F., Gomez, B., Page, M., Marden, M., Peacock, D., Richard, D., Trotter, C.M., 2005. Land-use change, sediment production and channel response in upland regions. *River Research and Applications* 21(7), 739-756. https://doi.org/10.1002/rra.880

Magliulo, P., Cusano, A., Giannini, A., Sessa, S., Russo, F., 2021. Channel Width Variation Phases of the Major Rivers of the Campania Region (Southern Italy) over 150 Years: Preliminary Results, *Earth* 2(3), 374-386. https://doi.org/10.3390/earth2030022.

Marco, J., Mateu, J., 2007. El fenómeno hidrológico. ETSICCP (Coord.), *Ciclo de Conferencias 50 años de la riada que transformó Valencia*. Octubre 18-25 y Noviembre 8-15, València.

Martín-Vide, J.P., Ferrer-Boix, C., Ollero, A., 2010. Incision due to gravel mining: modelling a case study from the Gállego River, Spain. *Geomorphology* 117(3-4), 261-271. https://doi.org/10.1016/j.geomorph.2009.01.019

Martínez-Fernández, V., González del Tánago, M., Maroto, J., García de Jalón, D., 2016. Fluvial corridor changes over time in regulated and non-regulated rivers (Upper Esla River, NW Spain). *River Research and Applications* 33(2), 214-223. https://doi.org/10.1002/rra.3032.

Mateu Bellés, J.F., Ruiz Pérez, J.M., Portugués Mollá, I., Carmona González, P., Bonache i Felici, X., Marco Segura, J.B., 2012. Materiales inéditos para el estudio de la riada del Turia en Valencia (octubre de 1957). *Cuadernos de Geografía* 91-92, 181-196.

Núñez, J.A., Riesco, J., 2007. *Climatología de la ciudad de Valencia*. Ministerio de Medio Ambiente, Instituto Nacional de Meteorología, Barcelona.

Ollero Ojeda, A., Conesa García, C., Vidal-Abarca Gutiérrez, M.R. (Coords.), 2021. *Buenas prácticas en gestión y restauración de cursos efímeros mediterráneos: resiliencia y adaptación al cambio climático*. Editum. Ediciones de la Universidad de Murcia. https://doi.org/10.6018/editum.2900

Pérez Cueva, A.J., 1985. *Geomorfología del sector oriental de la Cordillera Ibérica entre los ríos Mijares y Turia*. Universitat de València, Valencia.

Portugués, I., 2012. Una revisió de les crescudes de 1949 a la plana del Xúquer-Túria, *Cuadernos de Geografía* 91/92, 107-140.

Portugués, I., Mateu, J.F., 2012. Río y suburbio: el cauce del Turia en la Valencia de la autarquía (1939-1957). *Cuadernos de Geografía* 91/92, 141-160.

Portugués, I., Bonache, X., Mateu, J.F., Marco, J.B., 2016. A GIS-Based Model for the analysis of an urban flash flood and its hydro-geomorphic response. The Valencia event of 1957. *Journal of Hydrology* 541, 582-596. https://doi.org/10.1016/j.jhydrol.2016.05.048.

Puertes, C., Francés, F., 2016. La riada de Valencia de 1957: reconstrucción hidrológica y sedimentológica y análisis comparativo con la situación actual. *Ingeniería del agua* 20(4) 181-199, https://doi.org/10.4995/ia.2016.4772

Rovira, A., Batalla, R.J., Sala, M., 2005. Response of a river sediment budget after historical gravel mining (the lower Tordera, NE Spain). *River Research and Applications* 21 (7), 829-847. http://doi.org/10.1002/rra.885

Sanchis-Ibor, C., Segura-Beltrán, F., Almonacid-Caballer, J., 2017. Channel forms recovery in an ephemeral river after gravel mining (Palancia River, Eastern Spain). *Catena* 158, 357-370. https://doi.org/10.1016/j.catena.2017.07.012

Sanchis-Ibor, C., Segura-Beltrán, F., Navarro-Gómez, A., 2019. Channel forms and vegetation adjustment to damming in a Mediterranean gravel-bed river (Serpis River, Spain). *River Research and Applications* 35(1), 37-47. https://doi.org/10.1002/rra.3381

Scorpio, V., Aucelli, P.P., Giano, S.I., Pisano, L., Robustelli, G., Rosskopf, C.M., Schiattarella, M., 2015. River channel adjustments in southern Italy over the past 150 years and implications for channel recovery. *Geomorphology* 251, 77-90. https://doi.org/10.1016/j.geomorph.2015.07.008

Scorpio, V., Piégay, H., 2021. Is afforestation a driver of change in Italian rivers within the Anthropocene era? *Catena* 198, 105031. https://doi.org/10.1016/j.catena.2020.105031

Segura Beltrán, F., Sanchis Ibor, C., 2011. Efectos de una crecida en un cauce antropizado. La riada del Palancia de octubre de 2000. *Cuadernos de Geografía* 90, 147-168. http://doi.org/10.7203/CGUV..14215

Segura-Beltran, F., Sanchis-Ibor, C., 2013. Assessment of channel changes in a Mediterranean ephemeral stream since the early twentieth century. The Rambla de Cervera, eastern Spain. *Geomorphology* 201, 199-214. http://doi.org/10.1016/j.geomorph.2013.06.021

Surian, N., 2021. Fluvial Changes in the Anthropocene: A European Perspective, *Reference Module in Earth Systems and Environmental Sciences*, Elsevier, https://doi.org/10.1016/B978-0-12-818234-5.00109-7

Surian, N., Rinaldi, M., Pellegrini, L., Audisio, C., Maraga, F., Teruggi, L., Ziliani, L., 2009. Channel adjustments in northern and central Italy over the last 200 years, *Geol. Soc. Am. Spec. Pap*. 451, 83-95.

Tuset, J., Vericat, D., Batalla, R. 2015. Evolución morfo-sedimentaria del tramo medio del río Segre. *Cuadernos de Investigación Geográfica (Geographical Research Letters)* 41, 23-62. https://doi.org/10.18172/cig.2707

Cuadernos de Investigación Geográfica *Geographical Research Letters*	2022	Nº 48 (1)	pp. 23-40	EISSN 1697-9540

http://doi.org/10.18172/cig.4850

DESERTIFICATION AND DEGRADATION RISKS VS POVERTY: A KEY TOPIC IN MEDITERRANEAN EUROPE

JESÚS RODRIGO-COMINO[1]*, ROSANNA SALVIA[2], GIANLUCA EGIDI[3], LUCA SALVATI[4], ANTONIO GIMÉNEZ-MORERA[5], GIOVANNI QUARANTA[2]

[1]*Departamento de Análisis Geográfico Regional y Geografía Física, Facultad de Filosofía y Letras, Campus Universitario de Cartuja, University of Granada, 18071 Granada, Spain.*

[2] *Department of Mathematics, Computer Science and Economics, University of Basilicata, Via Nazario Sauro, 85, 85100 Potenza, Italy.*

[3] *Department of Agricultural and Forestry scieNcEs (DAFNE), Tuscia University, Via S. Camillo de Lellis, I-01100 Viterbo, Italy.*

[4] *Department of Methods and Models for Economy, Territory and Finances, Sapienza University of Roma, Via del Castro Laurenziano 9, 00161 Roma, Italy.*

[5] *Departamento de Economía y Ciencias Sociales, Escuela Politécnica Superior de Alcoy, Universitat Politècnica de València, Plaza Ferrandiz y Carbonell s/n, 03801 Alcoy, Alicante, Spain.*

ABSTRACT. Land degradation and, subsequently, desertification processes are conditioned by biophysical factors and human impacts. Nowadays, there is an increasing interest by social scientists to assess its implications. Especially, it is relevant to the potential changes and landscape deterioration on population, economic systems and feedbacks of local societies to such adjustments. Assessing social facets should also be related to desertification risks, integrated socio-economic inputs and environmentally sustainable development perspectives. However, investigations about the effects of land degradation conditioned by global socioeconomic-factors from a holistic point of view are scarce. In this review, we pretend to discuss past and recent findings on land degradation risks related to poverty, especially based on Mediterranean Europe. To achieve this goal, we focused on key socioeconomic forces such as developmental policy, production and market structure, social change and population mobility. Our review showed that regional disparities based on complex dynamics of demographic forces (e.g. migration, fertility and ageing) and economic drivers of change (e.g. industrial concentration, urbanization, crop intensification, tourism pressure, coastalization) are keys to understand Mediterranean regions such as Southern Italy, a region exposed to high desertification risk in Europe. We concluded that the overexploitation of territories, soil and water degradation urban expansion, tourism and unplanned industrialization are some sectors and activities which can be highly affected by political and socioeconomic forces leading to unsustainable forms of land management and types of development. Special attention should be paid to social policies, education and training schemes to reduce rural migration and potentiate territorial knowledge to avoid land degradation, considering other social issues such as poverty or centralization. The potential role of win-win policies abating poverty and reducing desertification risk is evident in Mediterranean Europe and achieving land degradation neutrality necessary.

Riesgos de desertificación y degradación vs pobreza: un tema clave en la Europa mediterránea

RESUMEN. Los procesos de degradación del territorio y, consecuentemente, los de desertificación están condicionados por factores biofísicos e condicionantes humanos. Hoy en día, existe un interés creciente por parte

de los científicos sociales por evaluar sus implicaciones. Especialmente, un interés por los posibles cambios y el deterioro del paisaje a consecuencia de la población, los sistemas económicos y las reacciones de las sociedades locales a dichos ajustes. La evaluación de las facetas sociales también debería estar relacionada con los riesgos de desertificación, los aportes socioeconómicos integrados y las perspectivas de desarrollo ambientalmente sostenible. Sin embargo, las investigaciones sobre los efectos de la degradación del territorio condicionado por factores socioeconómicos globales desde un punto de vista holístico son escasas. En esta revisión, pretendemos discutir los hallazgos pasados y recientes sobre los riesgos de degradación de la tierra relacionados con la pobreza, especialmente en la Europa mediterránea. Para lograr este objetivo, nos enfocamos en fuerzas socioeconómicas clave como la política de desarrollo, la estructura de producción y mercado, el cambio social y la movilidad de la población. Nuestra revisión demostró que las disparidades regionales basadas en la dinámica compleja de las fuerzas demográficas (por ejemplo, la migración, la fertilidad y el envejecimiento) y los impulsores económicos del cambio (por ejemplo, la concentración industrial, la urbanización, la intensificación de cultivos, la presión del turismo, la cosificación) son clave para comprender las regiones mediterráneas como el sur de Italia, una región expuesta a un alto riesgo de desertificación en Europa. Concluimos que la sobreexplotación de territorios, la degradación del suelo y el agua, la expansión urbana, el turismo y la industrialización no planificada son algunos sectores y actividades que pueden verse muy afectados por fuerzas políticas y socioeconómicas que conducen a formas insostenibles de ordenación territorial y tipos de desarrollo. Se debe prestar especial atención a las políticas sociales, los esquemas de educación y capacitación para reducir la migración rural y potenciar el conocimiento territorial para evitar la degradación de la tierra, considerando otros temas sociales como la pobreza o la centralización. El papel potencial de las políticas de beneficio mutuo para abatir la pobreza y reducir el riesgo de desertificación es evidente en la Europa mediterránea y es necesaria la neutralidad de la degradación del territorio.

Key words: Land degradation, regional geographical disparities, social processes, Southern Europe.

Palabras clave: Degradación del territorio, disparidades geográficas regionales, procesos sociales, Europa del sur.

Received: 19 August 2020

Accepted: 21 March 2021

*Corresponding author: Jesús Rodrigo Comino, Departamento de Análisis Geográfico Regional y Geografía Física, Facultad de Filosofía y Letras, Campus Universitario de Cartuja, University of Granada, 18071 Granada, Spain. E-mail address: jesusrc@ugr.es

1. Introduction

Environmental changes driven by biophysical factors and human impacts together arise interest among the social researchers (Xie *et al.,* 2020; Chasek *et al.,* 2019; Turner, 1994)**.** Usually, social scientists focus on the potential changes and landscape deterioration due to human activities, assessments of economic systems and feedbacks of local societies to such adjustments (Hussen, 2018; Berry *et al.,* 2019) While spatiotemporal uncertainty at the different scales and environmental risks are the key questions of the processes concerning social dynamics and political actions to be implemented (Nocenzi, 2005), the economic controversy about sustainable growth is still dominant. They are intrinsically defined by a complex synergy between environmental and social drivers (Giampietro, 2019; Bekun *et al.,* 2019). In these regards, Land Degradation (LD) leading to desertification risk is a complex phenomenon, which has received numerous definitions since the last decades (Akhtar-Schuster *et al.,* 2017; Reynolds *et al.,* 2011; Conacher and Sala, 1998). LD reduces soil fertility and leverages environmental and economic movements that define the territory at diverse temporal and spatial scales. In arid and semi-arid areas, land degradation or desertification could turn into potential processes of deterioration such as soil erosion (Borrelli *et al.,* 2016; Coelho and Sala, 1998). Implying a decline in soil fertility and reduced sustainability **(**Arshad and Martin, 2002), LD and desertification lead to an increase in land consumption affecting natural ecosystems

or protected areas (Smith *et al.,* 2020). In this regard, it is interesting to highlight the pioneering research conducted in the Spanish mountain areas, fertile soils close to the coast and rivers or abandoned territories during the 80s and 90s affected by LD processes and an imminent intensification of human activities (e.g. Garcia-Ruiz *et al.,* 1986; Lasanta *et al.,* 1995; Cerdà, 1995; Schnabel, 1994; Garcia-Ruiz *et al*., 1995).

In the past, LD was considered to be a specific issue of some territories due to particular sequences of natural drivers (Francke *et al.,* 2020; Larrey *et al.,* 2020). LD is generally associated to biophysical conditions (soil characteristics, steep slopes, lack of vegetation cover, (e.g. Kou *et al.,* 2016; Cerdà *et al.,* 2021; Boix-Fayos *et al.,* 2001; Vagen *et al.,* 2016) together with drought features when we talk about desertification (e.g. Ahmadi and Moradkhani, 2019; Ciais *et al.,* 2005; Emadodin *et al.,* 2019), but socioeconomic factors can also modify sensitive landscapes (García-Ruiz *et al.,* 2013; Butzer, 2005). Due to the current economic capitalism system (characterized by the importance of an elevated production, offer and consumption) and the over-use of the natural resources by an increase in the population, there has been a drastic acceleration of this process from western Europe in the 16th century to the Mediterranean countries (García Latorre *et al.,* 2001). This cannot be only explained as an explicit consequence of climate change or non-sustainable agricultural practices. It instead advocates that worldwide socioeconomic processes at the local and regional scales affect land degradation (Herrmann and Hutchinson, 2005). Some authors stated that it exists a 'poverty trap' thesis, which is defined as a kind of spiral relationship between poverty and environmental degradation: the poor people are both agents and victims of natural resource erosion (Prakash, 1997; Zambon *et al.,* 2018).

However, we consider that it is necessary to discuss social facets dealing with desertification risk and assessing the integrated socio-economic and environmentally sustainable development. To date, reviews that serve the readers as background to face this topic are scarce and its necessity vital to achieving land degradation neutrality (Collantes *et al.,* 2018; Dallimer and Stringer, 2018). Therefore, in this review, the role of selected social variables on LD processes was extensively debated. Specifically, the possible connection between land poverty and degradation was discussed considering rural areas of Southern Italy as examples, regarded as a desertification hotspot. Also, the desertification process under different social perspectives such as political, sociodemographic and economic ones and the implications of changing human behaviours and lifestyles will be introduced.

2. Regional questions related to LD and disparities

The concentration of rainfall events in heavy storms, long dry periods, high temperatures and evapotranspiration rates (Rodrigo-Comino *et al.,* 2019; Nadal-Romero *et al.,* 2015; García Marín, 2008), lack of vegetation (Fernández and Vega, 2014; Lozano-Parra *et al.,* 2015) and soil characteristics (Asadi *et al.,* 2012; Karamesouti *et al.,* 2015; Kosmas *et al.,* 2016) are the key degradation drivers impacting on land vulnerability at the regional scale. LD in arid and semi-arid areas such as the Mediterranean is affected by the evolution of regional changes and disparities, and their interactions at diverse spatiotemporal scales (García Latorre *et al.,* 2001; Martínez-Valderrama *et al.,* 2016). The most common determinants of land vulnerability include aridity, impoverished soil properties and the consolidation of population and activities in specific points such as coastal areas. This is the consequence of the urban development, migration and some human activities such as tourism, agriculture, transports or mining (Crossland *et al.,* 2018; Baumber *et al.,* 2019; Keesstra *et al.,* 2018). Moreover, land abandonment in rural areas is deteriorating the traditional agricultural system, which especially is more sensible in sloping areas, which may induce critical consequences in marginal rural landscapes (Puigdefábregas and Mendizabal, 1998). Especially, regional-scale investigations highly manifest these dynamics. For example, a multivariate analysis carried out to detect ecological indicators quantifying land sensitivity in Italy at a detailed geographical scale suggest that climate aridity and soil quality are the crucial variables explaining spatial patterns of LD through the highest proportion of variance (Salvati and Zitti, 2009; Salvati *et al.,* 2016). Another indicator highlighted in regional studies is the aridity, which may depict the effect of intensity of LD as the most evident result of climate change patterns (Amit *et al.,* 2006; Carrión *et al.,* 2010; McTainsh

et al., 1989). Physical processes involved in LD are also related to soil properties and erosion rates by water (Dunkerley, 2004; Koiter *et al.,* 2017) or wind (Gholami *et al.,* 2017; Marzen *et al.,* 2015). Finally, the impact of land-use changes and vegetation cover on LD are due to the agriculture and drastic intensification along with sloping or coastal areas (Squire *et al.,* 2015; Holland, 2004) and deforestation in lowlands and hilly zones (Gates and Ließ, 2001; Ruprecht and Schofield 1989), grazing (Abdalla *et al.,* 2018; Greenwood and McKenzie, 2001; Minea *et al.,* 2019) or abandonment in marginal interior land (Rey Benayas *et al.,* 2007; García-Ruiz and Lana-Renault, 2011), as well as unsustainable management of woodlands in mountain areas (Campos *et al.,* 2013). Destruction of natural ecosystems and biodiversity loss also leads to increased overland flows, modifying the antecedent balanced systems by runoff changes and altering the long-term social equilibrium existing in local communities depending on agriculture and forest economy (Brandt and Thorne, 1996; Brandt *et al.,* 2003; Sterk, 2003).

We developed a simplified framework showing the factors that would increase LD in Figure 1 based on specialized published literature (Baumber *et al.,* 2019; Rubio and Bochet, 1998; Knerr, 2004; Cuffaro, 2001; Tanrivermis, 2003; Cerdà 1998; Lal 1990; García-Ruiz *et al.,* 2015; Smith *et al.,* 2015; Thornes, 1985; Poesen, 2018; Tarolli, 2016). Drivers such as crop production, livestock, energy supply, industry, transport activities, mining, tourism, urban growth and climate change are exerting pressure on natural resources. Among economic and social factors, demographic and economic changes, especially in coastal territories affect urban growth and sprawl and migrations. The main populated areas are concentrated in coastal areas with non-sustainable using of natural resources (Duvernoy *et al.,* 2018; Salvati *et al.,* 2019). This is connected to rural depopulation, which accelerates the crisis conditions in traditional and marginal rural territories (Colucci, 2017; Pulido *et al.,* 2019). As a consequence, land abandonment leads to LD in steeper areas, especially, in bare lands. The loss of fertility, biodiversity and landscape fragmentation will also affect water and air quality, water shortage, biogeochemical cycles and human health (Smith *et al.,* 2015; Arnaez *et al.,* 2011; Hoffman *et al.,* 2001; Rodrigo-Comino *et al.,* 2020). Achieving land degradation neutrality and sustainability through scientific and local knowledge, generating human awareness and applying efficient policies is necessary, which allow developing efficient land management plans (Gichenje and Godinho, 2018; Zitti *et al.,* 2015). Organic farming (Rodrigo-Comino *et al.,* 2020) or the whole of the group of solutions named as nature-based ones (Kalantari *et al.,* 2018; Fini *et al.,* 2017) must be carefully designed and applied considering the environmental issue and local conditions.

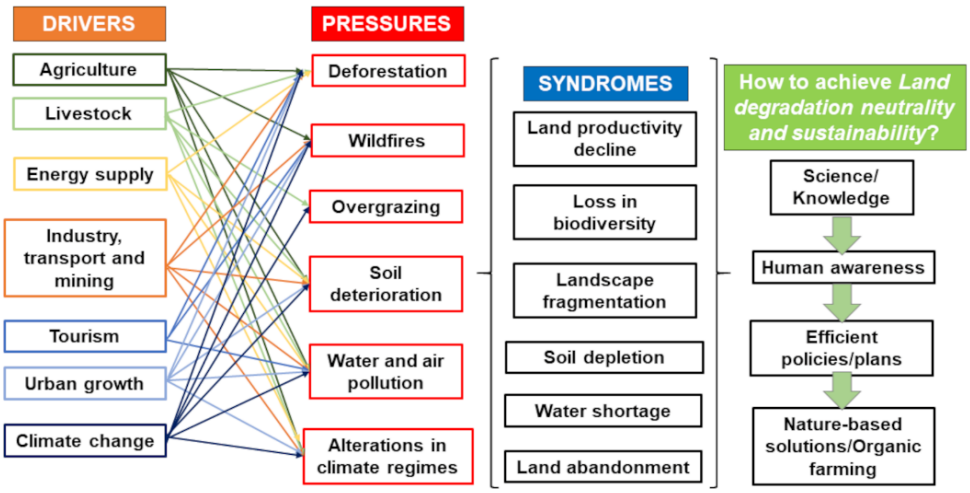

Figure 1. Forces leading to desertification risk and social consequences of poverty.

3. Increasing urbanization impacts

An increase of inhabitants can imply soil sealing by human spread into fertile lands (Bradford *et al.,* 1986; Fini *et al.,* 2017; Singer and Le Bissonais, 1998). Degradation of considered high-quality soils due to the urbanization growth can elevate the risks of wildfire, loss of biodiversity or the contamination of groundwater reservoirs (Askri and Al-Shanfari, 2017; Lotfi *et al.,* 2018; Bandala and Rodriguez-Narvaez, 2019). The tourism influx enhances land consumption of fragile natural areas and the overexploitation of water resources from coasts or mountains (Auernheimer and González, 2002; Bottrill, 2010). Especially, this concern affected land-use systems on the local communities (Philips and Jones, 2006).

3.1. Intensification of agriculture (quality and productivity) and urban sprawl

The intensification of the primary sector due to the use of machinery and low prices in the market represent an increase in crop surface and more elevated frequency of planting areas, which should be referred to the input of capital and labour. However, this is not generalized. The intensification of agriculture is considered by some authors as the major factor of soil and habitat deterioration due to deep-water drainage, irrigation, application of herbicides and pesticides, and tillage but also due to the low salaries and rural inhabitant rights, which promote rural depopulation (Serra *et al.,* 2014). There is evidence suggesting that in rural areas human impacts play a major role in the process of desertification due to overstocking, over-cultivation, and deforestation (Woods, 2009). Specific socio-economic factors that could be highlighted are nature of property rights on land ('environmental entitlements'), the institutions, cultural traditions as well as demographic dynamics. Notably, deforestation, overstocking and over-cultivation, determine a direct impact of human activities on the desertification (e.g. Cuffaro, 2001).

Low productivity is usually associated to arid and semi-arid areas or steep hillslopes which are affected by fluctuations of yields because of irregular pluviometric regimes and poor soils; however, this is also due to the non-sustainable agricultural practices. This tended to affect investments and the interest of novel scientific inputs to conserve land productivity and fertility. Although the priority to allocate development funds to the more productive landscapes could be assumed under economic criteria, policies (where applied) have set in motion a vicious circle with scarce economic and technological support. This would imply retrogressive management and weak economic performances in arid and semi-arid areas, because of the degradation of natural resources. The consequences are an accentuated difference between the rural and urban sectors and the rural itself, making clear "favourable" and "less favourable" land territories, causing disruptive influences on local communities (Suhrke, 1997). This can be also linked to non-controlled urban growth, which is related to LD processes. Urban sprawl in the Mediterranean is affecting natural ecosystems, soil fertility, the sustainability of coastal areas and quality of water resources among others (Barbero-Sierra *et al.,* 2013; Duvernoy *et al.,* 2018). It is understandable that in agriculture-dependent low-income countries land degradation could lead to a weak economic growth because the big share of the economy is made up of agriculture, but in advanced economies, the role of agriculture is very small. Therefore, this argument should be reconsidered in advanced economies as a factor for economic growth.

3.2. Social consequences of land degradation

Dynamics associated with migration, social inequality and underdevelopment are extremely linked with the local resource management. LD process carries out important socioeconomic implications. For example, LD may generate human displacement and induces migration. Because of the process of LD, especially in drylands, people may be forced to abandon the unproductive lands and seek for better income opportunities and a new source of livelihood in urban and coastal areas (Rey Benayas *et al.,* 2007). Notably, different human behaviours may represent, at the same time, a source of

LD. This would be affected by LD itself, suggesting a downward spiral, which is difficult to assess and mitigate through appropriate policies. In addition, other socioeconomic implications of LD stem from adaptive strategies and responses for mitigation to avoid political and institutional issues due to the scarcity of resources and environmental entitlements.

3.3. Migration, depopulation of rural areas and unemployment and social inequality

Rural migration and depopulation represent two different dynamics which could be directly or not linked to LD (Heat and Bingswangerb, 1996; Bilsborrow, 1992). Carrying capacity, population density and desertification risk are controversial and interrelated topics (Knerr, 2004). Past investigated experiences in rural areas of non-developing countries confirmed that arid and semi-arid areas could affect the number of inhabitants not able to conserve their living standards (Stern *et al.,* 1996; Amissah-Arthur *et al.,* 2000). Eroding environmental resources, therefore, does not continue an issue of the population staying there, but spreads to other regions even reaching neighboring territories by disseminating poverty and increasing disparities. This could generate future political or environmental conflicts, e.g. for natural or human resources (Chopra and Gulati, 1997; Drechsel *et al.*, 2001). We could consider that the type of living standard may be conditioned by the natural resources and less by human capabilities. The primary sector can improve land conservation or, on the contrary, can be the main degradation driver. In this situation, stakeholders, rural inhabitants and native natural ecosystems can be considered as victims. In addition, land abandonment could also represent another result of LD generating unbalanced population processes from inland to coastal areas. The densification processes of coastal territories could generate unemployment which may increase in more dense areas. Such process acts especially on vulnerable territorial elements such as women, old and young people, indirectly generating significant contributions to social deviance. Labour markets in rural areas associated with agriculture and rangelands are sensitive to trends in production, productivity and quality. Due to environmental conditioning factors linked to land degradation processes, even the tourism sector could suffer negative impacts by them (Bottrill, 2010; Barbier, 2000).

3.4. Loss of traditional practices, rural culture and poverty

The opportunity for technical support also plays an important role in sustainable land management. Although earlier studies have illustrated traditional skills of farmers able to maintain a high production level over structural aridity, there is little available information, at a wider level, about farmers' experiences in combating desertification. On the other hand, farmers-to-farmers visits should be encouraged to reduce the loss of traditional agricultural practices and to promote the sharing of experiences among communities, giving special consideration to women and youth. Poverty was analyzed considering this as a causal factor but also as a consequence of land degradation. Studies on the geography of poverty are scarce, but they use to insist upon the impoverishment could coincide with droughts, erosion or desertification (Sachs *et al.,* 2001). However, it is not clear if they present a linear or exponential correlation because of the extreme complexity of both phenomena. On the other, it is clearer that most cases of poverty show a mechanism through which institutions, policies or markets can affect land degradation (Powell *et al.,* 2001; Haan and Zoomers, 2003; Reidy, 2000). It intrinsically implies inappropriate public policies and institutional functions, which can cause i) geographical isolation; ii) vulnerability and increase of the occurrence in natural disasters; iii) demographic changes; and, iv) no access to a variety of public, private or social goods or services. The association of poverty and poor societies with marginality could also manifest some conditionals to this issue with clear implications on land degradation. Among them, land expropriation, demographic changes, intergenerational landscape fragmentation, privatization of common lands and expansion of commercial agriculture with reduced labour inputs could be considered as the main contributors' factors of LD because they motivate land abandonment and the reduction of land conservation strategies (Chopra and Gulati, 1997).

3.5. Emerging conflict for environmental resources, territorial dichotomy and social inequalities

The deterioration of the lands is increasing the number of conflicts because more territories have to share their resources. This provokes disparities among urban and rural areas especially about land ownership, cultivable and buildable surface availability or water storage (e.g., for both agricultural and domestic use) and energy source. Conflicts, especially for water resources, appear in developed countries affected to regular drought episodes such as the Mediterranean ones. Such conflicts may enhance migration movements and poverty among inland/marginal populations and represent a severe handicap to achieve land degradation neutrality and the sustainable development goals in arid and semi-arid areas. Human abuse or misuse of territory generating territorial divergences could suppose an important cause of conflicts and land degradation at the same time. In what measure human-related spatial dichotomy affect LD level or which social processes linking to inequality between populations can change desertification trends must be further investigated: i) land property rights; ii) political institutions; iii) cultural beliefs; and, iv) population structure and dynamics. Issues linked to resource unbalance, economic polarisation, and spatial dichotomy considering the possible influence on LD conditions along the Mediterranean basin are hot topics to be studied through a holistic point of view.

In Figure 2, a framework explaining the formation of social and environmental disparities in Southern Europe was designed. Disparities were represented along an elevation gradient, passing from coastal and lowland areas to inland, mountain and marginal ones. Dynamics of both poverty and LD depends on the elevation gradient. Along with a period (t0 and t1), land degradation would increase more in lowlands than in the mountain areas according to especially environmental pressures (e.g., increased aridity condition, poor soils and water resources, urban sprawl, fire impact, etc.) while poverty shows the reverse pattern due to especially social LD pressure. Such a framework allows us explaining different LD spatial patterns and the possible enhanced disparity among coastal and inland areas. Land resource management would depend on the structure of the primary production sector but it may be social unequal. Poverty can enhance to make decisions related to unsustainable methods to exploit resources and goods following a non-sustainable way. It should be tested if active participation occurs, local institutions can effectively manage the land.

Land accumulation and capitalist economic policies can enhance speculation and "throwaway" trends of resource exploitation, which could be ameliorated including strong programs of environmental education and understanding local traditions and religion. A key tool would be devoted to train and disseminate efficient economic incentives for sustainable development techniques to produce crops and animals (Rodrigo-Comino *et al.,* 2020; Hitzhusen, 2006; Nath, 2016). Concomitant factors could motivate poverty and degradation with irreversible soil loss and biodiversity. In arid lands, such condition may be defined as a downward spiral of 'poverty-LD'.

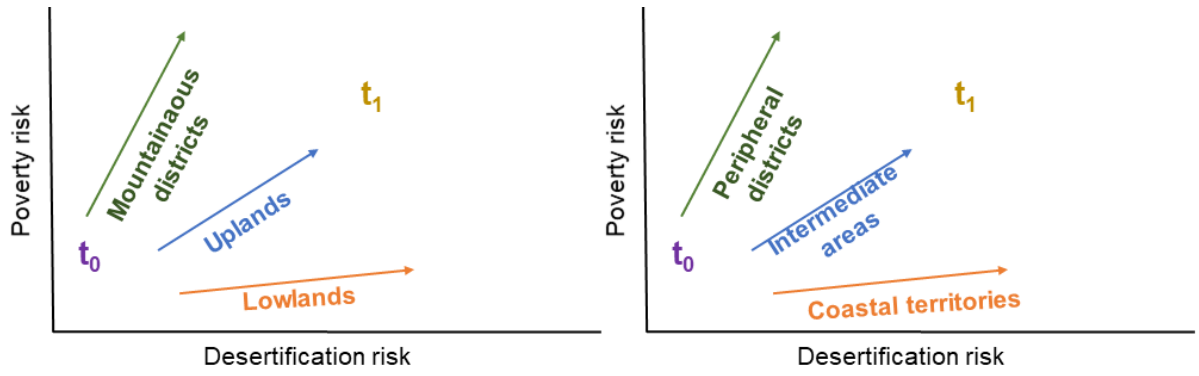

Figure 2. Hypothesis related to the trends over time in desertification and poverty risk in the Mediterranean context

4. Assessing the relationship between desertification risk and poverty: social indicators

Another critical point of the most recent literature on LD is the considerable lack in time series and scenarios analysis on vulnerable areas and the evolution of the main human factors involved. Although a multiplicity of statistical sources can be used in such studies, up to now, it is difficult to find data on human-induced LD trends at long-term periods and countries with different degree of development about (i) industrialisation during the fifties, (ii) intensification of the agriculture during sixties, (iii) higher demographic pressure up to seventies, (iv) increase in tourism pressure and urban sprawling along the coasts from early eighties, and (v) changes in the labour market from early nineties; and, (vi) land abandonment (extensification) of remote and rural areas. Low social variables are generally considered in the frameworks which built-up indexes of LD sensitivity such as the Environmental Sensitive Area (ESA) procedure (e.g. Karamesouti *et al.,* 2015; Kosmas *et al.,* 2016). Standard procedures to fix variables for these indexes should be easily computed at the highest spatial resolution and available, at least, every ten years. Setting up of metadata collection and the collection of multivariate tools (e.g., data mining, neural networks) should be carried out at different scales such as census section, municipality or province. This would make recognizable socioeconomic indicators. Also, the preparation of handbooks of good practices to be disseminated among the relevant authorities with the original datasets, final indicators and associated methodologies would be necessary. According to, a restricted panel of indicators able to depict social factors of LD in Mediterranean Europe is illustrated in Table 1, according to previous contributions on the topic (e.g. Salvati and Zitti 2009; Brandt *et al.,* 2003; Rubio and Bochet, 1998; Salvati *et al.,* 2008). Variables considered in this table are describing the most important characteristics of the society in terms of demographic, economic, and institutional elements.

Table 1. Examples of social indicators able to depict the human factors involved in LD processes.

Social	Demographic	Economic	Institutional/Policy
Poverty Gap Index	Population density	Gross domestic product	Scientific research funding
Unemployment rate	Demographic variation	Tourism density	Regional/local funding
GDP spent on education	Total fertility rate	Industrial concentration	Agri-environmental measures
Crime rate	Net migration rate	Agricultural intensity	Water use policy
Literacy index	Ageing rate	Farm income	Protected areas
Public perception of LD	Urban sprawl rate	Farm subsidies	Urban planning
	Farmer ageing	Crop productivity	Best practices

5. An example of downward spiral between poverty and desertification risk in Italy

In Italy, LD phenomena were visible in many inland and coastal municipalities of southern regions. Nowadays, Northern areas are becoming more sensitive to LD due to extreme drought episodes and the high agricultural intensification (Venezian Scarascia *et al.,* 2006; Munafò *et al.,* 2013). The dichotomy of LD sensitivity between coastal and inland zones increased during the seventies and maintained during the following decades. This was according to a progressive impact of human activities, especially, on the urban areas and more in general, on lowlands. The most sensitive areas include both southern part of the country as well as coastal zones along the Adriatic Sea and on the Po plain. LD sensitivity is moulded by complex geographic factors, where sensitivity increases in internal lowlands and coastal areas and decreases in mountain zones, according to a well-known increase in forests and decrease in human pressure and agriculture (Bouma *et al.,* 1998). Areas subjected to desertification risk are assessed based on a cartographic approach that takes into account mainly

ecological variables. It can be noted that only southern regions, namely Apulia, Sardinia, and Sicily present recent international literature in processes of desertification (Bajocco *et al.,* 2012).

Disparities among regions are well known in Italy not only at the environmental level but especially at the social and economic ones. While northern Italy represents one of the most European developed and rich regions, southern Italy includes regions with a marked growth deficit, high unemployment rate and evident gender disparity, both in the labour market and in participation to institutions and cultural life. Convergence in economic variables was observed among regions until the eighties but decreased in the last decade, suggesting that disparities among north and south still exist from a socioeconomic perspective. By integrating environmental and economic information, such a situation is confirmed by the inverse relationship between the level of per-capita income and LD rate (Fig. 3). Environmental and social drivers can mitigate ecological quality in low-income territories together like southern regions, generating the base background to begin a downward spiral 'Poverty – LD'. Such aspect is confirmed by an analysis of the positive relationship between relative poverty rate and LD rate at the regional level. While showing different levels of desertification risk, southern regions showed poverty rate always higher than 20% associated to a higher risk of desertification, while in many northern and central regions the poverty rate is considerably lower than 10% and sensitivity to LD is low or completely absent (Fig. 3).

To depict a downward spiral impacting natural and social factors, a logical framework (Fig. 4) is proposed here. We especially based on the effect of LD on the primary sector, which already explains more than 10% of the gross domestic product (compared to only 2% in northern Italy). Increasing agricultural intensification and mechanisation may provoke phenomena of LD through low-quality water management and unsustainable irrigation schemes.

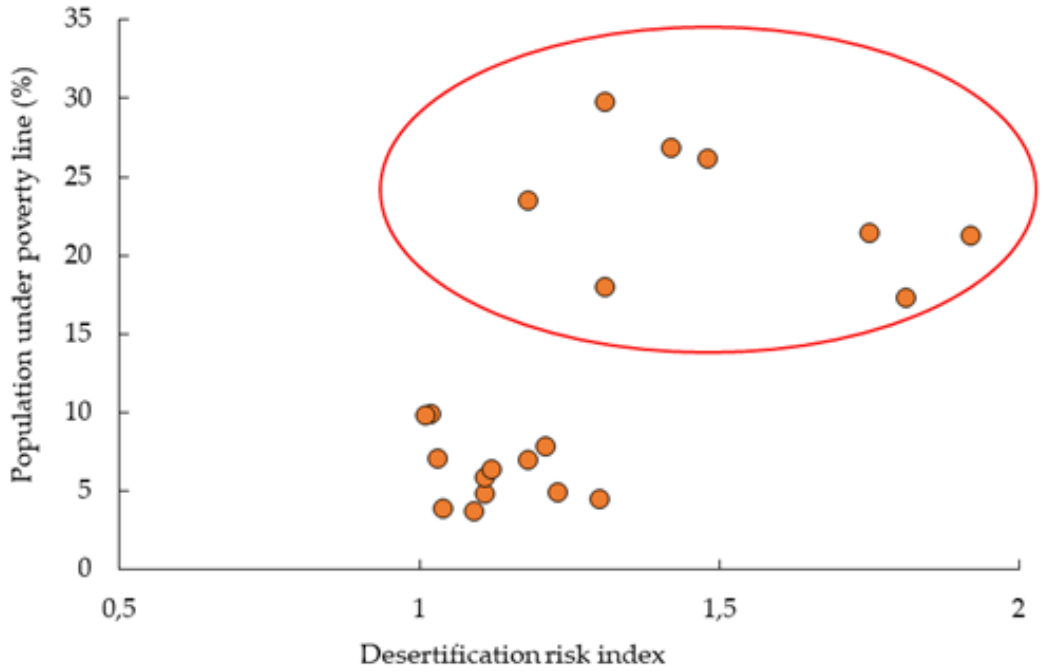

Figure 3. Relationship between desertification risk and population under the relative poverty line in Italy by administrative region (disseminated by National Institute of Statistics, ISTAT) in 2010 (Spearman rank correlation coefficient, rs = 0.54, p < 0.05, n = 20); red circle includes regions from Southern Italy; blue line indicates Central and Northern regions in Italy.

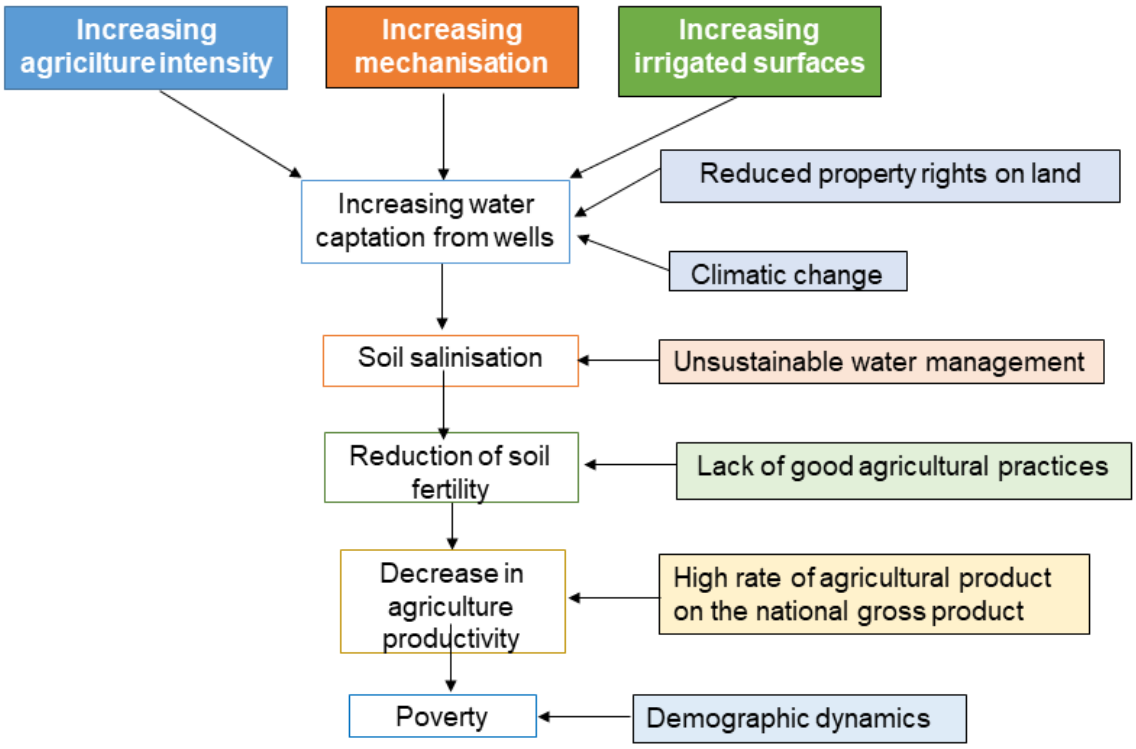

Figure 4. The downward spiral of desertification-poverty in Southern Italy.

At this point, climatic change may exacerbate local situations due to the lack of water resources and water extraction from wells combined with reduced property rights on lands with salinisation risks, subsequently, with a further reduction in land productivity. Compared to northern Italy, a weak application of good agricultural practices and low-sustainable management of land increase the medium-term risk of important economic loss in the primary sector. Since the primary sector significantly contributes to the total income, population movements and a consequent depopulation from inland, marginal areas are a reasonable response to this change. Territorial divergences increase and social disparities appear in rural, inland and coastal areas, increasing unemployment and poverty.

The importance of the interactions among LD and social determinants is highlighted by the analysis illustrated in Table 2. We classified the municipalities of southern Italy in four classes, according to their sensitivity to LD (Venezian Scarascia *et al.*, 2006). For each municipality, we calculated eleven social indicators (see paragraph before) and synthesize them per classes through their average figures weighted by commune surface. We can note that all the indicators, concerning labour market, education and social factors, are consistent in describing worse social conditions in high LD sensitivity areas, compared to the Italian average condition. The unemployment rate, especially those of women and youth, dramatically increase in the municipalities showing higher LD rate, while education levels showed a clear reversal pattern. Among the employees in the primary sector (which strongly increase in municipalities showing higher LD rate), ageing of farmers represents another key problem, especially in most degraded areas. Finally, taken as a proxy of 'social' life quality, crime rate showed the highest figures in the same areas.

Table 2. Relationship between level of land degradation and social variables in Southern Italy (disseminated by National Institute of Statistics, 2010, ISTAT).

Variable	Land degradation				Southern Italy	Italy
	Absent	Low	Medium	High		
Unemployment index (total)	18.6	18.8	20.0	23.3	20.8	11.9
Unemployment index (young)	48.1	48.9	49.2	54.4	50.9	30.7
Unemployment index (females)	24.7	25.5	27.5	32.0	28.5	16.6
Unemployment index (young females)	55.1	57.0	58.2	65.1	60.2	37.1
Employees in the primary sector (%)	12.0	14.0	16.0	14.0	15.0	10.0
Temporary employees in non-primary sector (%)	2.1	3.7	3.4	3.7	3.6	4.0
Population dropping out primary education (5)	11.8	12.3	13.7	14.4	13.6	11.1
Population with tertiary education degree (%)	4.6	5.1	5.0	4.9	5.0	5.0
Elderly index of farmers (% > 55 years)	18.0	20.0	21.0	21.0	21.0	23.0
Farmers with technical degree (%)	18.0	17.0	16.0	17.0	17.0	19.0
Crime rate (per 1.000 inhabitants)	14.6	13.0	17.6	24.3	18.8	20.4

6. Conclusions

Desertification risk is a social problem since land use is a socially constructed term. Reflections about land productivity and soil capacity, cropping systems and sustainable land management are products of a latent process of human-nature interactions. The socioeconomic structure, community integration, class inequality and developmental policy are discussed here in interaction with the theoretical framework of desertification risk. Assuming the underlying causes of desertification risk is directly related to human activities, anthropogenic pressure on natural resources leads to unsustainable ways of producing and living. The overexploitation of territories, soil and water, urban expansion, tourism and unplanned industrialization are some sectors and activities which come from political and socioeconomic forces leading to unsustainable forms of land management and types of unsustainable development. Social policies are important when combating desertification risk, and they can combat poverty and mitigate the impact of social inequality in rural areas. This is vital to achieving sustainable and equitable land. Education and training schemes to reduce rural migration and potentiate territorial knowledge could also help to avoid land degradation, affecting other social issues such as poverty or centralization. The potential role of win-win policies abating poverty and reducing desertification risk is evident in Mediterranean Europe.

References

Abdalla, M., Hastings, A., Chadwick, D. R., Jones, D. L., Evans, C. D., Jones, M. B., Rees, R. M., Smith, P., 2018. Critical review of the impacts of grazing intensity on soil organic carbon storage and other soil quality indicators in extensively managed grasslands. *Agriculture, Ecosystems and Environment* 253, 62-81. https://doi.org/10.1016/j.agee.2017.10.023

Ahmadi, B., Moradkhani, H., 2019. Revisiting hydrological drought propagation and recovery considering water quantity and quality. *Hydrological Processes* 33 (10), 1492-1505. https://doi.org/10.1002/hyp.13417

Akhtar-Schuster, M., Stringer, L.C., Erlewein, A., Metternicht, G., Minelli, S., Safriel, U., Sommer, S., 2017. Unpacking the concept of land degradation neutrality and addressing its operation through the Rio Conventions. *Journal of Environmental Management* 195, 4-15. https://doi.org/10.1016/j.jenvman.2016.09.044

Amissah-Arthur, A., Mougenot, B., Loireau, M., 2000. Assessing farmland dynamics and land degradation on Sahelian landscapes using remotely sensed and socioeconomic data. *International Journal of Geographical Information Science* 14 (6), 583-599. https://doi.org/10.1080/136588100415756

Amit, R., Enzel, Y., Sharon, D., 2006. Permanent quaternary hyperaridity in the Negev, Israel, resulting from regional tectonics blocking Mediterranean frontal systems. *Geology* 34 (6), 509-512. https://doi.org/10.1130/G22354.1

Arnaez, J., Lasanta, T., Errea, M.P., Ortigosa, L., 2011. Land abandonment, landscape evolution, and soil erosion in a Spanish Mediterranean mountain region: The Case of Camero Viejo. *Land Degradation & Development* 22 (6), 537-550. https://doi.org/10.1002/ldr.1032

Arshad, M. A., Martin, S., 2002. Identifying critical limits for soil quality indicators in agro-ecosystems. *Agriculture, Ecosystems and Environment* 88, 153-160. https://doi.org/10.1016/S0167-8809(01)00252-3

Asadi, H., Raeisvandi, A., Rabiei, B., Ghadiri, H., 2012. Effect of land use and topography on soil properties and agronomic productivity on calcareous soils of a semiarid region, Iran. *Land Degradation & Development* 23 (5), 496-504. https://doi.org/10.1002/ldr.1081

Askri, B., Al-Shanfari, R.A., 2017. Assessment of hydro-chemical processes inducing the groundwater salinisation in coastal regions: case study of the Salalah Plain, Sultanate of Oman. In: *Water Resources in Arid Areas: The Way Forward*, pp. 351-368. Springer.

Auernheimer, C., González, G., 2002. Repercussions of the national hydrological plan on the Spanish Mediterranean coast (water versus tourism and agriculture). In: D. Camarda, L. Grassini (Edrs.). *Local resources and global trades: environments and agriculture in the Mediterranean region,* pp. 179-185. Options Méditerranéennes: Série A. Séminaires Méditerranéens, 57.

Bajocco, S., De Angelis, A., Salvati, L., 2012. A satellite-based green index as a proxy for vegetation cover quality in a Mediterranean region. *Ecological Indicators* 23, 578-587. https://doi.org/10.1016/j.ecolind.2012.05.013

Bandala, E. R., Rodriguez-Narvaez, O.M., 2019. On the nature of hydrodynamic cavitation process and its application for the removal of water pollutants. *Air, Soil and Water Research* 12. https://doi.org/10.1177/1178622119880488

Barbero-Sierra, C., Marques, M.J., Ruíz-Pérez., M., 2013. The case of urban sprawl in Spain as an active and irreversible driving force for desertification. *Journal of Arid Environments* 90, 95-102. https://doi.org/10.1016/j.jaridenv.2012.10.014

Barbier, E. B. 2000. The economic linkages between rural poverty and land degradation: some evidence from Africa. *Agriculture, Ecosystems and Environment* 82 (1), 355-370. https://doi.org/10.1016/S0167-8809(00)00237-1

Baumber, A., Berry, E., Metternicht, G., 2019. Synergies between land degradation neutrality goals and existing market-based instruments. *Environmental Science and Policy* 94, 174-181. https://doi.org/10.1016/j.envsci.2019.01.012

Bekun, F. V., Alola, A.A., Sarkodie, S.A., 2019. Toward a sustainable environment: nexus between CO_2 emissions, resource rent, renewable and nonrenewable energy in 16-EU countries. *Science of The Total Environment* 657, 1023-1029. https://doi.org/10.1016/j.scitotenv.2018.12.104

Berry, E., Metternicht, G., Baumber, A., 2019. This country just hangs tight: Perspectives on managing land degradation and climate change in Far West NSW. *The Rangeland Journal* 41 (3), 197-210. https://doi.org/10.1071/RJ18030

Bilsborrow, R. E. 1992. Population growth, internal migration, and environmental degradation in rural areas of developing countries. *European Journal of Population* 8 (2), 125-148. https://doi.org/10.1007/BF01797549

Boix-Fayos, C., Calvo-Cases, A., Imeson, A. C., Mariano-Soto, M. D. 2001. Influence of soil properties on the aggregation of some Mediterranean soils and the use of aggregate size and stability as land degradation indicators. *Catena* 44, 47-67. https://doi.org/10.1016/S0341-8162(00)00176-4

Borrelli, P., Panagos, P., Ballabio, C., Lugato, E., Weynants, M., Montanarella, L., 2016. Towards a Pan-European assessment of land susceptibility to wind erosion. *Land Degradation & Development* 27 (4), 1093-1105. https://doi.org/10.1002/ldr.2318

Bottrill, C. 2010. *Sustainability and tourism*. Management Center Innsbruck. Austria 28.

Bouma, J., Varallyay, G., Batjes, N. H. 1998. Principal land use changes anticipated in Europe. *Agriculture, Ecosystems and Environment* 67 (2), 103-119. https://doi.org/10.1016/S0167-8809(97)00109-6

Bradford, J. M., Remley, P. A., Ferris, J. E., Santini, J. B., 1986. Effect of soil surface sealing on splash from a single waterdrop. *Soil Science Society of America Journal* 50 (6), 1547. https://doi.org/10.2136/sssaj1986.03615995005000060033x

Brandt, C. J., Thorne, C. R., 1996. *Mediterranean desertification and land use*. Wiley. USA. https://www.wiley.com/en-us/Mediterranean+Desertification+and+Land+Use-p-9780471942504

Brandt, C. J., Nichola, G., Imeson, A. C., 2003. *A Desertification indicator system for the Mediterranean Europe.* http://www.kcl.ac.uk/projects/desertlinks/downloads.htm

Butzer, K. W., 2005. Environmental history in the Mediterranean world: cross-disciplinary investigation of cause-and-effect for degradation and soil erosion. *Journal of Archaeological Science* 32 (12), 1773-1800. https://doi.org/10.1016/j.jas.2005.06.001

Campos, P., Huntsinger, L., Oviedo, J. L., Starrs, P. F., Diaz, M., Standiford, R. B., Montero, G., (Edrs.). 2013. *Mediterranean oak woodland working landscapes. Dehesas of Spain and ranchlands of California.* Landscape Series 16. Springer, 508 pag., https://doi.org/ 10.1007/978-94-007-6707-2

Carrión, J. S., Fernández, S., Jiménez-Moreno, G., Fauquette, S., Gil-Romera, G., González-Sampériz, P., Finlayson, C., 2010. The historical origins of aridity and vegetation degradation in southeastern Spain. *Journal of Arid Environments* 74 (7), 731-736. https://doi.org/10.1016/j.jaridenv.2008.11.014

Cerdà, A. 1995. Soil moisture regime under simulated rainfall in three years abandoned field in southeast Spain. *Physics and Chemistry of the Earth* 20 (3-4), 271-279. https://doi.org/10.1016/0079-1946(95)00037-2

Cerdà, A., 1998. Soil aggregate stability under different Mediterranean vegetation types. *Catena* 32 (2), 73-86. https://doi.org/10.1016/S0341-8162(98)00041-1

Cerdà, A., Novara, A., Dlapa, P., López-Vicente, M., Úbeda, X., Popovic, Z., Mekonnen, M., Terol, E., Janizadeh, S., Mbarki, S., Saldanha-Vogelmann, E., Hazrati, S. Sannigrahi, S., Parhizkar, M., Giménez-Morera, A., 2021. Rainfall and water yield in Macizo Del Caroig, Eastern Iberian Peninsula. Event runoff at plot scale during a rare flash flood at the Barranco de Benacancil. *Cuadernos de Investigación Geográfica (Geographical Research Letters)* 47. https://doi.org/10.18172/cig.4833

Chasek, P., Akhtar-Schuster, M., Orr, B. J., Luise, A., Rakoto Ratsimba, H., Safriel, U., 2019. Land degradation neutrality: The science-policy interface from the UNCCD to national implementation. *Environmental Science and Policy* 92, 182-190. https://doi.org/10.1016/j.envsci.2018.11.017

Chopra, K., Gulati, S. C., 1997. Environmental degradation and population movements: The role of property rights. *Environmental and Resource Economics* 9 (4), 383-408. https://doi.org/10.1007/BF02441758

Ciais, Ph, Reichstein, M., Viovy, N., Granier, A., Ogée, J., Allard, V., Aubinet, M., N. Buchmann, N., Bernhofer, Chr., Carrara, A., Chevallier, F., De Noblet, N., Friend, A. D., Friedlingstein, P., Grünwald, T., Heinesch, B., Keronen, P., Knohl, A., Krinner, G., Loustau, D., Manca, G., Matteucci, G., Miglietta, F., Ourcival, J.M., Papale, D., Pilegaard, K., Rambal, S., Seufert, G., Soussana, J. F., Sanz, M. J., Schulze, E. D., Vesala, T., Valentini, R., 2005. Europe-wide reduction in primary productivity caused by the heat and drought in 2003. *Nature* 437, 529-533. https://doi.org/10.1038/nature03972

Coelho, C. O. A., Sala, M., 1998. Erosion and land degradation in the Mediterranean. *Geoökodynamik* 19 (3/4), 318.

Collantes, V., Kloos, K., Henry, P., Mboya, A., Mor, T., Metternicht, G., 2018. Moving towards a twin-agenda: Gender equality and land degradation neutrality. *Environmental Science and Policy* 89, 247-253. https://doi.org/10.1016/j.envsci.2018.08.006

Colucci, A., 2017. Peri-urban/peri-rural areas: identities, values and strategies. In *Peri-Urban Areas and Food-Energy-Water Nexus*, pp. 99-104. Springer.

Conacher, A. J., Sala, M., (Edrs). 1998. *Land degradation in Mediterranean environments of the World: Nature and extent, causes and solutions*. Chichester , New York.

Crossland, M., Winowiecki, L. A., Pagella, T., Hadgu, K., Sinclair, F., 2018. Implications of variation in local perception of degradation and restoration processes for implementing land degradation neutrality. *Environmental Development* 28, 42-54. https://doi.org/10.1016/j.envdev.2018.09.005

Cuffaro, N. 2001. Population, economic growth and agriculture in less developed countries. Routledge, 188 pag., UK. https://www.routledge.com/Population-Economic-Growth-and-Agriculture-in-Less-Developed-Countries/Cuffaro/p/book/9780415202909

Dallimer, M., Stringer, L.C., 2018. Informing investments in land degradation neutrality efforts: A triage approach to decision making. *Environmental Science and Policy* 89, 198-205. https://doi.org/10.1016/j.envsci.2018.08.004

Drechsel, P., Gyiele, L., Kunze, D., Cofie, O., 2001. Population density, soil nutrient depletion, and economic growth in Sub-Saharan Africa. *Ecological Economics* 38 (2), 251-258. https://doi.org/10.1016/S0921-8009(01)00167-7

Dunkerley, D. 2004. Flow threads in surface run-off: Implications for the assessment of flow properties and friction coefficients in soil erosion and hydraulics investigations. *Earth Surface Processes and Landforms* 29 (8), 1011-1026. https://doi.org/10.1002/esp.1086

Duvernoy, I., Zambon, I., Sateriano, A., Salvati, L., 2018. Pictures from the other side of the fringe: Urban growth and peri-urban agriculture in a post-industrial city (Toulouse, France). *Journal of Rural Studies* 57, 25-35. https://doi.org/10.1016/j.jrurstud.2017.10.007

Emadodin, I., Reinsch, T., Taube, F., 2019. Drought and desertification in Iran. *Hydrology* 6 (3), 66. https://doi.org/10.3390/hydrology6030066

Fernández, C., Vega, J. A., 2014. Efficacy of bark strands and straw mulching after wildfire in NW Spain: Effects on erosion control and vegetation recovery. *Ecological Engineering* 63, 50-57. https://doi.org/10.1016/j.ecoleng.2013.12.005

Fini, A., Frangi, P., Mori, J., Donzelli, D., Ferrini, F., 2017. Nature based solutions to mitigate soil sealing in urban areas: Results from a 4-year study comparing permeable, porous, and impermeable pavements. *Environmental Research* 156, 443-454. https://doi.org/10.1016/j.envres.2017.03.032

Francke, A., Holtvoeth, J., Codilean, A. T., Lacey, J. H., Bayon, G., Dosseto, A., 2020. Geochemical methods to infer landscape response to Quaternary Climate Change and land use in depositional archives: A review. *Earth-Science Reviews* 207, 103218. https://doi.org/10.1016/j.earscirev.2020.103218

García Latorre, J., García-Latorre, J., Sanchez-Picón, A., 2001. Dealing with aridity: socio-economic structures and environmental changes in an arid Mediterranean region. *Land Use Policy,* 18 (1), 53-64. https://doi.org/10.1016/S0264-8377(00)00045-4

García Marín, R. 2008. La sequía: De riesgo natural a inducido. El ejemplo de la cuenca del río Segura (Sureste de España). *Vegueta* 10, 85-92.

García-Ruiz, J. M., Lana-Renault, N. 2011. Hydrological and erosive consequences of farmland abandonment in Europe, with special reference to the Mediterranean region–a review. *Agriculture, Ecosystems & Environment* 140 (3), 317-338. https://doi.org/10.1016/j.agee.2011.01.003

García-Ruiz, J. M., Lasanta-Martínez, T., Ortigosa-Izquierdo, L., Arnáez-Vadillo, J., 1986. Pipes in cultivated soils of La Rioja: Origin and evolution. *Zeitschrift Für Geomorphologie. Supplementband* 58, 93-100.

García-Ruiz, J. M., Lasanta, T., Martí, C., González, C., White, S., Ortigosa, L., Ruiz Flaño, 1995. Changes in runoff and erosion as a consequence of land-use changes in the Central Spanish Pyrenees. *Physics and Chemistry of The Earth* 20 (3-4), 301. https://doi.org/10.1016/0079-1946(95)00041-0

García-Ruiz, J. M., Nadal-Romero, E., Lana-Renault, N., Beguería, S., 2013. Erosion in Mediterranean landscapes: Changes and future challenges. Geomorphology 198, 20-36. https://doi.org/10.1016/j.geomorph.2013.05.023

García-Ruiz, J. M., Beguería, S., Nadal-Romero, E., González-Hidalgo, J.C., Lana-Renault, N., Sanjuán, Y., 2015. A meta-analysis of soil erosion rates across the world. *Geomorphology* 239, 160-173. https://doi.org/10.1016/j.geomorph.2015.03.008

Gates, L. D., Ließ, S., 2001. Impacts of deforestation and afforestation in the Mediterranean region as simulated by the MPI Atmospheric GCM. *Global and Planetary Change* 30, 309-328. https://doi.org/10.1016/S0921-8181(00)00091-6

Gholami, H., Telfer, M.W., Blake, W.H., Fathabadi, A., 2017. Aeolian sediment fingerprinting using a Bayesian mixing model. *Earth Surface Processes and Landforms* 42 (14), 2365-2376. https://doi.org/10.1002/esp.4189

Giampietro, M., 2019. On the circular bioeconomy and decoupling: Implications for sustainable growth. *Ecological Economics* 162, 143-156. https://doi.org/10.1016/j.ecolecon.2019.05.001

Gichenje, H., Godinho, S., 2018. Establishing a land degradation neutrality national baseline through trend analysis of GIMMS NDVI Time-Series. *Land Degradation & Development* 29 (9), 2985-2997. https://doi.org/10.1002/ldr.3067

Greenwood, K.L., McKenzie., B. M., 2001. Grazing effects on soil physical properties and the consequences for pastures: A review. *Australian Journal of Experimental Agriculture* 41 (8), 1231-1250. https://doi.org/10.1071/EA00102

Haan, L. D., Zoomers, A., 2003. Development geography at the crossroads of livelihood and globalisation. *Tijdschrift Voor Economische En Sociale Geografie* 94 (3), 350-362. https://doi.org/10.1111/1467-9663.00262

Heat, J., Bingswangerb, H., 1996. Natural resource degradation effects of poverty and population growth are largely policy-induced: The case of Colombia. *Environment and Development Economics* 1 (1), 65-84.

Herrmann, S. M., Hutchinson, C.F., 2005. The changing contexts of the desertification debate. *Journal of Arid Environments*, Special Issue on the "Greening" of the Sahel 63 (3), 538-555. https://doi.org/10.1016/j.jaridenv.2005.03.003

Hitzhusen, G. E. 2006. Religion and environmental education: Building on common ground. *Canadian Journal of Environmental Education* (CJEE) 11 (1), 9-25.

Hoffman, I., Gerlink, D., Kyiogwom, U. B., Mané-Bielfeldt, A., 2001. Farmers management strategies to maintain soil fertility in a remote area in northwest Nigeria. *Agriculture, Ecosystems and Environment* 86 (2001), 263-275. https://doi.org/10.1016/S0167-8809(00)00288-7

Holland, J. M. 2004. The environmental consequences of adopting conservation tillage in Europe: Reviewing the evidence. *Agriculture Ecosystems and Environment* 103, 1-25. https://doi.org/10.1016/j.agee.2003.12.018

Hussen, A. 2018. *Principles of environmental economics and sustainability: An integrated economic and ecological approach.* Routledge. UK.

Kalantari, Z., Ferreira, C. S. S., Keesstra, S., Destouni, G., 2018. Nature-based solutions for flood-drought risk mitigation in vulnerable urbanizing parts of East-Africa. *Current Opinion in Environmental Science and Health* 5, 73-78. https://doi.org/10.1016/j.coesh.2018.06.003

Karamesouti, M., Detsis, V., Kounalaki, A., Vasiliou, P., Salvati, L., Kosmas, C., 2015. Land-use and land degradation processes affecting soil resources: Evidence from a traditional Mediterranean cropland (Greece). *Catena* 132, 45-55. https://doi.org/10.1016/j.catena.2015.04.010

Keesstra, S., Mol, G., De Leeuw, J., Okx, J., Molenaar, C., De Cleen, M., Visser, S, 2018. Soil-related sustainable development goals: Four concepts to make land degradation neutrality and restoration work. *Land* 7 (4), 133. https://doi.org/10.3390/land7040133

Knerr, B. 2004. Desertification and human migration. In: D. Werner (Edr.), *Biological Resources and Migration,* Springer, 317-337 pp., Springer. Berlin, Heidelberg. https://doi.org/10.1007/978-3-662-06083-4_30

Koiter, A. J., Owens, P. N., Petticrew, E. L., Lobb., D.A., 2017. The role of soil surface properties on the particle size and carbon selectivity of interrill erosion in agricultural landscapes. *Catena* 153, 194-206. https://doi.org/10.1016/j.catena.2017.01.024

Kosmas, C., Karamesouti, M., Kounalaki, K., Detsis, V., Vassiliou, P., Salvati, L., 2016. Land degradation and long-term changes in agro-pastoral systems: An empirical analysis of ecological resilience in Asteroussia-Crete (Greece). *Catena* 147, 196-204. https://doi.org/10.1016/j.catena.2016.07.018

Kou, M., Jiao, J., Yin, Q., Wang, N., Wang, Z., Li, Y., Yu, W., Wei, Y., Yan, F., Cao, B. 2016. Successional trajectory over 10 years of vegetation restoration of abandoned slope croplands in the hill-gully region of the Loess Plateau. *Land Degradation & Development* 27 (4), 919-932. https://doi.org/10.1002/ldr.2356

Lal, R. 1990. Erosion measurement and evaluation. In: R. Lal (Edr.), *Soil Erosion in the Tropics: Principles and Management*. McGraw Hill, pp. 183-223, New York.

Larrey, M., Mouthereau, F., Masini, E., Huyghe, D., Gaucher, E.C., Virgone, A., Miegebielle, V., 2020. Quaternary tectonic and climate changes at the origin of travertine and calcrete in the Eastern Betics (Almería Region, SE Spain). *Journal of the Geological Society* 177, 939-954. https://doi.org/10.1144/jgs2020-025.

Lasanta, T., Perez-Rontome, C., García-Ruiz, J. M., Machín, J., Navas, A., 1995. Hydrological problems resulting from farmland abandonment in semi-arid environments: The Central Ebro Depression. *Physics and Chemistry of The Earth* 20 (3-4): 309.

Lotfi, D., Yann, L., Gerhard, S., Mohamed, H., Rajouene, M., 2018. Identifying the origin of groundwater salinisation in the Sidi El Hani Basin (Central-Eastern Tunisia). *Journal of African Earth Sciences* 147, 443-449. https://doi.org/10.1016/j.jafrearsci.2018.07.004

Lozano-Parra, J., Schnabel, S., Ceballos-Barbancho, A., 2015. The role of vegetation covers on soil wetting processes at rainfall event scale in scattered tree woodland of Mediterranean climate. *Journal of Hydrology* 529, 951-961. https://doi.org/10.1016/j.jhydrol.2015.09.018

Martínez-Valderrama, J., Ibáñez, J., Del Barrio, G., Sanjuán, M.E., Alcalá, F.J., Martínez-Vicente, S., Ruiz, A., Puigdefábregas. J., 2016. Present and future of desertification in Spain: Implementation of a surveillance system to prevent land degradation. *The Science of the Total Environment* 563-564, 169-178. https://doi.org/10.1016/j.scitotenv.2016.04.065

Marzen, M., Iserloh, T., Casper, M.C., Ries, J.B., 2015. Quantification of particle detachment by rain splash and wind-driven rain splash. *Catena* 127, 135-141. https://doi.org/10.1016/j.catena.2014.12.023

McTainsh, G. H., Burgess, R., Pitblado, J.R., 1989. Aridity, drought and dust storms in Australia (1960-84). *Journal of Arid Environments* 16 (1), 11-22. https://doi.org/10.1016/S0140-1963(18)31042-5

Minea, G., Ioana-Toroimac, G., Moro, G., 2019. The dominant runoff processes on grassland versus bare soil hillslopes in a temperate environment - An experimental study. *Journal of Hydrology and Hydromechanics* 67, 8. https://doi.org/10.2478/johh-2019-0018

Munafò, M., Salvati, L., Zitti, M. 2013. Estimating soil sealing rate at National level. Italy as a case study. *Ecological Indicators* 26, 137-140. https://doi.org/10.1016/j.ecolind.2012.11.001

Nadal-Romero, E., González-Hidalgo, J.C., Cortesi, N., Desir, G., Gómez, J. A., Lasanta, T., Lucía, A., Marín, C., Martínez-Murillo, J. F., Pacheco, E., Rodríguez-Blanco, M. L., Romero Díaz, A., Ruiz-Sinoga, J. D., Taguas, E. W., Taboada-Castro, M. M., Taboada-Castro, M. T., Úbeda, X., Zabaleta, A., 2015. Relationship of runoff, erosion and sediment yield to weather types in the Iberian Peninsula. *Geomorphology* 228, 372-381. https://doi.org/10.1016/j.geomorph.2014.09.011

Nath, B. 2016. *Environmental education and awareness. Religion, culture and sustainable development* -Volume III, II. EOLSS Publications, Oxford, UK.

Nocenzi, M. 2005. Environment and value challenge: Persistence and changes. International *Review of Sociology* 15 (2), 291-292. https://doi.org/10.1080/03906700500159623

Philips, M. R., Jones, A.L. 2006. Erosion and tourism infrastructure in the coastal zone: Problems, consequences and management. *Tourism Management* 27 (3): 517-524. https://doi.org/10.1016/j.tourman.2005.10.019

Poesen, J. 2018. Soil erosion in the Anthropocene: Research needs. *Earth Surface Processes and Landforms* 43 (1), 64-84. https://doi.org/10.1002/esp.4250

Powell, M., Boyne, G., Ashworth, R., 2001. Towards a Geography of People Poverty and Place Poverty. *Policy & Politics* 29 (3), 243–258. https://doi.org/10.1332/0305573012501332

Prakash, S., 1997. Poverty and environment linkages in mountains and uplands: Reflections on the 'Poverty Trap' Thesis. CREED Working Paper, 12. http://hdl.handle.net/10535/3659

Puigdefábregas, J., Mendizabal, T., 1998. Perspectives on desertification: Western Mediterranean. *Journal of Arid Environments* 39 (2), 209–224. https://doi.org/10.1006/jare.1998.0401

Pulido, M., Barrena-González, J., Alfonso-Torreño, A., Robina-Ramírez, R., Keesstra, S., 2019. The problem of water use in rural areas of Southwestern Spain: A local perspective. *Water* 11 (6), 1311. https://doi.org/10.3390/w11061311

Reidy, M. F. 2000. The longest commute: The Geography of poverty, employment, and services. *New England Journal of Public Policy* 16 (1), 53-68.

Rey Benayas, J. M., Martins, A., Nicolau, J. M., Schulz, J. J., 2007. Abandonment of Agricultural Land: An Overview of Drivers and Consequences. *CAB Reviews: Perspectives in Agriculture, Veterinary Science, Nutrition and Natural Resources* 2 (57), 1–14. https://doi.org/10.1079/PAVSNNR20072057

Reynolds, J. F., Grainger, A., Stafford Smith, D.M., Bastin, G., Garcia-Barrios, L., Fernández, R. J., Janssen, M.A., Jürgens, N., Scholes, R. J., Veldkamp, A., Verstraete, M. M., Von Maltitz, G., Zdruliet, P., 2011. Scientific Concepts for an Integrated Analysis of Desertification. *Land Degradation & Development* 22, 166-183. https://doi.org/10.1002/ldr.1104

Rodrigo-Comino, J., Senciales, J. M., Sillero-Medina, J.A., Gyasi-Agyei, Y., Ruiz-Sinoga, J.D., Ries, J.B., 2019. Analysis of weather-type-induced soil erosion in cultivated and poorly managed abandoned sloping vineyards in the Axarquía Region (Málaga, Spain). *Air, Soil and Water Research* 12. https://doi.org/10.1177/1178622119839403

Rodrigo-Comino, J., Giménez-Morera, A., Panagos, P., Pourghasemi, H. R., Pulido, M., Cerdà, A., 2020. The potential of straw mulch as a nature-based solution for soil erosion in olive plantation treated with glyphosate: A biophysical and socioeconomic assessment. *Land Degradation & Development* 31 (15), 1877-1889. https://doi.org/10.1002/ldr.3305

Rodrigo-Comino, J., López-Vicente, M., Kumar, V., Rodríguez-Seijo, A., Valkó, O., Rojas, C., Pourghasemi, H. R., Bakr, N., Vaudour, E., Brevik, E.C., Radziemska, M., Pulido, M., Di Prima, S., Dondini, M., de Vries, W, Santos, E.S., Mendonça-Santos, M., Yu, Y., Panagos, P., 2020. Soil science challenges in a new era: A transdisciplinary overview of relevant topics. *Air, Soil and Water Research* 13. https://doi.org/10.1177/1178622120977491

Rodrigo-Comino, J., Terol, E., Mora, G., Giménez-Morera, A., Cerdà, A., 2020. *Vicia Sativa Roth.* can reduce soil and water losses in recently planted vineyards (*Vitis Vinifera L.). Earth Systems and Environment* 4, 827-842. https://doi.org/10.1007/s41748-020-00191-5

Rubio, J. L., Bochet, E., 1998. Desertification indicators as diagnosis criteria for desertification risk assessment in Europe. *Journal of Arid Environments* 39, 113-120. https://doi.org/10.1006/jare.1998.0402

Ruprecht, J. K., Schofield, N. J., 1989. Analysis of streamflow generation following deforestation in Southwest Western Australia. *Journal of Hydrology* 105: 1-17. https://doi.org/10.1016/0022-1694(89)90093-0

Sachs, J. D., Mellinger, A. D., Gallup, J. L., 2001. The Geography of poverty and wealth. *Scientific American* 284 (3), 70-75.

Salvati, L., Zitti, M., 2009. Assessing the impact of ecological and economic factors on land degradation vulnerability through multiway analysis. *Ecological Indicators* 9 (2): 357-363. https://doi.org/10.1016/j.ecolind.2008.04.001

Salvati, L, Zitti, M., Ceccarelli, T., 2008. Integrating economic and environmental indicators in the assessment of desertification risk: A case study. *Applied Ecology and Environmental Research* 6, 129-138. https://doi.org/10.15666/aeer/0601_129138

Salvati, L., Zitti, Z., Perini, L., 2016. Fifty years on: long-term patterns of land sensitivity to desertification in Italy. *Land Degradation & Development* 27, 97-107. https://doi.org/10.1002/ldr.2226

Salvati, L., Ciommi, M.T., Serra, P., Chelli, M. 2019. Exploring the spatial structure of housing prices under economic expansion and stagnation: The role of socio-demographic factors in metropolitan Rome, Italy. *Land Use Policy* 81, 143-152. https://doi.org/10.1016/j.landusepol.2018.10.030

Schnabel, S., 1994. Using botanical evidence for the determination of erosion rates in semi-arid tropical areas. *Advances in GeoEcology* 27, 31-45.

Serra, P., Vera, A., Tulla, A.F., Salvati, L., 2014. Beyond urban-rural dichotomy: Exploring socioeconomic and land-use processes of change in Spain (1991-2011). *Applied Geography* 55, 71-81. https://doi.org/10.1016/j.apgeog.2014.09.005

Singer, M. J., Le Bissonais, Y., 1998. Importance of surface sealing in the erosion of some soils from a Mediterranean climate. *Geomorphology* 28, 79-85. https://doi.org/10.1016/S0169-555X(97)00102-5

Smith, P., Cotrufo, M. F., Rumpel, C., Paustian, K., Kuikman, P. J., Elliott, J. A., McDowell, R., Griffiths, R. I., Asakawa, S., Bustamante, M., House, J.I., Sobocká, J., Harper, R., Pan, G., West, P. C., Gerber, J. S., Clark, J. M., Adhya, T., Scholes, R. J., Scholes, M.J., 2015. Biogeochemical cycles and biodiversity as key drivers of ecosystem services provided by soils. *SOIL* 1, 665-685. https://doi.org/10.5194/soil-1-665-2015

Smith, P., Calvin, K., Nkem, J., Campbell, D., Cherubini, F., Grassi, G., Korotkov, V., Le Hoang, A., Lwasa, S., McElwee, P., Nkonya, E., Saigusa, N., Soussana, J. F., Taboada, M.A., Manning, F.C., Nampanzira, D., Arias-Navarro, C., Vizzarri, M., House, J., Roe, S., Cowie, A., Rounsevell, M., Almut, A., 2020. Which practices co-deliver food security, climate change mitigation and adaptation and combat land degradation and desertification? *Global Change Biology* 26 (3), 1532-1575. https://doi.org/10.1111/gcb.14878

Squire, G. R., Hawes, C., Valentine, T.A., Young, M.W., 2015. Degradation rate of soil function varies with trajectory of agricultural intensification. *Agriculture, Ecosystems & Environment* 202, 160-167. https://doi.org/10.1016/j.agee.2014.12.004

Sterk, G. 2003. Causes, consequences and control of wind erosion in Sahelian Africa: A review. *Land Degradation & Development* 14 (1), 95-108. https://doi.org/10.1002/ldr.526

Stern, D. I., Common, M.S., Barbier, E. B., 1996. Economic growth and environmental degradation: The environmental kuznets curve and sustainable development. *World Development* 24, 1151-1160. https://doi.org/10.1016/0305-750X(96)00032-0

Suhrke, A., 1997. Environmental degradation, migration, and the potential for violent conflict. In Gleditsch, N. P. (Edr.). *Conflict and the Environment.* NATO ASI Series. 255-272 pp., Springer Netherlands. https://doi.org/10.1007/978-94-015-8947-5_16

Tanrivermis, H. 2003. Agricultural land use change and sustainable use of land resources in the Mediterranean Region of Turkey. *Journal of Arid Environments* 54, 553-564. https://doi.org/10.1006/jare.2002.1078

Tarolli, P. 2016. Humans and the Earth's surface. *Earth Surface Processes and Landforms* 41 (15), 2301-2304. https://doi.org/10.1002/esp.4059

Thornes, J. B. 1985. The ecology of Erosion. *Geography* 70 (3), 222-235.

Turner, B. L. 1994. Local Faces, Global Flows: The Role of Land Use and Land Cover in Global Environmental Change. *Land Degradation & Development* 5 (2), 71-78. https://doi.org/10.1002/ldr.3400050204

Vagen, T. G., Winowiecki, L.A., Tondoh, J. E., Desta, L. T., Gumbricht, T., 2016. Mapping of soil properties and land degradation risk in Africa using MODIS reflectance. *Geoderma* 263, 216-225. https://doi.org/10.1016/j.geoderma.2015.06.023

Venezian Scarascia, M. E., Di Battista, F., Salvati, L., 2006. Water resources in Italy: Availability and agricultural uses. *Irrigation and Drainage* 55, 115-127. https://doi.org/10.1002/ird.222

Woods, M. 2009. Rural geography: Blurring boundaries and making connections. *Progress in Human Geography* 33 (6), 849-858. https://doi.org/10.1177/0309132508105001

Xie, H., Zhang, Y., Wu, Z., Lv., T., 2020. A bibliometric analysis on land degradation: Current status, development, and future directions. *Land* 9 (1), 28. https://doi.org/10.3390/land9010028.

Zambon, I., Benedetti, A., Ferrara, C., Salvati, L., 2018. Soil matters? A multivariate analysis of socioeconomic constraints to urban expansion in Mediterranean Europe. *Ecological Economics* 146, 173-183. https://doi.org/10.1016/j.ecolecon.2017.10.015

Zitti, M., Ferrara, C., Perini, L., Carlucci, M., Salvati, L., 2015. Long-term urban growth and land use efficiency in Southern Europe: Implications for sustainable land management. *Sustainability* 7 (3), 3359-3385. https://doi.org/10.3390/su7033359

Cuadernos de Investigación Geográfica *Geographical Research Letters*	2022	Nº 48	pp. 41-57	EISSN 1697-9540

http://doi.org/10.18172/cig.5212

IDENTIFICATION OF LEVELS OF ANTHROPIZATION AND ITS IMPLICATIONS IN THE PROCESS OF DESERTIFICATION IN THE CAATINGA BIOME (JEREMOABO, BAHIA-BRAZIL)

NÍVEA OLIVEIRA SANTOS[1], RICARDO AUGUSTO SOUZA MACHADO[2], RUBÉN CAMILO LOIS GONZÁLEZ[3*]

[1]Universidade Estadual de Feira de Santana, Rua Samuel Mota, n. 100, Bairro Dionísio Mota, Valente.Bahia, CEP 48890-000 Brazil.

[2]Universidade Estadual de Feira de Santana, Rua Francisco Jorge 147, Residencial Villa Bella, AP902, Luiz Anselmo, CEP 40261-065, Salvador, Bahia;, Brazil.

[3]Universidade de Santiago de Compostela. Pza. Universidade 1, 15782 Santiago de Compostela, Spain.

ABSTRACT. Desertification is one of the most serious current environmental problems and corresponds to the impoverishment and decrease of moisture in sandy soils located in regions with a sub-humid, arid and semiarid climate, with its main causes related to climatic variations and the resulting negative impacts of human activities. Studies show that the soils located in the Brazilian semiarid and especially in the Caatinga biome have been suffering an intense process of desertification due to the replacement of natural vegetation as a result of economic activities. Most municipalities that have an economy based on agropastoral activities are at the centre of desertification in several centres in Brazil. Based on this context and considering that the original vegetation cover is a preponderant factor for soil conservation, and subsequently for the maintenance of the ecological stability of the Caatinga biome, this work aimed to map the vegetation cover of the Vaza-Barris watershed corresponding to the municipality of Jeremoabo (Bahia-Brazil), with the purpose of identifying and quantifying, in terms of surface, the main types of interaction between human activities and the remnants of the vegetation cover, listing the potential impacts that have a direct consequence on the desertification processes. The delimitation of the vegetation cover was the result processing Sentinel 2A satellite images and the use of the Soil Adjusted Vegetation Index - SAVI. Five thematic classes representative of the study area were identified, classified according to the increasing level of anthropization that allowed us to conclude that desertification causes damage to agriculture, making the areas unproductive, as well as excessive agriculture with inappropriate practices causes the loss of fertility of the soils, aggravating the desertification process. With this, the environmental and social quality is threatened, considering that the main source of income in the municipality of Jeremoabo comes from agricultural activities and these are dependent on climatic conditions, soil conservation and water resources.

Identificación de niveles de antropización y sus implicaciones en el proceso de desertificación en la Caatinga (Jeremoabo, Bahía-Brasil)

RESUMEN. Actualmente la desertificación es uno de los problemas ambientales más graves y coincide con el empobrecimiento y disminución de la humedad de los suelos arenosos localizados en regiones de clima subhúmedo, árido y semiárido. Sus principales causas están relacionadas con las variaciones climáticas y los consiguientes impactos negativos de las actividades humanas. Los estudios muestran que los suelos ubicados en el semiárido brasileño y especialmente en el bioma Caatinga vienen sufriendo un intenso proceso de desertificación debido a la sustitución de la vegetación natural como resultado de las actividades económicas. La mayoría de los

municipios, que tienen una economía basada en actividades agro-pastorales, están en el centro de la desertificación en varias áreas de Brasil. En este contexto, y considerando que la cubierta vegetal original es un factor importante para la conservación del suelo y para el mantenimiento de la estabilidad ecológica del bioma Caatinga, este trabajo tiene como objetivo cartografiar la cubierta vegetal de la cuenca del río Vaza-Barris correspondiente al municipio de Jeremoabo (Bahía-Brasil). Se trata de identificar y cuantificar, en términos de superficie, los principales tipos de interacción entre las actividades humanas y los remanentes de la cubierta vegetal, enumerando los impactos potenciales que tienen una consecuencia directa sobre los procesos de desertificación. La delimitación de la cubierta vegetal fue resultado del procesamiento de imágenes del satélite Sentinel 2A y el uso del Índice de Vegetación Ajustado al Suelo - SAVI. Se identificaron cinco clases representativas de la zona de estudio, clasificadas según el nivel creciente de antropización que permitieron concluir que la desertificación provoca daños a la agricultura haciendo improductivas las áreas. También la agricultura excesiva con prácticas inadecuadas provoca la pérdida de fertilidad de los suelos, agravando el proceso de desertificación. De esta forma, la calidad ambiental y social se ve amenazada, considerando que la principal fuente de ingresos del municipio de Jeremoabo proviene de las actividades agropecuarias y éstas dependen de las condiciones climáticas, la conservación del suelo y los recursos hídricos.

Key words: Desertification, Caatinga, Anthropogenic Activities, SAVI, Sentinel 2A satellite.

Palabras clave: Desertificación, Caatinga, Actividades Antropogénicas, SAVI, Satélite Sentinel 2A.

Received: 15 October 2021

Accepted: 24 January 2022

***Corresponding author:** Rubén Camilo Lois González, Universidade de Santiago de Compostela, Pza. Universidade 1, 15782 Santiago de Compostela, Spain. E-mail address: rubencamilo.lois@usc.es

1. Introduction

Controlling occupation and soil use, a legal attribute in historically neglected Brazilian towns, has contributed over recent decades to the reduction in the conservation of environmental resources, including superficial and subterranean water resources, making it more difficult for human and animal populations to survive in areas which are characterised by their low annual precipitation rates, having a direct impact on the increase of the processes linked to desertification (Vieira *et al.,* 2013; Wijitkosum, 2016).

Desertification is one of the most serious current environmental problems (Mirzabaev *at al.,* 2019) and corresponds to the impoverishment and decrease of moisture in sandy soils located in regions with a sub-humid, arid and semiarid climate, with its main causes related to climatic variations and the resulting negative impacts of human activities, like the inadequate management of animal husbandry, the suppression of vegetation cover and the illegal practice of mining activities (Mouat *et al.,* 2019), as well as the salinization of the soil from irrigation, overgrazing, the unsustainable use of superficial and subterranean water resources (Salama *et al.,* 1999).

Studies show that the soils located in the Brazilian semiarid have been suffering an intense process of desertification due to the replacement of natural vegetation as a result of economic activities. Most municipalities that have an economy based on agropastoral activities are at the centre of desertification in several cities in the country (Brazil, 2005; Oliveira Junior, 2014; Souza, 2020).

A collaboration between the Ministry for the Environment, the State University of Feira de Santana, EmbrapaSemiárido and Embrapa Solos showed that only 40.5% of the original area of the Caatinga biome has remnants of its native vegetation (Sá *et al.,* 2010). The Caatinga is different in that

it is an exclusively Brazilian biome, located mainly in the north-east region where a semiarid climate is most predominant, characterised by precipitation levels below 800 millimetres/year, covering an area of approximately 735,000 km^2 (Silva *et al.* 2004). The Caatinga receives the official classification of a Stepiccal-Savannah (Veloso *et al.*, 1991).

This is where the area of study of this paper is located, the municipality of Jeremoabo, in the north of the State of Bahia (Fig. 1), where the main vegetation coverage is arboreal/shrub-like, branched and thorny, with different species of bromelia and cactus (Almeida *et al.,* 2011).

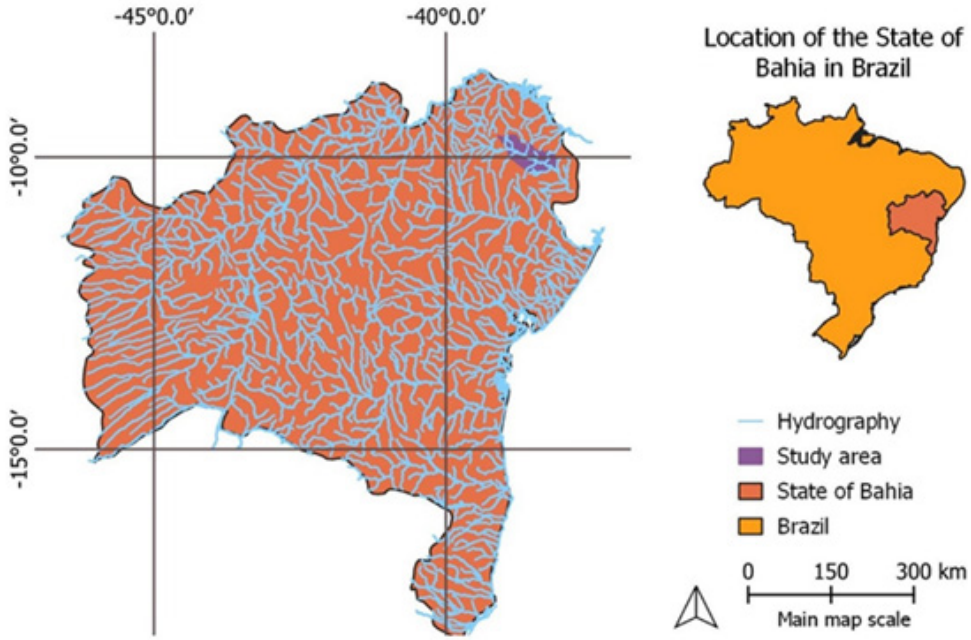

Figure 1. Location of the municipality of Jeremoabo in the State of Bahia, Brazil.

This individual type of tropical xerophile vegetation can only be found in the north-east of Brazil, as a result of the physiological defence mechanism of plants against the high level of transpiration (Brazil, 2005). In this region, the factors regarding the climate are more striking than other ecological factors when it comes to defining the type of vegetation coverage.

Jeremoabo has high temperatures throughout the year, with an average of 24º and a low rainfall index (a historical average of 654 mm/year), rainfall which is consolidated into the months from May to July and a high risk of drought, with it being more susceptible to erosion caused by the torrential rains (Grilo *et al.,* 2009). Such aspects are reflected in high evaporation rates or soil with a low liquid retention capacity, causing intermittence throughout rivers (Carvalho, 2010). In this type of environment, vegetation coverage is one of the main control factors of desertification, because as it is deciduous, it plays the role of protecting the soil from bad weather, thus lessening its deterioration (Sá *et al.,* 2010).

The reduction or disappearance of this vegetation coverage in recent decades has caused an imbalance in the thermal balance, leading to an increase in the reflectivity of solar radiation, thus intensifying the atmospheric subsistence and driving the dry air from the high troposphere to the surface, which ends up reducing the amount of cloud formation and the likelihood of rainfall. Besides this, soil that is directly exposed to solar radiation has less retention capacity for subterranean water (Castelletti *et al.,* 2003).

The main reason for this loss of vegetation coverage is linked to an economy which is based on farming and livestock, vegetation extraction and forestry which do not make use of the suitable technical

resources to make these activities compatible with the characteristics of the Caatinga biome, making the soil more susceptible to external variables, mainly regarding leaching and slipping processes and the evolution of gullies (Almeida *et al.,* 2011). It often causes the deterioration which contributes to desertification due to porous dryness and the loss of the soil's productive capacity (Oliveira Junior, 2014).

Based on this context and considering that the original vegetation cover is a preponderant factor for soil conservation, and subsequently for the maintenance of the ecological stability of the Caatinga biome, this work aimed to map the vegetation cover of the Vaza-Barris watershed corresponding to the municipality of Jeremoabo (Bahia-Brazil), with the purpose of identifying and quantifying, in terms of surface, the main types of interaction between human activities and the remnants of the vegetation cover, listing the potential impacts that have a direct consequence on the desertification processes.

The hydrographic basin in the Vaza-Barris river spans a total area of 16,787.47 km^2, with its sources in Serra da Canabrava in the Bahia municipality of Uauá. Its mouth is in the State of Sergipe, between the municipalities of Aracaju and Itaporanga d'Ajuda. The area covered by this study encompasses a population of 37,680 inhabitants which are unevenly distributed across 4,267.5 km^2, located in the Bahia Sertanejo lowland depression, a region which is known its low soil development (Marques *et al.,* 2009).

2. Method and Materials

In order to make a breakdown of the vegetation coverage, Sentinel 2A satellite images with bands 4 (red) and 8 (near infra-red) were used which were obtained from the site https://lv.eosda.com/, provided by the Earth Observation System, showing a spatial resolution of 10 metres.

Sentinel 2 is a multi-spectral sensor with a typical spatial resolution, which, according to the United States Geological Survey (USGS), is from an imaging mission carried out by the GMES Programme (Global Monitoring of the Environment and Security) together with the European Community and the ESA (European Space Agency), with the aim of gathering high-resolution soil, vegetation, humidity, river and coastal area data and data for atmospheric correction (up to 10m), with a short revisiting period (5 days), and is free and open for public access.

The images were pre-processed using the Semi-Automatic Classification of the ArcGIS (ESRI) software in order to carry out the atmospheric correction, considering the parameters present in the metadata on each band. After this stage, the composition of the bands used in the classification and the cutting process of the images was carried out in accordance with the limit of the hydrographic basin. After these procedures, the transformation of the Mapping Reference System (SRC) was made with the aim of matching the themed maps that would be produced with the SIRGAS 2000 geodetic reference system, used for the Brazilian Mapping Agency's activity.

Then, the differentiation of the types of soil use was made using the SAVI (Soil Adjusted Vegetation) calculation, a vegetation index adjusted to the soil developed by Huete (1988) with the aim of minimising the reflectance of the soil on the NDVI (Normalised Difference Vegetation Index), with the incorporation of an "L" constant which is adjusted according to the soil coverage, thus reducing the effects of the soil's colour in the classification results (Qi *et al.,* 1994; Lima *et al.,* 2017).

Using the near infra-red and red bands, Huete (1988) developed the SAVI by visiting areas of grasslands and agricultural crops, mainly canopies with around 50% of vegetation coverage, bearing in mind that the brightness of the soil, especially that of the darker shades, increases the value of the vegetation indexes and thus, the SAVI's aim is to produce vegetation isograms more separate from the soil (Huete, 1988 in Washington-Allen *et al.,* 2003; Gameiro *et al.,* 2016).

In accordance with Braz *et al*., 2015), the SAVI is calculated using the following equation:

$$SAVI = \left(\frac{NIR - R}{NIR + R + L} \right).(1 + L)$$

In it, according to the aforementioned authors, "NIR" is the Near Infra-Red band, "RED" is the Red band, and "L" represents the constant that reduces the effects of the soil and that can vary depending on the degree of density of the canopy in the studied area. The value of the L constant varies between 0 (identical to the NDVI) and 1, with the following being considered optimum values: value 1 for low vegetation densities; 0.5 for average densities; and 0.25 for low vegetation densities (Huete, 1988; Qi *et al.,* 1994; Rodondeaux *et al.,* 1996; Silva *et al.,* 2015).

In the majority of studies, the L value equal to 0.5 is the most common, regardless of the type of soil, since it covers a larger variation of vegetation (Washington-Allen *et al.,* 2003) and this is why it was the parameter used in this paper. Despite the results from the SAVI being similar to those from the NDVI, they are different in that the SAVI has wider values that highlight the characteristics of vegetated regions, non-vegetated rations and bodies of water, offering a more authentic view of the study area (Gameiro *et al.,* 2016).

In order to support the definition of the types with the different levels of anthropization, the studies developed for the São Francisco River Water Resources Plan (São Francisco River Hydrographic Basin Committee, 2016). Using the classification made by the SAVI, reference mapping was drafted to associate the vegetation coverage with the anthropic activity, the respective potential environmental impacts arising from this interaction and their relationship with the desertification processes, as well as the ascertainment of the surface area occupied by each type and its percentage in relation to the total area of the basin in the municipality of Jeremoabo.

3. Results

Five representative subject types of the study area were identified and classified in accordance with the growing level of anthropization (Fig. 2), which are: Caatinga with Possible Crops, Caatinga Interspersed with Grasslands, Grasslands and Crops Interspersed by Caatinga, Agriculture and the Urban Area, which were dealt with as follows.

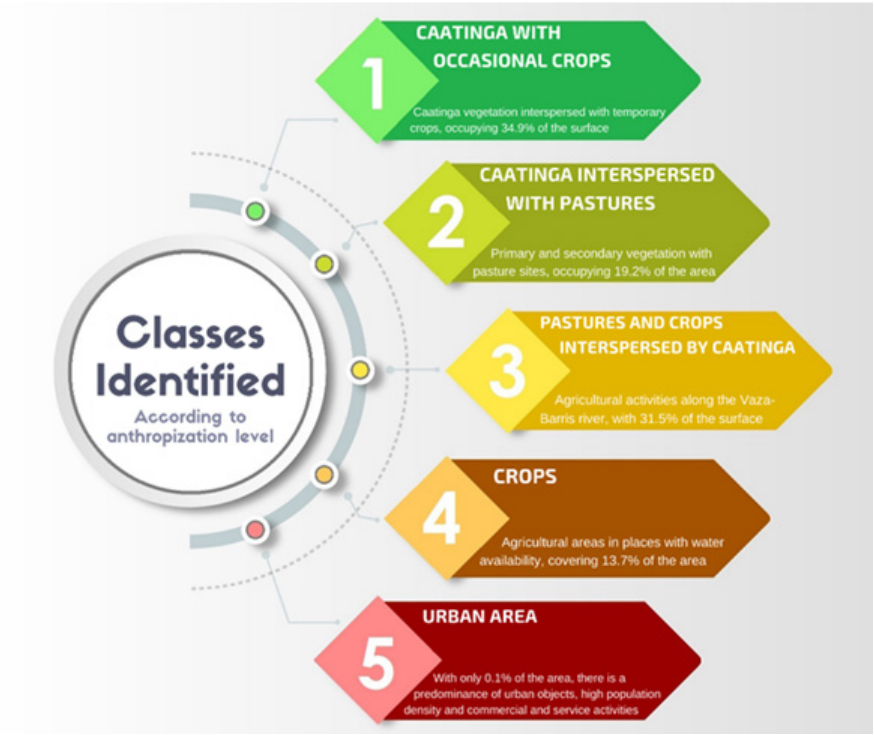

Figure 2. Subject types with a growing level of anthropization.

3.1 Caatinga with Possible Crops

The Caatinga with Possible Crops type corresponds to around 34.9% of the study area and covers around 1,364 km^2. It tends to be located in the central-northern and central-southern part of the municipality and boasts a larger concentration of vegetation coverage. It is located in higher altitude areas at between 550 and 766m (Grilo *et al.,* 2009). It is made up of Caatinga vegetation interspersed by seasonal crops such as beans, cassava, melon and corn (IBGE, 2019).

Taking into account the climate characteristics in Jeremoabo, a typical quality which is consistent with the dry areas during the 3 wet months per year can be observed, which rejuvenate the Caatinga and provide the temporary crops (Almeida, 2011). In the other 9 dry months there is a considerable drop in farming activity. The Caatinga provides species of different sizes like the *Commiphora leptophloeoes,* the *Bromelia antiacantha,* the *Schinopsis brasiliensis,* the *Pilocereus gounellei,* the *Mimosa hostilis,* the *Cereus jamacaru,* the *Cnidoscolus quercifolius,* amongst others, with it now being dense and open (Almeida, 2011), as shown in Figure 3.

Figure 3. Arboreal/shrub Caatinga. Source: Almeida (2011).

A large part of the areas of crops are monocultures that cause significant changes to the environment's fauna and flora and a reduction in the biodiversity, mainly due to the replacement of the original vegetation cover by non-autochthonous species (Rohila *et al.,* 2017; Killebrew and Wolff, 2010), as well as creating problems for the crop itself, as is the case with corn that has increased grain and cob rot which was burnt due to the practice (Trento *et al.,* 2002).

In accordance with the IBGE (2019), between 2004 and 2018 there was a dramatic fall in the production of seasonal crops, such as beans, which in 2004 equated to around 13,680 tonnes, and that by 2018 had fallen to just 51 tonnes. This substantial drop in production could be related to the process of desertification, bearing in mind that desertification and farming find themselves in a cycle: desertification causes damage to farming, making areas barren, and excess farming with unsuitable practices, such as the intensive use of irrigation, which results in soil compaction, increased erosion, decreased productivity and salinization, makes the soil less fertile, which in turn exacerbates the process of desertification (Dourado, 2017; Mirzabaec *et al.,* 2019).

3.2 Caatinga Interspersed by Grasslands

The Caatinga Interspersed by Grasslands occupies around 19.2% of the study area, spanning some 750 km^2 and mainly being found in the north-east of the municipality. This type is predominant at altitudes of between 195 and 550m (Grilo *et al.,* 2009), is only slightly entropized, and characterised by prickly, deciduous species with microfolia and floral diversity, encompassing plants with varied vertical structures (arboreal, grassy, herbal and shrubby) and varied densities of coverage, including primary and secondary vegetation where grazing takes place with loose cattle, often without any fencing, as shown in Figure 4 (Oliveira Junior, 2014).

Figure 4. The Caatinga and the area allocated for cattle grazing. Source: Oliveira Junior (2014) y Almeida (2011).

3.3 Grasslands and Crops Interspersed by Caatinga

The Grasslands and Crops Interspersed by Caatinga cover 31.5% of the area, occupying 1,230 km^2. This type can be found at altitudes of between 195 and 550m (Grilo, 2009), boasting land which is harvested using subsistence methods (where there is no mechanization and farming depends mainly on the occurrence of rain) and modern methods (exportation), and is occupied by the traditionally-handled livestock (Oliveira Junior, 2014), interspersed with farming mainly to the east of the municipality and the outskirts of the Vaza-Barris river, bearing in mind the need for the availability of water resources that support the farming and livestock activity and irrigation (Fig. 5).

Figure 5. Grasslands and crops along the Vaza-Barris river. Source: Almeida (2011).

The livestock is characterised by its extensive nature (Oliveira Junior, 2014), grazing and the use of vast areas for production, which usually takes places without heavy investment or the use of the latest technology that would enrich the grassland. Production has fallen as a result of this, and it has been affecting the livestock in the municipality throughout recent years. Goat farming, which in 2012 had a total count of 40,414, fell to 19,263 in 2018, which is a 52.3% drop in production (IBGE, 2019). More data from the IBGE (2019) shows that sheep farming also fell, with a total count of 41,476 in 2012 in comparison with 21,015 in 2018, representing a 49.3% drop.

Within this type, two areas with different features are noticeable (Fig. 6): one to the west, with an area where agricultural output is lower, superficial soil (New soils) and low annual rainfall rates (up to 600 mm), and another to the east, with higher annual rainfall rates (up to 700 mm), more developed soil (Latosols and Acrisols) and, as a result, an increased use of the soil for farming and livestock activity (Marques, 2009).

Figure 6. Contrast between the landscapes on the western side (on the left) and the eastern side (on the right). Source: Marques et al. *(2009).*

3.4 Agriculture

Agriculture corresponds to 13.7% of the total area, spanning 535 km^2. It is found at the lower altitudes in the municipality, varying between 195 and 403m (Grilo, 2009), and mainly found to the east and along the Vaza-Barris river, bearing in mind that these farming areas are located in places with more water availability and depend highly on irrigation (Almeida *et al.,* 2011). As a result, an increase in the demand for water (one of the most limiting factors of the region) could cause social, economic and environmental conflict in the event that there is less of it available, considering that it is an area susceptible to desertification (Brasil, 2005).

As per the IBGE (2019), the main permanent crops in the municipality are: bananas, coconuts, guavas and papaya. Like with seasonal crops, they also experienced a decline in production; for instance, the number of bananas produced in 2004 (2,100 tonnes) and 2018 (960 tonnes), with approximately a 54.2% fall.

3.5 Urban Area

The Urban Area type occupies just 0.1% of the total study area, covering around 4 km^2. There is an urban density of 4,359 people/km^2 with a population of 17,437 inhabitants (IBGE, 2018). It is located in the east where the town centre is found (Fig. 7). Figure 8 shows the spatial distribution of the different types of anthropization in the municipality.

Figure 7. Urban centre of the municipality of Jeremoabo. Source: Google Earth (2021).

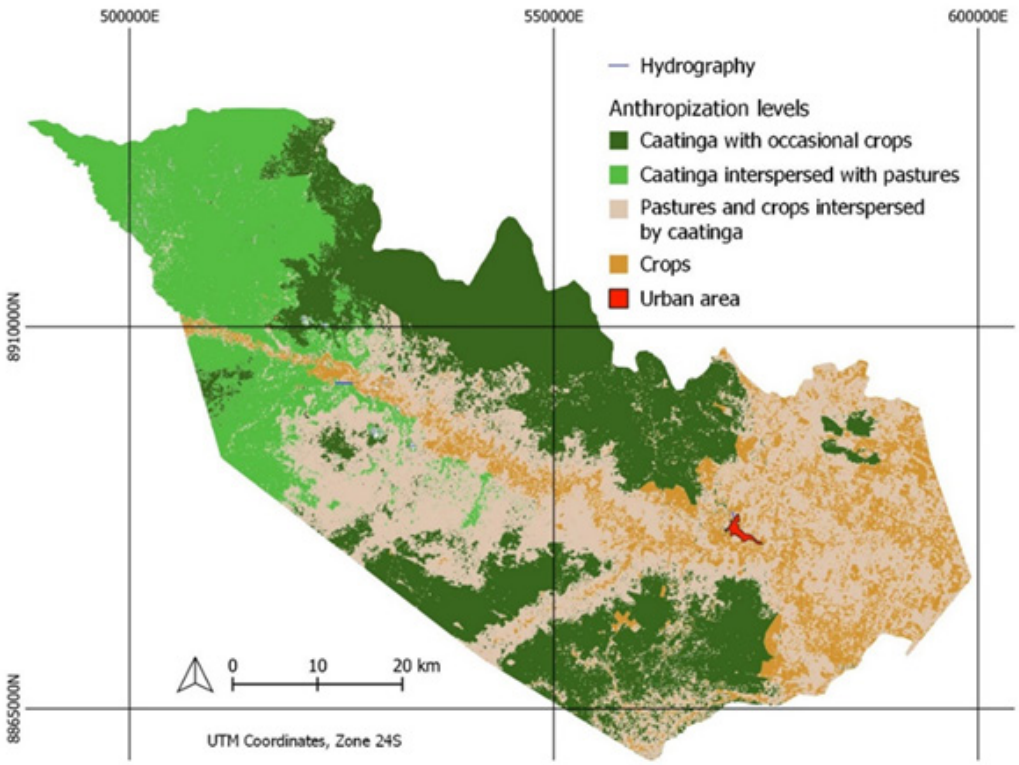

Figure 8. Spatialisation of the types of anthropization.

4. Discussion

The inappropriate treatment of the semiarid agricultural ecosystems is one of the main causes of deterioration in the studied area, where anthropic interference associated to the particular climate conditions causes negative impacts on the entire ecosystem, as well as significant rates of desertification (Rossi, 2020).

The majority of the species present in the Caatinga tend to regrow after being cut down. Meanwhile, burning the soil, which is one of the most aggressive preparation techniques, progressively decreases vegetation regrowth, where the rate of colonization by woody species is much slower, and with a much smaller population in areas cultivated over a long period than in newly opened areas within a mature forest, causing effects on the biomass that last for over 6 years (Sampaio *et al.,* 2005; Dourado, 2017). Furthermore, the use of fire destroys the humus layer and the microbial life, forming a crust under the soil through the deposit of particles and materials that are susceptible to pollution, which prevents water filtration (Sá *et al.,* 2010; Martín *et al.,* 2016). Continuous burning in one area also reduces the soil's humidity, limiting infiltration and the level of organic material, increasing the evapotranspiration and flooding (Oliveira and Montebello, 2014; Almeida *et al.,* 2011).

Around 80% of Caatinga's natural ecosystems have already been modified, which is mainly due to deforestation and burning. Recent research shows a 25.9% fall in wood, coal and firewood production in areas that are susceptible to desertification, displaying a serious lack of vegetation (Dourado, 2017; CGEE, 2016).

Of the types identified in this article, the area made up of grasslands and crops interspersed by the Caatinga appear to be the most susceptible to desertification, considering that there is more human intervention within this type, characterised by crops and inappropriate animal farming techniques, thus reducing the amount of native vegetation particularly in areas closest to the Vaza-Barris river (Grilo *et al.,* 2009). This activity involves alternate output between agriculture and livestock, something that has

been common since the 17th century, with land being used for ploughing and grazing with a seasonal dynamic due to the cyclicity of the rainfall and droughts, which are common for the municipality's type of climate (Oliveira Junior, 2014).

In most cases, the native vegetation was replaced with grassy pastures or short-cycle crops that have different sizes compared with the Caatinga's original vegetation, which makes the soil more exposed, causing a loss of fertility and leading to processes of erosion, resulting from surface rainfall, where recurrence reason the opening of gullies, which are mainly caused by torrential rain. Subsequently, there is the evolution of land and sand bank slides in river and streams (Sampaio *et al.,* 2005; Grilo *et al.,* 2009).

In a large part of the municipality, particularly in the areas closest to water courses, the *Prosopis Juliflora* can be observed; it is a perennial, drought-resistant plant that has a high wood and coal supply potential (Fig. 9), besides serving as food for cows and goats, but it is not native to the region (Almeida, 2011).

Figure 9. The expansion of the Prosopis juliflora through the municipality. Source: Almeida (2011).

However, competing for space, the *Prosopis Juliflora* prevent the native vegetation from evolving, as it consumes a large amount of water. The heavy presence of the *Prosopis Juliflora* reduces the soil's protection to erosive processes and increases the risk of fires due to an accumulation of biomass, which impacts the ecosystem and alters the local water regime, whilst also lowering the area's biodiversity, as it overshadows other species (Pegado *et al*., 2006). The chemical composition of its pods may cause dental and digestive problems for goats, sheep and cows, and may even be fatal when it is consumed in excess for extended periods of time (Aboud *et al.,* 2005).

In grassland areas, the main factor for desertification is the removal of the native vegetation (Nascimiento, 2013), leading to a reduction in organism diversity, which affects the self-regulation mechanisms present in natural ecosystems (Matches, 1992 in Bilotta *et al.,* 2007). The expansion of goat rearing makes it difficult for the vegetation which is typical of the Caatinga to evolve, consuming up to 70% of the existing species and having a negative impact on their growth (Dourado, 2017).

The large livestock infrastructure generates different environmental impacts that cause deterioration and is difficult to reverse (Oliveira Junior, 2014). Overgrazing causes excessive treading which significantly alters the structure of the superficial later of the soil, intensifying its aggregation and diminishing the vegetation coverage, which in turn bolsters the process of erosion and affects the replenishment of fresh water, reducing its infiltration into the water tables (Souza, 2010; Bilotta *et al.,* 2007; Mirzabaev *et al.,* 2019). Livestock production is responsible for a part of the greenhouse gas emissions into the atmosphere and is generally something which consumes a lot of water (Vera and Muñoz, 2017).

Other important issues are linked to the commercial planting of fruits and vegetables, which is responsible for the lack of availability and deterioration in water quality, considering that the consumption made by irrigated crops exceeds that of the native species. Removing water for irrigation leads to a decrease in river flow, thus modifying the rates of evotranspiration (Sá *et al.,* 2010; Bilotta *et al.,* 2005). In these irrigated areas, the use of the water with high salt levels (above 5g/l of chlorides), the inappropriate handling of the wetting cycles and the lack of drainage leads the soil to salinization (Castelletti *et al.,* 2003), as in Figure 10.

Figure 10. Development of saline crust as a result of irrigation. Source: Almeida (2011).

Added to this are the agrochemicals and heavy metals in the pesticides used during ploughing that reach the Vaza-Barris river by being intentionally dumped or due to superficial draining, causing risks to human and animal health, polluting the soil through the infiltration of the water which transports particles present in the pesticides (Almeida, 2011; Killebrew and Wolff, 2010; Rohila *et al.,* 2017).

Generally speaking, crops are lower in height that the typical shrubs in the Caatinga and have lower stomatic resistance, leading to an increase in the susceptibility to biotic and abiotic stress, and to modifications in the water, energy and coal balances on the surface (Cunha, *et al.,* 2013). Given the permanence of these crops without their nutrients being duly replenished, there is a loss of fertility in the soil as a result (Sampaio *et al.,* 2003).

Continuously harvesting the soil for extended periods of time, the removal of the vegetation and burning the soil cause changes to its physical properties, particularly to its porosity, causing temporary or permanent changes, such as the reduction in the organic material that lowers its fertility, with losses greater than 50% of themicrobial biomass (Pereira, 2013), accelerating the process of erosion, the evolution of gullies and ravines, which are common in areas that are susceptible to desertification (Narain and Kar, 2005; Almeida, 2011), as can be seen in Figure 11.

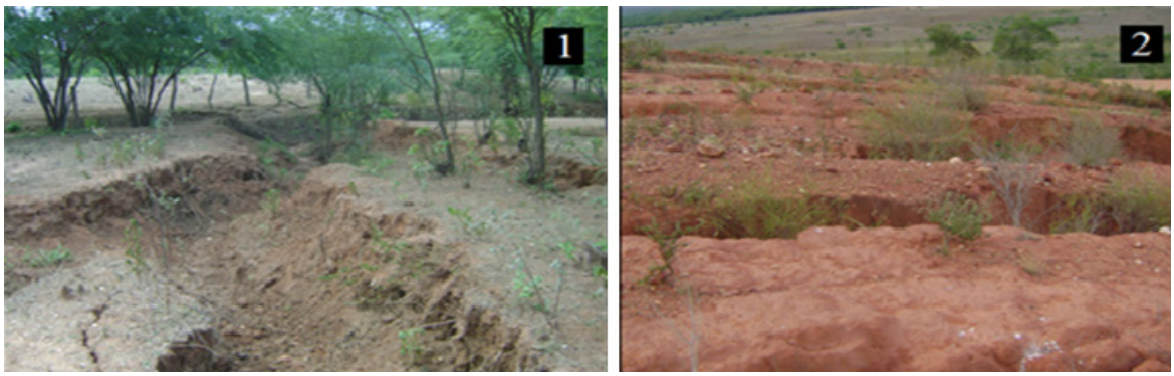

Figure 11: Processes of erosion in Jeremoabo: development of gullies (1) and exposed soil with gullies (2). Source: Almeida (2011).

Not adhering to the time required to restore the soil in farming practices gradually reduces its productivity and contributes to the onset of conditions that occur prior to desertification, which could be long-lasting or even irreversible (Brito, 2016). In some cases, they are a potential indicator of progression in the desertification process (Sampaio, 2005).

The reduction in the soil's productivity is just one consequence of desertification and causes problems for many sectors, mainly the agricultural sector, generating damage to production and crop failures, besides the high cost of recovering the soil and the plantations (Rossi, 2020; Dourado, 2017).

In Jeremoabo's case, the conversion of rural land into urban land, as well as being crude, is also characterised by pressures, interests and disputes, causing risk situations and socio-environmental vulnerabilities beyond the city limits and mainly affecting the conservation of the superficial water resources.

Of the main impact factors are the contamination caused by domestic effluents; the suppression of the vegetation coverage, which has a large effect on the conservation of the riverbanks; the paving of the streets, which reduces the potential for rainfall infiltration into the soil and all the other factors related to the increase in the speed of draining, the production of solid waste and sediment that are carried to the drains and change the natural features of the bodies of water, causing hydrological alterations (Silva *et al.,* 2016; Carpio and Fath, 2011; Ameen and Mourshed, 2017).

All these issues are linked to a lack of scientific knowledge and an inefficiency of technical means, as well as the ethical and social principles of the government and the local population, which are embodied by short-term policies with no comprehensive environmental or developmental view (Leff, 2002). In Brazil, it is the municipality's responsibility to regulate the occupation and use of the soil, as well as to establish territorial planning.

In the specific case inherent to the area of study, it is the municipal administration's responsibility to develop intervention capacity from interdisciplinary analyses and the activity of different sectors or levels of the public administration, as well as its standardisation with those representing private initiatives. Considering territorial planning are a process of organisation or an obvious condition ascribes it one or more goals that must be reached.

Of these goals, the protection and recovery of the Caatinga's environment are considered a key factor for maintaining the water resources, the soil and the economic activity concerning the processes of desertification. As a practical mechanism for enforcement, Brazilian legislation has a set of Natural Protected Area (NPA) categories (Brasil, 2000) which can be combined with local or mosaic systems in order to obtain more efficiency with regards protection and to better reconcile production activity with the principles of sustainability.

In addition, there is also the resource for Damper Areas (DA), which was introduced around the NPAs to establish different levels of restrictions regarding the occupation and use of the soil, with the aim of alleviating the environmental pressure on the protected areas and reducing the impacts on the environment (Machado *et al.,* 2020). Edmiston *et al.* (2017) suggests that the Damper Areas should work as areas peripheral to a protected area and as a way of integrating and familiarising people with the conservation and preservation goals and challenges of the different ecosystems.

The conservation of the current context of Jeremoabo's evolution, in the absence of territorial planning that would consider the environment as a space-organising agent and a basic condition for sustainability and economic development, tends to emphasise the causes that contribute to the increase in the processes related to desertification and the impoverishment of biological diversity. These issues will have a direct impact on the local human population, which could lead to an increase in social vulnerability (Vieira *et al.,* 2020).

5. Conclusion

Taking into account that the area of study is in a semiarid environment, linked to droughts and damaging human activity, the process of desertification ends up being the cause and the consequence of certain indicators, such as the reduction in ecological diversity, the growing depletion of the soil, the loss of water resources and the decline in productivity, which as a whole could lead to definitive desert-like conditions being established.

In this scenario, the use of geotechnology, particularly Remote Sensoring, is highly important for making diagnostics, facilitating data collection and analysis, especially in remote and environmentally vulnerable areas like Jeremoabo, thus offering the possibility of obtaining essential information for territorial planning.

Likewise, the classification of the use and coverage of the soil based on the different levels of anthropization made understanding the local productive system and its spatial layout possible, which was marked by the intensive and erroneous use of the soil for farming purposes that have a direct impact on the environment and are linked to the process of desertification.

Such practices, which are linked to the climate aspects that are typical of the area (high temperatures and rainfall concentrated into just 3 months of the year) break the dynamic balance of the environment, reducing the availability of water resources and favouring an increase in the process of desertification. This materialises with landscapes that show accelerated deterioration, displaying gullies, ravines, land with low levels of productivity and a high salinization of the soil. This process of erosion leads to the onset of irrecoverable areas or high recovery costs.

In relation to the classification made, the types Caatinga with Possible Crops and Caatinga Interspersed with Pastures are characterised by a lower concentration of anthropic activity, which is a result of unfavourable rainfall conditions, superficial soil and low water availability. The types Agriculture, Pastures and Crops Interspersed by Caatinga are characterised by the high level of human intervention, arising from conditions that are more suitable for the growth of animal husbandry activities, mainly to the east of the municipality and along the Vaza-Barris river, granting these types higher susceptibility to desertification as this phenomenon is directly linked to how the soil is occupied or used.

Hence, the social and environmental quality is threatened, taking into consideration that the main source of income for the municipality comes from animal husbandry activities and they depend on the weather conditions, the conservation of the soil and the water resources. In general, areas that are susceptible to desertification are characterised by low development, which shows the need for better geo-environmental conditions so as to foster improved management practices and the development of sustainable technologies.

Despite being in an area that is susceptible to desertification with an aridity rate lower than 0.20, agricultural soil potential being inadvisable and a high frequency of droughts, the area of study is not so severely affected by desertification when compared with other areas in north-west Brazil, as stated in a study carried out by the MMA in 2007, which identifies Ceará, Paraíba, Pernambuco, Rio Grande do Norte and Sergipe as being in an extreme state due to the process of desertification.

Given these circumstances, it is considered highly important that the local population is mobilised together with the public authorities in order to plan actions aimed at recovering the deteriorated areas, the creation and implementation of management programmes for water resources, environmental education and the promotion of improved agroecological exploitation techniques and the use of the municipality's natural resources. Together, measures to monitor and control deforestation and burning practices as a form of soil protection are essential, as are crop diversification and reduction of extensive agricultural areas. Other alternatives include the use of allelochemicals extracted from plants to combat pests in the plantations and the establishment of an irrigation plan with a control on the amount

of water used, as well as the adoption of a fertirrigation practice, which consists of the irrigation system applying water and fertiliser simultaneously.

References

Aboud, A.A., Kisoyan, P.K., Coppock, D.L., 2005. *Agro-Pastoralists' wrath for the Prosopis tree: The case of the IL Chamus of Baringo District, Kenya.* Research Brief 05-02-PARIMA. Global Livestock Collaborative Research Support Program. University of California at Davis. 3 pag.

Almeida, A.S., 2011. *Avaliação da Vulnerabilidade Ambiental à Perda de Solo no Município de Jeremoabo (Ba). Feira de Santana (BA).* Thesis (Modalagemen Ciências da Terra e do Ambiente) - Departmentof Natural Sciences, StateUniversityof Feira de Santana.

Almeida, A.S., Santos, R.L., Chaves, J.M., 2011. *Mapeamento de Uso e Ocupação do Solo no Município de Jeremoabo-Ba: Uso do Algoritmo Máxima Verossimilhança (Maxver).* Papers from the XV Brazilian Remote Sensoring Symposium - SBSR, Curitiba, PR, Brazil, 30th April to 5th May 2011, INPE, p. 7255.

Ameen, R.F.M., Mourshed, M., 2017. Urban environmental challenges in developing countries-A stakeholder perspective. *Habitat International* 64, 1-10. https://doi.org/10.1016/j.habitatint.2017.04.002

Bilotta, G.S., Brazier, R.E., Haygarth, P.M., 2007. The impacts of grazing animals on the quality of soils, vegetation, and surface waters in intensively managed grasslands. *Advances in Agronomy* 94, 237-280. https://doi.org/10.1016/S0065-2113(06)94006-1

Brasil, 2000. *Imposes the National System of Nature Conservation Units and provides other provisions.* Law no. 9985 of 18 July 2000.

Brasil, 2005. *The National Action Plan for Fighting Desertification and Mitigating the Effects of the Drought PAN-Brazil.* Ministry of the Environment - Secretariat for Water Resources, 242 pag.

Braz, A.M., Águas, T. de A., Garcia, P.H.M., 2015. Análise de índices de vegetação NDVI e SAVI e índice de área folear (IAF) para a comparação da cobertura vegetal na bacia hidrográfica do córrego do ribeirãozinho, município de Selvíria – MS. *Revista Percurso – NEMO* 7 (2), 5-22.

Brito, A.S. de., 2016. Análise ambiental e desertificação no pólo de Jeremoabo: explicação a partir da análise dos indicadores sociais de desenvolvimento. *XX Seminário de Iniciação Científica* 20. https://doi.org/10.13102/semic.v0i20.3134

Carpio, O.V., Fath, B.D., 2011. Assessing the environmental impacts of urban growth using land use/land cover, water quality and health indicators: A case study of Arequipa, Peru. *American Journal of Environmental Sciences* 7 (2), 90-101. https://doi.org/10.3844/ajessp.2011.90.101

Carvalho, M.E.S., 2010. *A questão hídrica na bacia sergipana do rio vaza Barris*. These (PhD in Geography), Federal University of Sergipe.

Castelletti, C.H.M., Cardoso da Silva, J.M., Tabarelli, M., Santos, A.M.M., 2003. Quanto ainda resta da caatinga? Uma estimativa preliminar. In: J.M.C. Silva *et al.* (Ed). *Biodiversidade da caatinga: áreas e ações prioritárias para a conservação*. Ministry of the Environment, Federal University of Pernambuco, Brasilia, pp. 91-100.

CGEE (Centre for Management and Strategic Studies), 2016. *Desertificação, degradação da terra e secas no Brasil*, Brasilia, 252 pag.

Cunha, A. P. M. do A., Alvala, R. C. dos S., Oliveira, G. S. de, 2013. Impactos das mudanças de cobertura vegetal nos processos de superfície na região semiárida do Brasil. *Revista Brasileira de Meterologia* 28 (2), 139-152.

Dourado, C. da S., 2017. *Áreas de risco de desertificação: cenários atuais e futuros frente às mudanças climáticas.* Doctoral thesis - State University of Campinas, Faculty of Agricultural Engineering. Campinas, SP.

Edmiston, J.T., Hyman, G., McNeely, J.A., Trzyna, T., 2017. Áreas protegidas urbanas: perfis e diretrizes para melhores práticas. *Best Practice Protected Area Guidelines Series* 22. IUCN Publication, 110 pag.

Gameiro S., Teixeira C.P.B., Silva Neto T.A.S., Lopes M.F.L., Duarte C.R., Souto M.V.S., Zimback C.R.L., 2016. Avaliação da cobertura vegetal por meio de índices de vegetação (NDVI, SAVI e IAF) na Sub-Bacia Hidrográfica do Baixo Jaguaribe, CE. *Terræ* 13 (1-2), 15-22.

Grilo, D.C., Franca-Rocha, W.J.S., Vale, R.M.C., 2009. Caracterização Geoambiental associada a processos de desertificação no município de Jeremoabo/Bahia. *Papers from the XIV Brazilian Remote Sensoring Symposium - SBSR*, Natal, Brazil, 25th-30th April 2009, INPE, pp. 5243-5249.

Huete, A.R., 1988. A soil-adjusted vegetation index (SAVI). *Remote Sensing of Environment* 25, 295-309. https://doi.org/10.1016/0034-4257(88)90106-X

IBGE (Brazilian Institute of Geography and Statistics). *Demographic Census.* Available at: http://www.ibge.gov.br/cidades. Accessed: 6th Dec 2019.

IBGE (Brazilian Institute of Geography and Statistics). *Cities.* Available at: http://www.ibge.gov.br/cidades. Accessed: 6th Dec 2019.

Killebrew, K., Wolff, H., 2010. *Environmental Impacts of Agricultural Technologies,* Working Papers UWEC-2011-01, University of Washington, Department of Economics.

Leff, E., 2002. *Epistemologia Ambiental*. Cortez, São Paulo.

Lima, D.R.M. de., Dlugosz, F.L., Iurk, M.C., Pesck, V.A., 2017. Uso de NDVI e SAVI para Caracterização da Cobertura da Terra e Análise Temporal em Imagens RapidEye. *Spacios* 38 (36), 7.

Machado, R.A.S; Lima, E.C. de; Oliveira, A.G. de, 2020. Evolução da cobertura e uso do solo na Zona de Amortecimento da Estação Ecológica Raso da Catarina entre 1985 e 2015 e sua relação com o processo de desertificação. *Brazilian Applied Science Review* 4 (5), 3107-3122. https://doi.org/10.34115/basrv4n5-028

Marques, L. de S., Mello, F.R., CHAVES, J.M., 2009. *Mapeamento de uso e cobertura do solo do município de Jeremoabo (Ba) por meio de sensoriamento remoto*. XIII SBGFA - Symposium of Applied Physical Geography Minas Gerais.

Martin, D., Tomida, M., Meacham, B., 2016. Environmental impact of fire. Fire Science Reviews 5. https://doi.org/10.1186/s40038-016-0014-1

Mirzabaev, A., Wu, J., Evans, J., Garcia-Oliva, F., Hussein, I.A.G., Iqbal, M.H., Kimutai, J., Knowles, T., Meza, F., Nedjroaoui, D., Tena, F., Türkeş, M., Vázquez, R.J., Weltz, M., 2019. Desertification. In: P. R. Shukla, J. Skeg, E. Calvo Buendia, V. Masson-Delmotte, H.-O. Pörtner, D. C. Roberts, P. Zhai, R. Slade, S. Connors, S. van Diemen, M. Ferrat, E. Haughey, S. Luz, M. Pathak, J. Petzold, J. Portugal Pereira, P. Vyas, E. Huntley, K. Kissick, M. Belkacemi & J. Malley (eds.). *Climate Change and Land: an IPCC special report on climate change, desertification, land degradation, sustainable land management, food security, and greenhouse gas fluxes in terrestrial ecosystems.* https://philpapers.org/rec/NGCD

Mouat, D., Thomas, S., Lancaster, J., 2019. Desertification and Impact on Sustainability of Human Systems. In: J. LaMoreaux (ed). *Environmental Geology. Encyclopedia of Sustainability Science and Technology Series*. Springer, New York, NY. https://doi.org/10.1007/978-1-4939-8787-0_268

Narain, P., Kar, A., 2005. *Desertification. Agriculture and Environment*. Publishers: Malhotra Publishing House, New Delhi, India.

Nascimento, F. R. do, 2013. *O fenômeno da desertificação*. Goiânia: Editora UFG.

Oliveira, A.P.N., Montebello, A.E.S., 2014. Aspectos Econômicos e Impactos Ambientais da Pecuária Bovina de Corte Brasileira. *Revista UNA* 9 (2), 1-20.

Oliveira Junior, I. de, 2014. *O processo de desertificação: a vulnerabilidade e degradação ambiental no Polo Regional de Jeremoabo*. Thesis (Dissertation in Geography). Federal University of Bahia, Salvador, Bahia.

Pegado, C.M.A., Anfrade, L.A., Félix, L.P., Pereira, I.M., 2006. Efeitos da invasão biológica de algaroba - Prosopisjuliflora (Sw.) DC. sobre a composição e a estrutura do estrato arbustivo-arbóreo da caatinga no Município de Monteiro, PB, Brasil. *Acta Botanica Brasilica* 20(4), 887-898.

Pereira, V. L., 2013. Impacto do desmatamento da Caatinga sobre a comunidade microbiana do solo. Universidade Federal de Pernambuco. https://repositorio.ufpe.br/handle/123456789/12672

Qi, J., Chehbouni, A., Huete, A.R., Kerr, Y. H., Sorooshian, S., 1994. A modified soil adjusted vegetation index. *Remote Sensing of Environment* 48, 119-126. https://doi.org/10.1016/0034-4257(94)90134-1

Rondeaux, G., Steven, M., Baret, F., 1996. Optimization of soil-adjusted vegetation indices. *Remote Sensing of Environment* 55, 95-107. https://doi.org/10.1016/0034-4257(95)00186-7

Rohila, A. K., Ansul, Maan, D., Kumar, A., Kumar, K., 2017. Impact of agricultural practices on environment. *Asian Jr. of Microbiol. Biotech. Env. Sc.* 19 (2), 145-148.

Rossi, R., 2020. *Desertification and agriculture*. EPRS–European Parliamentary Research Service.

Sá, I.B., Cunha, T.J.F., Teixeira, A.H.C., Angelotti, F., Drumond, M.A., 2010. Processos de desertificação no Semiárido Brasileiro. In I.B. Sá, P.C.G. da Silva (Eds). *Semiárido Brasileiro: pesquisa, desenvolvimento e inovação.* Embrapa Semiárido, Petrolina, pp. 125-158.

Salama, R., Otto, C., Fitzpatrick, R., 1999. Contributions of groundwater conditions to soil and water salinization. *Hydrogeology Journal* 7, 46-64. https://doi.org/10.1007/s100400050179

Sampaio, E.V.S.B, Araújo, M. dos S; Sampaio, Y.S.B., 2005. Impactos ambientais da agricultura no processo de desertificação no nordeste do Brasil. *Revista de Geografia*, 22, 1.

São Francisco River Hydrographic Basin Committee, 2016. *São Francisco River Hydrographic Basin Water Resources Plan 2016-2025*. Alagoas, 520 pag. (Volumes 1 and 2).

Silva, J.M.C., Tabarelli, M., Fonseca, M.T., Lins, L.V., 2004. *Biodiversidade da Caatinga: áreas e ações prioritárias para a conservação*. MMA/UFPE/ConservationInternational – Biodiversitas – Embrapa Semi-árido, Brasília (DF), 382 pag.

Silva, M.V.R., Chaves, J.M., de Vasoncelos, R.N., Duverger, S. G., Da Capes, B.D. M., 2015. Aplicação do índice de vegetação ajustado ao solo-SAVI para a identificação de fragmentos de caatinga em cultivos de Agave sisalana Perrine na região Semiárida do Brasil. A*nais XVII Simpósio Brasileiro de Sensoriamento Remoto- SBSR, João Pessoa-PB*, Brasil, INPE.

Silva, R.F., Santos, V.A., Galdino, S.M.G., 2016. Análise dos impactos ambientais da Urbanização sobre os recursos hídricos na sub-bacia do Córrego Vargem Grande em Montes Claros-MG. *Caderno de Geography* 26 (47), 966-976.

Souza, J., S., 2020. *O impacto ambiental atribuído à pecuária.* Post-Graduate Diploma in Animal Husbandry at the State University of Maringá, 2010. *Revista CRMV- PR.* Ed. 30.

Souza, R. B. de., 2010. *Sensoriamento Remoto: conceitos fundamentais e plataformas.* South Regional Centre for Space Research - CRS. National Institute of Space Research - INPE. IV CEOS WGE du Workshop, Santa Maria, RS, Brazil.

Trento, S.M., Irgang, H., Reis, E.M., 2002. Efeito de rotação de culturas, de monocultura e de densidade de plantas na incidência de grãos ardidos em milho. *Fitopatologia Brasileira* 27, 609-613.

USGS (U.S. Geological Survey), 2007. *Investigating the Environmental Effects of Agriculture Practices on Natural Resources*: *Scientific Contributions of the U.S. Geological Survey to Enhance the Management of Agricultural Landscapes.* Fact Sheet 2007-3001, Geological Survey (U.S.). https://doi.org/10.3133/fs20073001

Veloso, H.P., Rangel-Filho, A.L.R., Lima, J.C.A., 1991. *Classificação da vegetação brasileira, adaptada a um sistema universal.* Departamento de Recursos Naturais e estudios Ambientais. Ministerio da Economia, Fazenda e Planejamiento, IGBE, Rio de Janeiro, 124 pag.

Vera, L., Muñoz, E., 2017. Environmental Impact of Livestock Production. *Agricultural Research &Techology: Open Access J.* 8(4), 555745. https://doi.org/10.19080/ARTOAJ.2017.08.555745

Vieira, R. M. da S. P., Feitosa F. da F., Rosemback, R., Sestini, M.F., Cunha, A.P.M. do A., Alvala, R.C. dos S., 2013. Influência das mudanças de uso da terra e da degradação do solo na dinâmica populacional do núcleo de desertificação de Gilbués (PI). *Papers from the XVI Brazilian Remote Sensoring Symposium - SBSR*, Foz do Iguaçu, PR, INPE.

Vieira, R. M. da S. P., Sestini, M.F., Tomasella, J., Marchezini, V., Pereira, G.R., Barbosa, A.A., Santos, F.C., Rodriguez, D.A., Rodrigues do Nascimento, F., Santana, M.O., Campello, F.C.B., Ometto, J.P.H.B., 2020. Characterizing spatio-temporal patterns of social vulnerability to droughts, degradation and desertification in the Brazilian northeast. *Environmental and Sustainability Indicators* 5, 100016. https://doi.org/10.1016/j.indic.2019.100016

Washington-Allen, R.A., West, N.E., Ramsey, R.D., 2003. Remote sensing-based dynamical systems analysis of sagebrush steppe vegetation in rangelands. In: N. Allsopp, A.R. Palmer, S.J. Milton, K.P. Kirkman, G.I.H. Kerley, C.R. Hurt, C.J. Brown N. (Eds). *Proceedings of the 7th International Rangelands Congress*, Durban, South Africa, pp. 416-418.

Wijitkosum, S., 2016. The impact of land use and spatial changes on desertification risk in degraded areas in Thailand. *Sustainable Environment Research* 26 (2). https://doi.org/10.1016/j.serj.2015.11.004.

Cuadernos de Investigación Geográfica *Geographical Research Letters*	2022	Nº 48	pp. 59-78	EISSN 1697-9540

http://doi.org/10.18172/cig.5098

IDENTIFICATION OF DESERTIFIED AND PRESERVED AREAS IN A CONSERVATION UNIT IN THE STATE OF PARAÍBA - BRAZIL

LEANDRO F. DA SILVA[1], BARTOLOMEU I. SOUZA[1], RAFAEL CÁMARA ARTIGAS[2]*

[1]Dept. Geography, University of Paraíba, Brazil.

[2]Dept. Physical Geography and Regional Geographic Analysis, University of Seville, Spain.

ABSTRACT. The objective of this study is to identify and analyse the main characteristics of areas potentially degraded by desertification and of preserved areas using the Soil Surface Moisture Index (SSMI), alongside the Land Surface Temperature (LST) and Normalized Difference Vegetation Index (NDVI). The study is based on a set of points obtained in the field and from the RGB false colour image for the Environmental Protection Areas (EPA) of the Cariri, in the semi-arid region of Paraíba, using a space-time cross-section covering both rainy and dry periods. The results showed that at all points in Desertified Areas, the main characteristics were a low SSMI, high LST and low NDVI in both periods. The Preserved Areas, on the other hand, presented a high SSMI, moderate LST and high NDVI in the rainy period, with the same characteristics repeated in the dry period for SSMI and NDVI, but with a low LST. Timely identification of these characteristics, both in areas degraded by desertification and in better preserved areas, can provide useful information for future decisions relating to the physical and territorial management of the Conservation Unit.

Identificación de áreas desertificadas y preservadas en una unidad de conservación en el Estado de Paraíba - Brasil

RESUMEN. El objetivo de este estudio fue identificar y analizar las principales características de áreas potencialmente degradadas por desertificación y de áreas preservadas. Para ello se utilizaron el Índice de Humedad Superficial del Suelo (IHSS), junto con la Temperatura de la Superficie de la Tierra (TS) y el Índice de Vegetación de Diferencia Normalizada (IVDN). El estudio está basado en un conjunto de puntos obtenidos en el campo y en la composición de la imagen de falso color RGB para el Área de Protección Ambiental (APA) del Carirí, en la región semiárida de Paraíba, utilizando un corte espacio-temporal que abarca la estación lluviosa y seca. Los resultados mostraron que en todos los puntos de las Áreas Desertificadas las principales características fueron el IHSS bajo, TS alto y IVDN bajo en ambos períodos. Las Áreas Preservadas, por su parte, presentaron IHSS alto, TS moderado e IVDN alto en la época de lluvias, con las mismas características repetidas en el periodo seco para IHSS y IVDN, pero con TS bajo. La identificación puntual de estas características, tanto en áreas degradadas por desertificación como en las más conservadas, puede aportar información útil para la toma de decisiones futuras relacionadas con la gestión territorial y física de la Unidad de Conservación.

Key words: Desertification, Carirí EPA, SSMI.

Palabras clave: Desertificación, APA del Carirí, IHSS.

Received: 4 Mayo 2021

Accepted: 6 October 2021

*Corresponding author: Rafael Cámara Artigas. Dept. Physical Geography and Regional Geographic Analysis, University of Seville, Spain. E-mail address: rcamara@us.es

1. Introduction

Brazil has the second highest proportion of dry forests degraded by human activity of all the countries in the Americas (Portillo-Quintero and Sánchez-Azofeifa, 2010). Among Brazil's different ecosystems, the Caatinga, which is the dominant biome in the Brazilian Northeast, is one of the most threatened and disrupted. The main threats to this ecosystem are the illegal extraction of wood for energy and for producing fences, as well as the expansion of farming, which has created large areas of desertified land (Castelletti *et al.,* 2003) and has even affected the Conservation Units (CU) created by the state.

These CUs are defined by the Brazilian Ministry of the Environment (MMA) as territorial units with noteworthy natural characteristics, which serve to ensure the representation of important, ecologically viable samples of the different populations, habitats and ecosystems present in the country and to preserve the existing biological heritage (MMAUC, 2020).

These areas allow traditional, sustainable, rational use of natural resources to continue, with special rules and regulations in place for local communities to engage in sustainable economic activity. They are created in law by the federal, state and municipal governments after technical studies are carried out on the areas of land in question and local people consulted where necessary (MMAUC, 2020).

CUs in Brazil are divided into two main categories: 1) Fully Protected and 2) Sustainable Use. The latter includes the country's Environmental Protection Areas or EPAs (MMAUC, 2020), where people can make direct use of natural resources, albeit in a carefully controlled manner.

Desertification is defined by the United Nations (UN) as the reduction or destruction of biological potential, starting with alterations to natural vegetation by human intervention in arid, semi-arid and dry sub-humid regions. These processes are exacerbated by climatic fluctuations (MMA, 2020).

In 1994, the UN oversaw the drafting of a global plan to tackle desertification and the effects of drought by adopting effective measures at all levels, based on cooperation agreements and international collaboration (MTERD, 2020). Nevertheless, many of the countries affected by the issue, including Brazil, have been slow to take action and their measures have had little practical impact.

According to data from the National Semi-Arid Institute (INSA, 2015)) in Brazil, the area of the country susceptible to desertification covers 1,340,863km² and includes 1,488 municipalities in nine states in the semi-arid region in the Brazilian Northeast. The main hotspots for desertification in Brazil's semi-arid region are: Seridó in the states of Rio Grande do Norte and Paraíba; Cariris Velhos in Paraíba; Inhamuns in Ceará; Gilbués in Piauí; Sertão Central in Pernambuco; and Sertão do São Francisco in Bahía. These areas are the product of inadequate or non-existent measures to mitigate the interaction between productive activity and the natural resources available in an ecologically fragile environment (INSA, 2015). However, there is still a lack of knowledge of these degrading processes and their extent, and constant updates of this knowledge are required (INSA, 2015).

A significant proportion of the damage to natural resources, especially plant cover, is the result of people in regions at risk of desertification seeking to provide for their basic needs. Other causes

include commercial agriculture and excessive demand for raw materials for industrial use (Zhou *et al.,* 2015; Bezerra *et al.,* 2020).

The impacts of this overexploitation can be seen in escalating soil erosion, especially sheet erosion, and in processes of salinisation in both irrigated agricultural land and non-irrigated land (MMA, 2020).

In desertified areas, vegetation is sparse with many dwarf plants and low levels of diversity (MMA, 2020). Therefore, desertification has a severe social and economic impact and is considered to be one of the most significant environmental issues facing the world at this time (Nascimento, 2015; Bezerra *et al.,* 2020).

In the Cariris Velhos region, Paraíba, Brazil, the desertification process is very acute and is related primarily to i) geoecological predisposition or the unstable balance resulting from climatic, edaphic and topographic factors; and ii) different types of direct or indirect human activity, which begin with the removal or degradation of plant cover (Sobrinho, 1982; MMA, 2020).

Given these characteristics, a wide range of studies have sought to address the issue in this region specifically (Souza *et al.,* 2009; Souza *et al.,* 2015a; Lemos *et al.,* 2020). As this type of degradation progresses, it is increasingly important to understand the causes in order to develop alternative measures and solutions to mitigate the problem and attempt to slow its advance.

With this in mind, current technologies can make a significant contribution to studies of desertification and have already been used in research on the issue from a wide variety of disciplines (Sousa *et al.,* 2012; Vieira *et al.,* 2020).

In recent years, the number of methods drawing on computational techniques to identify and situate environmental phenomena has also increased, using tools such as remote sensing and geotechnologies applied specifically to arid and semi-arid environments around the world.

These methods are based on bio-geophysical parameters obtained via a series of freely available sensors, such as MODIS (Moderate-resolution Imaging Spectroradiometer) on the Terra and Aqua satellites, and TM (Thematic Mapper) and OLI (Operational Land Imager) on the Landsat satellites, which are mostly used to analyse parameters such as land surface temperature (Sousa *et al.,* 2015b; Santos *et al.,* 2020) and different vegetation indices, including the traditional NDVI - Normalized Difference Vegetation Index and the SAVI - Soil-Adjusted Vegetation Index (Aquino *et al.,* 2012; Silva Filho *et al.,* 2020).

Other techniques and methodologies have been used to perform important tasks such as quantifying and situating the influence of moisture on the soil. Some of these allow the surface retention capacity, infiltration, evaporation, influence on vegetation and desertification to be estimated, as in studies conducted by Lopes *et al.* (2011), Francisco *et al. (*2017) and Inocêncio *et al.* (2020), based on the interactions between the different indices and bio-geophysical parameters obtained via remote sensing.

Against this backdrop, this study aimed to identify and analyse the main characteristics of areas potentially degraded by desertification and preserved areas in a Conservation Unit (CU) for sustainable use, located in the semi-arid region of Paraíba, Brazil, using the Soil Surface Moisture Index (SSMI) proposed by Lopes *et al. (*2011), the land surface temperature (LST) and the Normalised Difference Vegetation Index (NDVI).

2. Methodology

2.1. Study area

The Cariri EPA is situated between the municipalities of Boa Vista, Cabaceiras and São João do Carirí, between the latitudes 07º20’00” and 7º25’00” S and the longitudes 36º25’00” and 36º15’00” O, as shown in Figure 1.

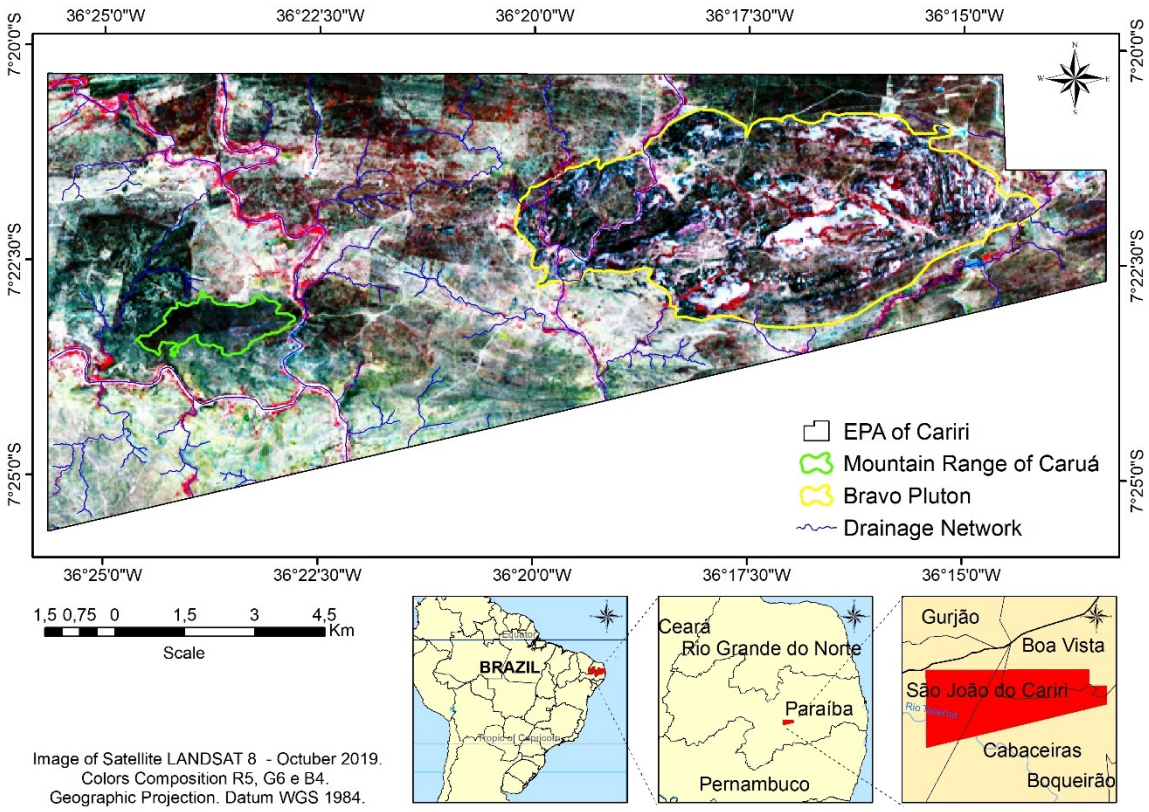

Figure 1. Map showing the location of the Cariri EPA and the areas with the most extensive plant cover in this CU.

The Cariri EPA is located in the micro-region of Cariris Velhos in the state of Paraíba, Northeast Brazil. This CU for sustainable use was created by the Secretariat of Environment in the State of Paraíba under State Decree 25083 of 8 June 2004 and covers an area of approximately 156 km².

The predominant vegetation in the region is Caatinga, which comprises a variety of physiognomies ranging from tree and shrub formations dominated by xerophilous deciduous species, as well as cacti and bromeliads (Ballén *et al.,* 2016; Souza and Souza, 2016; Lima *et al.,* 2017). Some sectors are characterised by differentiated vegetation, comprising species from humid and sub-humid areas of other Brazilian biomes. These are referred to here as Exceptional Areas and their soils and topography result in locally higher water levels, differentiating them from surrounding areas. This can be seen on varying scales across the interior of Northeast Brazil (Melo, 1988; Mello Neto *et al.,* 1985).

The climate in the region is classified by Koppen (1931) as semi-arid (BSh) or dry semi-arid, with low rainfall averaging between 400 mm and 500 mm a year (AESA, 2020a) and an average annual temperature ranging from 25 to 27°C, making this the driest region in Brazil (Souza *et al.,* 2009; Silva *et al.,* 2019a).

The main soil types found in the region are Regolith Neosol, Litholic Neosol and Chromic Luvisol, as well as Fluvic Neosol on floodplains (Ballén *et al.,* 2016; Silva *et al.,* 2019a).

From a geological perspective, the region is made up of granite rock with large rocky outcrops commonly known as *lajedos* (Lages *et al.,* 2013); one of the most prominent outcrops in this area is the Bravo Pluton, an ellipsoidal stock formed by granitic orthogneisses with a high metamorphic content (Romano *et al.,* 2018). Its surface is ellipsoidal, measuring almost 12 km long and 5 km wide (Sousa and Xavier, 2017), emerging in the centre-east of Paraíba between the municipalities of Cabaceiras and Boa Vista (Romano *et al.,* 2018).

In this CU, the most common landforms have a convex, tabular topography. The highest topographies are linked to the large rocky outcrops in the Bravo Pluton region to the West (W), with small mountain groups to the East (E) such as the Caruá Mountains, where elevations exceed 600m (Fig. 2).

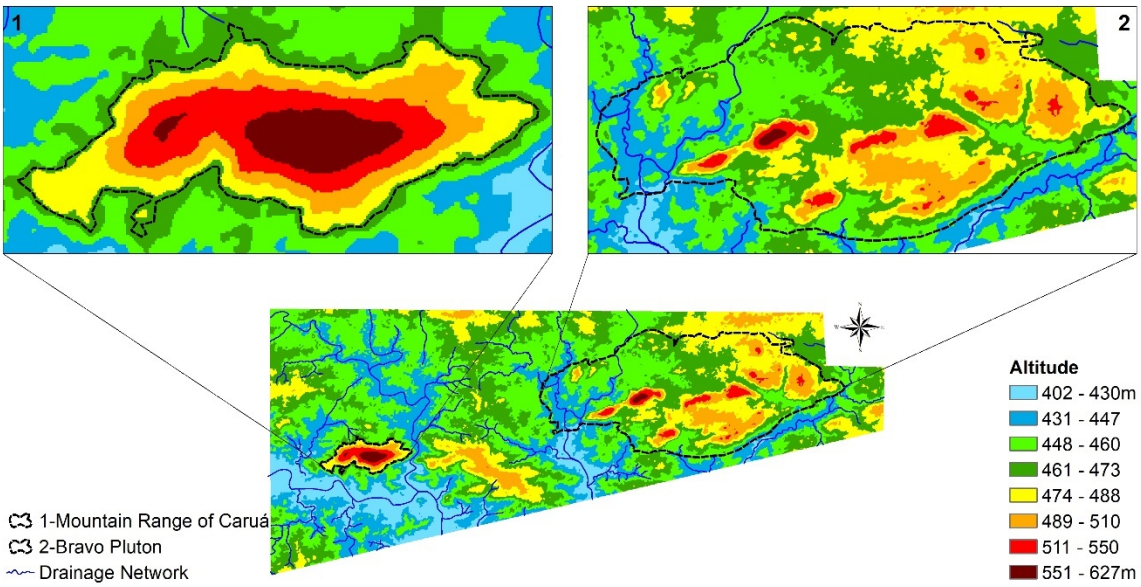

Figure 2. Map of Altitude.

2.2. Methodological procedures

The images used were produced by the Landsat 8 – OLI satellite in April (rainy period) and October (dry period) 2019 and geometrically corrected at the Q1 level (l1T) to all multispectral bands, including band 10 in the thermal infrared region, the TIR (thermal infrared sensor), orbit 215 point 065, freely available from the United States Geological Survey via USGS Earth Explorer.

The multispectral images then underwent radiometric correction and were loaded one by one into the ENVI 5.3 software in MTL format. Using the Radiometric Calibration tool, the correction algorithm was applied simultaneously to all bands. Once they had all been radiometrically corrected, the bands underwent atmospheric correction using the FLAASH Atmospheric Correction tool, which employs one of the most advanced algorithms for this type of correction: Moderate Resolution Atmospheric Transmission or MODTRAN. Using the same tool, a series of parameters were set: the type of sensor was set to OLI, the Tropical category was defined for the atmospheric model, the Rural category was set for the aerosol model, 2-band (K-T) was set for aerosol retrieval and 40km for the initial visibility.

The next step was to normalise the corrected atmospheric images, automatically balancing the levels of each pixel by applying a Gaussian function using the Band Math tool in ENVI 5.3.

2.2.1. Land Surface temperature (LST)

To obtain the land surface temperature (LST), thermal infrared band 10 (B10) from the TIRS sensor with a spectral range of 10.6 -11.19 µm was used for both months, with three key steps required:

I. conversion of the grey levels of the thermal band into spectral radiance, via the following equation (eq. 1):

$$L_\lambda = \left(\frac{L\max_\lambda - Lmin_\lambda}{Q_{\text{cal max}} - Q_{\text{cal min}}}\right) * (Q_{cal} - Q_{\text{cal min}}) + L_{min\lambda} \quad \text{eq. 1}$$

Where: L_λ= spectral radiance (W/m²M.¹·µm¹); Q_{cal}= quantified pixel value and digital level calibration (DN); Q_{calmin} = minimum value of pixel levels (DN = 1); Q_{calmax}= maximum value of pixel levels (DN = 255); $L_{min\lambda}$= minimum spectral radiance (1.238 W/ m² sr¹ µm¹); $L_{max\lambda}$= maximum spectral radiance (15.303 W/ m² sr¹ µm¹).

II. conversion of radiance values into temperature, represented in degrees Kelvin (K), via the following equation (eq. 2):

$$\text{LST} = \frac{K_2}{ln\,(K_1/L_\lambda + 1)} \quad \text{eq. 2}$$

Where: LST= land surface temperature; ln= constant of the equation; L_λ= spectral radiance (result of eq.1); K_1= calibration constant 1 (607.76 W/ m² sr¹ µm¹); K_2= calibration constant 2 (1260.56 W/ m² sr¹ µm¹).

The calibration constants (K_1 and K_2) used were obtained from the metadata (MTL) file in the information package for the bands provided when downloading images from the USGS website.

III. conversion of the ST in degrees Kelvin (K) to degrees Celsius (C), via the following expression (exp.1):

$$ST_{\circ C} = ST_K - 273.15 \quad \text{exp. 1}$$

Where: $ST_{\circ C}$= surface temperature in Celsius; ST_K= surface temperature in Kelvin (result of equation 2); 273.15= temperature equivalent to 0° degrees Celsius.

The following tools were used for these three steps: ArcToolbox – Spatial Analyst Tools – Map Algebra – Raster Calculator in ArcGIS 10.3.

2.2.2. Normalised Difference Vegetation Index (NDVI)

The Normalised Difference Vegetation Index (NDVI) was proposed by Rouse *et al. (*1973) and is obtained via the equation (eq. 3.):

$$NDVI = \frac{\rho_{NIR} - \rho_{RED}}{\rho_{NIR} + \rho_{RED}} \quad \text{eq. 3}$$

Where: ρNIR= near-infrared reflectance; ρRED= red reflectance

The values vary from -1, which indicates an absence of vegetation, to 1, which shows maximum vegetation. This process used the red (B4) and near-infrared (B5) bands corrected for two months. ArcGis 10.3 software was then used and equation 3 applied via the following tools: ArcToolbox - Spatial Analyst Tools - Map Algebra - Raster Calculator.

2.2.3. Soil Surface Moisture Index (SSMI)

The Soil Surface Moisture Index (SSMI) was initially suggested by Zhan *et al. (*2004) and adjusted by Wang *et al. (*2010) for semi-arid regions in China. It was subsequently adapted by Lopes *et al. (*2011) for the semi-arid region in Brazil. The index considers biophysical and geophysical parameters from remote sensing, like the LST and NDVI, and consists of three steps:

I. application of the SSMI calculation to the LST values obtained (Zhan *et al.,* 2004; Lopes *et al.,* 2011), via equation 4 (eq. 4):

$$SSMI_{LST} = \frac{LST_{max} - LST}{LST_{max} - LST_{min}} \quad \text{eq. 4}$$

Where: $SSMI_{LST}$= moisture index calculated directly from LST; LST= land surface temperature; LST_{min}= minimum ST value; LST_{max}= maximum ST value.

II. application of the SSMI calculation adjusted to NDVI (Wang *et al.,* 2010; Lopes *et al.,* 2011) via equation 5 (eq. 5):

$$SSMI_{NDVI} = 1 - \left(\frac{NDVI_{max} - NDVI}{NDVI_{max} - NDVI_{min}}\right) \quad \text{eq. 5}$$

Where: $SSMI_{NDVI}$= moisture index calculated directly from NDVI; NDVI= normalised difference vegetation index; $NDVI_{min}$= minimum NDVI value; $NDVI_{max}$= maximum NDVI value.

Constant 1 relates to the reversal of values as the higher the NDVI value, the higher the soil surface moisture level (Wang *et al.,* 2010; Lopes *et al.,* 2011).

III. The last calculation is then applied to obtain the final SSMI (Lopes *et al.,* 2011), using the average SSMI generated from the relationship between the $SSMI_{LST}$ and the $SSMI_{NDVI}$, via equation 6 (eq. 6):

$$SSMI = \frac{SSMI_{LST} + SSMI_{NDVI}}{2} \quad \text{eq. 6}$$

Where: SSMI= soil surface moisture index; $SSMI_{LST}$= moisture index calculated directly from LST; $SSMI_{NDVI}$= moisture index calculated directly from NDVI.

The final SSMI displays values ranging from 0 for drier surfaces to 1 for damper surfaces (Zhan *et al.,* 2004; Wang *et al.,* 2010; Lopes *et al.,* 2011).

All calculations for this step were carried out using ArcGis 10.3 and the tools ArcToolbox - Spatial Analyst Tools - Map Algebra - Raster Calculator.

2.2.4. Fieldwork and analysis

The fieldwork was carried out using a GNSS receiver at the collection points. The landscape at each collection point was also described, with particular reference to the use and occupation of the land over time. Images were recorded using a camera. Fieldwork was carried out in May and June 2018 (rainy period) and November 2019 (dry period), covering a large proportion of the Cariri EPA.

Back in the office, the points collected in the field with coordinates from the UTM map used for reference were converted individually to Shapefile format before being separated into two categories for analysis: 1) Desertified areas and 2) Preserved areas.

Eleven real points (RP) were obtained for Desertified Areas, which were made up of open shrubby Caatinga at different stages of degradation, and fourteen points were obtained for Preserved Areas, comprising closed shrubby arboreal Caatinga and areas of differentiated vegetation referred to here as Exceptional Areas.

The field information relating to the points in the Desertified Areas was classified according to the intensity of desertification following the system proposed by Conti (2007) and organised by Araújo and Lima (2019), as shown in Table 1.

The 11 points obtained in the field fell into two desertification categories—slight and moderate—as shown in Table 1. Therefore, the term Desertified Areas was used for all points with these characteristics in this study.

Table 1. Intensity of desertification.

Classification	Characteristics
Slight	Minor deterioration of plant cover and soil.
Moderate	Significant deterioration of plant cover and appearance of sand nodules. Evidence of salinisation of soils and formation of gullies and holes.
Severe	Significant expansion of areas prone to gullies and appearance of sand. Expansion of wind erosion. Increase in ruts and holes in the soil.
Very severe	Almost complete disappearance of biomass. Sealing and intense salinisation of soils.

Source: Conti (2007); Araújo and Lima (2019b).

To increase and equalise the number of points to be analysed for each category and ensure greater representation of the areas which were not monitored during fieldwork in particular, the points obtained from the false colour images were added between bands B4, R6 and G5 for each period, according to the characteristics of the real points (Table 2).

Table 2. Characteristics of the real points (RP) in the false colour images B4, R6 and G5.

Real Points	Colour				Texture	Shape
Period	Rainy		Dry		Rainy/Dry	Rainy/Dry
Desertified Areas	White, Light Green and Cyan	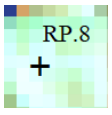	White, Brown and Cyan		Smooth, not very rough	Regular and Irregular
Preserved Areas	**Colour**				**Texture**	**Shape**
Period	Rainy		Dry		Rainy/Dry	Rainy/Dry
Shrubby arboreal Caatinga	Red and Black		Dark Green and Black		Smooth, not very rough	Irregular
Exceptional Areas	Red		Dark Red		Smooth, not very rough	Rectangular, Thin and Irregular

Source: Compiled by the authors using data from the Landsat 8 OLI satellite - bands B4, R6 and G5 – USGS Explorer 2019.

The points obtained from the images, based on the characteristics of the real points, were labelled IP, taking into account aspects such as the colour, texture and shape of both categories. In this way, 15 points were obtained for Desertified Areas (IP.11-IP.25) and 11 points for Preserved Areas (IP.40-IP.50), which were added to the real points (RP) to produce a total of 50 points (Table 3) for analysis.

Table 3. Final points.

Desertified Areas	Preserved Areas
RP.1 – RP.10	RP.26 – RP.39
IP.11 – IP.25	IP.40 – IP.50

3. Results and discussion

3.1. Land Surface Temperature (LST) and Normalised Difference Vegetation Index (NDVI)

The first results obtained were the LST and NDVI values, which were calculated and then described for the entire Cariri EPA during the two periods analysed (rainy and dry), as shown in Figure 3.

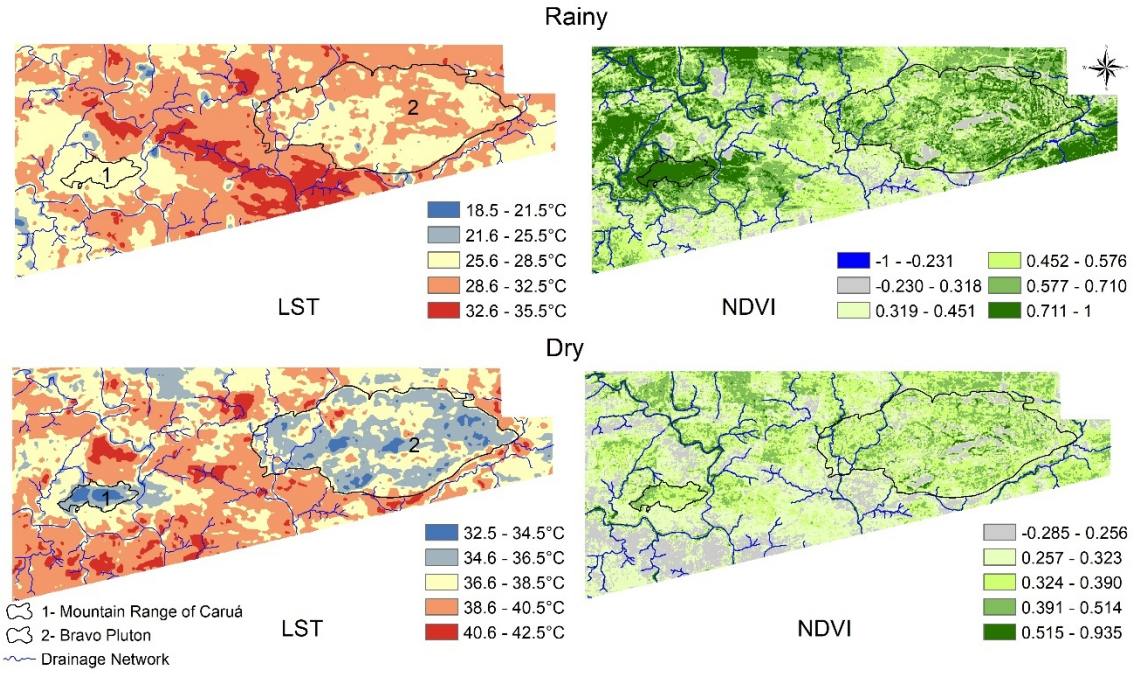

Figure 3. LST and NDVI values.

The LST value calculated for the whole EPA for the month of April (rainy period) varied between 18.5°C and 35.5°C. The NDVI displayed values of -1, relating to water bodies, and 1, indicating the maximum biomass. High levels of water bodies and biomass can be found at this time of year across most of the Cariris Velhos, as February and March are the months of greatest rainfall in the region, with precipitation events extending into July (Medeiros *et al.,* 2015; Silva *et al.,* 2018; Sena *et al.,* 2019).

The rains directly influence the vigour of plant growth, as most of the plants in the Caatinga are deciduous and display rapid leaf renewal during the rainy period (Amorim *et al.,* 2009) due to the availability of more water.

It is important to note that the rains in the Cariri region of Paraíba are not homogeneous and display spatial variability, as well as differences in the volume and time of rainfall (Souza *et al.,* 2009), with a direct impact on the dynamics of the plant cover.

Meanwhile, in October (dry period), the minimum LST value was 32.5°C and the maximum was 42.5°C. The NDVI varied from -0.285, representing areas of exposed soil, to 0.935, the peak biomass recorded, which is most apparent in the few perennial plants growing in the study area. These species are found in more preserved areas such as the Exceptional Areas in the Bravo Pluton and the closed shrubby arboreal Caatinga in the Caruá Mountains, as we will see later.

In the two months prior to October, rainfall tends to decline; August is viewed as a transitional month marking the end of the rainy period, while September has very low or no rainfall in some places. October and November are the driest months of the year (Medeiros *et al.,* 2015; Silva *et al,* 2018; Sena *et al.,* 2019). This can be seen in the rainfall data for 2019, which was obtained from 8 weather stations run by the Executive Agency for Water Management (AESA) of the State of Paraíba (AESA, 2020b) and scattered across the area surrounding the Cariri EPA (Fig. 4).

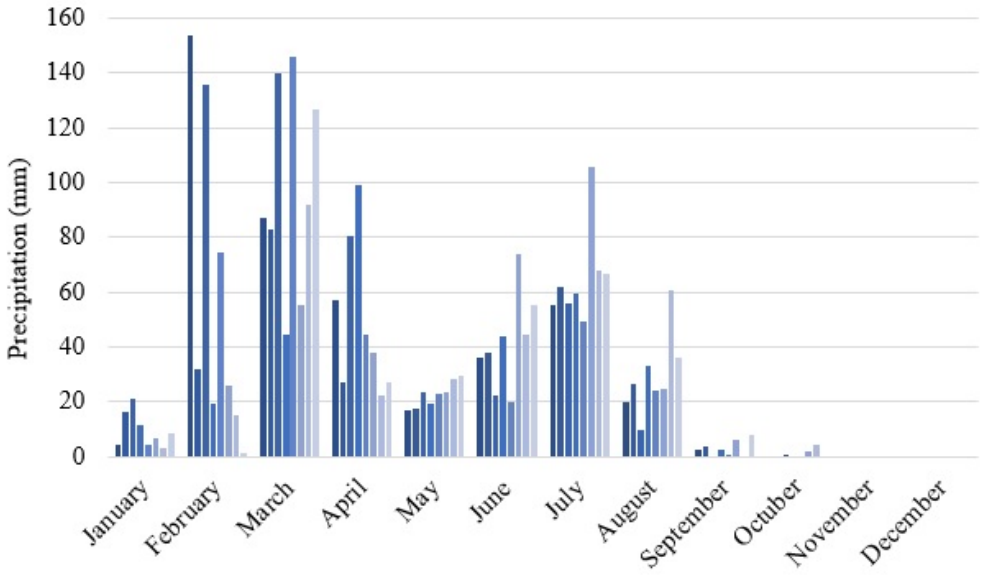

Figure 4. Average monthly rainfall around the Cariri EPA in 2019.

3.2. Soil Surface Moisture Index (SSMI)

The results of the SSMI mapping for April and October 2019 were divided into six categories ranging from 0.0 to 1.0. A result closer to 0.0 indicates that there is less surface moisture, while a result closer to 1.0 suggests a greater concentration of moisture at the surface, according to the scale drawn up by Lopes *et al.* (2011).

By inserting the real validation points (RP) and the points obtained from the images (IP) into the SSMI map (Fig. 5), it was possible to perform a spatial analysis of the points in Desertified Areas and Preserved Areas and link these points to the values for each LST and NDVI category, allowing the interactions between the values for each variable to be observed.

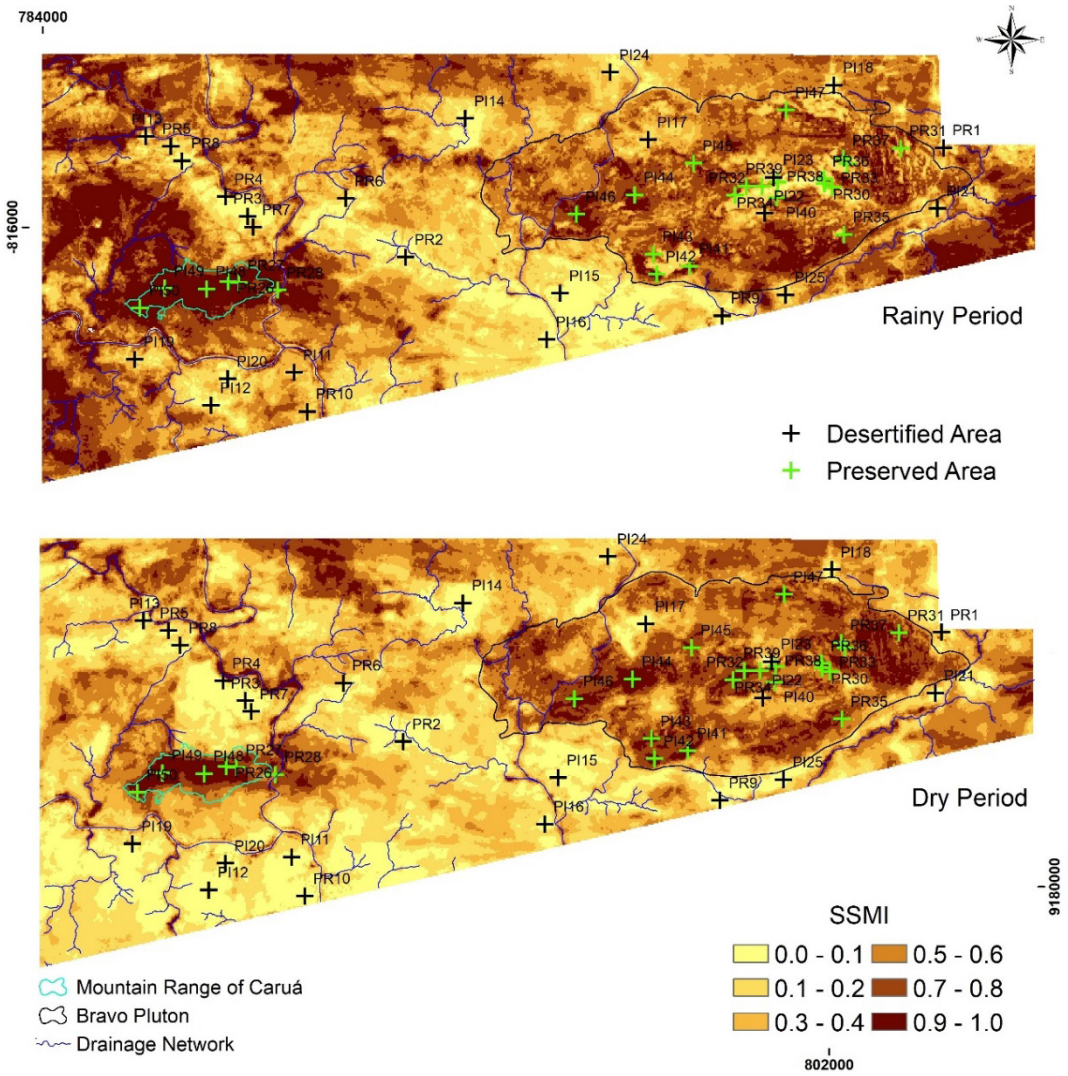

Figure 5. Soil Surface Moisture Index.

The first group of points to be analysed were those relating to Desertified Areas (Fig. 6), which cover large areas as a result of human activity resulting in the intensive removal of native vegetation. These areas are characterised by exposed soils, limited diversity of native plant species contrasting with the presence of exotic species, including mesquite (*Prosopis juliflora*) in particular, and varying degrees of erosion, which is generally advanced (Souza *et al.,* 2015a; Souza and Souza, 2016; Silva *et al.,* 2019a; Araújo and Lima, 2019).

RP.6 - Desertified Area - Rainy Period RP.3 - Desertified Area - Dry Period

Figure 6. Desertified Areas.

During the rainy period, the points in the Desertified Areas (RP.1-IP.25) fell into the SSMI categories 0.0-0.2 (Table 4), indicating lower concentrations of soil surface moisture. The land surface temperatures (LST) were also high at these points, varying from 28.6 to 35.5°C on the maximum scale calculated for this period, with temperatures of 32.6 - 35.5°C predominating at most of the points. The NDVI ranged from -0.230 (exposed soil) to 0.318 (low density vegetation) at most of the points analysed, and from 0.319 to 0.451 between RP.2, 3 and 6 and IP. 16, 17, 21 and 22, indicating higher levels of biomass but significantly altered vegetation with predominantly exotic species.

Table 4. Relationship between the points and the LST, NDVI and SSMI values for the rainy period.

Point	UTM coord.	Category	LST	NDVI	SSMI
RP.1	804573/9185922	Desertified Area	28.6 - 32.5°C	-0.230 - 0.318	0.1 - 0.2
RP.2	792283/9183321	Desertified Area	32.6 - 35.5°C	0.319 - 0.451	0.0 - 0.1
RP.3	788674/9184254	Desertified Area	32.6 - 35.5°C	0.319 - 0.451	0.0 - 0.1
RP.4	788169/9184906	Desertified Area	32.6 - 35.5°C	-0.230 - 0.318	0.0 - 0.1
RP.5	786917/9185856	Desertified Area	32.6 - 35.5°C	-0.230 - 0.318	0.0 - 0.1
RP.6	790913/9184657	Desertified Area	32.6 - 35.5°C	0.319 - 0.451	0.0 - 0.1
RP.7	788804/9184005	Desertified Area	28.6 - 32.5°C	-0.230 - 0.318	0.1 - 0.2
RP.8	787179/9185522	Desertified Area	32.6 - 35.5°C	-0.230 - 0.318	0.0 - 0.1
RP.9	799512/9181981	Desertified Area	32.6 - 35.5°C	-0.230 - 0.318	0.0 - 0.1
RP.10	790032/9179793	Desertified Area	28.6 - 32.5°C	-0.230 - 0.318	0.1 - 0.2
IP.11	789734/9180685	Desertified Area	28.6 - 32.5°C	-0.230 - 0.318	0.1 - 0.2
IP.12	787841/9179933	Desertified Area	32.6 - 35.5°C	-0.230 - 0.318	0.0 - 0.1
IP.13	786350/9186076	Desertified Area	32.6 - 35.5°C	-0.230 - 0.318	0.0 - 0.1
IP.14	793643/9186488	Desertified Area	32.6 - 35.5°C	-0.230 - 0.318	0.0 - 0.1
IP.15	795813/9182495	Desertified Area	32.6 - 35.5°C	-0.230 - 0.318	0.0 - 0.1
IP.16	795509/9181437	Desertified Area	32.6 - 35.5°C	0.319 - 0.451	0.0 - 0.1
IP.17	797821/9186005	Desertified Area	28.6 - 32.5°C	0.319 - 0.451	0.1 - 0.2
IP.18	802062/9187249	Desertified Area	32.6 - 35.5°C	-0.230 - 0.318	0.0 - 0.1
IP.19	786092/9180985	Desertified Area	32.6 - 35.5°C	-0.230 - 0.318	0.0 - 0.1
IP.20	788216/9180538	Desertified Area	32.6 - 35.5°C	-0.230 - 0.318	0.0 - 0.1
IP.21	804429/9184427	Desertified Area	32.6 - 35.5°C	0.319 - 0.451	0.0 - 0.1
IP.22	800512/9184301	Desertified Area	28.6 - 32.5°C	0.319 - 0.451	0.1 - 0.2
IP.23	800692/9185145	Desertified Area	32.6 - 35.5°C	-0.230 - 0.318	0.0 - 0.1
IP.24	796954/9187546	Desertified Area	32.6 - 35.5°C	-0.230 - 0.318	0.0 - 0.1
IP.25	800962/9182454	Desertified Area	32.6 - 35.5°C	-0.230 - 0.318	0.0 - 0.1

Key: RP=Real points collected in the field; IP=Points collected from the RGB image composition.

The degraded vegetation in the Cariri region in Paraíba is open Caatinga scrubland, where three to four species predominate, usually pioneers with greater resistance to lengthy periods of drought: *pereiro* (*Aspidosperma pyrifolium*); *catingueira* (*Caesalpinia pyramidalis*) and *jurema-preta* (*Mimosa hostilis)*, as well as mesquite (*Prosopis juliflora*), some bromeliads and cacti (Souza *et al.,* 2015b; Bállen *et al.,* 2016; Souza and Souza, 2016; Silva *et al.,* 2019a).

Souza *et al.* (2015b) obtained similar surface temperature values to those observed in this study in their analysis of the end of the rainy period in the upper course of the Paraíba River between 1989 and 2004/2005, with values between 27°C and 35°C for the Cariri EPA. This highlights the issue of the relationship between soil degradation and high ST values in this area.

When analysed during the dry period, the same 25 points displayed an SSMI of only 0.0 to 0.1, as shown in Table 5.

Table 5. Relationship between the points and the LST, NDVI and SSMI values for the dry period.

Point	UTM coord.	Category	LST	NDVI	SSMI
RP.1	804573/9185922	Desertified Area	38.6 - 40.5°C	-0.285 - 0.256	0.0 - 0.1
RP.2	792283/9183321	Desertified Area	38.6 - 40.5°C	-0.285 - 0.256	0.0 - 0.1
RP.3	788674/9184254	Desertified Area	38.6 - 40.5°C	-0.285 - 0.256	0.0 - 0.1
RP.4	788169/9184906	Desertified Area	40.6 - 42.5°C	-0.285 - 0.256	0.0 - 0.1
RP.5	786917/9185856	Desertified Area	38.6 - 40.5°C	-0.285 - 0.256	0.0 - 0.1
RP.6	790913/9184657	Desertified Area	38.6 - 40.5°C	-0.285 - 0.256	0.0 - 0.1
RP.7	788804/9184005	Desertified Area	38.6 - 40.5°C	-0.285 - 0.256	0.0 - 0.1
RP.8	787179/9185522	Desertified Area	38.6 - 40.5°C	-0.285 - 0.256	0.0 - 0.1
RP.9	799512/9181981	Desertified Area	38.6 - 40.5°C	-0.285 - 0.256	0.0 - 0.1
RP.10	790032/9179793	Desertified Area	38.6 - 40.5°C	-0.285 - 0.256	0.0 - 0.1
IP.11	789734/9180685	Desertified Area	38.6 - 40.5°C	-0.285 - 0.256	0.0 - 0.1
IP.12	787841/9179933	Desertified Area	40.6 - 42.5°C	-0.285 - 0.256	0.0 - 0.1
IP.13	786350/9186076	Desertified Area	38.6 - 40.5°C	-0.285 - 0.256	0.0 - 0.1
IP.14	793643/9186488	Desertified Area	40.6 - 42.5°C	-0.285 - 0.256	0.0 - 0.1
IP.15	795813/9182495	Desertified Area	38.6 - 40.5°C	-0.285 - 0.256	0.0 - 0.1
IP.16	795509/9181437	Desertified Area	40.6 - 42.5°C	-0.285 - 0.256	0.0 - 0.1
IP.17	797821/9186005	Desertified Area	40.6 - 42.5°C	-0.285 - 0.256	0.0 - 0.1
IP.18	802062/9187249	Desertified Area	40.6 - 42.5°C	-0.285 - 0.256	0.0 - 0.1
IP.19	786092/9180985	Desertified Area	40.6 - 42.5°C	-0.285 - 0.256	0.0 - 0.1
IP.20	788216/9180538	Desertified Area	40.6 - 42.5°C	-0.285 - 0.256	0.0 - 0.1
IP.21	804429/9184427	Desertified Area	40.6 - 42.5°C	-0.285 - 0.256	0.0 - 0.1
IP.22	800512/9184301	Desertified Area	38.6 - 40.5°C	-0.285 - 0.256	0.0 - 0.1
IP.23	800692/9185145	Desertified Area	38.6 - 40.5°C	-0.285 - 0.256	0.0 - 0.1
IP.24	796954/9187546	Desertified Area	40.6 - 42.5°C	-0.285 - 0.256	0.0 - 0.1
IP.25	800962/9182454	Desertified Area	40.6 - 42.5°C	-0.285 - 0.256	0.0 - 0.1

Key: RP=Real points collected in the field; IP=Points collected from the RGB image composition.

In this case, all 25 points displayed the highest LST levels calculated, ranging from 38.6°C to 42.5°C, with an NDVI varying from -0.285 to 0.256, with negative values indicating areas of exposed soil (-0.285) and positive values suggesting low levels of biomass. At points where the NDVI values were higher than in the rainy period (0.319 - 0.451), such as RP.2, 3, 6 and IP.16, 17, 21 and 22, positive biomass values were observed in the dry period; however, in the case of the latter, these values did not exceed 0.256, indicating a degree of biomass in the areas occupied by pioneer plants and mesquite.

The LST for these points followed a similar pattern to that observed during the rainy period, with higher levels displayed. IP.17 was an exception, scoring the second highest ST (28.6 - 32.5°C) and an SSMI of 0.1-0.2 in the rainy period and the maximum LST value (40.6 to 42.5°C) and the minimum SSMI (0.0 – 0.1) in the dry period.

In this regard, the points obtained in the field and from the images for the Desertified Areas analysed display very similar patterns when the LST, NDVI and SSMI values for the rainy and dry periods are compared. These patterns are shaped by a high LST and a low NDVI or no biomass, resulting in a low SSMI, which is indicative of drier areas owing largely to the process of degradation.

Especially during rainy periods, high surface temperatures and low levels of biomass in areas potentially degraded by desertification are a warning sign, revealing the difficulty of spontaneous regeneration of the native vegetation in the Caatinga since the process of seed germination for most of the plants in this biome occurs primarily during this period (Souza *et al.,* 2015b).

According to Lemos *et al.* (2020), the rising surface temperatures caused primarily by the removal of native vegetation result in high exposure of the soil to solar radiation, hindering the germination of seeds from the different plant species, as this process depends on a certain temperature in order to be able to occur, thus obstructing the ecological succession as a result of changes to part of

the system. Like other tropical and sub-tropical biomes, ideal temperatures in the Caatinga are considered to lie between 20 and 30ºC (Carvalho and Nakagawa, 2000).

These areas degraded by desertification are located on gently undulating and flat terrain, usually close to the drainage network (Silva *et al.,* 2019a), and are the result of human activity linked to forms of land use which have been practised since settlement began in the region in the 17th century. Deforestation of native vegetation began with the introduction of farming activities, with a second, more intense period resulting from cotton cultivation between the 19th century and the mid-1980s (Souza *et al.,* 2015a).

More recently, in the 1970s, further changes to the landscape of Cariri occurred with the introduction of exotic tree species such as mesquite by the Federal Government to provide an economic alternative for the region. The species serves as feed for livestock and led to intensifying deforestation of the remaining native vegetation to make room for cultivation (Souza *et al.,* 2015a), with a negative environmental impact. Fuel is also extracted as a source of energy for making fences and structures for homes (Travassos and Souza, 2014).

It is noteworthy that even in areas where mesquite predominates, indicating slightly higher biomass values, especially in the dry period, they do not have similar characteristics to the Preserved Areas or the same ecological features, as they do not present plant diversity of native species, being mesquite extremely competitive and which makes it predominant over other plant species. And because they are very resistant to long periods of drought and endowed with biomass, they also end up influencing human action in their introduction in a disorderly way. Thus, configuring another type of environmental degradation favoring the desertification process.

The analysis was extended into the Preserved Areas in the EPA, using another 25 points (RP.26 to IP.50). These areas were dominated by two main types of plant formation: shrubby arboreal Caatinga and Exceptional Areas.

Shrubby arboreal Caatinga (Fig. 7) is characterised by a greater, denser presence of trees. This type of vegetation was mostly identified in an area of higher altitude, the Caruá Mountains located in the southwest of the EPA. Meanwhile, the Exceptional Areas can be found in areas located near the large rocky outcrops (*lajedos*) in the Bravo Pluton region (Souza and Souza, 2016; Silva *et al.,* 2019a; Silva *et al.,* 2019b).

RP.26 - Preserved Area - Rainy Period RP.28 - Preserved Area - Dry Period

Figure 7. Preserved Area - Shrubby arboreal Caatinga.

The Exceptional Areas in the Cariri EPA (Fig. 8) occupy narrow strips between the *lajedos* of Bravo Pluton measuring approximately 10 to 20 metres wide. They are largely made up of tree species, many of which belong to other Brazilian biomes, including Amazon, Cerrado and Atlantic Forest, where higher rainfall and moisture levels are found (Lunguinho *et al.,* 2015; Silva *et al.,* 2019b), mixed with

typical species from the Caatinga commonly found in riverside areas. Therefore, the presence of these species indicates higher moisture levels at the local level.

RP.34 - Preserved Area - Rainy Period RP.32 - Preserved Area - Dry Period

Figure 8. Preserved Area - Exceptional Areas.

During the rainy period, the SSMI values identified at the points in these areas were the highest in the EPA, oscillating between 0.7 and 1.0 (Table 6) and indicating high levels of soil surface moisture.

Table 6. Relationship between the points and the LST, NDVI and SSMI values for the rainy period.

Point	UTM coord.	Category	LST	NDVI	SSMI
RP.26	788235/9182755	Shrub.Arbo.Caat.	25.6 - 28.5°C	0.711 - 1	0.9 - 1.0
RP.27	788475/9182734	Shrub.Arbo.Caat.	25.6 - 28.5°C	0.711 - 1	0.9 - 1.0
RP.28	788363/9182567	Shrub.Arbo.Caat.	25.6 - 28.5°C	0.577 – 0.710	0.9 - 1.0
RP.29	802368/9185462	Exceptional Areas	28.6 - 32.5°C	0.711 - 1	0.7 - 0.8
RP.30	801848/9185002	Exceptional Areas	28.6 - 32.5°C	0.711 - 1	0.7 - 0.8
RP.31	803593/9185805	Exceptional Areas	25.6 - 28.5°C	0.711 - 1	0.9 - 1.0
RP.32	799812/9184732	Exceptional Areas	25.6 - 28.5°C	0.711 - 1	0.9 - 1.0
RP.33	802026/9184919	Exceptional Areas	28.6 - 32.5°C	0.711 - 1	0.7 - 0.8
RP.34	800425/9184939	Exceptional Areas	28.6 - 32.5°C	0.711 - 1	0.7 - 0.8
RP.35	802298/9183836	Exceptional Areas	25.6 - 28.5°C	0.711 - 1	0.9 - 1.0
RP.36	801832/9185110	Exceptional Areas	25.6 - 28.5°C	0.711 - 1	0.9 - 1.0
RP.37	802283/9185583	Exceptional Areas	25.6 - 28.5°C	0.711 - 1	0.9 - 1.0
RP.38	800788/9185034	Exceptional Areas	28.6 - 32.5°C	0.711 - 1	0.7 - 0.8
RP.39	800065/9184941	Exceptional Areas	25.6 - 28.5°C	0.711 - 1	0.9 - 1.0
IP.40	800760/9184679	Exceptional Areas	28.6 - 32.5°C	0.711 - 1	0.7 - 0.8
IP.41	798775/9183112	Exceptional Areas	25.6 - 28.5°C	0.711 - 1	0.9 - 1.0
IP.42	798018/9182933	Exceptional Areas	25.6 - 28.5°C	0.711 - 1	0.9 - 1.0
IP.43	797945/9183390	Exceptional Areas	25.6 - 28.5°C	0.711 - 1	0.9 - 1.0
IP.44	797515/9184745	Exceptional Areas	25.6 - 28.5°C	0.711 - 1	0.9 - 1.0
IP.45	798861/9185463	Exceptional Areas	25.6 - 28.5°C	0.711 - 1	0.9 - 1.0
IP.46	796185/9184299	Exceptional Areas	25.6 - 28.5°C	0.577 – 0.710	0.7 - 0.8
IP.47	800974/9186686	Exceptional Areas	25.6 - 28.5°C	0.577 – 0.710	0.7 - 0.8
IP.48	787737/9182588	Shrub.Arbo.Caat.	25.6 - 28.5°C	0.711 - 1	0.9 - 1.0
IP.49	786774/9182608	Shrub.Arbo.Caat.	25.6 - 28.5°C	0.711 - 1	0.9 - 1.0
IP.50	786217/9182160	Shrub.Arbo.Caat.	25.6 - 28.5°C	0.711 - 1	0.9 - 1.0

Key: RP = Real points collected in the field; IP = Points collected from the RGB image composition; Shrub. Arbo.Caat. = Shrubby arboreal Caatinga.

In these areas, the surface temperature varied from 25.6 to 32.5°C, with temperatures of 25.6 to 28.5°C predominant at most points and especially in the areas of shrubby arboreal Caatinga, where this LST value was found at every point. In the Exceptional Areas, at points RP.29, 30, 33, 34, 38 and IP.40,

the ST was higher, ranging from 28.6 - 32.5°C. This is due to the fact that these points are located in more open areas of vegetation, which are influenced by smaller, more widely spaced *lajedos*.

Most of the points analysed displayed an NDVI of 0.711 - 1, with lower values found only at RP.28 and IP.46 and 47 (0.577 – 0.710), which are located in areas with a greater presence of dense arboreal Caatinga (another common vegetation type in the region) on steeper slopes in the Caruá Mountains and between the *lajedos* of Bravo Pluton.

During the rainy period, the vast majority of the points analysed in both Preserved Areas saw LST values below 30°C, while temperatures did not exceed 32°C at the other points in these areas. Echoing the findings of Carvalho and Nakagawa (2000) and Souza *et al. (*2015b), these areas are characterised by improved conditions for germination for the majority of the Caatinga plant species compared to areas with a higher LST, such as the Desertified Areas, especially during the rainy period, where there is an expansion of biomass and greater retention of soil surface moisture due to the availability of water and the type of vegetation found in these areas.

Confirming this observation, during the dry period, the 25 points analysed (RP.26 to IP.50) also had an SSMI of 0.7 - 1.0, indicating that there was a high concentration of soil surface moisture at these locations, as Table 7 shows.

Table 7. Relationship between the points and the LST, NDVI and SSMI values for the dry period.

Point	UTM coord.	Category	LST	NDVI	SSMI
RP.26	788235/9182755	Shrub.Arbo.Caat.	32.5 - 34.5°C	0.324 - 0.390	0.9 - 1.0
RP.27	788475/9182734	Shrub.Arbo.Caat.	34.6 - 36.5°C	0.324 - 0.390	0.9 - 1.0
RP.28	788363/9182567	Shrub.Arbo.Caat.	32.5 - 34.5°C	0.324 - 0.390	0.7 - 0.8
RP.29	802368/9185462	Exceptional Areas	34.6 - 36.5°C	0.391 - 0.514	0.9 - 1.0
RP.30	801848/9185002	Exceptional Areas	34.6 - 36.5°C	0.515 - 0.935	0.9 - 1.0
RP.31	803593/9185805	Exceptional Areas	32.5 - 34.5°C	0.515 - 0.935	0.9 - 1.0
RP.32	799812/9184732	Exceptional Areas	32.5 - 34.5°C	0.391 - 0.514	0.9 - 1.0
RP.33	802026/9184919	Exceptional Areas	34.6 - 36.5°C	0.515 - 0.935	0.9 - 1.0
RP.34	800425/9184939	Exceptional Areas	34.6 - 36.5°C	0.515 - 0.935	0.9 - 1.0
RP.35	802298/9183836	Exceptional Areas	34.6 - 36.5°C	0.515 - 0.935	0.9 - 1.0
RP.36	801832/9185110	Exceptional Areas	34.6 - 36.5°C	0.515 - 0.935	0.9 - 1.0
RP.37	802283/9185583	Exceptional Areas	32.5 - 34.5°C	0.515 - 0.935	0.9 - 1.0
RP.38	800788/9185034	Exceptional Areas	34.6 - 36.5°C	0.515 - 0.935	0.9 - 1.0
RP.39	800065/9184941	Exceptional Areas	32.5 - 34.5°C	0.515 - 0.935	0.9 - 1.0
IP.40	800760/9184679	Exceptional Areas	34.6 - 36.5°C	0.515 - 0.935	0.9 - 1.0
IP.41	798775/9183112	Exceptional Areas	32.5 - 34.5°C	0.515 - 0.935	0.9 - 1.0
IP.42	798018/9182933	Exceptional Areas	32.5 - 34.5°C	0.515 - 0.935	0.9 - 1.0
IP.43	797945/9183390	Exceptional Areas	34.6 - 36.5°C	0.515 - 0.935	0.9 - 1.0
IP.44	797515/9184745	Exceptional Areas	32.5 - 34.5°C	0.391 - 0.514	0.9 - 1.0
IP.45	798861/9185463	Exceptional Areas	34.6 - 36.5°C	0.515 - 0.935	0.9 - 1.0
IP.46	796185/9184299	Exceptional Areas	34.6 - 36.5°C	0.391 - 0.514	0.7 - 0.8
IP.47	800974/9186686	Exceptional Areas	34.6 - 36.5°C	0.391 - 0.514	0.9 - 1.0
IP.48	787737/9182588	Shrub.Arbo.Caat.	32.5 - 34.5°C	0.391 - 0.514	0.9 - 1.0
IP.49	786774/9182608	Shrub.Arbo.Caat.	32.5 - 34.5°C	0.391 - 0.514	0.9 - 1.0
IP.50	786217/9182160	Shrub.Arbo.Caat.	34.6 - 36.5°C	0.391 - 0.514	0.9 - 1.0

Key: RP = Real points collected in the field; IP = Points collected from the RGB image composition; Shrub. Arbo.Caat. = Shrubby arboreal Caatinga.

The LST values ranged from 32.5 to 36.5°C, representing the lowest level calculated for this period. Moreover, the NDVI varied from 0.324 to 0.935, indicating high levels of biomass at most of the points during this period of the year, especially in the Exceptional Areas, as shown in Table 4.

In the points relating to areas of shrubby arboreal Caatinga, the NDVI oscillated between 0.324 and 0.390 in areas located on the slopes of the Caruá Mountains, where the dominant vegetation is Caatinga scrubland, and from 0.391 to 0.514 at the highest points in this area, IP.48, 49 and 50, where the phytophysiognomy is still denser and more arboreal.

In the Exceptional Areas, some points displayed an NDVI ranging between 0.391 and 0.514, such as RP.29 and 32 and IP.44, 46 and 47, where closed Caatinga scrubland is more dominant. However, the remaining points in this area had biomass values between 0.515 and 0.935, located in strips around the *lajedos* of Bravo Pluton. These areas of high biomass are clearly visible during the dry period in the region (Figure 6), when many evergreen species can maintain themselves due to higher local moisture levels. In the more distant Bravo Pluton area, the predominant vegetation is open shrubby Caatinga, usually deciduous.

Comparing the rainy and dry periods for these points in Preserved Areas, the SSMI and NDVI were high in both and only the LST varied. The lowest temperature values were found in the dry period, while moderate temperatures ranging from 25.5 to 28.0ºC were observed in the rainy period at most points, with the exception of more open areas where maximum temperatures of 32.5°C were found.

In our understanding, these factors are only possible in these areas due to the presence of certain specific natural characteristics: in the case of shrubby arboreal Caatinga, the relative altitude of the mountains is linked to low local levels of anthropisation, while in the Exceptional Areas, the geological and geomorphological conditions generated by the large rocky outcrops in the Bravo Pluton encourage the concentration of moisture. In the latter case in particular, a kind of micro-environment with unique characteristics develops, contrasting with its surroundings in terms of soil type, moisture retention and nutrient availability, as well as soil and air temperature, shade and other important conditions that make these places conducive to vigorous growth of the species colonising them (Lunguinho *et al.,* 2015; Silva *et al.,* 2019b).

It is also relevant to note that conservation of the plant cover is facilitated in these areas by the conditions imposed by the topography and geomorphology, making it difficult for human activities making more direct, impactful use of the land to take place. This is the case of the Caruá Mountains, due to their striking topographic relief, and the Bravo Pluton, due to the presence of large rocky outcrops.

4. Conclusions

Combining the points used with the biophysical and geophysical data captured by orbital sensors enabled two different types of environmental conditions to be identified and described and a number of highly relevant characteristics to be observed regarding the two categories analysed in this study.

In Desertified Areas, factors such as a higher surface temperature, low levels of biomass and low soil surface moisture are present throughout the year, although they are exacerbated by the dry period.

Analysis of the points linked to the Preserved Areas revealed the presence of factors that were more conducive to the balance and maintenance of plant cover, with high levels of biomass and a concentration of surface moisture, as well as surface temperatures sufficient for seed germination in the rainy period and lower temperatures than other areas during the dry period.

These results may be combined with other information as part of the management process and search for mitigation measures in degraded areas, especially those areas suffering desertification in semi-arid regions. In the case of Conservation Units like the Cariri EPA, the methodology employed in this study may be used to inform land-use management plans and, more broadly, to plan a more rational use of the natural resources available in biomass like that found in the Caatinga and other biomes with a similar climate.

Acknowledgements

The first author is grateful to CAPES/Brazil for the PhD scholarship awarded via FAPESQ, Public Notice no. 003/2016, Case no. 88887.369009/2019-00, and to the Postgraduate Programme in Geography at the Federal University of Paraíba in Brazil.

References

AESA (Agência Executiva de Gestão das Águas do Estado da Paraíba), 2020a. Bacia Hidrográfica do Rio Paraíba. Available in: http://www.aesa.pb.gov.br/aesa-website/comite-de-bacias/rio-paraiba/

AESA (Agência Executiva de Gestão das Águas do Estado da Paraíba), 2020b Meteorologia – Chuvas. Available in: http://www.aesa.pb.gov.br/aesa-website/meteorologia-chuvas/

Amorim, I. L., Sampaio, E.V.S.B., Araújo, E. L., 2009. Fenologia de espécies lenhosas da caatinga do Seridó, RN. *Revista Árvore* 33(3), 491-499. Available in: https://www.scielo.br/pdf/rarv/v33n3/11.pdf

Aquino, C.M.S., Almeida, J.A.P., Oliveira, J.G.B. 2012. Estudo da cobertura vegetal/uso da terra nos anos de 1987 e 2007 no núcleo de degradação/desertificação de São Raimundo Nonato – Piauí. *Revista RA´EGA o Espaço Geográfico em Análise* 25, 252-278. https://doi.org/10.5380/raega.v25i0.28013

Aráujo, S.M.S., Lima, E.R.V., 2019. Semiárido Brasileiro e Desertificação. In Araújo, S.M.S. and Lima, E.R.V. (Coord.), *Desertificação no semiárido brasileiro e paraibano abordagens conceituais, metodologias e indicadores,* pp. 55-62, Bahia: Paulo Afonso. Available in: http://www.sabeh.org.br/?mbdb_book=desertificacao-no-semiarido-brasileiro-e-paraibano

Ballén, L.A.C., Souza, B.I., Lima, E.R.V., 2016. Análise espaço-temporal da cobertura vegetal na área de proteção ambiental do Cariri, Paraíba, Brasil. *Boletim Goiano de Geografia* 36(3), 55-571. https://doi.org/10.5216/bgg.v36i3.44558

Bezerra, F.G.S., Aguiar, A.P.D., Alvalá, R.C., Giarolla, A., Bezerra, K.R.A., Lima, P.V.P.S., Nascimento, F.R., Arai, E. 2020. Analysis of areas undergoing desertification, using EVI2 multi-temporal data based on MODIS imagery as indicator. *Ecological Indicators* 117, 01-15. https://doi.org/10.1016/j.ecolind.2020.106579

Carvalho, N., Nakagawa, M., 2000. *Sementes: ciência, tecnologia e produção.* 4ª ed. Jaboticabal: FUNEP.

Castelletti, C.H.M., Santos, A.M.M., Tabarelli M., Silva, J.M.C., 2003. Quanto ainda resta da Caatinga? In: *Ecologia e conservação da Caatinga*. Editora Universitária da UFPE, pp. 719-734, Recife.

Conti, J.B. 2007. *Clima e meio ambiente.* Atual. São Paulo.

Francisco, P.R.M., Chaves, I.B., Chaves, L.H.G., Lima, E.R.V., Silva, B.B. 2017. Umidade antecedente e índice de vegetação da diferença normalizada no mapeamento da Caatinga. *Agropecuária Científica no Semiárido* 13(2), 82-91. http://revistas.ufcg.edu.br/acsa/index.php/ACSA/index

Inocêncio, T.M., Neto, A.R., Souza, A.G.S.S. 2020. Soil moisture obtained through remote sensing to assess drought events. *Revista Brasileira de Engenharia Agrícola e Ambiental* 24(9), 575-580. http://doi.org/10.1590/1807-1929/agriambi.v24n9p575-580

INSA (INSTITUTO NACIONAL DO SEMIÁRIDO), 2015. *Relatórios. Relatório do seminário nacional combate à desertificação, degradação das terras e convivência com a semiaridez para redução da pobreza e um desenvolvimento sustentável.* Instituto Nacional do Semiárido. Departamento de Combate à Dertificaçao, FAO, Instituto Interamericano de Cooperaçao para Agricultura.

Köppen, W.P. 1931. *Grundriss der Klimakunde.* Walter de Gruyter. Berlín. Available in: https://www.worldcat.org/title/grundriss-der-klimakunde/oclc/2549942

Lages, G.A. Marinho, M.S., Nascimento, M.A.L., Medeiros, V.C., Dantas, E.L. Fialho, D., 2013. Mar de Bolas do Lajedo do Pai Mateus, Cabaceiras, PB - Campo de matacões graníticos gigantes e registros rupestres de civilização pré-colombiana. *In*: Winge, M., Schobbenhaus, C., Souza, C.R.G., Fernandes, A.C.S., Berbert-Born,M., Sallun Filho, W., Queiroz, E.T. (Edit.). *Sítios Geológicos e Paleontológicos do Brasil.* Available in: http://sigep.cprm.gov.br/sitio068/sitio068.pdf

Lemos, J.E., Souza, B.I., Diniz, M.T.M., 2020. Sistemas, caos e o processo de desertificação no semiárido brasileiro: complexidade e interações. *Ateliê Geográfico* 14(01), 136-154. https://doi.org/10.5216/ag.v14i1.57004

Lima, F.S., Almeida, N.V., 2017. Dinâmica espaço-temporal da cobertura vegetal na Área de Proteção Ambiental (APA) do Cariri, Paraíba-PB, Brasil. *Revista Brasileira de Geografia Física* 10(3), 699-721. https://doi.org/10.5935/1984-2295.20170046

Lopes, H.L., Accioly, L.J.O., Silva, F.H.B.B., Sobral, M.C.M., Araújo Filho, J.C., Candeias, A.L.B., 2011. Espacialização da umidade do solo por meio da temperatura da superfície e índice de vegetação. *Revista Brasileira de Engenharia Agrícola e Ambiental* 15(09) 973-980. https://doi.org/10.1590/S1415-43662011000900014

Lunguinho, R.L., Souza, B.I., Queiroz, R.T., Cardoso, E.C.M.A. 2015. Influência dos lajedos na composição florística do seu entorno, no sítio Salambaia – Cabaceiras – PB. *Revista Equador* 4(3), 230-237. Available in: https://revistas.ufpi.br/index.php/equador/article/view/3643/2119

Medeiros, R.M., Santos, D.C., Francisco, P.R.M., Gomes Filho, M.F., 2015. Análise hidroclimática da região de São João Do Cariri-PB. *Revista Educação Agrícola Superior* 30(2), 59-65.

Melo, M.L. 1988. *Áreas de exceção da Paraíba e dos sertões de Pernambuco*. SUDENE. Recife, 8 pp.

Mello Neto, A.V. de, Lins, R.C., Coutinho, S.F.S., 1985. Áreas de exceção do Nordeste brasileiro considerações conceituais. In: *SUDENE, Fundação Joaquim Nabuco - Áreas de exceção do Nordeste (Coord). Pernambuco e Paraíba*, pp. 1-11. Recife. Available in: http://observatoriogeograficoamericalatina.org.mx/egal3/Geografiasocioeconomica/Geografiaagricola/01.pdf

MMAUC (Ministério do Meio Ambiente. Unidades de Conservação), 2020. Available in: https://www.gov.br/mma/pt-br

MMA (Ministério do Meio Ambiente), 2020. In *Programa de Ação Nacional de Combate à Desertificação e Mitigação dos Efeitos da Seca PAN-Brasil*. Available in: https://www.gov.br/mma/pt-br

MTERD (Ministerio para la Transición Ecológica y Reto Demográfico), 2020. Available in: https://www.miteco.gob.es/es/biodiversidad/legislacion/legislacion-y-convenios/convenios-internacionales/convencion_desertificacion.aspx

Nascimento, F.R., 2015. Os semiáridos e a desertificação no Brasil. REDE-*Revista Eletrônica do PRODEMA* 9(2), 7–26.

Portillo-Quintero, C.A., Sánchez-Azofeifa, G.A., 2010. Extent and conservation of tropical dry forests in the Americas. *Biological Conservation* 143(1), 144-155. https://doi.org/10.1016/j.biocon.2009.09.020

Rouse, J.W., Haas, R.H., Schell, J.A., Deering, D.W., 1973. Monitoring vegetation systems in the Great Plains with ERTS. *NTRS – NASA Technical Reports Server.* 1, 309-317. Available in: https://ntrs.nasa.gov/api/citations/19740022614/downloads/19740022614.pdf

Romano, M.P.C.G., Rocha, J.G., Santos, M.L.F., Souza, M.C.S., 2018. Unidades paisagísticas no semiárido paraibano: porção Leste do Plúton Bravo, Cabaceiras-PB. In: Plataforma Espaço digital (pp. 1-10). Actas del II Congresso Internacional Da Diversidade Do Semiárido. Paraíba, novembro 8-10 de 2017. Available in: http://www.editorarealize.com.br/index.php/artigo/visualizar/33912

Santos, C.V.B., Carvalho, H.F.S., Silva, M.J., Moura, M.S.B., Galvíncio, J.D., 2020. Uso de sensoriamento remoto na análise da temperatura da superfície em áreas de floresta tropical sazonalmente seca. *Revista Brasileira de Geografia Física* 13(03), 941-953. https://doi.org/10.26848/rbgf.v13.3.p941-957

Sena, J.P.O., Moraes Neto, J.M., Lucena, D.B., 2019. Variabilidade da precipitação em Sumé e São João do Cariri e suas consequências na agropecuária. *Revista Brasileira de Climatologia* 25**,** 278-293. http://doi.org/10.5380/abclima.v25i0.65182

Silva, G.S., Silva, W.S., Silva, A.L., Almeida, N.V., Araújo, L.E., 2018. Análise da precipitação da microrregião do Cariri oriental paraibano. *Revista REGNE* 4(1), 42-57. Available in: https://periodicos.ufrn.br/revistadoregne/article/view/13938

Silva, L.F., Souza, B.I., Bacani, V.M., 2019a. Intensidade da ação antrópica na área de proteção ambiental do Cariri paraibano. *Caminhos de Geografia* 20(71), 364-383.

Silva, L.F., Souza, B.I., Bacani, V.M., 2019b. Desempenho comparativo entre classificadores supervisionados no mapeamento de áreas de Ecótono em região de Caatinga. *Caderno de Geografia* 29(59), 1083-1105. https://doi.org/10.5752/P.2318-2962.2019v29n59p1083

Silva Filho, R., Vasconcelos, R.S., Galvão, C.O., Rufino, I.A.A., Cunha, E.B.L., 2020. Representação matemática do comportamento intra-anual do NDVI no bioma Caatinga. *Ciência Florestal* 30(2), 473-488. https://doi.org/10.5902/1980509837279

Sobrinho, J.V., 1982. *Processos de desertificação no Nordeste do Brasil: sua gênese e sua contenção*. Sudene, 101 pp., Recife.

Sousa, F.P., Ferreira, T.O., Mendonça, E.S., Romero, R.E., Oliveira, J.G.B., 2012. Carbon and nitrogen in degraded Brazilian semi-arid soils undergoing desertification. *Agriculture, Ecosystems and Environment*, 148, 11-21. https://doi.org/10.1016/j.agee.2011.11.009

Souza, B.I., Suertegaray, D.M.A., Lima, E. R.V., 2009. Desertificação e seus efeitos na vegetação e solos do Cariri Paraibano. *Mercator* 8(16), 217-232. Available in: http://www.mercator.ufc.br/mercator/article/view/250

Souza, B.I., Queiroz, R.T., Cardoso, E.C.M., 2015a. Degradação e riscos à desertificação no alto curso do rio Paraíba – PB/Brasil. *Revista da Associação Nacional de Pós-graduação e Pesquisa em Geografia (Anpege)* 11(16), 201-222. https://doi.org/10.5418/RA2015.1116.0009

Souza, B.I. Macêdo, L.A., Silva, G.J.F., 2015b. Temperatura dos solos e suas influências na regeneração natural da Caatinga nos Cariris Velhos – PB. *Revista RA'EGA* 35, 261-287. http://doi.org/10.5380/raega.v35i0.41609

Souza, B.I., Souza, R.S., 2016. Processo de ocupação dos Cariris Velhos – PB e efeitos na cobertura vegetal: contribuição à Biogeografia Cultural do semiárido. *Caderno de Geografia* 26(2) 229-258. https://doi.org/10.5752/p.2318-2962.2016v26nesp2p229

Souza, N.R.L., Xavier, R.A., 2017. A importância dos "lajedos" na paisagem geomorfológica do Cariri Paraibano. In: Os desafios da Geografia Física na Fronteira do Conhecimento. Actas del XVII Simpósio Brasileiro De Geografia Física Aplicada. Campinas, june 28-30 and 02 july, pp. 6561-6566. Available in: https://www.researchgate.net/publication/321304297_A_importancia_dos_lajedos_na_paisagem_geomorfologica_do_Cariri_Paraibano

Travassos, I.S., Souza, B.I., 2014. Desmatamento e Desertificação no Cariri Paraibano. *Revista Brasileira de Geografia Física* 07(1), 103-116. https://periodicos.ufpe.br/revistas/rbgfe/article/viewFile/232905/26887

Vieira, R.M.S.P., Sestini, M.F., Tomasella, J., Marchezini, V., Pereira, G.R., Barbosa, A.A., Santos, F.C., Rodriguez, D.A., Nascimento, F.R., Santana, M. O., Campello, F.B. C., Ometto, J.P.H., 2020. Characterizing spatio-temporal patterns of social vulnerability to droughts, degradation and desertification in the Brazilian northeast. *Environmental and Sustainability Indicators* 5, 01-09. https://doi.org/10.1016/j.indic.2019.100016

Wang, H., Li, X., Long, H., Xu, X., Bao, Y., 2010. Monitoring the effects of land use and cover type changes on soil moisture using remote-sensing data: A case study in China's Yongding River basin. *Catena* 82, 135-145. https://doi.org/10.1016/j.catena.2010.05.008

Zhan, Z., Qin, Q., Wang, X., 2004. The application of LST/NDVI index for monitoring land surface moisture in semiarid area. *IEEE Transactions on geosciences and Remote Sensing* 3, 1551-1554. https://doi.org/10.1109/IGARSS.2004.1370609

Zhou, W., Gang, C., Zhou, F., Li, J., Dong, X., Zhao, C., 2015. Quantitative assessment of the individual contribution of climate and human factors to desertification in northwest China using net primary productivity as an indicator. *Ecological Indicators* 48, 560-569. https://doi.org/10.1016/j.ecolind.2014.08.043

Cuadernos de Investigación Geográfica *Geographical Research Letters*	2022	Nº 48	pp. 79-96	EISSN 1697-9540

http://doi.org/10.18172/cig.4951

SUBGRID SNOW DEPTH COEFFICIENT OF VARIATION SPANNING ALPINE TO SUB-ALPINE MOUNTAINOUS TERRAIN

GRAHAM A. SEXSTONE[1,2], STEVEN R. FASSNACHT[1,2,3*], JUÁN I. LÓPEZ-MORENO[4], CHRISTOPHER A. HIEMSTRA[5]

[1] *ESS-Watershed Science, Colorado State University, USA.*

[2] *Natural Resources Ecology Laboratory, Colorado State University, USA.*

[3] *Cooperative Institute for Research in the Atmosphere, USA.*

[4] *Instituto Pirenaico de Ecología, Spain.*

[5] *U.S. Army Cold Regions Research and Engineering Laboratory, USA.*

ABSTRACT. Given the substantial variability of snow in complex mountainous terrain, a considerable challenge of coarse scale modeling applications is accurately representing the subgrid variability of snowpack properties. The snow depth coefficient of variation (CV_{ds}) is a useful metric for characterizing subgrid snow distributions but has not been well defined by a parameterization for mountainous environments. This study utilizes lidar-derived snow depth datasets spanning alpine to sub-alpine mountainous terrain in Colorado, USA to evaluate the variability of subgrid snow distributions within a grid size comparable to a 1000 m resolution common for hydrologic and land surface models. The subgrid CV_{ds} exhibited a wide range of variability across the 321 km^2 study area (0.15 to 2.74) and was significantly greater in alpine areas compared to subalpine areas. Mean snow depth was the dominant driver of CV_{ds} variability in both alpine and subalpine areas, as CV_{ds} decreased nonlinearly with increasing snow depths. This negative correlation is attributed to the static size of roughness elements (topography and canopy) that strongly influence seasonal snow variability. Subgrid CV_{ds} was also strongly related to topography and forest variables; important drivers of CV_{ds} included the subgrid variability of terrain exposure to wind in alpine areas and the mean and variability of forest metrics in subalpine areas. Two statistical models were developed (alpine and subalpine) for predicting subgrid CV_{ds} that show reasonable performance statistics. The methodology presented here can be used for characterizing the variability of CV_{ds} in snow-dominated mountainous regions, and highlights the utility of using lidar-derived snow datasets for improving model representations of snow processes.

Coeficiente de variación del espesor de la nieve a escala de subcuadrícula en áreas montañosas alpinas y subalpinas

RESUMEN. Dada la variabilidad de la nieve en áreas de montaña complejas, un reto importante de las aplicaciones de modelado a gran escala es representar con precisión la variabilidad de las propiedades de la capa de nieve a escala de subcuadrícula. El coeficiente de variación (CV_{ds}) del espesor de la nieve es una medida útil para caracterizar la distribución de la nieve en subcuadrículas, pero no ha sido bien definido mediante una parametrización para entornos montañosos. Este estudio utiliza datos de espesor de la nieve derivados de LIDAR en áreas montañosas alpinas y subalpinas de Colorado, EE. UU. La finalidad es evaluar la variabilidad de la distribución de la nieve a escala de subcuadrícula dentro de un tamaño de cuadrícula de una resolución de 1000 m habitual para modelos hidrológicos y de superficie del terreno. Los CV_{ds} de la subcuadrícula mostraron un amplio rango de variabilidad en el área de estudio de 321 km^2 (0,15 a 2,74) y fueron significativamente mayores en las

áreas alpinas en comparación con las áreas subalpinas. El espesor medio de la nieve fue el factor determinante de la variabilidad del CV_{ds} tanto en áreas alpinas como subalpinas, ya que el CV_{ds} disminuyó de forma no lineal con el incremento del espesor de la nieve. Esta correlación negativa se atribuye al tamaño estático de los elementos rugosos (topografía y dosel) que influyen fuertemente en la variabilidad estacional de la nieve. El CV_{ds} de la subcuadrícula también estuvo muy relacionado con la topografía y las variables forestales. Los controladores determinantes del CV_{ds} fueron la variabilidad a escala de subcuadrícula de la exposición del terreno al viento en áreas alpinas y la media y variabilidad de las métricas forestales en áreas subalpinas. Se desarrollaron dos modelos estadísticos (alpino y subalpino) para predecir el CV_{ds} a escala de subcuadrícula que muestran estadísticamente rendimientos razonables. La metodología presentada aquí puede ser utilizada para caracterizar la variabilidad de CV_{ds} en regiones montañosas dominadas por la nieve, y subraya la utilidad de usar conjuntos de datos de nieve derivados de LIDAR para mejorar las representaciones de modelos de procesos de nieve.

Key words: Snow distribution, subgrid variability, coefficient of variation, lidar, modeling.

Palabras clave: Distribución de la nieve, variabilidad de la subcuadrícula, coeficiente de variación, lidar, modelos.

Received: 9 December 2020

Accepted: 19 April 2021

Corresponding author: Steven R. Fassnacht. ESS-Watershed Science, Colorado State University. E-mail address: steven.fassnacht@colostate.edu

1. Introduction

Snow plays an important role in hydrological, ecological, and atmospheric processes within much of the Earth System, and for this reason, considerable research has focused on understanding the spatial and temporal distribution of snow depth (d_s) and snow water equivalent (*SWE*) across the landscape (Clark *et al.*, 2011). Snowpacks tend to exhibit substantial spatiotemporal variability (López-Moreno *et al.*, 2015) that is shaped by processes at varying spatial scales (Blöschl, 1999). The variability of the snowpack through space and time at a given scale of interest is often driven by meteorology and its interactions with topography and forest features as well as land-cover changes from forest disturbance and deforestation (Berris and Harr, 1987). Mountainous areas, which often accumulate large seasonal snowpacks, generally exhibit a high range of snow variability because of these effects (Sturm *et al.,* 1995). Given that this variability occurs over relatively short distances (Fassnacht and Deems, 2006; López-Moreno *et al.*, 2011), accurately modeling the distribution of snow in mountainous areas requires a detailed understanding of the characteristics of snow variability at the model scale of interest (Trujillo and Lehning, 2015).

An important challenge of physically-based modeling is often the ability to represent subgrid processes, or the spatial variability of critical input parameters (Seyfried and Wilcox, 1995). Accurate representation of subgrid snow distribution is critical for reliably simulating energy and mass exchanges between the land and atmosphere in snow-covered regions (Liston, 1999), yet various studies have highlighted a deficiency with this representation in hydrologic and land-surface models (Pomeroy *et al.*, 1998; Slater *et al.*, 2001; Liston, 2004; Clark *et al.*, 2011; Liston and Hiemstra, 2011). Liston (2004) presented an approach of effectively representing subgrid snow distributions in coarse-scale models by using a lognormal probability density function and an assigned coefficient of variation (*CV*). This approach only requires an estimation of the *CV* parameter (i.e. standard deviation divided by the mean), which has generally been estimated from field data and is a measure of snow variability that allows for comparisons that are independent of the amount of snow accumulation. Representative values of the *CV*

of snow water equivalent (CV_{SWE}) and snow depth (CV_{ds}) have been published by many field studies (refer to Table 1 and Figure 2 from Clark *et al.*, 2011) and have been summarized based on vegetation and landform type (Pomeroy *et al.*, 1998) and classified globally, based on air temperature, topography, and wind speed regimes (Liston, 2004). However, the range of published CV_{SWE} and CV_{ds} in complex mountainous terrain (i.e. the mountain snow class from Sturm *et al*., 1995) is quite variable and a parameterization has not been well defined.

The recent developments of snow depth mapping capabilities from ground-based and airborne lidar (Deems *et al.*, 2013) as well as digital photogrammetry (Bühler *et al.*, 2015; Nolan *et al.*, 2015] have provided a high definition view of snow depth distributions, albeit at fixed locations in space and time, that have not been historically available by traditional field measurements. These detailed snow depth datasets have aided in an improved understanding of the scaling properties of snow distributions (Deems *et al.*, 2006; Trujillo *et al.*, 2007), the temporal evolution of snow distributions (Grünewald *et al.*, 2010; López-Moreno *et al.*, 2015), the relation of snow depth with topography (Grünewald *et al.*, 2013; Kirchner *et al.*, 2014; Revuelto *et al.*, 2014) and canopy (Broxton *et al.,* 2015; Revuelto *et al.,* 2015; Zheng *et al.*, 2016) characteristics, as well as the nature of fine scale subgrid variability of snow depth (López-Moreno *et al.*, 2015). Grünewald *et al.* (2013) present a novel study in which lidar-derived snow depth datasets are aggregated to coarse scale grids to evaluate the drivers of snow distribution at the catchment scale. Evaluations of lidar snow depth datasets within coarser scale grid resolutions can be analogous to the grid resolution of many modeling applications, thus lidar-derived snow datasets have potential to serve as an important tool for evaluating the representation of subgrid snow distributions within physically-based models.

In this study, we evaluate the snow depth coefficient of variation (CV_{ds}) as a metric of subgrid snow variability within complex mountainous terrain spanning alpine to sub-alpine land covers in north-central Colorado, U.S.A. We evaluate CV_{ds} at a grid resolution comparable to 1000 m resolution of hydrologic and land surface models. The objectives of this research were to (1) determine the range of CV_{ds} values that are observed within varying grid resolutions throughout the study area, (2) evaluate the effects of mean snow depth, forest, and terrain characteristics on subgrid CV_{ds}, and (3) develop a methodology for characterizing CV_{ds} within complex mountainous terrain. This research aims to help advance understanding of the variability of subgrid snow distributions, and inform more accurate representations of subgrid snow variability that can be used within physically-based models.

2. Methods

2.1. Site description

This research was conducted in the Front Range Mountains of north-central Colorado, located in the western United States (Fig. 1). Spatial lidar datasets collected by the Boulder Creek Critical Zone Observatory (CZO) (http://criticalzone.org/boulder/, accessed 17 April 2016) were investigated in this study. The study area ranges in elevation from 2190 m to 4117 m and is dominated by of ponderosa pine (*Pinus ponderosa*) and lodgepole pine (*Pinus contorta*) forests at lower elevations; Engelmann spruce (*Picea engelmannii)* and subalpine fir (*Abies lasiocarpa*) forests at higher elevations, and alpine tundra at the highest elevations (Fig. 1). The mean winter (1 October to 1 May) precipitation and temperature for water years 2006-2010 at the Niwot SNOTEL site (3021 m; Fig. 1) is 452 mm and 2.7°C (Harpold *et al.*, 2014). The mountainous terrain in this region is complex, varying from gentle topography at lower elevations to steep and rugged slopes closer to the Continental Divide. The majority of the study area has a southeastern aspect and is located on the eastern side of the Continental Divide (Fig. 1). The Front Range Mountains are characterized by a continental seasonal snowpack (Trujillo and Molotch, 2014), with the persistent snow zone at elevations greater than 3050 m (Richer *et al.*, 2013), generally exhibiting peak snow accumulation during the springtime months of April and May each year.

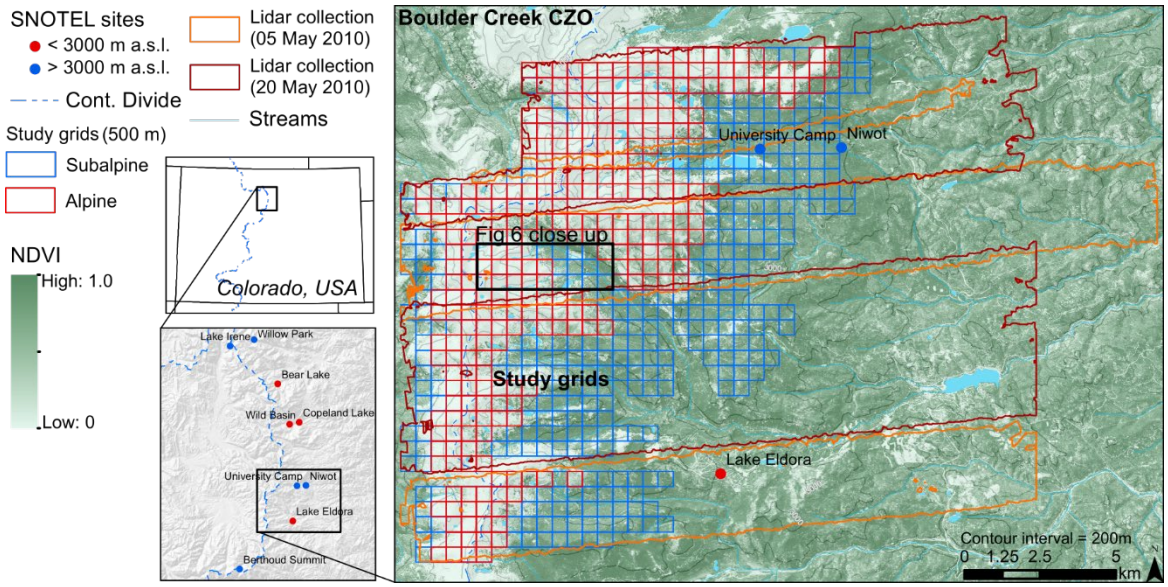

Figure 1. Map of the Boulder Creek CZO study area located within the Front Range Mountains of northern Colorado, USA. NRCS SNOTEL sites in the region are shown in blue (sites greater than 3000 m elevation) and red (sites less than 3000 m elevation). The extent of the snow-covered lidar collection on 05 May 2010 (20 May 2010) is shown in orange (red). The 500 m resolution study grids (n = 642) are shown in gray. The blue rectangle highlights the area of close up shown in Figure 5.

2.2. Spatial datasets

This study uses the publicly available lidar-derived snow depth (d_s), elevation (z), and vegetation height (VH) raster datasets (1 m resolution) from the Boulder Creek CZO (ftp://snowserver.colorado.edu/pub/WesternCZO_LiDAR_data, accessed 27 August 2015) that are described in detail by Harpold *et al.* (2014). Airborne lidar campaigns were completed during snow-covered (May 2010) and snow free (August 2010) periods across the study area and lidar surfaces were differenced to derive d_s (Harpold *et al.*, 2014). The snow-covered lidar returns were collected on two dates, 05 May 2010 and 20 May 2010, and the combined snow-covered lidar extent is 321 km^2 (Fig. 1). A comparison of the lidar d_s dataset to in situ d_s sensors within research catchments in the Boulder Creek CZO showed a Root Mean Squared Error (RMSE) of 27 cm (44% relative to lidar catchment mean) and 7 cm (117% relative to lidar catchment mean) at the Como Creek catchment (16 sensors) and Gordon Gulch catchment (5 sensors), respectively (Harpold *et al.*, 2014).

The lidar-derived digital elevation model (DEM) was resampled from a 1 m to a 10 m resolution for representation of the resolution of commonly available DEMs (USGS National Elevation Dataset, http://ned.usgs.gov) and was subsequently used to derive terrain variables for each 10 m cell that have been shown to influence d_s distributions (Elder *et al.*, 1998; Winstral *et al.*, 2002; Erickson *et al.*, 2005; Kerr *et al.*, 2013; Revuelto *et al.*, 2014) using a Geographic Information System (GIS). Surface slope (S) was calculated by fitting a plane to a 3 x 3 cell window around each DEM cell. Winter clear-sky incoming solar radiation ($Q_{sw\downarrow}$) was determined using the Area Solar Radiation tool in ArcGIS, which calculates mean incoming solar radiation for clear-sky conditions across a DEM surface for a specified time interval based on solar zenith angle and terrain shading. The time interval used for the calculation of $Q_{sw\downarrow}$ was 01 October through 01 May. Aspect was not considered because it was highly correlated with $Q_{sw\downarrow}$. Maximum upwind slope (Sx) (Winstral *et al.*, 2002), which can be used as a measure of the exposure to or sheltering from wind, was calculated for each cell as:

$$Sx_{\alpha,d\max}(x_i,y_i)=\max\left(\tan^{-1}\left\{\frac{z(x_v,y_v)-z(x_i,y_i)}{\left[(x_v-x_i)^2+(y_v-y_i)^2\right]^{0.5}}\right\}\right) \quad (1)$$

where α is the azimuth of the search direction, *dmax* is the maximum distance for the search direction, z is elevation, and (x_v, y_v) are all cells along the vector defined by α and *dmax*. Given the prevailing westerly winds within the study area (Winstral *et al.*, 2002; Erickson *et al.*, 2005], an average *Sx* was calculated for a *dmax* of 200 m and a range of α from 240° to 300° at 5° increments (Molotch *et al.*, 2005). Topographic position index (*TPI*) (Weiss, 2001), which is a measure of the relative position of the cell to surrounding terrain, was calculated for each cell as:

$$TPI = z_0 - \bar{z} \tag{2}$$

$$\bar{z} = \frac{1}{n_R} \sum_{i \in R} z_i \tag{3}$$

where z_0 is the elevation of the cell and $\bar{z}$ is the average elevation of the surrounding cells within a specified cell window (R). TPI was calculated for 3 x 3 (i.e. 30 m resolution), 11 x 11, and 21 x 21 windows around each cell. Additionally, a 30 m resolution 2011 canopy density (*CD*) dataset was downloaded for the study area (http://www.mrlc.gov/nlcd2011.php, accessed 04 December 2015).

2.3. Aggregation of study grids

Operational snow models (Carroll *et al.*, 2006] often have a 1000 m horizontal grid resolution and snow representations within land surface models (Slater *et al.*, 2001) have generally been designed for a coarser resolution (Yang *et al.*, 1997) but are being developed to operate at finer scales (Kumar *et al.*, 2006; Wood *et al.*, 2011; Bierkens *et al.*, 2015). This study attempts to evaluate the subgrid variability of d_s at a comparable grid resolution to this 1000 m model grid size. Therefore, the subgrid variability of d_s within study grids of 100 m, 200 m, 300 m, 400 m, 500 m, 750 m, and 1000 m resolutions was evaluated. For example, subgrid statistics for each 500 m study grid (with 100% d_s coverage) were calculated based on 250000 lidar-derived d_s cells. The goal of this was to identify an appropriate grid size for evaluation that exhibited similar characteristics of snow variability to the 1000 m resolution grids, but maximized the number of grids available for analysis within the study area. At least 80% coverage of each study grid by the lidar d_s datasets was required, and the d_s dataset with the greatest coverage was utilized for cases of the overlapping snow-covered lidar datasets (Fig. 1). When the 05 May 2010 and 20 May 2010 lidar d_s datasets were overlapping and both datasets had 100% study grid coverage, the 05 May 2010 dataset was used.

For each study grid, the mean and standard deviation (σ) of d_s were determined and used to calculate CV_{ds}. The mean and standard deviation of each of the terrain and canopy variables outlined above were also calculated for each study grid. A categorical variable representing ecosystem type was also determined for each study grid. The alpine ecosystem type was assigned to study grids that had a mean elevation greater than 3300 m and a mean *VH* less than 0.5 m, while the remaining study grids were assigned to the subalpine ecosystem type; treeline elevation in this area generally varies between 3400 m and 3700 m (Suding *et al.*, 2015). Lastly, only study grids with a mean elevation greater than 3000 m (i.e. the persistent snow zone) were evaluated in this study. Table 1 provides a list of all variables used in this study.

Table 1. Symbols of variables and metrics used in this study.

Symbol	Variable
CV_{ds}	snow depth coefficient of variation
d_s	snow depth
σ_{ds}	standard deviation of snow depth
VH	vegetation height

σ_{VH}	standard deviation of vegetation height
CD	canopy density
σ_{CD}	standard deviation of canopy density
z	elevation
σ_z	standard deviation of elevation
S	surface slope
σ_S	standard deviation of surface slope
$Q_{sw\downarrow}$	winter clear-sky incoming solar radiation
$\sigma_{Qsw\downarrow}$	standard deviation of winter clear-sky incoming solar radiation
Sx	maximum upwind slope
σ_{Sx}	standard deviation of maximum upwind slope
TPI	topographic position index
σ_{TPI}	standard deviation of topographic position index

2.4. Statistical analysis

Pairwise relations between CV_{ds} and d_s, terrain variables and vegetation variables were explored for both alpine and subalpine study grids to evaluate drivers of subgrid d_s variability. CV_{ds} was expected to have a strong nonlinear relation with d_s (Fassnacht and Hultstrand, 2015); therefore, this relation was detrended for both the alpine and subalpine study grids, and residuals were used to evaluate further terrain and vegetation effects on CV_{ds} using Pearson's r coefficient. Additionally, multiple linear regression models (refer to Table 3 for general model equation) were developed to predict CV_{ds} for both alpine and subalpine study grids based on the variables presented in Table 1. Variables included in the models were selected by an all-subsets regression procedure in which both Mallows' C_p (Mallows, 1973) and Akaike information criterion (AIC) (Akaike, 1974) were used as a measure of relative goodness of fit of the models (Sexstone and Fassnacht, 2014). Final independent variables within the models were required to be statistically significant (p value < 0.05) and not exhibit multicollinearity. Multicollinearity was defined as model parameters exhibiting a variance inflation factor greater than 2. Given that a non-normal distribution of snow depth (Liston, 2004) and other terrain and vegetation variables was expected, natural log and square root transformations of model variables (Table 1) were explored. Model diagnostics of residuals were used to ensure the model assumptions of normality, linearity, and homoscedasticity. Model performance was evaluated using the Nash-Sutcliffe efficiency (NSE) and RMSE. Additionally, model verification was assessed using a 10-fold cross-verification procedure which runs 10 iterations of removing a randomly-selected 10 percent of the dataset, fitting the regression to the remainder of the data, and subsequently comparing modeled values to the independent observations that were removed.

3. Results

3.1. Snowpack conditions

In a hypothetical uniform snowmelt scenario (Egli and Jonas, 2009), the subgrid mean d_s is expected to decrease faster than the σ_{ds}, thus the CV_{ds} will increase without a corresponding increase in subgrid snow variability (Winstral and Marks, 2014). Therefore, in this study, an evaluation of the snowpack conditions was important for assessing if the subgrid CV_{ds} may have been influenced by a melting snowpack. *SWE* data from nine Natural Resources Conservation Service (NRCS) SNOTEL stations located in the Front Range Mountains of northern Colorado (Fig. 1) were evaluated to assess snowpack conditions. A snowmelt event occurred across the study area on 10 April 2010 (Fig. 2a) that caused considerable snowmelt at stations below an elevation of 3000 m and a loss of 10% of peak *SWE* on average at stations above 3000 m. Following this snowmelt event, substantial snow accumulation continued at SNOTEL stations above 3000 m until 17 May 2010, when the onset of snowmelt began

(Fig. 2a). A plot of σ_{ds} versus mean d_s among the SNOTEL stations highlights the hysteretic dynamics of accumulation and melt across the region (Egli and Jonas, 2009), and confirms that the lidar data were collected prior to and at the beginning of snowmelt across the study area (Fig. 2b). Given that the lidar-derived snow depth was collected before substantial snowmelt had occurred within the persistent snow zone, we are confident that the subgrid CV_{ds} evaluated in this study is representative of snow variability at peak snow accumulation in this region.

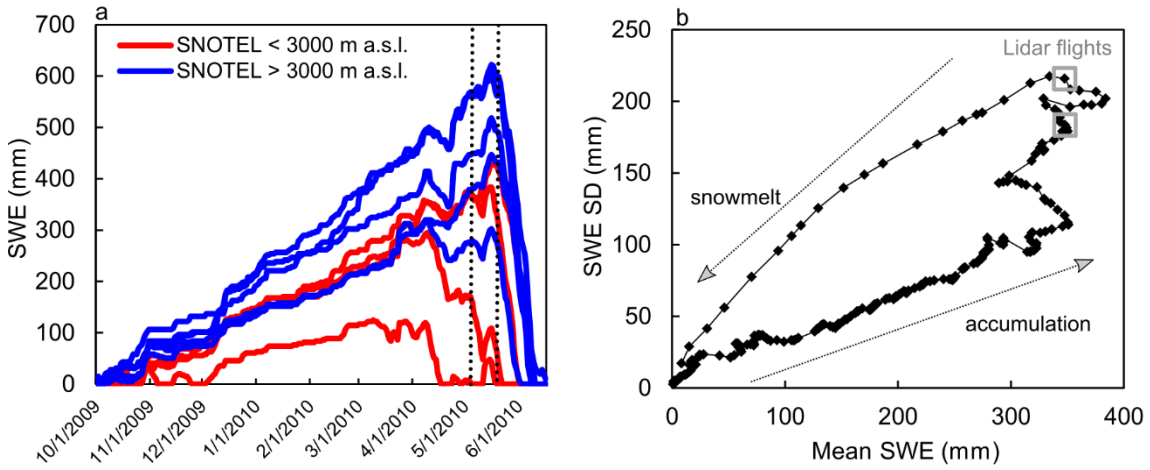

Figure 2. Snow water equivalent (SWE) data from nine NRCS SNOTEL sites within the region of the study area displayed as (a) niveographs showing snow accumulation and snowmelt throughout water year 2010 with the timing of 05 May 2010 and 20 May 2010 lidar flights plotted as vertical dashed lines and (b) a scatter plot of the standard deviation of SWE versus mean SWE from the SNOTEL sites highlighting the hysteretic dynamics of snow accumulation and snowmelt across the region based on nine SNOTEL stations (Egli and Jonas, 2009).

3.2. Subgrid snow depth variability

Snow depth *CV* (CV_{ds}) and σ_{ds} were consistently greater in the alpine versus subalpine at each of the varying grid resolutions (Fig. 3). The mean CV_{ds} across the study grids was generally consistent with changes in grid resolution; however, the standard deviation of CV_{ds} decreased with increasing grid resolution and stabilized around a 500 m grid size. The mean σ_{ds} across the study grids tended to increase with increasing grid size for all study grids, but stabilized around 400 m for subalpine study grids only. The 500 m resolution study grids (n = 642) were chosen for analysis in this study (Fig. 1) and is believed to be representative of the subgrid snow variability at the 1000 m resolution.

The median d_s, σ_{ds}, and CV_{ds} across all study grids (500 m resolution) was equal to 1.27 m, 0.88 m, and 0.74, respectively, and subgrid CV_{ds} ranged from 0.15 to 2.74 across the study area. The variability of CV_{ds} collected on 05 May 2010 (n = 219 study grids) and 20 May 2010 (n = 423 study grids) (Fig. 1) was similar, with the 05 May grids exhibiting a slightly smaller CV_{ds} (median = 0.64) than the 20 May grids (median = 0.81). Statistically significant differences (p value < 0.001) between the alpine and subalpine study grids were observed for d_s, σ_{ds}, and CV_{ds} by the nonparametric Mann-Whitney test (Fig. 4). The alpine study grids exhibited a greater mean and range of snow accumulation and variability than the subalpine study grids. The range of CV_{ds} from the 10th to the 90th percentiles within the alpine and subalpine study grids was equal to 0.61 to 1.57 and 0.30 to 0.98, respectively. Figure 5 highlights the abrupt change of subgrid snow depth variability characteristics observed in a transition from the subalpine to alpine ecosystem; the forest structure and terrain characteristics appears to exert a strong influence on subgrid CV_{ds} and these relations were investigated further.

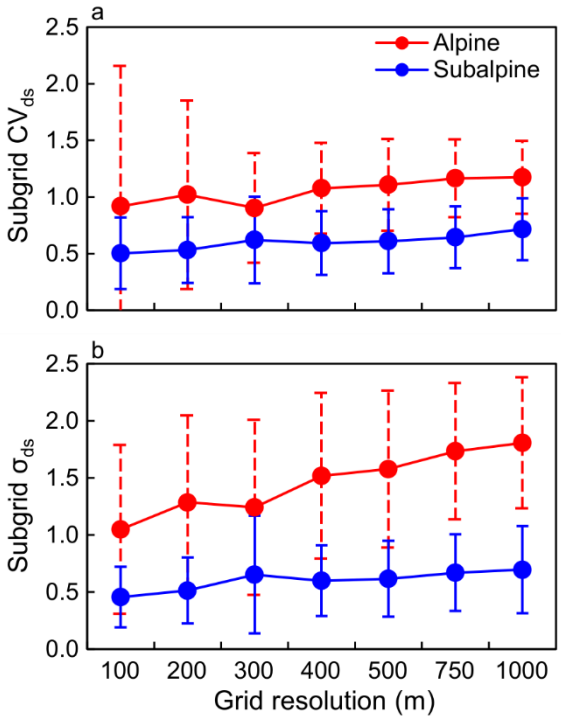

Figure 3. Mean subgrid (a) CV_{ds} and (b) σ_{ds} across the study area plotted versus study grid resolution for alpine (red) and subalpine (blue) study grids. Error bars represent the standard deviation of CV_{ds} and σ_{ds} across the study area.

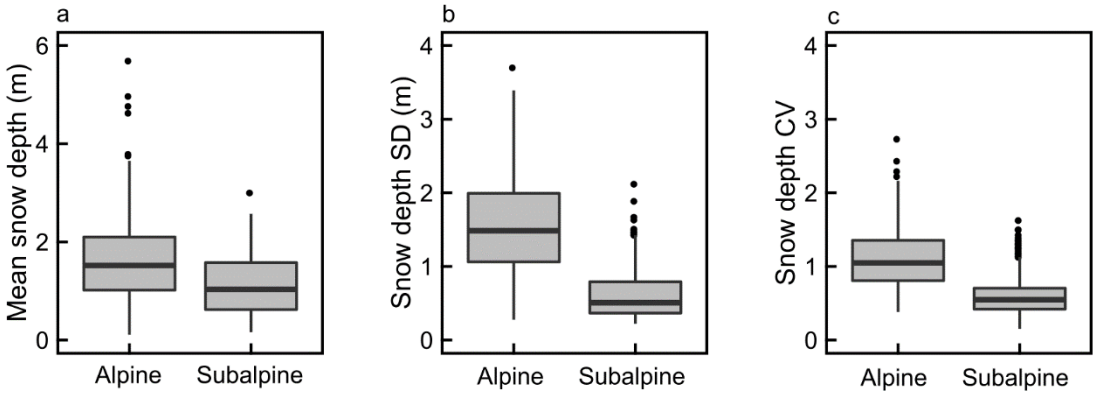

Figure 4. Boxplots showing the outliers (black circles), 10th and 90th percentiles (whiskers), 25th and 75th percentiles (box) and median (black horizontal line) for the (a) d_s, (b) σ_{ds}, and (c) CV_{ds} of the alpine and subalpine study grids (500 m resolution).

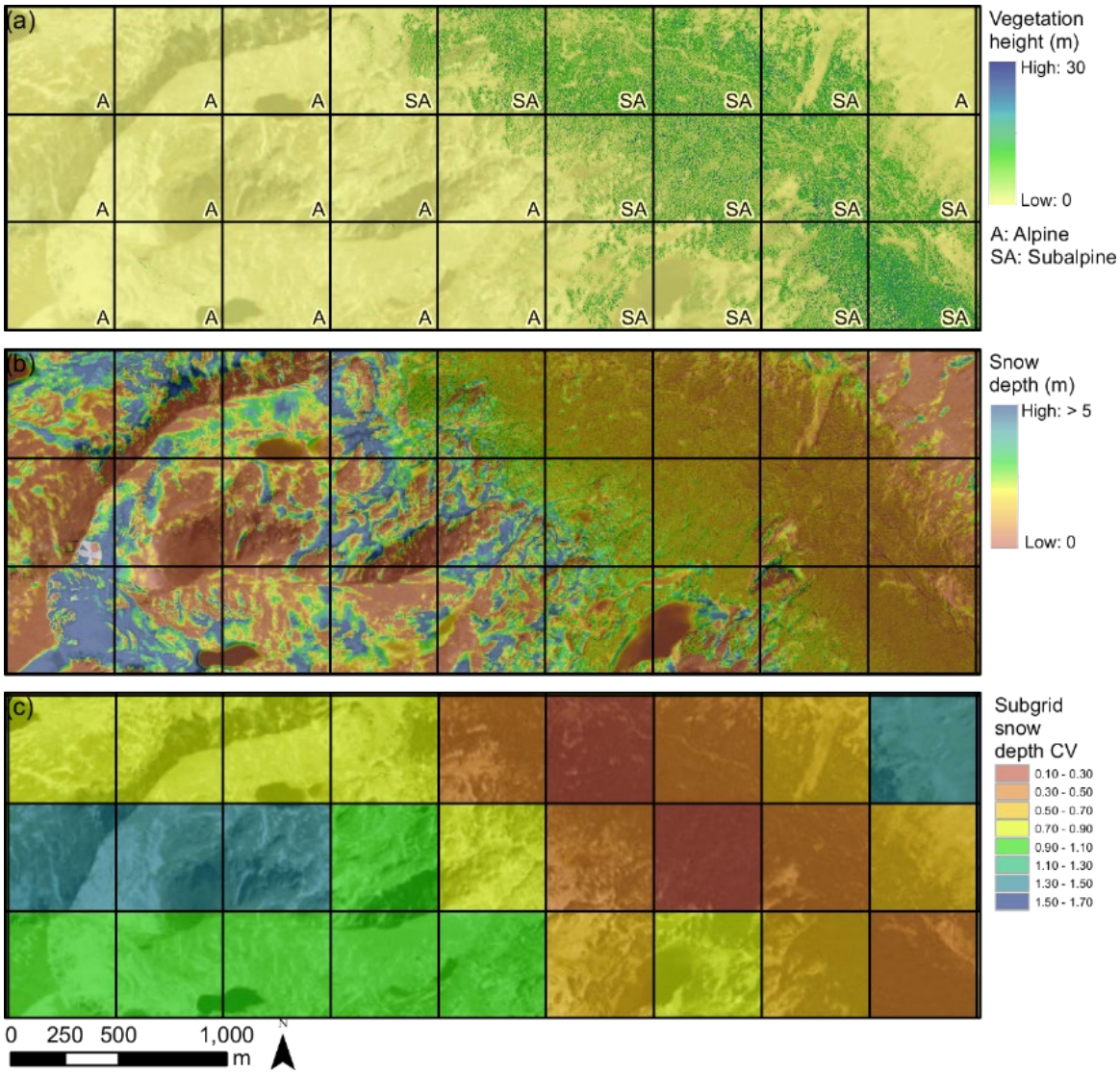

Figure 5. Close up map of selected study grids showing the distribution of (a) vegetation height and ecosystem type, (b) snow depth, and (c) subgrid CV_{ds} value. Area of close up is highlighted in Figure 1.

3.3. Relation of subgrid snow depth variability with terrain and forest characteristics

A statistically significant linear correlation (Pearson's r coefficient; p value < 0.05) between CV_{ds} and d_s was observed to be -0.60 and -0.45 for the alpine and subalpine study grids, respectively (Table 2). However, further evaluation showed this relation to be nonlinear and best described by a power function (Fig. 6). This function suggests that CV_{ds} exhibits a systematic decrease with increasing d_s and suggests that relative subgrid snow variability is importantly related to the total snow accumulation of a given year. The power relation between CV_{ds} and d_s was greatly improved when split between alpine and subalpine study grids, as a CV_{ds} for a corresponding d_s tended to be greater for alpine versus subalpine study grids (Fig. 6). The power functions (CV_{ds} versus d_s) were detrended (i.e. removing the influence of d_s on CV_{ds}) and the residuals of the functions were compared to terrain and forest characteristics (Table 2). The alpine study grids were most positively correlated with σ_{Sx} suggesting that the variability of wind exposure and sheltering and thus wind redistribution within a study grid is a strong control on CV_{ds}. The subalpine study grids were most negatively correlated with the *VH* and *CD* variables suggesting that forest structure is important driver of subalpine subgrid variability with increases in forest canopy coverage generally reducing CV_{ds}.

Table 2. Bivariate correlations (Pearson's r coefficient) between snow depth coefficient of variation (CV_{ds}) and the mean and standard deviation (σ) of snow depth (d_s), vegetation height (VH), canopy density (CD), elevation (z), slope (S), winter clear-sky incoming solar radiation ($Q_{sw}\downarrow$), maximum upwind slope (Sx), and topographic position index (TPI) for both alpine and subalpine study grids. Correlations are also shown for the residuals from the detrended nonlinear relation of CVd_s and d_s. Bold values represent statistical significance (p value < 0.05)

	CV_{ds} *(alpine)*	CV_{ds} *(subalpine)*	CV_{ds} (alpine) d_s residuals	CV_{ds} (subalpine) d_s residuals
d_s	**-0.60**	**-0.45**	---	---
σ_{ds}	-0.06	**0.25**	---	---
VH	**-0.38**	**-0.48**	**-0.28**	**-0.71**
σ_{VH}	**-0.38**	**-0.57**	**-0.24**	**-0.59**
CD	-0.06	**-0.32**	**-0.21**	**-0.64**
σ_{CD}	-0.06	**0.30**	**-0.26**	**0.50**
z	**0.17**	**-0.22**	**0.32**	**0.18**
σ_z	-0.07	0.09	**0.16**	**0.29**
S	-0.03	0.06	**0.25**	**0.28**
σ_S	-0.06	0.13	**0.37**	**0.38**
$Q_{sw}\downarrow$	0.10	-0.02	-0.07	**-0.17**
$\sigma_{Qsw}\downarrow$	-0.07	-0.03	**0.21**	**0.21**
Sx	0.02	0.08	**0.29**	0.09
σ_{Sx}	0.07	0.10	**0.43**	**0.28**
TPI	**0.28**	**0.11**	**0.15**	0.04
σ_{TPI}	-0.09	0.09	**0.29**	**0.33**

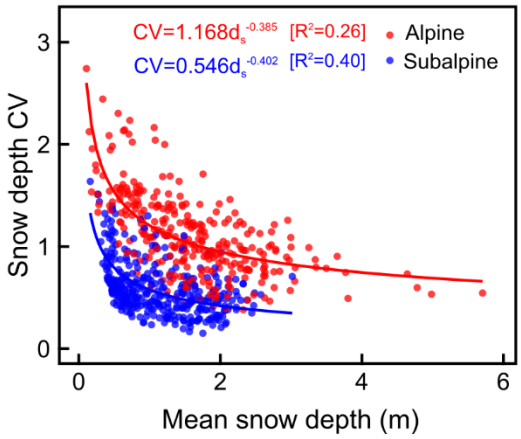

Figure 6. Nonlinear relation of CV_{ds} and d_s for alpine (red) and subalpine (blue) study grids (500 m resolution).

3.4. Statistical models

We evaluated a range of independent variables to be included within the multiple linear regression models (refer to variables in Table 1). However, to make the model analysis most transferable to other mountainous environments, some of the variables were deemed unsuitable and excluded from model testing. For example, mean *z* was not included in model testing as it was believed to be a site-specific variable that may not have been transferable to independent data. Additionally, *VH* and *σVH* were not tested despite their strong correlation with subalpine CV_{ds} as these variables are not commonly available as spatial datasets, such as the USGS National Land Cover Database

(http://www.mrlc.gov/index.php) land cover type and canopy density products. Variables that were shown to significantly improve model diagnostics and performance and suggested relations with CV_{ds} that make physical sense were included in the final models. The multiple linear regression models developed for predicting CV_{ds} in both alpine and subalpine seasonal snowpacks are presented in Table 3. Variable transformations were necessary to CV_{ds} and d_s in both models and to σ_{Sx} in the alpine model and *CD* in the subalpine model to account for the nonlinearity of these datasets (Table 3). Snow depth exhibited the greatest explanatory ability within both the alpine and subalpine models, with standardized regression coefficients equal to -0.92 and -0.95, respectively (not shown). Standardized regression coefficients of σ_{Sx} and *CD* were equal to 0.50 and -0.72 for the alpine and subalpine models, respectively, and both showed the second strongest explanatory power in their respective models. For the model calibration dataset (10-fold cross-verification dataset), the alpine model had a NSE of 0.66 (0.65) and RMSE of 0.24 (0.24) while the subalpine model had an NSE of 0.79 (0.78) and RMSE of 0.12 (0.13) (Fig. 7). A total NSE of 0.81 was calculated for the entire dataset based on predictions from both models. These performance statistics suggest that the models perform reasonably well predicting CV_{ds} and cross-verification suggests the model may be transferable to independent data within the bounds of the original dataset.

Table 3. Multiple linear regression equation variables and coefficients of the alpine and subalpine CV_{ds} *models. The multiple linear regression is of the form:* $y=\beta_0 + \beta_1 X_1 + \beta_2 x_2 + \ldots + \beta_n x_n$ *where y is the dependent variable,* x_1 *through* x_n *are n independent variables,* β_0 *is the regression intercept, and* β_1 *through* β_n *are n regression coefficients.*

	Alpine model	Subalpine model
Y	$\log(CV_{ds})$	$CV_{ds}^{0.5}$
β_0	9.00E-03	8.45E-01
β_1	-1.02E+00	-2.84E-01
x_1	$d_s^{0.5}$	$\log(d_s)$
β_2	1.00E-02	-9.79E-05
x_2	Sx	CD^2
β_3	3.42E-01	1.12E-02
x_3	$\log(\sigma_{Sx})$	σ_S
β_4	1.84E-03	---
x_4	$Q_{SW\downarrow}$	---

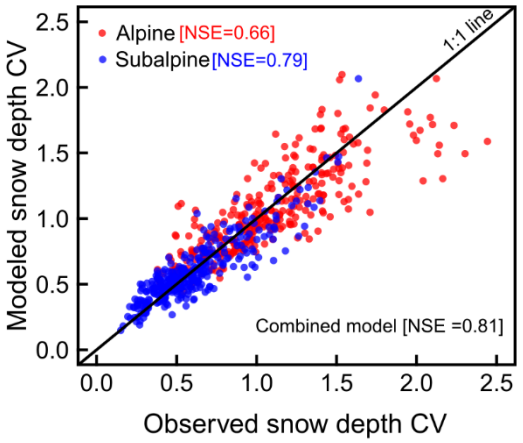

Figure 7. Modeled versus observed CV_{ds} *for the alpine (red) and subalpine (blue) multiple linear regression models.*

4. Discussion

Based on an evaluation of CV_{ds} at a 500 m grid resolution, subgrid snow variability across a mountainous subalpine and alpine study area is shown to exhibit a wide range of spatial variation and be well correlated with ecosystem type, snow amount, as well as terrain characteristics and forest structure. Alpine CV_{ds} was most correlated with mean snow depth and the variability of exposure to wind while mean snow depth and canopy height and density were most correlated with CV_{ds} in subalpine areas. A statistical model for both alpine and subalpine ecosystems was able to reasonably predict subgrid CV_{ds} based on these relations and could be used to support improving model parameterizations of subgrid snow variability in mountainous terrain.

The range of CV_{ds} observed over relatively small distances in this study (Fig. 5) highlights the importance of further characterizing the spatial variability of this parameter within mountainous terrain. The global classification of CV_{SWE} defined by Liston (2004) performed well predicting the average conditions observed in this study. Liston (2004) define the CV_{SWE} of mid-latitude mountainous forest (i.e. subalpine) as 0.60 and of mid-latitude treeless mountains (i.e. alpine) as 0.85, whereas this study found a median CV_{ds} of 0.55 for subalpine study grids and 1.05 for alpine study grids. However, the global classification was unable to adequately represent the range and variability of CV_{ds} across the study area (Fig. 4c), and the results presented herein further characterize the distribution and variability of CV_{ds} in mountainous terrain.

Mean snow depth was the main driver of CV_{ds} variability across alpine and subalpine areas within the study area. As subgrid d_s increased, the CV_{ds} decreased, which is a result that is consistent with previous studies at various spatial scales (Fassnacht and Deems, 2006; Fassnacht and Hultstrand, 2015; López-Moreno *et al.*, 2015). A positive correlation was observed between σ_{ds} and d_s in alpine and subalpine areas, which had a dampening effect on this overall negative correlation between the relative subgrid variability (CV_{ds}) with d_s. The relative subgrid variability of d_s likely decreases with increasing snow accumulation because of the consistent size of the roughness elements of terrain and canopy that drive snow variability; as d_s increases, the relative influence of these terrain and canopy features tends to decrease (Fassnacht and Deems, 2006; López-Moreno *et al.*, 2011; López-Moreno *et al.*, 2015]. The range of CV_{ds} observed in this study (Fig. 4) is similar to previous studies conducted in mountainous mid-latitude forested and alpine areas [refer to Figure 2 from Clark *et al.*, 2011 and references therein]. Future research could further investigate CV_{ds} and d_s across different geographic regions and snow regimes as well as across multiple snow seasons and compare results to the functions presented in Figure 6 to better understand the dynamics and consistency of this relation. An understanding of how the subgrid variability of snow depth for a given set of terrain and canopy elements scales between low and high snow years could be particularly important.

Within the alpine study grids, the variability of the exposure/sheltering from wind (σ_{Sx}) was an important driver of CV_{ds}. Study grids with the greatest σ_{Sx} were generally positioned over large breaks in terrain. For example, a given study grid with a large σ_{Sx} likely contained areas with both wind exposure ($Sx < 0°$) where snow accumulation is scoured by wind and sheltering from wind ($Sx > 0°$) where preferential deposition of wind transported snow occurs. Study grids with a consistent Sx showed a lower CV_{ds} with greater variability observed in sheltered grids than in exposed grids. Winstral *et al*. (2002) and many subsequent studies (Erickson *et al.*, 2005; Molotch *et al.*, 2005; Revuelto *et al.*, 2014; McGrath *et al.*, 2015) have highlighted this control of wind exposure on snow depth distribution in tree-less areas. The degree of importance of σ_{Sx} for describing CV_{ds} is likely variable from year-to-year, and would be expected to be well correlated with observed wind speeds [*Winstral and Marks*, 2014]. However, in alpine areas where high wind speeds are ubiquitous, σ_{Sx} is expected to be a consistently important driver of subgrid snow variability.

Subgrid snow variability within subalpine study grids was well correlated with *VH* and *CD*. As mean study grid *VH* and *CD* increased, CV_{ds} tended to decrease. Forest structure has been shown by various studies to have a strong influence on snow variability because of a variety of physical process

interactions. Interception of snow (Hedstrom and Pomeroy, 1998; Suzuki and Nakai, 2008] and subsequent canopy sublimation (Montesi *et al.*, 2004; Molotch *et al.*, 2007), influences of trees on shortwave (Ellis and Pomeroy, 2007; Musselman *et al.*, 2012) and longwave (Pomeroy *et al.*, 2009; Yamazaki and Kondo, 1992) radiation dynamics, and the effect of trees on wind redistribution of snow (Hiemstra *et al.,* 2006) can each drive snow accumulation and evolution in forested areas. Broxton *et al.* (2015) utilized lidar-derived snow depth datasets and showed that the variability of snow depth in subalpine forests tended to be greatest beneath the forest canopy and near the forest canopy edge and the least snow depth variability occurred in forested openings that were distant from the forest edge, relating to fetch and area contributing to snow deposition. Also, substantial differences in accumulated d_s were observed between subcanopy areas and forest openings. The increased CV_{ds} with decreasing *VH* and *CD* observed in this study can be explained by a greater occurrence of transitional areas between subcanopy areas and forest openings (i.e., forest edges) occurring in study grids with smaller mean *VH* and *CD*. Across the study area, subalpine forest openings that spanned an entire study grid were not present; therefore, study grids with consistent forest cover tended to exhibit the least subgrid snow variability.

This study was limited by the spatial and temporal coverage of the lidar-derived snow datasets that were used (Fig. 1). Although the alpine and subalpine areas evaluated are representative of mountainous terrain in the region and snowpacks in this area are representative of the continental snow regime (Trujillo and Molotch, 2014), further analysis of subgrid snow variability across a greater geographic area and across other regions with differing snow regimes could improve the applicability of a CV_{ds} parameterization for snow distributions in mountains areas in general. Additionally, spatial patterns of snow variability have been shown to be temporally consistent from year-to-year (Erickson *et al.*, 2005; Deems *et al.*, 2008; Sturm and Wagner, 2010], but future studies with multiple years of lidar collection could help understand the inter-annual variability of CV_{ds} and the consistency of its driving variables (Fassnacht *et al.*, 2012]. Of particular interest would be the temporal consistency of the relation between CV_{ds} and d_s.

This study evaluates the subgrid variability of d_s, but *SWE* is the most fundamental snowpack variable of interest in land surface processes (Sturm *et al.*, 2010). Snow depth and *SWE* have been shown by many studies to be well correlated (Jonas *et al.*, 2009; Sturm *et al.*, 2010; Sexstone and Fassnacht, 2014), and the subgrid *CV* of these variables is expected to exhibit similar characteristics (Fassnacht and Hultstrand, 2015). We suggest that a parameterization of CV_{ds} could be sufficient for representing subgrid *SWE* variability, but further investigation into this hypothesis is needed. In order to directly investigate CV_{SWE} from lidar-derived snow data in future studies, an estimation of snow density would be needed. Statistically-derived snow density models have been successfully developed over varying domain sizes for estimating *SWE* from d_s (Jonas *et al.*, 2009; Sturm *et al.*, 2010; Sexstone and Fassnacht, 2014), and these models make use of the fact that *SWE* and d_s variability is much greater than the variability of snow density (Mizukami and Perica, 2008; Lopez-Moreno *et al.*, 2013).

The snow distributions and variability characteristics evaluated in this study were likely influenced by the occurrence of snowmelt conditions within the study area. Although substantial snowmelt had not occurred prior to data collection within the study grids (Figure 2), the mid-season melt events and onset of snowmelt may have caused an increase in CV_{ds} and this effect may have differed between the two dates of lidar-derived d_s. López-Moreno *et al.* (2015) observed a sharp increase in CV_{ds} just following the onset of snowmelt yet a fairly consistent CV_{ds} for the remainder of snowmelt season. Future studies evaluating subgrid snow variability should investigate the intra-annual variability CV_{ds} to further understand the seasonal evolution of this parameter.

The development of high-resolution snow depth mapping from lidar has provided a unique ability for detailed snapshot views of the spatial distribution of snow in complex mountains areas. Although some key advantages of these datasets are related to validating satellite-based remote sensing products and direct use within water resources forecasting, this study also suggests that lidar-derived

snow datasets can be an important tool for the improvement of snow representations within modeling applications. Future research should utilize lidar-derived snow datasets to directly evaluate the ability of physically-based models to represent snow distributions as well as to continue to improve the representation of subgrid variability of snow. Additionally, other key snow modeling questions such as how representative snow monitoring stations are of surrounding areas (Molotch and Bales, 2005; Meromy *et al.*, 2013) could also be investigated further by lidar-derived snow datasets. Lastly, the analysis methods that have been developed in this study may also be useful in future studies for characterizing the subgrid variability of other variables that can be measured remotely at a fine scale through lidar or other measurement techniques.

5. Conclusions

This study outlines a methodology for utilizing lidar-derived snow datasets for investigating subgrid snow depth (d_s) variability and potentially improving its representation within physically-based modeling applications. At fine grid resolutions, subgrid snow depth coefficient of variation (CV_{ds}) generally increased and its variability decreased with increasing grid resolution, while study grid CV_{ds} characteristics were similar among a range of coarser resolutions (from 500 m to 1000 m). Study grids (500 m resolution) exhibited a wide range of CV_{ds} across the study area (0.15 to 2.74) and subgrid d_s variability was found to be greater in alpine areas than subalpine areas. Snow depth was the most important driver of CV_{ds} variability in both alpine and subalpine areas and a systematic nonlinear decrease in CV_{ds} with increasing d_s was observed; the negative correlation between CV_{ds} and d_s is attributed to the static size of roughness elements (terrain and canopy) that strongly influence seasonal snow variability. The variability of wind exposure in alpine areas as well as mean vegetation height and canopy density in subalpine areas were also found to be important drivers of study grid CV_{ds}. Two statistical models were developed (alpine and subalpine) for predicting subgrid CV_{ds} from mean d_s and terrain/canopy features. They show reasonably good performance statistics and suggest this methodology can be used for characterizing CV_{ds} in snow-dominated mountainous areas. This research highlights the utility of using lidar-derived snow datasets for improving model representations of subgrid snow variability.

Acknowledgements

This work was partially funded by the NASA Terrestrial Hydrology Program (award NNX11AQ66G ‘Improved Characterization of Snow Depth in Complex Terrain Using Satellite Lidar Altimetry’ PI Michael F. Jasinski NASA GSFC). The airborne lidar data were collected in collaboration between the Boulder Creek CZO and the National Center for Airborne Laser Mapping, both of which are funded by the National Science Foundation. The lidar-derived elevation, vegetation, and snow datasets were processed and made publicly available as described in *Harpold et al.* [2014] and were invaluable datasets for this study. Thanks to Adam Winstral for providing the *Sx* code.

References

Akaike, H. 1974. A new look at the statistical model identification. *IEEE Transactions on Automatic Control* 19(6), 716-723. https://doi.org/10.1109/TAC.1974.1100705

Berris, S.N., Harr, R.D. 1987. Comparative snow accumulation and melt during rainfall in forested and clear-cut plots in the Western Cascades of Oregon. *Water Resources Research* 23(1), 135–142. https://doi.org/10.1029/WR023i001p00135

Bierkens, M.F.P., Bell, V.A., Burek, P., Chaney, N., Condon, L.E., David, C.H., de Roo, A., Döll, P.P.D., Drost, N., Famiglietti, J.S., Flörke, M., Gochis, D.J., Houser, P., Hut, R., Keune, J., Kollet, S., Maxwell, R.M., Reager, J.T., Samaniego, L., Sudicky, E., Sutanudjaja, E.H., van de Giesen, N., Winsemius, H., Wood,

E.F. 2015. Hyper-resolution global hydrological modelling: what is next? "Everywhere and locally relevant". *Hydrological Processes* 29 (2), 310-320. https://doi.org/10.1002/hyp.10391

Blöschl, G. 1999. Scaling issues in snow hydrology. *Hydrological Processes* 13 (14-15), 2149-2175.https://doi.org/10.1002/(SICI)1099-1085(199910)13:14/15<2149::AID-HYP847>3.0.CO;2-8

Broxton, P.D., Harpold, A.A., Biederman, J.A., Troch, P.A., Molotch, N.P., Brooks, P.D. 2015. Quantifying the effects of vegetation structure on snow accumulation and ablation in mixed-conifer forests. *Ecohydrology* 8 (6), 1073-1094. https://doi.org/10.1002/eco.1565

Bühler, Y., Marty, M., Egli, L.,Veitinger, J., Jonas, T., Thee, P., Ginzler, C. 2015. Snow depth mapping in high-alpine catchments using digital photogrammetry. *The Cryosphere* 9 (1), 229-243. https://doi.org/10.5194/tc-9-229-2015

Carroll, T., Cline, D., Olheiser, C., Rost, A., Nilsson, A., Fall, G., Bovitz, C., Li, L. 2006. NOAA's National Snow Analyses, paper presented at *74th Annual Western Snow Conference*, Las Cruces, NM.

Clark, M.P., Hendrikx, J., Slater, A.G., Kavetski, D., Anderson, B., Cullen, N.J., Kerr, T., Hreinsson, E.O., Woods, R.A. 2011. Representing spatial variability of snow water equivalent in hydrologic and land-surface models: A review. *Water Resources Research* 47 (7). https://doi.org/10.1029/2011WR010745

Deems, J.S., Fassnacht, S.R., Elder, K.J. 2006. Fractal distribution of snow depth from Lidar data. *Journal of Hydrometeorology* 7 (2), 285-297. https://doi.org/10.1175/JHM487.1

Deems, J.S., Fassnacht, S.R., Elder, K.J. 2008. Interannual consistency in fractal snow depth patterns at Two Colorado Mountain Sites. *Journal of Hydrometeorology* 9 (5), 977-988. https://doi.org/10.1175/2008JHM901.1

Deems, J.S., Painter, T.H., Finnegan, D.C. 2013. Lidar measurement of snow depth: a review. *Journal of Glaciology* 59 (215), 467-479. https://doi.org/10.3189/2013JoG12J154

Egli, L., Jonas, T. 2009. Hysteretic dynamics of seasonal snow depth distribution in the Swiss Alps. *Geophysical Research Letters*, 36 (2), L02501. https://doi.org/10.1029/2008GL035545

Elder, K., Rosenthal, W., Davis, R.E. 1998. Estimating the spatial distribution of snow water equivalence in a montane watershed. *Hydrological Processes* 12 (10-11), 1793-1808. https://doi.org/10.1002/(SICI)1099-1085(199808/09)12:10/11<1793::AID-HYP695>3.0.CO;2-K

Ellis, C.R., Pomeroy, J.W. 2007. Estimating sub-canopy shortwave irradiance to melting snow on forested slopes. *Hydrological Processes* 21(19), 2581-2593. https://doi.org/10.1002/hyp.6794

Erickson, T.A., Williams, M.W., Winstral, A. 2005. Persistence of topographic controls on the spatial distribution of snow in rugged mountain terrain, Colorado, United States, *Water Resources Research* 41 (4). https://doi.org/10.1029/2003wr002973

Fassnacht, S.R., Deems, J.S. 2006. Measurement sampling and scaling for deep montane snow depth data. *Hydrological Processes* 20 (4), 829-838. https://doi.org/10.1002/hyp.6119

Fassnacht, S.R., Dressler, K.A., Hultstrand, D.M., Bales, R.C., Patterson, G. 2012. Temporal inconsistencies in coarse-scale snow water equivalent patterns: Colorado River Basin snow telemetry-topography regressions. *Pirineos* 167(0), 165-185. https://doi.org/10.3989/Pirineos.2012.167008

Fassnacht, S.R., Hultstrand, M. 2015. Snowpack variability and trends at long-term stations in northern Colorado, USA. *Proceedings of the International Association of Hydrological Sciences* 371, 131-136. https://doi.org/10.5194/piahs-371-131-2015

Grünewald, T., Schirmer, M., Mott, R., Lehning, M. 2010. Spatial and temporal variability of snow depth and ablation rates in a small mountain catchment. *The Cryosphere* 4 (2), 215-225. https://doi.org/10.5194/tc-4-215-2010

Grünewald, T., Stötter, J., Pomeroy, J.W., Dadic, R., Moreno Baños, I., Marturià, J., Spross, M., Hopkinson, C., Burlando, P., Lehning, M. 2013. Statistical modelling of the snow depth distribution in open alpine terrain. *Hydrology and Earth System Sciences* 17 (8), 3005-3021. https://doi.org/10.5194/hess-17-3005-2013

Harpold, A.A., Guo, Q., Molotch, N., Brooks, P.D., Bales, R., Fernandez-Diaz, J.C., Musselman, K.N., Swetnam, T.L., Kirchner, P., Meadows, M.W., Flanagan, J., Lucas, R. 2014. LiDAR-derived snowpack data sets from mixed conifer forests across the Western United States. *Water Resources Research* 50 (3), 2749-2755. https://doi.org/10.1002/2013WR013935

Hedstrom, N.R., Pomeroy, J.W. 1998. Measurements and modelling of snow interception in the boreal forest. *Hydrological Processes* 12(10-11), 1611-1625. https://doi.org/10.1002/(SICI)1099-1085(199808/09)12:10/11%3C1611::AID-HYP684%3E3.0.CO;2-4

Hiemstra, C.A., Liston, G.E., Reiners, W.A. 2006. Observing, modelling, and validating snow redistribution by wind in a Wyoming upper treeline landscape. *Ecological Modelling* 197 (1-2), 35-51. https://doi.org/10.1016/j.ecolmodel.2006.03.005

Jonas, T., Marty, C., Magnusson, J. 2009. Estimating the snow water equivalent from snow depth measurements in the Swiss Alps. *Journal of Hydrology* 378 (1-2), 161-167. https://doi.org/10.1016/j.jhydrol.2009.09.021

Kerr, T., Clark, M., Hendrikx, J., Anderson, B. 2013. Snow distribution in a steep mid-latitude alpine catchment. *Advances in Water Resources* 55, 17-24. https://doi.org/10.1016/j.advwatres.2012.12.010

Kirchner, P. B., Bales, R. C., Molotch, N. P., Flanagan, J., Guo, Q. 2014. LiDAR measurement of seasonal snow accumulation along an elevation gradient in the southern Sierra Nevada, California. *Hydrology and Earth System Sciences*, 18 (10), 4261-4275. https://doi.org/10.5194/hess-18-4261-2014

Kumar, S.V., Peters-Lidardb, C.D., Tian, Y., Houser, P.R., Geiger, J., Olden, S., Lighty, L., Eastman, J.L., Doty, B., Dirmeyer, P., Adams, J., Mitchell, K., Wood, E.F., Sheffield, J. 2006. Land information system: An interoperable framework for high resolution land surface modeling. *Environmental Modelling & Software* 21 (10), 1402-1415. https://doi.org/10.1016/j.envsoft.2005.07.004

Liston, G.E. 1999. Interrelationships among snow distribution, snowmelt, and snow cover depletion: Implications for atmospheric, hydrologic, and ecologic modeling. *Journal of Applied Meteorology* 38 (10), 1474-1487. https://doi.org/10.1175/1520-0450(1999)038<1474:IASDSA>2.0.CO;2

Liston, G.E. 2004. Representing subgrid snow cover heterogeneities in regional and global models. *Journal of Climate* 17 (6), 1381-1397. https://doi.org/10.1175/1520-0442(2004)017<1381:RSSCHI>2.0.CO;2

Liston, G.E., Hiemstra, C.A. 2011. Representing Grass- and Shrub-Snow-Atmosphere Interactions in Climate System Models. *Journal of Climate* 24 (8), 2061-2079. https://doi.org/10.1175/2010JCLI4028.1

López-Moreno, J.I., Fassnacht, S.R., Beguería, S., Latron, J.B.P. 2011. Variability of snow depth at the plot scale: implications for mean depth estimation and sampling strategies. *The Cryosphere* 5 (3), 617-629. https://doi.org/10.5194/tc-5-617-2011

Lopez-Moreno, J.I., Fassnacht, S.R., Heath, J.T., Musselman, K.N., Revuelto, J., Latron, J., Moran-Tejeda, E., Jonas, T. 2013. Small scale spatial variability of snow density and depth over complex alpine terrain: Implications for estimating snow water equivalent. *Advances in Water Resources* 55, 40-52. https://doi.org/10.1016/j.advwatres.2012.08.010

López-Moreno, J.I., Revuelto, J., Fassnacht, S.R., Azorín-Molina, C., Vicente-Serrano, S.M., Morán-Tejeda, E., Sexstone, G.A. 2015. Snowpack variability across various spatio-temporal resolutions. *Hydrological Processes*, 29 (6), 1213-1224. https://doi.org/10.1002/hyp.10245

Mallows, C.L. 1973. Some Comments on Cp. *Technometrics* 15 (4), 661.

McGrath, D., Sass, L., O'Neel, S., Arendt, A., Wolken, G., Gusmeroli, A., Kienholz, C., McNeil C. 2015. End-of-winter snow depth variability on glaciers in Alaska. *Journal of Geophysical Research: Earth Surface* 120 (8), 1530-1550. https://doi.org/10.1002/2015JF003539

Meromy, L., Molotch, N.P., Link, T.E., Fassnacht, S.R., Rice, R. 2013. Subgrid variability of snow water equivalent at operational snow stations in the western USA. *Hydrological Processes* 27 (17), 2383-2400. https://doi.org/10.1002/hyp.9355

Mizukami, N., Perica, S. 2008. Spatiotemporal characteristics of snowpack density in the mountainous regions of the Western United States. *Journal of Hydrometeorology* 9 (6), 1416-1426. https://doi.org/10.1175/2008JHM981.1

Molotch, N.P., Bales, R.C. 2005. Scaling snow observations from the point to the grid element: Implications for observation network design. *Water Resources Research* 41 (11), W11421. https://doi.org/10.1029/2005WR004229

Molotch, N.P., Colee, M.T., Bales, R.C., Dozier, J. 2005. Estimating the spatial distribution of snow water equivalent in an alpine basin using binary regression tree models: the impact of digital elevation data and independent variable selection. *Hydrological Processes* 19 (7), 1459-1479. https://doi.org/10.1002/hyp.5586

Molotch, N.P., Blanken, P.D., Williams, M.W., Turnipseed, A.A., Monson, R.K., Margulis, S.A. 2007. Estimating sublimation of intercepted and sub-canopy snow using eddy covariance systems. *Hydrological Processes* 21 (12), 1567-1575. https://doi.org/10.1002/hyp.6719

Montesi, J., Elder, K., Schmidt, R.A., Davis, R.E. 2004. Sublimation of intercepted snow within a Subalpine Forest Canopy at Two Elevations. *Journal of Hydrometeorology* 5 (5), 763-773. https://doi.org/10.1175/1525-7541(2004)005<0763:SOISWA>2.0.CO;2

Musselman, K.N., Molotch, N.P., Margulis, S.A., Kirchner, P.B., Bales, R.C. 2012. Influence of canopy structure and direct beam solar irradiance on snowmelt rates in a mixed conifer forest. *Agricultural and Forest Meteorology* 161, 46-56. https://doi.org/10.1016/j.agrformet.2012.03.011

Nolan, M., Larsen, C., Stur, M. 2015. Mapping snow depth from manned aircraft on landscape scales at centimeter resolution using structure-from-motion photogrammetry. *The Cryosphere*, 9 (4), 1445-1463. https://doi.org/10.5194/tc-9-1445-2015

Pomeroy, J.W., Gray, D.M., Shook, K.R., Toth, B., Essery, R.L.H., Pietroniro, A., Hedstrom, N. 1998. An evaluation of snow accumulation and ablation processes for land surface modelling. *Hydrological Processes* 12 (15), 2339-2367. https://doi.org/10.1002/(SICI)1099-1085(199812)12:15<2339::AID-HYP800>3.0.CO;2-L

Pomeroy, J.W., Marks, D., Link, T., Ellis, C., Hardy, J., Rowlands, A., Granger, R. 2009. The impact of coniferous forest temperature on incoming longwave radiation to melting snow. *Hydrological Processes* 23 (17), 2513-2525. https://doi.org/10.1002/hyp.7325

Revuelto, J., López-Moreno, J.I. Azorin-Molina, C., Vicente-Serrano, S.M. 2014. Topographic control of snowpack distribution in a small catchment in the central Spanish Pyrenees: intra- and inter-annual persistence. *The Cryosphere* 8 (5), 1989-2006. https://doi.org/10.5194/tc-8-1989-2014

Revuelto, J., Lopez-Moreno, J.I., Azorin-Molina, C., Vicente-Serrano, S. M. 2015. Canopy influence on snow depth distribution in a pine stand determined from terrestrial laser data. *Water Resources Research* 51 (5), 3476-3489. https://doi.org/10.1002/2014WR016496

Richer, E.E., Kampf, S.K., Fassnacht, S.R., Moore, C.C. 2013. Spatiotemporal index for analyzing controls on snow climatology: application in the Colorado Front Range. *Physical Geography* 34 (2), 85-107. https://doi.org/10.1080/02723646.2013.787578

Sexstone, G.A., Fassnacht, S.R. 2014. What drives basin scale spatial variability of snowpack properties in northern Colorado? *The Cryosphere* 8 (2), 329-344. https://doi.org/10.5194/tc-8-329-2014

Seyfried, M.S., Wilcox, B.P. 1995. Scale and the nature of spatial variability - Field examples having implications for hydrologic modeling. *Water Resources Research* 31 (1), 173-184. https://doi.org/10.1029/94WR02025

Slater, A.G., Schlosser, C.A., Desborough, C.E., Pitman, A.J., Henderson-Sellers, A., Robock, A., Ya Vinnikov, K., Entin, J., Mitchell, K., Chen, F., Boone, A., Etchevers, P., Habets, F., Noilhan, J., Braden, H., Cox, P.M., de Rosnay, P., Dickinson, R.E., Yang, Z-L, Dai, Y-J, Zeng, Q., Duan, Q., Koren, V., Schaake, S., Gedney, N., Gusev, Ye M., Nasonova, O.N., Kim, J., Kowalczyk, E.A., Shmakin, A.-B., Smirnova, T.G., Verseghy, D., Wetzel, P., Xue, Y. 2001, The representation of snow in land surface schemes: Results from PILPS 2(d). *Journal of Hydrometeorology* 2 (1), 7-25. https://doi.org/10.1175/1525-7541(2001)002<0007:TROSIL>2.0.CO;2

Sturm, M., Holmgren, J., Liston, G.E. 1995. A seasonal snow cover classification-system for local to global applications. *Journal of Climate* 8 (5), 1261-1283. https://doi.org/10.1175/1520-0442(1995)008<1261:ASSCCS>2.0.CO;2

Sturm, M., Wagner, A.M. 2010. Using repeated patterns in snow distribution modeling: An Arctic example. *Water Resources Research* 46 (12), W12549. https://doi.org/10.1029/2010WR009434

Sturm, M., Taras, B., Liston, G.E., Derksen, C., Jonas, T., Lea, J. 2010. Estimating snow water equivalent using snow depth data and climate classes. *Journal of Hydrometeorology* 11 (6), 1380-1394. https://doi.org/10.1175/2010JHM1202.1

Suding, K.N., Farrer, E.C., King, A.J., Kueppers, L., Spasojevic, M.J. 2015. Vegetation change at high elevation: scale dependence and interactive effects on Niwot Ridge. *Plant Ecology & Diversity* 8 (5-6), 713-725. https://doi.org/10.1080/17550874.2015.1010189

Suzuki, K., Nakai, Y. 2008. Canopy snow influence on water and energy balances in a coniferous forest plantation in northern Japan. *Journal of Hydrology* 352, 126-138. https://doi.org/ 10.1016/j.jhydrol.2008.01.007

Trujillo, E., Ramirez, J.A., Elder, K.J. 2007. Topographic, meteorologic, and canopy controls on the scaling characteristics of the spatial distribution of snow depth fields. *Water Resources Research*, 43 (7), W07409. https://doi.org/10.1029/2006WR005317

Trujillo, E., Molotch, N P. 2014. Snowpack regimes of the Western United States. *Water Resources Research* 50 (7), 5611-5623. https://doi.org/10.1002/2013WR014753

Trujillo, E., Lehning, M. 2015. Theoretical analysis of errors when estimating snow distribution through point measurements. *The Cryosphere* 9, 1249-1264. https://doi.org/10.5194/tc-9-1249-2015

Weiss, A.D. 2001. Topographic position and landforms analysis, in *ESRI User Conference*, edited, San Diego, USA.

Winstral, A., Elder, K., Davis, R.E. 2002. Spatial snow modeling of wind-redistributed snow using terrain-based parameters. *Journal of Hydrometeorology* 3 (5), 524-538. https://doi.org/10.1175/1525-7541(2002)003<0524:SSMOWR>2.0.CO;2

Winstral, A., Marks, D. 2014. Long-term snow distribution observations in a mountain catchment: Assessing variability, time stability, and the representativeness of an index site. *Water Resources Research* 50 (1), 293-305. https://doi.org/10.1002/2012WR013038

Wood, E.F., Roundy, J.K., Troy, T.J., van Beek, L. P.H., Bierkens, M.F.P., Blyth, E., de Roo, A., Döll, P., Ek, M., Famiglietti, J., Gochis, D., van de Giesen, N., Houser, P., Jaffé, P.R., Kollet, S., Lehner, B., Lettenmaier, D.P., Peters-Lidard, C., Sivapalan, M., Sheffield, J., Wade, A., Whitehead, P. 2011. Hyperresolution global land surface modeling: Meeting a grand challenge for monitoring Earth's terrestrial water. *Water Resources Research* 47 (5). https://doi.org/10.1029/2010WR010090

Yamazaki, T., Kondo, J., Watanabe, T., Sato, T. 1992. A heat-balance model with a canopy of one or two layers and its application to field experiments. *Journal of Applied Meteorology and Climatology* 31, 86–103. https://doi.org/10.1175/1520-0450(1992)031<0086:AHBMWA>2.0.CO;2

Yang, Z.L., Dickinson, R.D., Robock, A., Vinnikov, K.Y. 1997. Validation of the snow submodel of the biosphere-atmosphere transfer scheme with Russian snow cover and meteorological observational data. *Journal of Climate* 10 (2), 353-373. https://doi.org/10.1175/1520-0442(1997)010<0353:VOTSSO>2.0.CO;2

Zheng, Z., Kirchner, P.B., Bales, R.C. 2016. Topographic and vegetation effects on snow accumulation in the southern Sierra Nevada: a statistical summary from lidar data. *The Cryosphere* 10 (1), 257-269. https://doi.org/10.5194/tc-10-257-2016

Cuadernos de Investigación Geográfica *Geographical Research Letters*	2022	Nº 48	pp. 97-110	EISSN 1697-9540

http://doi.org/10.18172/cig.5022

VARIABILIDAD TEMPORAL DE LA ISLA DE CALOR URBANA DE LA CIUDAD DE ZARAGOZA (ESPAÑA)

JOSÉ M. CUADRAT[1,2]*, ROBERTO SERRANO-NOTIVOLI[3], SAMUEL BARRAO[1,2], MIGUEL ÁNGEL SAZ[1,2], ERNESTO TEJEDOR[4]

[1]Departamento de Geografía y Ordenación del Territorio, Universidad de Zaragoza, España.

[2]Instituto Universitario de Ciencias Ambientales, Universidad de Zaragoza, España.

[3]Departamento de Geografía, Universidad Autónoma de Madrid, España.

[4]Department of Atmospheric and Environmental Sciences, University at Albany, United States.

RESUMEN. En este artículo se analiza la intensidad y la variabilidad temporal de la isla de calor urbana (ICU) de la ciudad de Zaragoza (España) y se evalúa la acción del viento como importante factor atmosférico condicionante de la misma. A partir de los datos horarios proporcionados por la red meteorológica urbana de mesoescala de la ciudad, se calculó la diferencia de temperatura entre dos observatorios, uno urbano (Plaza Santa Marta) y otro en las afueras del área urbana (Ciudad Deportiva), en el periodo 2015-2020. Los resultados indican que la temperatura en el centro de la ciudad es, con mucha frecuencia, 1º o 2ºC más elevada que en el entorno, y en ocasiones ha llegado a superar los 8ºC. La ICU es más intensa en verano (promedios horarios de 2,5ºC) que en invierno (promedio de 2,2ºC) y es más intensa durante la noche que durante el día. El valor máximo de la ICU se alcanza en situaciones de calma atmosférica; en cambio, se debilita claramente con vientos de más de 10 km/h y llega prácticamente a desaparecer con velocidades superiores a 50 km/h.

Temporal variability of the urban heat island in Zaragoza (Spain)

ABSTRACT. We analyse the temporal intensity and variability of the urban heat island (UHI) in the city of Zaragoza (Spain), and assess the role of wind as an important atmospheric conditioning factor. Based on the time data provided by the city's urban mesoscale meteorological network, the temperature difference between two observatories, one urban (Plaza Santa Marta) and one located on the outskirts of the urban area (Ciudad Deportiva), was calculated for the 2015-2020 period. The results indicate that the temperature in the city centre is very frequently 1º or 2ºC higher than in the surroundings, sometimes even more than 8ºC higher. The UHI is more intense in summer (an average of 2.5ºC per hour) than in winter (an average of 2.2ºC per hour) and more intense during the night than during the day. The maximum UHI value is reached in calm atmospheric situations; however, this value is very limited with winds over 10 km/h and it practically disappears with wind speeds over 50 km/h.

Palabras clave: clima urbano, isla de calor urbano (ICU), velocidad del viento, Zaragoza, España.

Key words: urban climate, Urban Heat Island (UHI), wind speed, Zaragoza, Spain.

Recibido: 8 Febrero 2021

Aceptado: 30 Junio 2021

*Correspondencia: José María Cuadrat. Departamento de Geografía y Ordenación del Territorio, Universidad de Zaragoza, 50009 Zaragoza, España. E-mail: cuadrat@unizar.es

1. Introducción

Es bien conocido que las ciudades transforman el medio físico donde se asientan. Su masa compacta de edificios supone una alteración profunda del paisaje natural, la cubierta vegetal es sustituida por un substrato impermeable y las actividades de sus habitantes son una fuente considerable de calor y contaminación. Estos cambios afectan al conjunto de sus condiciones ambientales, pero de manera especial al clima, cuya consecuencia más perceptible es el desarrollo de la denominada isla de calor urbano (ICU), que se define por la mayor temperatura del aire del centro de la ciudad en relación con el espacio rural circundante (Oke, 1995). La ICU es un fenómeno de escala local o, a lo sumo regional, que puede suponer diferencias térmicas, en noches de viento en calma o muy débil y cielo despejado, de más de 7-8ºC en las grandes urbes: p. ej. New York (Gedzelman *et al*., 2003), Londres (Kolokotroni y Giridharan, 2008), Paris (APUR, 2012), Moscú (Lokoshchenko, 2014) o Berlín (Fenner, 2014). Por el contrario, al aumentar la velocidad del viento la ICU disminuye y llega hacerse prácticamente imperceptible. Algunos autores han sugerido la existencia de una "velocidad límite del viento" a partir de la cual la ICU es nula (Oke y Hannell, 1970). Las velocidades del viento de 35-40 km son valores de referencia de este límite crítico encontrado para ciudades muy desiguales como Seúl (Kim y Baik, 2002) y Salamanca (Alonso *et al.,* 2007). En Zaragoza es superior, y se parece más al límite de 50 Km/h encontrado en otras ciudades, como por ejemplo Buenos Aires (Camilloni y Barrucand, 2012). No obstante, se trata de valores muy dispares, no siempre fáciles de precisar, que están relacionados con las características morfológicas de cada ciudad. La intensidad de la ICU y su configuración tienen que ver con el tamaño, la población y la latitud de la ciudad (Hogan y Ferrick, 1988), y por lo general, es mayor en verano que en invierno (Morris *et al*., 2001). Es muy evidente durante la noche, y puede llegar a desaparecer durante el día (Jauregui, 1997; Steinecke, 1999).

La ICU es una característica climática observada científicamente desde el siglo XIX en los trabajos pioneros de Howard (1818) sobre la ciudad de Londres. Desde entonces la preocupación por el conocimiento del clima urbano ha ido en aumento, y en la actualidad ocupa un lugar privilegiado como tema de estudio por la trascendencia económica y social que tiene el fenómeno urbano y la incidencia del clima sobre el confort, la salud humana y la calidad de vida (p. ej. Alcoforado y Matzarakis, 2010; Taylor *et al.,* 2015; Román *et al.,* 2017). Este interés aplicado es el que está en el origen de las primeras investigaciones del clima de la ciudad de Zaragoza, centradas primero en el análisis de la relación clima-contaminación atmosférica (Ascaso, 1969) y más tarde en las características bioclimáticas y confort urbanos (Calvo-Palacios, 1976).

Los trabajos siguientes han progresado en dos niveles de análisis: uno inicial, de estudio de los rasgos generales y patrones espaciales de las islas de calor y de sequedad, y otro más reciente, que contempla los principales factores que influyen sobre el clima de la ciudad (Cuadrat *et al.,* 1993; De la Riva *et al*., 1997; Cuadrat *et al.,* 2005; López Martín, 2011; Cuadrat *et al.*, 2015). La metodología de trabajo se apoyó en los datos procedentes de los observatorios meteorológicos, los transectos urbanos en automóvil y el uso de imágenes de satélite. Sin embargo, esta información no permite un seguimiento continuo de la ICU, ni conocer la acción relevante que sobre la misma tienen buen número de factores, como es el caso particular del viento en Zaragoza, donde sopla con reiteración e intensidad. Para avanzar en la investigación, el año 2015 se monitorizó la ciudad con una amplia red de sensores termohigrométricos ubicados en lugares seleccionados del interior urbano y área rural circundante que permiten un examen más preciso de muchos rasgos del clima urbano todavía poco estudiados. Con estos nuevos datos, el objetivo de esa investigación es analizar en detalle la intensidad y la variabilidad en el

tiempo de la isla de calor, y evaluar la acción del viento como muy significativo factor condicionante de la misma.

2. Fuentes y Metodología

2.1. Área de estudio

Zaragoza es una ciudad compacta y multifuncional, de 716.000 habitantes (Instituto Nacional de Estadística de 2020), situada al Nordeste de España, en la zona central de la Depresión del Ebro, asentada sobre ambas márgenes de dicho río (Fig. 1). El área urbana ocupa 967 km^2 de una amplia zona llana, con variaciones topográficas inferiores a 100 metros entre el eje del río Ebro y la zona más elevada de la ciudad, denominada Pinares de Venecia, a 280 metros de altitud. La textura urbana es variada, pero no tiene edificios de gran altura, sólo unos pocos superan los 30 m. Tradicionalmente ha ido creciendo a partir de un extenso núcleo histórico, de alta densificación de edificios, calles estrechas y plazas sin formas definidas, en torno al cual se han desarrollado los ensanches y los nuevos barrios que añaden complejidad a la trama urbana. En los últimos años la expansión de la ciudad se realiza alrededor de nuevos suelos urbanizables de tipo residencial de baja y media densidad en el exterior del área urbana, y la recualificación de áreas estratégicas ubicadas en el interior del casco histórico.

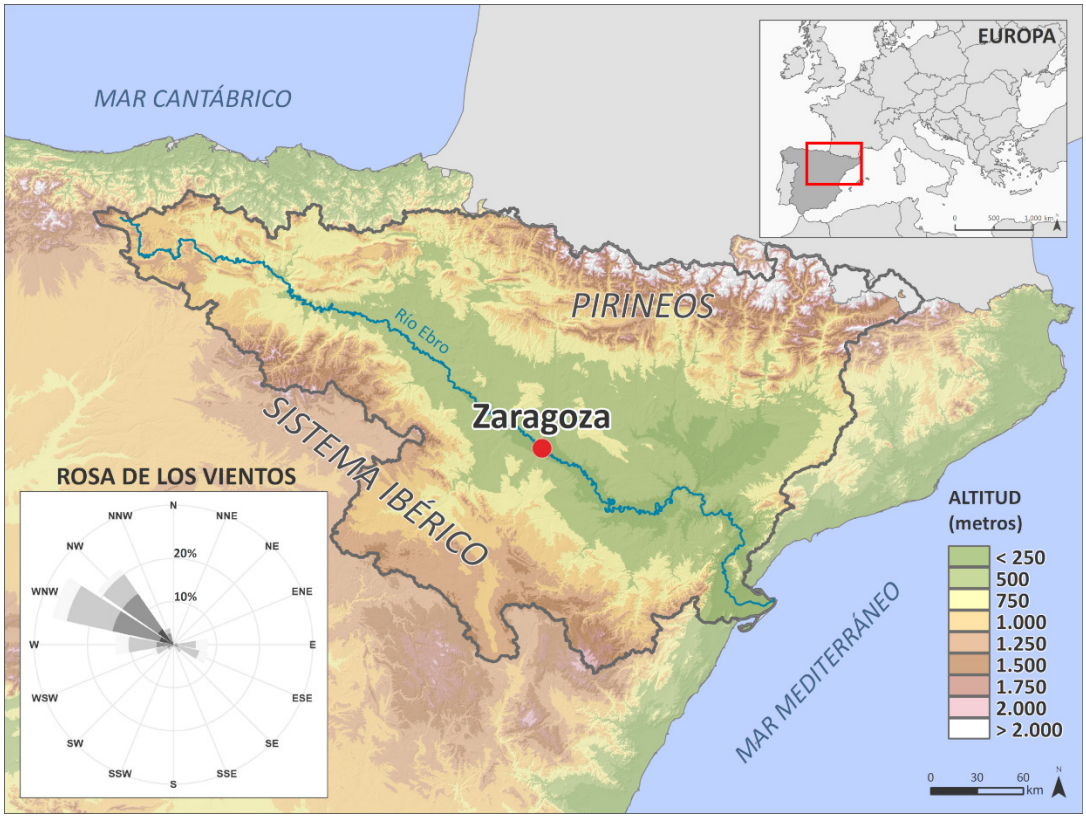

Figura 1. Mapa de localización de Zaragoza y rosa de vientos de la ciudad.

La estructura viaria muestra un esquema radial constituido por cuatro cinturones urbanos concéntricos, vías convergentes al núcleo o radiales y ejes transversales mediante los cuales se realiza la conexión inter e intrazonal de la ciudad. La articulación de este viario está condicionada por el cruce del río Ebro que únicamente puede realizarse a través de los puentes que conectan sus márgenes y que unen los distintos barrios. Por sus grandes avenidas circulan a diario más de 30.000 vehículos; sin embargo, la organización de la red viaria evita fuertes concentraciones de tráfico en el núcleo central.

El clima es mediterráneo, con marcada influencia continental, caracterizado por la escasez de las precipitaciones (326 mm anuales), el contraste entre un largo y frío invierno (6,2ºC es la temperatura media de enero) y un cálido y continuado verano (24,3ºC), y reiteradas situaciones anticiclónicas, de cielo despejado y viento en calma, que propician la formación de la isla de calor. El viento tiene gran significación por la frecuencia y por la intensidad que alcanza, superior en ocasiones a 100 km/h, consecuencia de un claro efecto orográfico (Cuadrat, 1999): los diferentes flujos de aire de cualquier procedencia se canalizan en el corredor abierto entre dos sobresalientes alineaciones montañosas, los Pirineos al Norte y el Sistema Ibérico al Sur, y adquiere dos claras componentes, Noroeste y Sureste (Fig. 1).

2.2. Bases de datos

Para el desarrollo de este trabajo se ha utilizado la información horaria de temperaturas desde febrero del año 2015 a marzo de 2020, procedente de la red de sensores termohigrométricos instalados por el Departamento de Geografía de la Universidad de Zaragoza, en colaboración con el Departamento de Medio Ambiente del Ayuntamiento de Zaragoza y con la Agencia Estatal de Meteorología. Los aparatos de medición están colocados en postes públicos, aproximadamente a 3 m del suelo. Son del tipo HOBO Pro v2, con sensor de temperatura y humedad, y un data-logger para el almacenamiento de la información. Su rango de funcionamiento en las temperaturas es de los -40ºC a los 70ºC, con una precisión de 0,04ºC y una resolución de 0,02 grados. Para protegerlos de la radiación solar directa y del efecto de la lluvia, los sensores están colocados dentro de un soporte tipo M-RSA.

La red está formada por 24 sensores, ubicados en lugares representativos de distintos ambientes de la urbe y su periferia inmediata siguiendo los criterios definidos por Steward y Oke (2012), que clasifica los espacios urbanos en Zonas Climáticas Locales (Local Climate Zones, LCZ) según la trama de la ciudad (Fig. 2). Los datos registrados por esta red han sido sometidos a un riguroso control de calidad para evaluar la presencia de lagunas de información, datos aberrantes e inhomogeneidades. Para ello se ha creado un paquete de funciones en lenguaje R, de código abierto, que consiguen minimizar la presencia de errores en la base de datos y garantizan su consistencia. Los pasos seguidos han sido los siguientes:

1) En primer lugar, se ha realizado la detección de datos repetidos y observaciones anormales. Para ello se han aplicado los métodos de Tukey (rango intercuartílico) y Chauvenet (desviación típica) para evitar marcar como outliers datos que son correctos. Además, se ha utilizado como referencia la media para cada hora del año de todos los sensores para comparar con cada dato y eliminar posibles datos aberrantes.

2) A continuación, se ha analizado la variabilidad horaria de las observaciones con la finalidad de evitar posibles saltos con valores ilógicos en la serie temporal de datos. Se han encontrado descensos térmicos bruscos de más de 10ºC, sobre todo en verano, provocados por situaciones atmosféricas con episodios de tormentas fuertes; por este motivo, se estableció un umbral límite de 8ºC para señalar los datos erróneos, y además se hizo una completa revisión de los mismos para evitar excluir datos reales.

Mayores detalles sobre el proceso aplicado a la base de datos pueden consultarse en Tejedor *et al.* (2016).

La base de datos creada es la fuente básica de esta investigación, y ha permitido también las primeras aproximaciones al análisis de las olas de calor y el confort térmico (Tejedor *et al.*, 2016), además del estudio de las relaciones entre los extremos térmicos y las enfermedades cardiorrespiratorias (Barrao *et al.,* 2020). Para determinar la influencia de la velocidad del viento sobre la intensidad de la isla de calor zaragozana se han utilizado los datos horarios del periodo 2015-2020 del observatorio

oficial de la Agencia Estatal de Meteorología, instalado en el aeropuerto de Zaragoza, a 249 m de altitud s.n.m, y a 10 km de distancia de la capital. El anemocinemógrafo climatológico se encuentra a 10 m del suelo, en área despejada y libre de obstáculos.

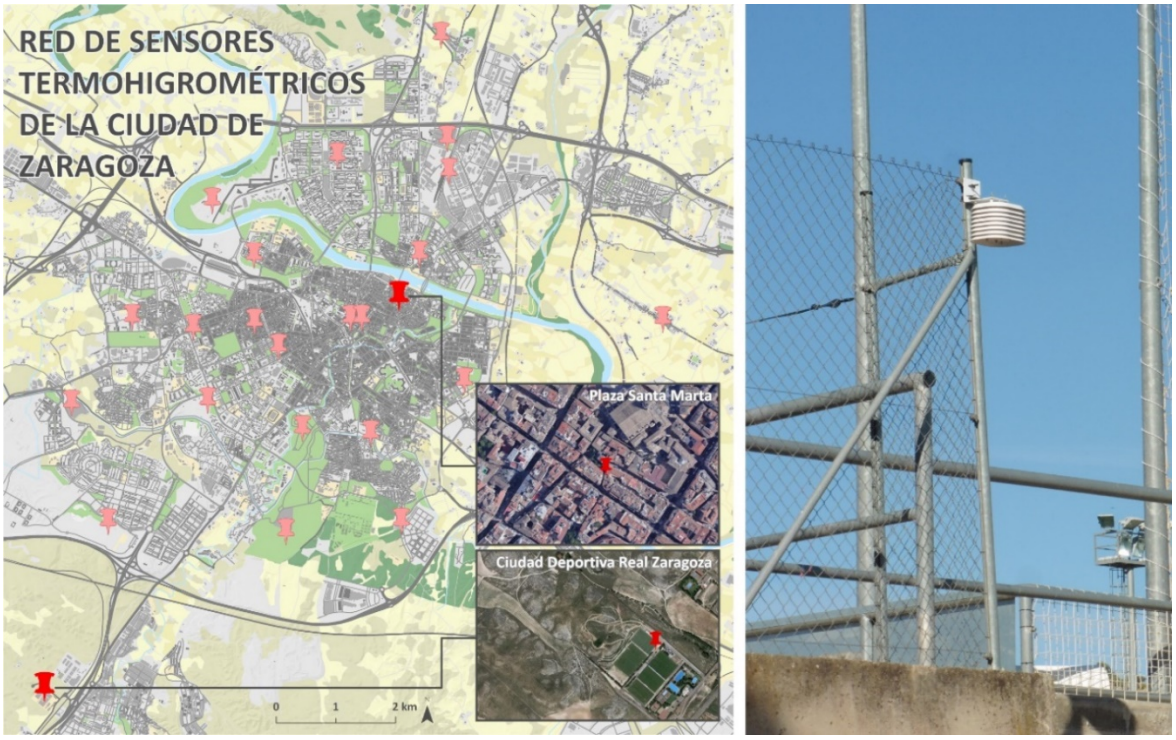

Figura 2. A la izquierda, red de sensores termo-higrométricos de la ciudad de Zaragoza y detalle de la localización del observatorio urbano (Plaza de Santa Marta) y del observatorio rural (Ciudad Deportiva del Real Zaragoza) utilizados en el trabajo. Fuente: Imagen extraída de Google Earth. A la derecha, soporte protector del termohigrómetro instalado en la Ciudad Deportiva del Real Zaragoza.

2.3. Metodología

La isla de calor urbana resulta del hecho de que la temperatura del aire de la ciudad suele ser más elevada que la temperatura del espacio no urbano próximo (Oke, 1996). Siguiendo la misma fuente, la diferencia térmica entre el sector más cálido de la ciudad y el espacio rural limítrofe define la intensidad de la isla de calor.

Formalmente:

$$\Delta T_{u-r} = T_u - T_r$$

donde ΔT_{u-r} es la intensidad de la isla de calor, T_u la temperatura del punto urbano y T_r la temperatura del punto rural.

Como han señalado Steward (2010) y Martín-Vide *et al.* (2015a), se debe prestar especial atención a la selección de estos puntos y procurar que sean térmica y geográficamente comparables para que la diferencia entre ambos exprese el efecto de la ciudad, que constituye nuestro objetivo. En el presente estudio, se ha utilizado la información térmica de dos sensores: uno urbano, localizado en la Plaza de Santa Marta, y otro rural, instalado en la Ciudad Deportiva del Real Zaragoza.

1) El sensor de la Plaza de Santa Marta es puramente urbano, en pleno centro histórico, muy representativo del corazón de la ciudad, a 214 m. de altitud (24 m superior al cauce del río Ebro), en una LCZ del tipo *compact mid-rise* (LCZ-2), espacio densamente urbanizado, edificios de mediana altitud (4-5 plantas), poco arbolado, suelo en su mayor parte pavimentado y tráfico

muy restringido. Como indican todos los estudios previos, forma parte del entorno más cálido de Zaragoza (Cuadrat *et al.*, 2005; López Martín, 2011).

2) El sensor de la Ciudad Deportiva del Real Zaragoza es representativo del medio rural. Se localiza a 3 km de distancia, al sudoeste de la ciudad, a una altitud 40 m superior al sensor urbano. Se localiza en un espacio abierto, en una LCZ del tipo C (*Bush, scrub*), con arbustos y árboles leñosos cortos, contiguos a unas instalaciones deportivas y prácticamente sin tráfico rodado. Comparte las condiciones climáticas generales de Zaragoza y está expuesta al viento dominante del Oeste sin interferencias de la ciudad.

El cálculo de la intensidad de la ICU, su frecuencia y sus variaciones temporales se ha realizado con los datos horarios del periodo 2015-2019. En el caso de las variaciones diarias, debido al amplio rango de intensidades, los datos se dividieron en observaciones diurnas (10:00 a 18:00 h) y observaciones nocturnas (20:00 a 06:00 h). Al seleccionar estos momentos se evitan parcialmente las condiciones de radiación que pueden causar anomalías térmicas debido a las sombras que se proyectan al amanecer y al atardecer.

3. Resultados y Discusión

3.1. Frecuencia de la isla de calor urbana

Para el conjunto de los cinco años analizados se calculó la distribución de frecuencias de los valores de las diferencias entre las temperaturas horarias del observatorio urbano (Plaza de Santa Marta) y del observatorio rural (Ciudad Deportiva), y se trazó el histograma correspondiente que se muestra en la Figura 3. La temperatura en la Plaza de Santa Marta fue inferior a la de la Ciudad Deportiva solo el 16 % de las horas; en las 84 % restantes la temperatura fue igual o superior en la ciudad, lo cual indica claramente la existencia de una anomalía térmica positiva muy visible en la urbe respecto al medio rural circundante.

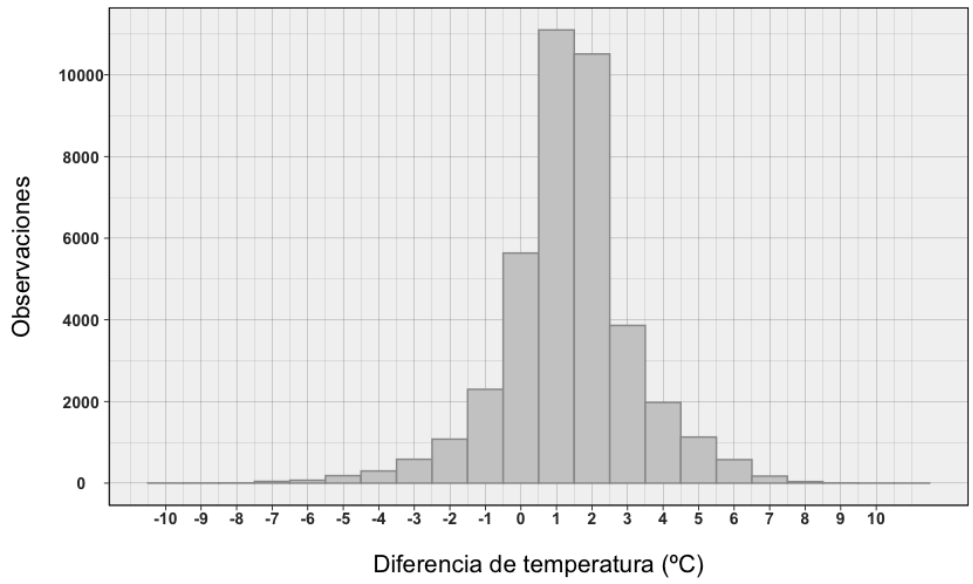

Figura 3. Histograma de las diferencias entre las temperaturas horarias del observatorio urbano (Plaza de Santa Marta) y las del observatorio rural (Ciudad Deportiva), en el período 2015-2020. Eje de abscisas: diferencias de temperatura, en ºC; eje de ordenadas: número absoluto de casos.

Los intervalos de clase de mayor frecuencia son 1º y 2ºC, con el 29 % de casos. El dato es digno de destacar y es acorde con los promedios esperados en una ciudad de estas características (Fernández *et al.,* 1998). El resto de intervalos es bastante menor, aunque en varios momentos las diferencias ciudad-campo han superado los 8ºC; y en el caso excepcional del día 9 de junio de 2019 se llegaron a alcanzar los 10,5ºC, a las 20.00h, como consecuencia de un particular episodio tormentoso, acompañado de precipitación y descenso de las temperaturas, que tuvo mayor incidencia en el sur de la ciudad. Con bastante menos frecuencia el centro urbano está más frío que el entorno rural. En este caso, las diferencias más habituales son de 1º y 2ºC en favor del medio rural; aunque también se han observado anomalías térmicas negativas de hasta 5ºC, en el 2% de las ocasiones, o cercanas a los 6ºC, en algún momento muy puntual.

3.2. Intensidad de la isla de calor urbana

La isla de calor es un fenómeno esencialmente nocturno, cuando la energía almacenada en el interior de la ciudad es remitida a la atmósfera limitando su enfriamiento. Por el contrario, durante el día las diferencias campo-ciudad se reducen y la isla puede llegar a desaparecer e incluso provocar una verdadera isla de frescor. Estos contrastes térmicos están relacionados con el distinto ritmo de calentamiento y enfriamiento de las áreas urbanas y rurales, y lógicamente con el ciclo diario y anual de la radiación solar.

En la capital zaragozana la intensidad máxima de la isla de calor se alcanza a primeras horas de la noche, alrededor de las 21-22 horas (más del 70 % de los casos), con valores promedio superiores a los 2ºC (véase la Fig. 4); la intensidad de la isla disminuye lentamente hacia el amanecer y por la mañana desaparece con rapidez cuando la zona rural comienza a recibir radiación y el ascenso de la temperatura en ella aumenta más deprisa que en la ciudad. Durante las horas centrales del día, entre las 11 y 13 horas, el efecto de sombra de los edificios frente a la radiación más directa que recibe el medio rural, invierte la situación y se origina una débil isla de frescor, inferior a 1ºC. Por la tarde, la isla de calor se recupera al mismo ritmo que se produjo el descenso de la mañana, hasta llegar la noche, momento en que se inicia un nuevo ciclo. La evolución observada guarda consonancia con los resultados de estudios previos realizados de la ICU de Zaragoza (Cuadrat, 2004; López Martín, 2011), pero siempre con matices como consecuencia de las distintas fuentes utilizadas y los años estudiados.

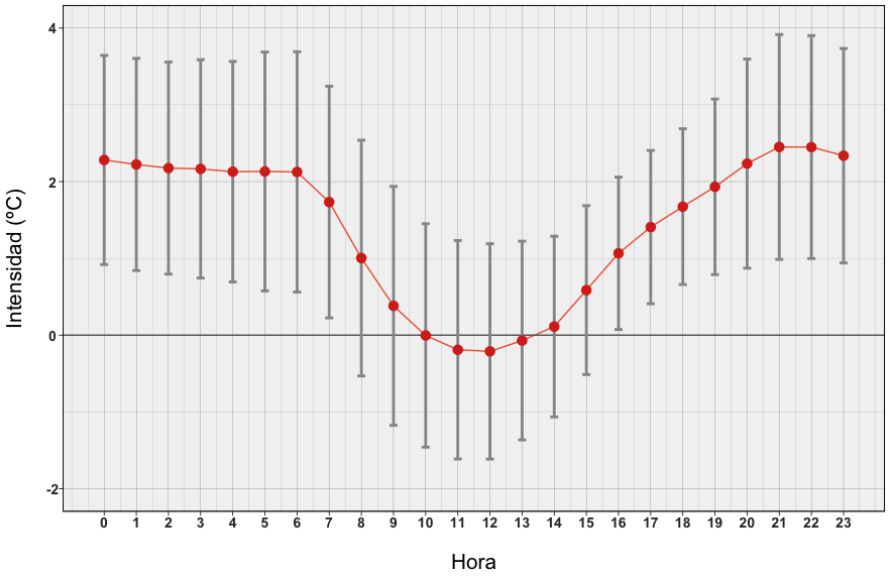

Figura 4. Variaciones horarias medias de la intensidad de la isla de calor (línea roja continua: media; líneas verticales: desviación estándar).

La división en observaciones diurnas (10:00 a 18:00 h) y observaciones nocturnas (20:00 a 06:00 h) revela más detalles de la variación diaria de la isla de calor porque elimina las horas cercanas al amanecer y al atardecer, cuando las condiciones de radiación pueden distorsionar las temperaturas. De hecho, dependiendo de la hora, el día, la estación y la disposición de los edificios, pueden surgir particularidades climáticas muy locales no relacionadas con los factores climáticos generales de la ciudad. En el periodo estudiado, la intensidad de la ICU es más elevada por la noche (1,7ºC) que por el día (0,9ºC). Como se observa en los diagramas de la Figura 5, durante las horas nocturnas el 50 % de la intensidad de la ICU cambia de 1,4ºC a 2,9ºC, mientras que durante el día lo hace de -0,2ºC a 1,5ºC. Se observa, además, mayor dispersión de los datos en el caso diurno, lo cual indica también la mayor variabilidad que en ese momento tiene la intensidad de la isla. Este patrón, con pocas variaciones, responde al esquema general explicado por Oke (1996), y se repite en trabajos similares publicados en ciudades tan diferentes como Lisboa (Lopes *et al.,* 2013; Alcoforado *et al.,* 2014) o Berlín (Fenner *et al.,* 2014), p. ej.; pero en todos los casos se concluye que estos resultados esconden grandes diferencias temporales y espaciales que exigen ser analizados con estudios de mayor detalle.

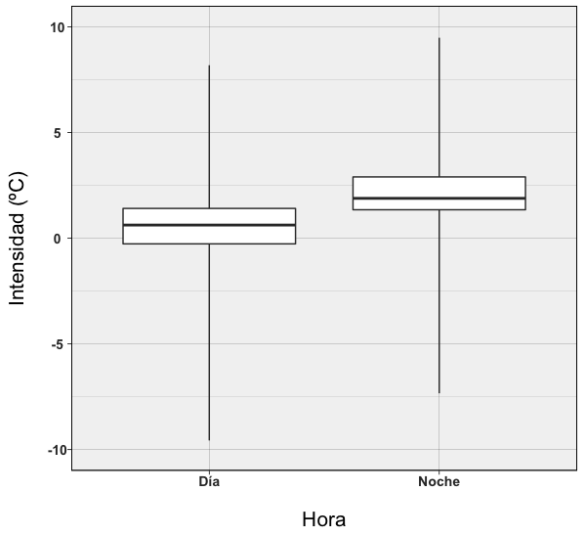

Figura 5. Variabilidad observada de la intensidad de la isla de calor urbana diurna (10:00 a 18:00 h) y nocturna (20:00 a 06:00 h) de la ciudad de Zaragoza.

3.3. Variabilidad estacional de la isla de calor urbana

Las diferencias de temperatura del aire entre el centro de la ciudad y el espacio rural de su entorno también muestran considerables variaciones estacionales. La característica principal es que las mayores diferencias ocurren en verano, se reducen en invierno y alcanzan los valores más bajos en primavera y otoño (Fig. 6). En los meses de junio, julio y agosto la intensidad de la isla de calor alcanza promedios de 2,5ºC, con máximos absolutos nocturnos de 8ºC. En esta época del año son frecuentes las situaciones atmosféricas anticiclónicas, acompañadas de muchas horas de sol, que unidas la capacidad de acumulación y también generación de calor de la ciudad, son la causa del incremento de la ICU. En sentido contrario, también es en este periodo cuando es más frecuente la formación de islas de frescor, próximas a -0,5ºC. Ocurre al final de la mañana, cuando la radiación solar incide de manera directa sobre el medio rural, mientras que las sombras proyectadas por los edificios se cruzan parcialmente con la radiación solar que llega al interior de la urbe; como consecuencia, la temperatura del aire aumenta con mayor lentitud dentro del contexto urbano en comparación con las áreas rurales. En invierno, las condiciones favorables a la formación de la ICU son menos comunes. De diciembre a febrero predominan también las situaciones anticiclónicas; sin embargo, la intensidad de la ICU es más débil y menos frecuente que en verano. Probablemente una de las causas principales sean las nieblas que se

forman en el Valle del Ebro por la estabilidad atmosférica, las cuales mitigan la radiación solar y las diferencias térmicas ciudad-campo. En otoño y primavera las intensidades de la ICU, por lo general, son menores.

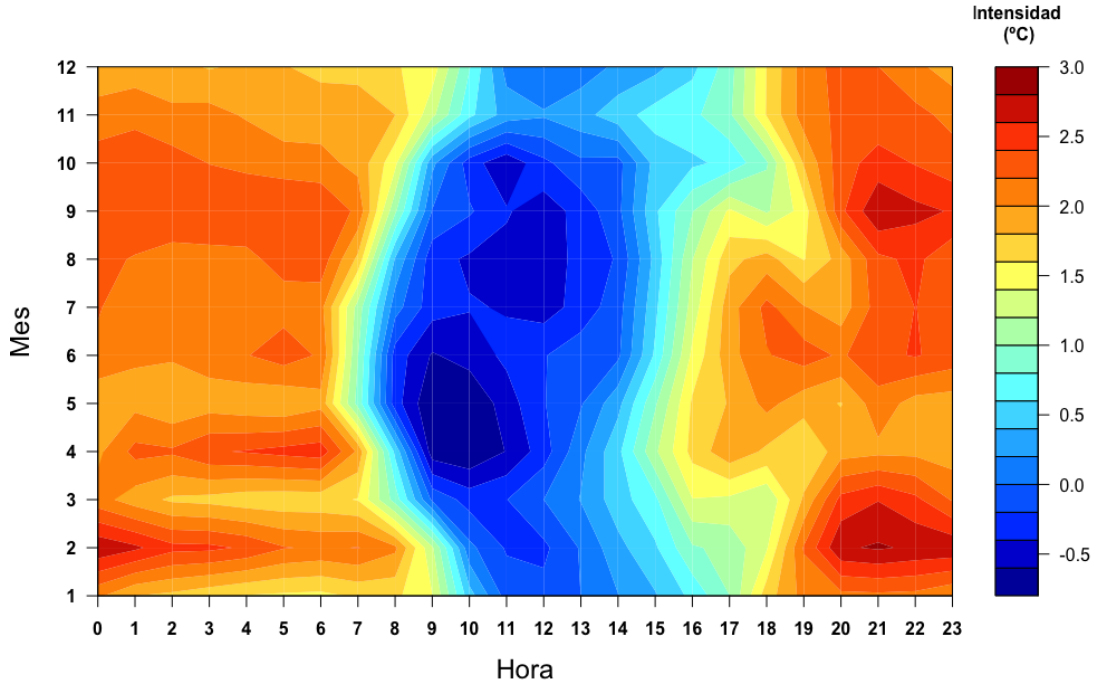

Figura 6. Intensidad media mensual y horaria de la isla de calor urbana en Zaragoza (2015-2020).

Estas diferencias estacionales se reconocen muy bien cuando se observa la evolución de la intensidad de la isla de calor en los dos meses extremos del año, enero y junio (Fig. 7). La amplitud del ciclo diario en el mes de junio es superior al de enero como resultado de las mayores intensidades de la isla de calor por la noche y una apreciable isla de frescor por el día. En junio, poco después del amanecer, la temperatura del medio rural, por la menor modificación de la radiación incidente y práctica ausencia de sombras, está en promedio unas décimas de grado más elevada que el interior de la ciudad y se genera una isla de frescor durante 3-4 horas. La situación cambia al final de la tarde y por la noche. En este momento, la gran inercia calórica de la ciudad retrasa el enfriamiento del aire y se crea una permanente isla de calor de varias horas, cuyos valores rebasan los 2,5ºC. En enero el ciclo es bastante similar, pero las diferencias térmicas campo-ciudad son menores: la isla de calor alcanza una intensidad de 2,2ºC unas pocas horas al comienzo de la noche, y la isla de frescor de mediodía es casi nula.

Coinciden estos resultados con la mayoría de los estudios de clima urbano: la ICU es un fenómeno nocturno, cuyo valor máximo aparece pocas horas después de la puesta del sol y puede perdurar hasta cerca del amanecer. Estacionalmente, en Zaragoza la intensidad de la isla de calor se incrementa en verano, al igual que ocurre en buen número de ciudades; sin embargo, existen notables diferencias según las regiones, no siempre fáciles de explicar: en Madrid (Fernández, 2009; Yagüe *et al*., 1991) y Lisboa (Alcoforado *et al.,* 2014), por ejemplo, la ICU es mayor en verano; en Barcelona (Martín-Vide *et al.,* 2015b) es más intensa en invierno; y en ocasiones, existe bi-estacionalidad, con máximos entre otoño-verano, como ocurre en Nueva York (Gedzelman *et al.,* 2003). De hecho, la variación estacional tiende a depender de la ubicación de la ciudad, con sus factores atmosféricos y geográficos condicionantes; y aunque existen muchos puntos en común, el clima urbano es bastante específico para cada ciudad.

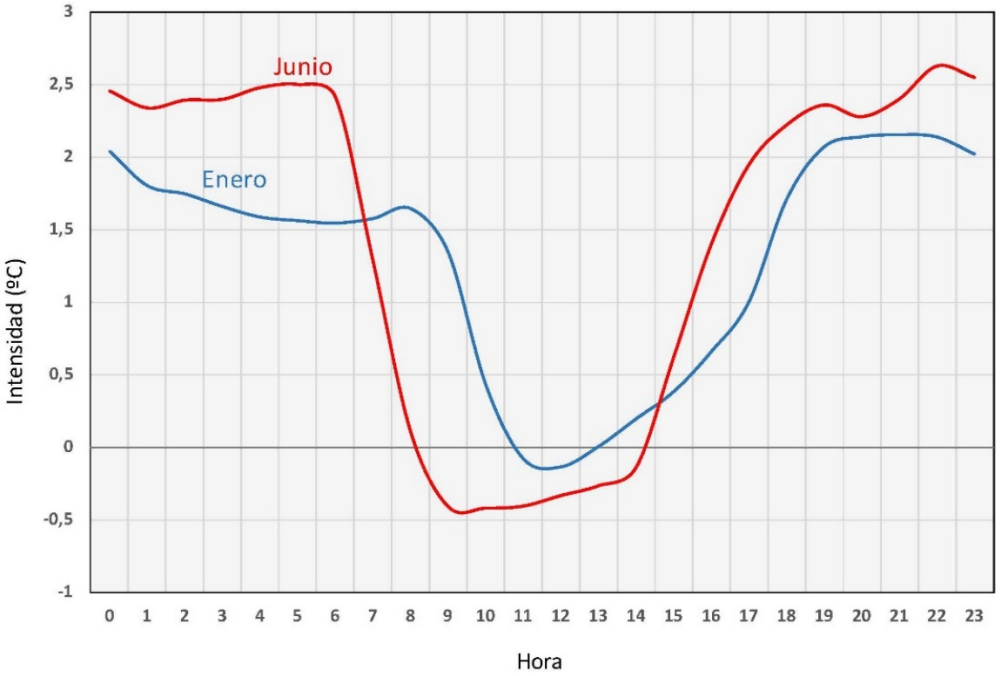

Figura 7. Variación horaria de la isla de calor urbana en junio y enero (periodo 2015-2020).

3.4. La isla de calor y la acción del viento

La ICU está condicionada por muchos factores, pero de manera especial por el viento, del cual depende una parte fundamental de sus cambios de magnitud y frecuencia. La intensidad máxima de la isla de calor se alcanza en noches de tiempo estable, viento en calma o flojo y cielo despejado, características que corresponden a situaciones atmosféricas de tipo anticiclónico; en sentido opuesto, el tiempo perturbado, la nubosidad, lluvia y viento son factores negativos que debilitan la isla y pueden hacerla desaparecer. En el caso de Zaragoza, el viento es uno de los elementos más genuinos del clima por la frecuencia con la que sopla y por la intensidad que en ocasiones alcanza. Sus mecanismos son, especialmente, un efecto topográfico: los diferentes flujos de aire de cualquier procedencia se canalizan y aumentan su velocidad en el corredor abierto entre los Pirineos y el Sistema Ibérico, adquiriendo dos claras componentes oeste-noroeste, al que se denomina cierzo, y este-sureste, llamado bochorno. Por esta razón, las rosas de los vientos se deforman y alargan en el sentido NO-SE, que es precisamente el de la dirección del rio Ebro (Fig. 1).

La influencia de la velocidad del viento sobre la ICU se ilustra en la Figura 8, y confirma que los valores más altos de la isla de calor se alcanzan con viento en calma o muy débil. En efecto, en ausencia de viento o soplo de una ligera brisa, las diferencias térmicas campo-ciudad alcanzan su máximo desarrollo, más de 7ºC en ocasiones, y tiene promedios de 2,7ºC (Tabla 1). Las velocidades bajas, inferiores a 10 km/h, implican una alta variabilidad, aunque siempre dominando las intensidades positivas. A partir de este valor se produce una reducción esperada de la intensidad de la ICU, pero aún puede sobrepasar los 4ºC y mantiene promedios de 1,57ºC. Con velocidades superiores a 50 km/h la ICU prácticamente desaparece, aunque no llega a ser nula, lo cual significa que el efecto refugio de la ciudad, con su morfología y sus edificios, es sin duda importante. En general, la tasa media de descenso de la ICU es de -0,02ºC por cada km/h de incremento en velocidad del viento, aunque con gran variabilidad por debajo de 10 km/h y muy estable por encima de 30 km/h, mostrando una distribución más similar a una exponencial negativa que a una relación completamente lineal.

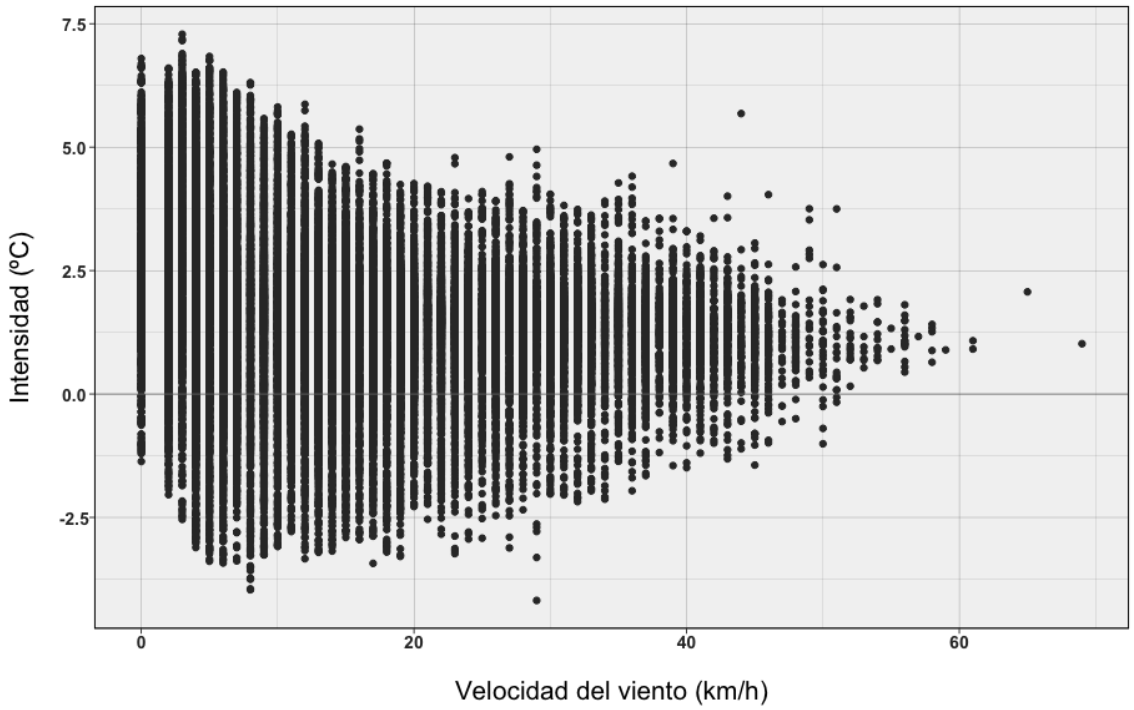

Figura 8. Intensidad de la isla de calor urbana de Zaragoza y su relación con la velocidad del viento.

Tabla 1. Velocidades del viento y valores promedio de la isla de calor. (VEL: velocidad del viento en Km/h. MED: intensidad media de la isla de calor. SD: desviación estándar. OBS: número de observaciones. CV: coeficiente de variación.).

VEL	MED	SD	OBS	CV
0	2,70	1,72	821	63,82
2 - 5	2,35	1,96	5113	83,16
5 - 10	1,57	1,75	6884	111,19
10 - 15	1,27	1,40	5938	110,26
15 - 20	1,14	1,27	4659	111,39
20 - 25	1,18	1,14	3394	96,93
25 - 30	1,22	1,05	3055	86,22
30 - 50	1,17	0,85	4573	72,65
> 50	1,12	0,42	87	37,85

4. Conclusiones

La ICU de Zaragoza reúne todas las generalizaciones empíricas indicadas por Oke (1982) en el ámbito del clima urbano: 1) La intensidad de la isla de calor urbana es mayor por la noche. 2) La isla de calor urbana puede desaparecer durante el día y la ciudad puede ser más fresca que los alrededores rurales. 3) La intensidad de la isla de calor urbana es mayor en verano. 4) La isla de calor urbano disminuye al aumentar la velocidad del viento.

Este fenómeno no es constante ni tiene siempre la misma magnitud: factores geográfico-urbanos, factores meteorológicos, referidos al estado del tiempo, y factores temporales, como la hora del día o la estación del año, son los que definen sus variaciones y rasgos esenciales. En la capital zaragozana, en este periodo de estudio 2015-2020, la temperatura en el centro de la ciudad es con mucha frecuencia 1 o 2ºC más elevada que en el entorno, y en ocasiones muy puntuales, ha llegado a superar los 8ºC. Las mayores diferencias entre el observatorio urbano y el observatorio rural se alcanzan 2-3 horas más tarde de la puesta de sol, persisten varias horas (en particular en verano) y disminuyen lentamente hacia el amanecer.

De estos valores se concluye, asimismo, otro rasgo muy común en los núcleos urbanos: en el interior de Zaragoza hay menor contraste térmico, pues las amplitudes diarias son menores; por el contrario, en el medio rural se comprueba una mayor amplitud, ya que en los momentos centrales del día las temperaturas suelen ser algo más altas y por la noche sensiblemente más frías.

La influencia del viento sobre la ICU es también muy evidente. En situaciones de calma atmosférica o ligera brisa la isla de calor alcanza su máxima intensidad, pero se debilita claramente conforme aumenta la velocidad del viento. El valor de 50 km/h puede fijarse como referencia de límite crítico a partir del cual la ICU se vuelve nula; no obstante, siempre permanece una débil isla por el efecto abrigo que genera la ciudad frente al medio rural.

Un aspecto a resaltar es la importancia que tiene la selección adecuada de los observatorios meteorológicos utilizados para comparar las temperaturas de la ciudad y del espacio no urbano próximo. Posiblemente es una de las tareas más difíciles en el análisis de la ICU. En este estudio se han elegido dos puntos que consideramos térmica y geográficamente correctos, porque respetan los requisitos exigidos en este tipo de estudios: el primero está ubicado en un lugar central y denso de la urbe, y el segundo en un medio rural, abierto y alejado de la influencia urbana. Lógicamente, la elección de otros puntos de observación puede introducir pequeños cambios en los resultados finales, sin embargo, los rasgos fundamentales de la isla de calor están bien definidos en esta investigación.

Los resultados de esta investigación suponen un paso más en el conocimiento de la ICU de Zaragoza y confirman la importancia del fenómeno en términos de calentamiento nocturno en el centro de la ciudad por contraste con el espacio periurbano. Buena parte de los estudios previos de la ICU zaragozana se han apoyado en los registros térmicos directos obtenidos en recorridos del área urbana y su periferia. Esta metodología utilizada hasta ahora ha servido para determinar la configuración de la isla de calor, conocer la ubicación de los valores máximos de la misma y observar la diversidad microclimática de la ciudad. La recién instalación de la red de sensores termohigrométricos amplía las posibilidades de estudio y ha permitido en esta investigación estimar con cierto detalle la intensidad de la ICU y analizar su variabilidad en el tiempo; además de explicar la importante acción condicionante del viento. La suma de todo este conocimiento facilita emprender nuevos objetivos por las implicaciones que esta característica climática urbana tiene sobre cuestiones ambientales relevantes como el confort térmico, la salud humana, el consumo de energía o la calidad de vida en nuestras ciudades.

Referencias

Alcoforado, M.J., Matzarakis, A. 2010. Planning with urban climate in different climatic zones. *Geographicalia* 57, 5-39. http://doi.org/10.26754/ojs_geoph/geoph.201057808

Alcoforado, M.J., Lopes, A., Lima, E., Canário, P. 2014. Lisboa Heat Island. Statistical study (2004-2014). *Finisterra* 98, 61-80. https://doi.org/10.18055/Finis6456

Alonso, M.S., Fidalgo, M.R., Labajo, J.L. 2007. The urban heat island in Salamanca (Spain) and its relationship to meteorological parameters. *Climate Research* 34, 39-46. https://doi.org/10.3354/cr034039

Ascaso, A. 1969. Contaminación y contaminadores atmosféricos. El problema en Zaragoza. *Las Ciencias* 1, 22-34.

Barrao, S., Cuadrat, J.M., Saz, M.A., Serrano-Notivoli, R., Tejedor, E. 2020. Olas de calor y olas de frío en la ciudad de Zaragoza (España) y sus efectos sobre las enfermedades cardiorrespiratorias, 2011-2015. En: *Crisis y espacios de oportunidad. Retos para la Geografía.* Asociación Española de Geografía, Valencia, págs. 343-358. ISBN: 978-84-947 787-2-8.

Calvo-Palacios, J.L. 1976. Aportación metodológica al estudio geográfico del microclima urbano. *Boletín de la Real Sociedad Geográfica* 42, 95-110.

Camilloni, I., Barrucand, M. 2012. Temporal variability of the Buenos Aires, Argentina, urban heat island. *Theoretical and Applied Climatology* 107, 47-58. https://doi.org/10.1007/s00704-011-0459-z

Cuadrat, J.M., Vicente-Serrano, S., Saz, M.A. 2005. Los efectos de la urbanización en el clima de Zaragoza (España): la isla de calor y sus factores condicionantes. *Boletín de la AGE* 40, 311-327. https://bage.age-geografia.es/ojs/index.php/bage/article/view/2019

Cuadrat, J.M. 2004. Patrones temporales de la isla de calor urbana de Zaragoza. En: M.C. Faus (Coord.), *Aportaciones geográficas en homenaje al profesor Higueras*. Universidad de Zaragoza. Zaragoza, págs. 63-70. ISBN: 84-96214-32-X.

Cuadrat, J.M. 1999. El clima de Aragón*.* Institución Fernando El Católico. Zaragoza. ISBN 84-88305-72-9.

Cuadrat, J.M., De La Riva, J., López, F., Martí, A. 1993. El medio ambiente urbano en Zaragoza. Observaciones sobre la isla de calor. *Anales Universidad Complutense* 13, 127-138. https://revistas.ucm.es/index.php/AGUC/article/view/AGUC9393110127A

Cuadrat, J.M., Vicente-Serrano, S., Saz, M.A. 2015. Influence of different factors on relative air humidity in Zaragoza, Spain. *Frontiers in Earth Science* 3 (10). https://doi.org/10.3389/feart.2015.00010

De La Riva, J., Cuadrat, J.M., López, F., Martí A. 1997. Aplicación de las imágenes Landsat TM al estudio de la isla de calor térmica de Zaragoza. *Geographicalia* 35, 24-36. https://doi.org/10.26754/ojs_geoph/geoph.1997351701

Fenner, D., Meier, F., Scherer, D., Polze, A. 2014. Spatial and temporal air temperature variability in Berlin, Germany, during the years 2001-2010. *Urban Climate* 10, 308-331. https://doi.org/10.1016/j.uclim.2014.02.004

Fernández, F. 2009. Ciudad y cambio climático: aspectos generales y aplicación al área metropolitana de Madrid. *Investigaciones Geográficas* 49, 173-195. https://doi.org/10.14198/INGEO2009.49.09

Fernández, F., Galán, E., Cañada, R. 1998. *Clima y ambiente urbano en ciudades ibéricas e iberoamericanas.* Editorial Parteluz, 215 p. Madrid, ISBN: 84-8230-016-4.

Gedzelman, S.D., Austin, S., Cermak, R. N., Stefano, R., Partridge, S., Quesenberry, S., Robinson, D.A. 2003. Mesoscale aspects of the Urban Heat Island around New York City. *Theoretical and Applied Climatology* 75, 29-42. https://doi.org/10.1007/s00704-002-0724-2

Hogan, A.W., Ferrick, M.G. 1988. Observations in nonurban heat islands. *Journal of Applied Meteorology* 37, 232-236. https://doi.org/10.1175/1520-0450(1998)037<0232:OINHI>2.0.CO;2

Howard, L. 1818. *The Climate of London*. Longman, London., 221 p.

Jauregui, E. 1997. Heat island development in Mexico City. *Atmospheric Environment* 31, 3821-3831. https://doi.org/10.1016/S1352-2310(97)00136-2

Kim, Y.H., Baik, J.J. 2002. Maximum urban heat island intensity in Seoul. *Journal of Applied Meteorology* 41, 651-659. https://doi.org/10.1175/1520-0450

Kolokotroni, M., Giridharan, R. 2008. Urban heat island intensity in London: an investigation of the impact of physical characteristics on changes in outdoor air temperature during summer. *Solar Energy* 82, 986-998. https://doi.org/10.1016/j.solener.2008.05.004

Lokoshchenko, M.A. 2014. Urban heat island in Moscow. *Urban Climate* 10 (3), 550-562. https://doi.org/10.1016/j.uclim.2014.01.008

Lopes, A., Alves, E., Alcoforado, M.J., Machete, R. 2013. Lisbon Urban Heat Island Updated: New Highlights about the Relationships between Thermal Patterns and Wind Regimes. *Advances in Meteorology* 15, 1-15. https://doi.org/10.1155/2013/487695

López-Martín, F. 2011. *Clima urbano y ciudad. El caso de Zaragoza*. Universidad San Jorge-Colegio de Geógrafos. Zaragoza, 118 p. ISBN: 978-84-615-2098-5.

Martín-Vide, J., Sarricolea, P., Moreno-García, M.C. 2015a. On the definition of urban heat island intensity: the "rural" reference. *Frontiers in Earth Science* 3, 3 p. https://doi.org/10.3389/feart.2015.00024

Martín-Vide, J., Cordobilla, M.J., Artola, V.M., Moreno-García, M.C. 2015b. *La isla de calor en el Área Metropolitana de Barcelona y la adaptación al cambio climático.* Barcelona, Área Metropolitana de Barcelona. 120 p.

Morris, C.J., Simmonds, I., Plummer, N. 2001. Quantification of the influences of wind and cloud on the nocturnal urban heat island of a large city. *Journal of Applied Meteorology* 40, 169-182. https://doi.org/10.1175/1520-0450

Oke, T.R., 1982. The energetic basis of the urban heat island. *Quarterly Journal of the Royal Meteorological Society* 108, 1-24. https://doi.org/10.1002/qj.49710845502

Oke, T.R. 1995. *The heat island of the urban boundary layer: characteristics, causes and effects*. En: J.E. Cermak, A.G. Davenport, E.J. Plate, D.X., Viegas, (Eds.). *Wind Climate in Cities*. Kluwer-Academic Publ. Norwell, 81-107. ISBN 978-94-017-3686-2

Oke, T.R. 1996. *Boundary layer climates*. 2nd ed. Routledge, London. ISBN 0-415-04319-0.

Oke, T.R., Hannell, F.G. 1970. *The form of the urban heat island in Hamilton,* Canada. WMO Tech Note 108, págs. 113–126.

Román, E., Gómez, G., de Luxán, M. 2017. *Urban Heat Island of Madrid and its influence over Urban Thermal Comfort.* En: P. Mercader-Moyano (Ed.). *Sustainable Development and Renovation in Architecture, Urbanism and Engineering.* Springer, Cham, pp 415-425. http://doi.org/10.1007/978-3-319-51442-0_34

Steinecke, K. 1999. Urban climatological studies in the Reykjavík subartic environment, Iceland. *Atmospheric Environment* 33, 4157-4162. https://doi.org/10.1016/S1352-2310(99)00158-2

Stewart, I., Oke, T.R. 2012. Local Climate Zones for Urban Temperature Studies. *Bulletin American Meteorological Society* 93 (12), 1879-1900. http://doi.org/10.1175/BAMS-D-11-00019.1

Stewart, I.D. 2010. A systematic review and scientific critique of methodology in modern urban heat island literature. *International Journal of Climatology* 31, 200-217. https://doi.org/10.1002/joc.2141

Taylor, J., Wilkinson, P., Davies, M., Armstrong, B., Chalabi, Z., Mavrogianni, A., Symonds, P., Oikonomou, E., Bohnenstengel, S. 2015. Mapping the effects of urban heat island, housing, and age on excess heat-related mortality in London. *Urban Climate* 14, pp.517-528. http://doi.org/10.1016/j.uclim.2015.08.001

Tejedor, E., Cuadrat, J.M., Saz, M.A., Serrano-Notivoli, R., López, N., Aladrén, M. 2016. *Islas de calor y confort térmico en Zaragoza durante la ola de calor de julio de 2015.* En: J. Olcina, A. Rico, E. Moltó (Eds.). *Clima, sociedad, riesgos y ordenación del territorio*. Asociación Española de Climatología. Vol. 10. Alicante, págs. 141-152. http://doi.org/10.14198/XCongresoAECAlicante2016-13

Yagüe, C., Zurita, E., Martínez, A. 1991. Statistical analysis of the Madrid urban heat island. *Atmospheric Environment* 25B, 327-332. https://doi.org/10.1016/0957-1272(91)90004-X

Cuadernos de Investigación Geográfica *Geographical Research Letters*	2022	Nº 48	pp. 111-132	EISSN 1697-9540

http://doi.org/10.18172/cig.5049

IDENTIFICATION OF CHANGES IN THE RAINFALL REGIME IN CHIHUAHUA'S STATE (MÉXICO)

INDALECIO MENDOZA-URIBE

Instituto Mexicano de Tecnología del Agua, Jiutepec, México.

ABSTRACT. The impacts of Climate Change are not homogeneous globally or for a country or region as a whole. Consequently, it is essential to carry out studies to identify its effects in particular areas. Due to its geographical and topographic characteristics, Chihuahua's state is vulnerable to the adverse effects of Climate Change. The scarce availability of water resources leads to problems of social pressure and economic impact. This paper analyzes the alteration of the rainfall regime in Chihuahua's state and its association with Climate Change. For this, historical characterization is used; trend analysis using the Mann Kendall test; and calculation of 10 indices of climatic extremes proposed by the Group of Experts for Detection and Climate Change Indices for the precipitation variable. The results showed that the precipitation patterns in the south and southeast of Chihuahua's state have been gradually modifying, with a downward trend in annual accumulated and reduction of wet days. Still, in counterpart, there is a slight intensification of extreme rainfall. This fact added to the growing demand for water resources in the entity, requests for public policies for sustainable management and responsible use by users. Otherwise, there is a risk of experiencing negative effects associated with the over-exploitation of water, not only for the resource users but also for the environment.

Identificación de cambios en el régimen pluvial en el estado de Chihuahua, México

RESUMEN. Los impactos del Cambio Climático no son homogéneos de manera global ni para un país o región en su totalidad. En consecuencia, es imprescindible realizar estudios para identificar sus efectos en zonas particulares. Por sus características geográficas y topográficas, el estado de Chihuahua es vulnerable a los efectos adversos del Cambio Climático. La escasa disponibilidad del recurso hídrico conlleva problemas de presión social y de impacto económico. En este trabajo se analiza la alteración del régimen pluvial en el estado de Chihuahua y su asociación a Cambio Climático. Para ello se recurre a la caracterización histórica; análisis de la tendencia mediante la prueba de Mann Kendall; y, cálculo de 10 índices de extremos climáticos propuestos por el Grupo de Expertos de Detección e Índices de Cambio Climático para la variable de precipitación. Los resultados demostraron que los patrones de precipitación en el sur y sureste del estado de Chihuahua se han ido modificando paulatinamente, con una tendencia a disminución en los acumulados anuales y reducción de los días húmedos. Pero en contraparte, existe una ligera intensificación de las precipitaciones extremas. Este hecho, sumado a la creciente demanda del recurso hídrico en la entidad demanda de políticas públicas de gestión de forma sustentable y uso responsable por parte de los usuarios, de lo contrario se corre el riesgo de experimentar efectos negativos asociados a la sobreexplotación del agua, no solo para los usuarios del recurso, sino también para el medio ambiente.

Key words: Standard Normal Homogeneity test, Mann Kendall test, Pettitt test, trend analysis, interannual variability.

Palabras clave: prueba de Homogeneidad Normal Estándar, prueba Mann Kendall, prueba Pettitt, análisis de tendencia, variabilidad interanual.

Received: 22 February 2021

Accepted: 21 May 2021

Corresponding author: Indalecio Mendoza Uribe, Instituto Mexicano de Tecnología del Agua, 62550 Jiutepec, México. E-mail address: indalecio_mendoza@tlaloc.imta.mx

1. Introduction

Climate Change, in a simplified way, can be understood as an alteration of the environmental characteristics and their variability in the average climate that occurs in a given region so that it can involve both heating and cooling conditions (Flores-Campaña *et al.*, 2012). These climate changes occur both naturally and through human actions that contribute to the increase in greenhouse gas emissions, main agents responsible for Climate Change (Benavides-Ballesteros *et al.*, 2007; Miller, 2007; Useros-Fernández, 2013). There is an accepted consensus among the scientific community, and in a multidisciplinary way, on the evidence of Climate Change and its effects at a global level (Watkiss *et al.*, 2005; Caballero *et al.*, 2010; Loyola-Martínez *et al.*, 2011; Sánchez-Cohen *et al.*, 2011; Serrano-Vincenti *et al.*, 2017; Pérez-Palmar, 2017; Pacheco *et al.*, 2019). Nevertheless, the impacts of Climate Change are not homogeneous globally or for a country or region as a whole. Likewise, some areas are more sensitive to change than others (IPCC, 2014; Greenpeace, 2018). For this reason, it is essential to carry out studies to identify the effects of Climate Change in particular areas.

The scarce availability of water resources in Chihuahua leads to social pressure and economic impact since agriculture and livestock depend on this vital element, primary activities of great importance in the entity (Government of the State of Chihuahua, 2005). This fact, from a scientific point of view, denotes the importance of studying changes in precipitation patterns in the state, that quantitatively demonstrate the existing variability and the prevailing trend. Which may allow authorities to design policies aimed at planning the use of water resources in a sustainable way, which is more important in regions where this vital resource is scarce (Ferrelli *et al.*, 2020), as is the state of Chihuahua.

Of the 67 municipalities that make up the Chihuahua´s state, 79.10% have a vulnerability to climate change from very low to low, while 19.40% have a medium vulnerability and only 1.49% a high vulnerability (UACJ, 2019). Vulnerable points in the state are found in underserved groups such as female-headed households, indigenous communities and the high population in food poverty. This situation is closely related to the use of the entity's natural resources, because the ecosystems of the area do not allow adapting them to generate a good natural capital, with which the population would be better prepared to respond to the adversities of climate change (Monterroso, 2012).

This work aims to answer the questions: Is there evidence of changes in the rainfall regime that may alter the availability of water in the state of Chihuahua? Are the droughts of recent years in Chihuahua the consequence of natural climate variability or Climate Change? Can we attribute the increase in more extreme and frequent rainfall in Chihuahua to Climate Change? For this, historical characterization, trend analysis, and calculation of climatic extreme indices for the precipitation variable are used.

2. Study Area

The state of Chihuahua is located in the northwest region of Mexico between 25°29' - 31°54' north latitude and between 103°16' - 109°17' west longitude. To the north, it borders the United States of America; to the west with Sonora and Sinaloa's states; to the south with Durango and to the east with Coahuila de Zaragoza. Chihuahua has an area of 247,456 km^2 and includes altitudes ranging from 1,000 to 3,300 m elevation. 18.1% of the territory belongs to the Great Plateau and Canyons of Chihuahuenses and 17.4% to the plains and dunes of the north (Fig. 1). The rest corresponds to other physiographic areas (INEGI, 2013).

In the state, arid, semi-arid and temperate sub-humid climates predominate with 40%, 33%, and 24% of the total territory. In accordance with Cervera-Gómez *et al.* (2018), has both surface water supply sources (Rio Conchos and Rio Bravo) like underground (aquifers: Sauz Encinillas, Valle de Juárez, Parral Valle Verano and Bolsón del Hueco). The rains are scarce, with an average annual rainfall of 462 mm (Esparza, 2014). However, although water scarcity is a limitation for agricultural activity, this is practiced as temporary and irrigated. Corn, beans, oats, alfalfa, cotton, sorghum, wheat, apple, among others, are grown. The arid and semi-arid climate favors the growth of grasslands in the plains, which has selected the development of livestock (Stock Informático, 2012).

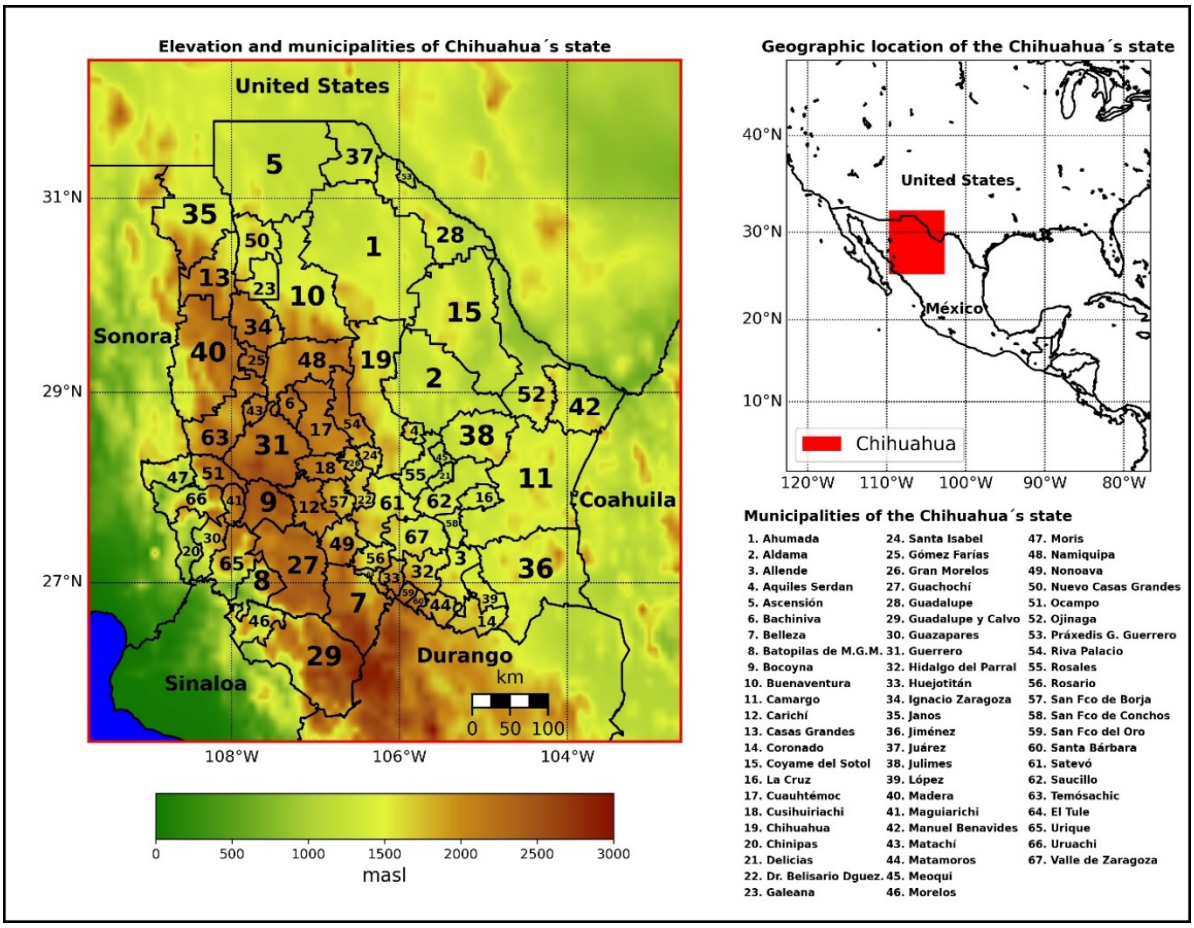

Figure 1. Geographic location of the Chihuahua's state.

3. Methodology

The study was carried out in 4 steps. First, the data set and quality control metrics were defined to select representative weather stations of Chihuahua's state. Second, the annual and monthly climatology was obtained at the state and weather stations for different periods. Third, the precipitation trend was analyzed using the Mann Kendall test. Fourth and last, 10 indices of climatic extremes of precipitation were calculated.

3.1. Dataset

Historical data was consulted from the CLICOM climate data management system (WMO, 1986) for Mexico, currently operated by the National Meteorological Service. The study period was defined as between 1961 and 2012. This last year corresponds to the most recent data stored in the database for the state of Chihuahua. The inventory amounts to 279 conventional weather stations installed in the entity. In this type of station, the data is collected by an observer at 8 in the morning and recorded in a notebook to later capture and process data. To identify possible errors in the data, either due to data collection, failures in measuring instruments, data capture and/or relocation of climate observation stations, three quality control criteria were applied to identify the stations that contained reliable data series. The tests are minimum availability of 80% of the data for the study period and operation; logical congruence of daily data; and homogeneity test (Guajardo-Panes *et al.*, 2017).

3.1.1. Minimum availability of 80% of data and in operation

The first requirement of a practical climatic series is to meet the minimum data number conditions and the climatological station's current state, operating or suspended. This last indicator indicates that the observation site is in operation and that the data series has a high possibility of being updated and maintaining continuity for future studies. For this study, as the first filter, the weather stations with at least 80% of data for the study period 1960-2012 and with operating status were selected.

3.1.2. Logical congruence of daily precipitation data

This test validates the integrity of the data, that is to say, the data correspond to values within a valid range. For this test, the daily precipitation records were compared against a limit established by the UNE 500540: 2004 standard (AENOR, 2004). Since the rains are scarce in the study area, the valid range of rainfall was set between 0 and 100 mm per day (Equation 1). The values of -99999 present in the database correspond to null values, that is, without observation.

$$validity(X_{ij}) = \begin{cases} Valid\ record\ if\ 0 \leq X_{ij} \leq 100 \\ Invalid\ record\ if\ X_{ij} < 0\ \ or\ if\ X_{ij} > 100 \\ Null\ record\ if\ X_{ij} = -99999 \end{cases} \quad (1)$$

where X_{ij} corresponds to the precipitation data in the year *i* and day *j*.

3.1.3. Homogeneity test

For an adequate climate study, it is necessary that the data series be of the exact nature and have been obtained through similar procedures. They represent the normal variability of the observation sites. The station environment's characteristics may change over time, how can be the increase urbanization, but these changes must occur gradually. Abrupt discontinuities, which are the most common type of inhomogeneities, can be caused by changes in the weather station's site and/or modification of the measuring instrument (WMO, 2018). Instrument-related maintenance or calibration problems may also

occur. Consequently, before starting any analysis, modeling or forecasting, these inhomogeneities should be detected and removed from the series, if possible (Yozgatligil *et al.*, 2015).

To validate the homogeneity of the data series, the Pettitt and Standard Normal Homogeneity (SNHT) tests have been widely accepted and applied by the scientific community (Zarenistanak *et al.*, 2014; Mallakpour *et al.*, 2016; Guajardo-Panes *et al.*, 2017; Khosravi *et al.*, 2017; Palaniswami *et al.*, 2018).

The Pettitt test (Pettitt, 1979), is a rank-based nonparametric statistical test. The null hypothesis of the test is that, by arbitrarily dividing the sample into two segments, there is no change in each segment's mean value. At the same time, the alternative hypothesis is accepted when, by arbitrarily dividing the sample into two pieces, there is a significant change in each segment's mean value. This test does not require normalized data series. The test is based on the ranking order of the ranks r_1, r_2, …, r_n of the series (Equation 2).

$$U_d = 2\sum_{i=1}^{d} r_i - d(n+1) \quad for\ d = 1,2,\dots,n \tag{2}$$

The test statistic U_0, critical value, is the maximum vector's total value (Equation 3). The probable turning point is where U_d has its maximum.

$$U_0 = \max|U_d| \quad where\ 1 \le d \le n \tag{3}$$

For his part, test SNHT, initially developed by Alexanderson (1986) and later modified by Alexanderson *et al.* (1997), is a widely used likelihood ratio test to detect inhomogeneities in a time series. The test identifies the breaks at the beginning and end of the time series. It is based on the ordered values of the observations under the assumption of independence and normality. Uses normalized values using standard deviation. The statistician T_d of the test is used to compare the mean of the first d observations with the mean of the remaining (n - d) observations (Equation 4).

$$T_d = d\bar{z_1}^2 + (n-d)\bar{z_1}^2 \quad for\ d = 1,2,3,\dots,n \tag{4}$$

$$\bar{z_1} = \frac{1}{d}\sum_{i=1}^{d}\frac{(Y_i - \bar{Y})}{s} \tag{5}$$

$$\bar{z_2} = \frac{1}{n-d}\sum_{i=d+1}^{n}\frac{(Y_i - \bar{Y})}{s} \tag{6}$$

where Y_i is the value observed at position i, $\bar{Y}$ is the mean and S the standard deviation of the series.

The turning point, break, is where T_d gets its maximum value. The test statistic T_0, critical value, is defined in Equation 7.

$$T_0 = \max T_d \quad where\ 1 \le d \ge 0 \tag{7}$$

3.2. Rainfall climatology

Climatological normals are a reference against which the non-linear fluctuations of the climate in a given region can be defined and compared (WMO, 2007). As a first analysis, the climatological normals of annual and monthly accumulated precipitation were calculated for periods 1961-1990, 1981-2010, and 1961-2012. The climatology was obtained by observation site and at the state level.

3.3. Rainfall trend

As a second analysis, the precipitation trend was calculated using the Mann-Kendall test (Mann, 1945; Kendall, 1975) for each data series and the state average. This test has been widely used in the evaluation of trends in climate data series (Berger, 1986; Kundzewicz *et al.*, 2000; Peña-Quiñones *et al.*, 2010; Alencar de Silva-Alves *et al.*, 2017). It corresponds to a non-parametric test that consists of the sequential comparison between the values that make up the same time series. The null hypothesis considers that the values of the time series are independent and identically distributed. In contrast, the alternative hypothesis assumes that the data follow a monotonic trend (Peña-Quiñones *et al.*, 2010). Equation 8 represents the *S* statistic of the Mann Kendall test.

$$S = \sum_{k=1}^{n-1} \sum_{j=k+1}^{n} sgn(x_j - x_k) \tag{8}$$

$$sgn(x) = \begin{cases} +1, & X > 0 \\ 0, & X = 0 \\ -1, & X < 0 \end{cases} \tag{9}$$

where *j* y *k* corresponds to two consecutive positions, precedent and antecedent respectively, within data series X_n.

The result of *S* indicates the possible existence of a trend and its direction. A positive value of *S* indicates an increasing trend. In opposition, a negative value of *S* indicates a decreasing trend. Therefore, since *S* is different from zero, the null hypothesis is rejected, and the alternative hypothesis is accepted (Mann, 1945).

On the other hand, the existence of a statistically significant trend is evaluated by the *Z* statistic (Equation 10). Table 1 presents the interpretation of the *Z* statistic for a level of significance α=0.05.

$$Z = \begin{cases} \dfrac{S-1}{(Var(S))^{1/2}} & if\ S > 0 \\ 0 & if\ S = 0 \\ \dfrac{S+1}{(Var(S))^{1/2}} & if\ S < 0 \end{cases} \tag{10}$$

Table 1. Interpretation of the Z statistic of the Mann Kendall test.

Meaning	**Symbology**	**Z**
Significantly increasing trend	SIT	Z > +1.96
Not significantly increasing trend	NSIC	0 > Z < +1.96
No trend	NT	Z = 0
Not significantly decreasing trend	NSDT	-1.96 > Z < 0
Significantly decreasing trend	SDT	Z < -1.96

Source: Alves *et al.* (2015)

3.4. Extreme climatic indices of precipitation

The Expert Team on Climate Change Detection and Indices (ETCCDI) formulated a set of 27 Climate Change indices for the detection and monitoring of changes in the extremes of the climate associated with the variables of precipitation, maximum temperature and minimum temperature (Karl *et al.*, 1999; Peterson *et al.*, 2008). These indices provide a common theoretical basis so that they can be consistently calculated in different regions of the planet. For this study, the 10 indices of climatic extremes corresponding to the precipitation variable were calculated (Table 2). The calculation of the indices was performed using the RClimdex software (Zhang *et al.*, 2018).

Table 2. Extreme climatic indices for the precipitation variable proposed by the ETCCDI.

Index	Description	Unit
CDD	Consecutive dry days	Days
CWD	Consecutive wet days	Days
PRCPTOT	Annual precipitation on wet days	mm
R10MM	Days with precipitation greater than 10 mm	Days
R20MM	Days with precipitation greater than 20 mm	Days
R95P	Annual precipitation on very humid days	mm
R99P	Annual precipitation on extremely humid days	mm
RX1DAY	Maximum rainfall in one day	mm
RX5DAY	Maximum rainfall in five days	mm
SDII	Simple daily intensity index	mm

Source: Zhang *et al.* (2018).

3.4.1. Consecutive dry days (CDD)

Let RR_{ij} the daily amount of precipitation on day i in period j. Count the largest number of consecutive days where

$$RR_{ij} < 1\ mm \tag{11}$$

3.4.2. Consecutive wet days (CWD)

Let RR_{ij} the daily amount of precipitation on day i in period j. Count the largest number of consecutive days where

$$RR_{ij} \geq 1\ mm \tag{12}$$

3.4.3. Annual precipitation on wet days (PRCPTOT)

Let RR_{ij} the daily amount of precipitation on day i in period j. If I represents the number of days in period j, then

$$PRCPTOT = \sum_{i=1}^{I} RR_{ij}\,, \qquad where\ RR_{ij} \geq 1\ mm \tag{13}$$

3.4.4. Days with precipitation greater than 10 mm (R10MM)

Let RR_{ij} the daily amount of precipitation on day i in period j. Count the number of days where

$$RR_{ij} \geq 10\ mm \tag{14}$$

3.4.5. Days with precipitation greater than 20 mm (R20MM)

Let RR_{ij} the daily amount of precipitation on day i in period j. Count the number of days where

$$RR_{ij} \geq 20\ mm \tag{15}$$

3.4.6. Annual precipitation on very humid days (R95P)

Let RR_{wj} the daily amount of precipitation on a wet day *w* (where RR ≥ 1 mm) in period *j*, and let $RR_{wn}95$ be the 95th percentile of precipitation on wet days in the study period. If *W* represents the number of wet days in the period, where $RR_{wj} > 1\ mm$, then

$$R95P_j = \sum_{w=1}^{W} RR_{wj}, \qquad where\ RR_{wj} > RR_{wn}95 \tag{16}$$

3.4.7. Annual precipitation on extremely humid days (R99P)

Let RR_{wj} the daily amount of precipitation on a wet day *w* (where RR ≥ 1 mm) in period *j*, and let $RR_{wn}99$ be the 99th percentile of precipitation on wet days in the study period. If *W* represents the number of wet days in the period, where $RR_{wj} > 1\ mm$, then

$$R95P_j = \sum_{w=1}^{W} RR_{wj}, \qquad where\ RR_{wj} > RR_{wn}99 \tag{17}$$

3.4.8. Maximum rainfall in one day (RX1DAY)

Let RR_{ij} the daily amount of precipitation on day *i* in period *j*. Then the maximum 1-day values for period *j* are

$$RX1DAY_j = \max(RR_{ij}) \tag{18}$$

3.4.9. Maximum rainfall in five days (RX5DAY)

Let RR_{kj} the amount of precipitation for the five-day interval ending in *k*, of period *j*. Then, the maximum 5-day values for period *j* are

$$RX5DAY_j = \max(RR_{kj}) \tag{19}$$

3.4.10. Simple daily intensity index (SDII)

Let RR_{wj} the daily amount of precipitation on wet days. If *W* represents the number of wet days in period *j*, where $RR_{wj} >= 1$, then

$$SDII_j = \frac{\sum_{w=1}^{W} RR_{wj}}{W} \tag{20}$$

4. Results

4.1. Selected datasets

Of the 279 weather stations installed in Chihuahua, only 21 stations had 80% minimum data and as a status in operation (Table 3). The data were organized in time series to facilitate their processing. With the daily data logical congruence test, 12 records were identified that exceeded 100 mm. Anomalous data were verified by comparing them with values from neighboring stations and with contiguous values (previous and next) from the same series. Also, the occurrence of tropical cyclones on the data's date that could explain the extreme value was investigated. After finding no evidence of these values' validity, in all cases, the displacement of the decimal point was attributed as a capture error,

so the data was corrected manually (Table 4). Pettitt and SNHT homogeneity tests were applied using Python's pyhomogeneity library, defining a significance level of α=0.05. Tables 5 and 6 list the parameters obtained in the tests.

Table 3. Weather stations with at least 80% data for 1961-2012 and with status in operation.

Station ID	Name	Municipality	Latitude	Longitude	Altitude	%
8004	Bachiniva	Bachiniva	28.7717	-107.2556	2017	98.11
8038	Creel	Bocoyna	27.7500	-107.6375	2348	87.40
8044	Delicias	Delicias	28.1942	-105.4636	1173	98.86
8049	Luis L. León	Aldama	28.9786	-105.3117	1080	90.64
8052	El Mulato	Ojinaga	29.3942	-104.1689	774	92.08
8059	El Tintero	Namiquipa	29.2636	-107.4572	2450	96.25
8081	Jiménez	Jiménez	27.1333	-104.9167	1370	94.71
8084	Ascensión	Ascensión	31.0964	-108.0128	1290	84.09
8085	La Boquilla	San Fco. de Conchos	27.5439	-105.4119	1323	94.79
8097	Madera	Madera	29.1900	-108.1414	2100	85.78
8099	Majalca	Chihuahua	28.8028	-106.4847	2119	93.81
8156	Villa Coronado	Coronado	26.7386	-10.1600	1516	90.77
8167	Chinipas	Chinipas	27.3931	-108.5361	440	86.59
8172	Guadalupe y Calvo	Guadalupe y Calvo	26.1083	-106.9750	2279	95.26
8182	Moris	Moris	28.1472	-108.5200	754	95.11
8194	Villa López	López	27.0031	-105.0361	1424	92.07
8202	Dam Fco. I. Madero	Rosales	28.1672	-105.6275	1242	98.71
8215	Las Chepas	Bachiniva	28.7153	-107.2458	2076	92.15
8219	Peñitas	Madera	29.2519	-108.0928	2135	95.92
8246	Basuchil	Guerrero	28.5181	-107.4019	2020	87.92
8270	La Mesa	Aldama	28.7733	-105.9636	1250	96.05

Table 4. Anomalous precipitation values detected with the logical congruence test, values from neighboring stations and corrected value.

Date	Station ID	Abnormal value	Values of neighboring stations						Corrected value
			Station 1	Value 1	Station 2	Value 2	Station 3	Value 3	
2006/08/28	8044	113.0	8049	1.0	8202	25.0	8270	42.0	11.3
1973/07/26	8049	107.9	8044	10.0	8052	0.0	8270	0.0	10.8
1987/10/22	8059	105.0	8004	0.0	8097	1.0	8219	5.0	10.5
2008/09/01	8085	101.0	8044	0.5	8194	0.1	8202	1.0	10.1
1973/08/29	8099	110.0	8004	28.0	8215	7.0	8270	0.0	11.0
1980/09/25	8099	120.0	8004	2.0	8215	0.0	8270	19.0	12.0
2000/10/21	8167	105.3	8038	0.0	8182	56.0	8246	8.0	10.5
1979/01/24	8172	131.4	8156	2.5	8167	61.7	8194	3.0	13.1
1983/03/03	8172	118.5	8156	5.0	8167	49.2	8194	0.0	11.9
1987/12/24	8172	111.0	8156	0.0	8167	0.0	8194	0.0	11.1
1989/12/17	8172	106.0	8156	0.0	8167	36.0	8194	0.0	10.6
1976/06/06	8246	114.0	8004	1.0	8059	1.0	8215	2.0	11.4

Table 5. Statistical values of the Pettitt homogeneity test by climatological station.

Station ID	Breaking point (Year/Month)	Value P	U_0	Middle value		Homogeneous series
				Before PC	After PC	
8004	92 (1968/09)	0.88	2.91	43.71	32.84	Yes
8038	536 (2005/09)	0.13	8.20	58.44	37.35	Yes
8044	597 (2010/10)	0.45	5.37	25.36	9.11	Yes
8049	597 (2010/10)	0.68	4.06	25.10	10.65	Yes
8052	556 (2007/05)	0.00	28.43	6.44	21.51	No
8059	618 (2012/07)	1.00	1.57	28.08	51.60	Yes
8081	597 (2010/10)	0.67	4.11	28.00	7.55	Yes
8084	396 (1994/01)	0.00	18.28	21.68	11.09	No
8085	250 (1981/11)	0.31	6.24	29.25	21.41	Yes
8097	453 (1998/10)	0.01	14.94	60.85	38.9	No
8099	498 (2002/07)	0.00	18.36	13.46	35.59	No
8156	316 (1987/05)	0.00	59.29	39.54	9.66	No
8167	65 (1966/06)	0.01	13.39	22.58	62.69	No
8172	453 (1998/10)	0.00	16.80	95.68	56.69	No
8182	137 (1972/06)	0.00	40.22	0.10	41.41	No
8194	102 (1969/07)	0.00	24.75	0.03	20.63	No
8202	597 (2010/10)	0.95	2.34	26.37	14.29	Yes
8215	450 (1998/07)	0.00	63.98	6.59	33.30	No
8219	144 (1973/01)	0.00	81.06	0.10	44.56	No
8246	162 (1974/07)	0.00	53.47	0.51	29.89	No
8270	176 (1975/09)	0.00	62.67	0.46	25.62	No

Table 6. Statistical values of the SNHT homogeneity test by climatological station.

Station ID	Breaking point (year/month)	Value P	T_0	Middle value		Homogeneous series
				Before PC	After PC	
8004	92 (1968/09)	0.89	2.91	43.71	32.84	Yes
8038	536 (2005/09)	0.14	8.20	58.44	37.35	Yes
8044	597 (2010/10)	0.45	5.37	25.36	9.11	Yes
8049	597 (2010/10)	0.68	4.06	25.10	10.65	Yes
8052	556 (2007/05)	0.00	28.43	6.44	21.51	No
8059	618 (2012/07)	1.00	1.57	28.08	51.60	Yes
8081	597 (2010/10)	0.67	4.11	28.00	7.55	Yes
8084	396 (1994/01)	0.00	18.28	21.68	11.09	No
8085	250 (1981/11)	0.32	6.24	29.25	21.41	Yes
8097	453 (1998/10)	0.00	14.94	60.85	38.90	No
8099	498 (2002/07)	0.00	18.36	13.46	35.59	No
8156	316 (1987/05)	0.00	59.29	39.54	9.66	No
8167	65 (1966/06)	0.01	13.39	22.58	62.69	No
8172	453 (1998/10)	0.00	16.80	95.68	56.69	No
8182	137 (1972/06)	0.00	40.22	0.10	41.41	No
8194	102 (1969/07)	0.00	24.75	0.03	20.63	No
8202	597 (2010/10)	0.96	2.34	26.37	14.29	Yes
8215	450 (1998/07)	0.00	63.98	6.59	33.30	No
8219	144 (1973/01)	0.00	81.06	0.10	44.56	No
8246	162 (1974/07)	0.00	53.47	0.51	29.89	No
8270	176 (1975/09)	0.00	62.67	0.46	25.62	No

Based on the results obtained in the three quality control tests, only stations 8004, 8038, 8044, 8049, 8059, 8081, 8085 and 8202 demonstrated consistency and reliability in their corresponding data series. Therefore, statistical analysis was only applied in these eight stations. Figure 2 shows the geographic location of the 21 stations with at least 80% data and in operation, differentiating the stations with homogeneous data series from those with no.

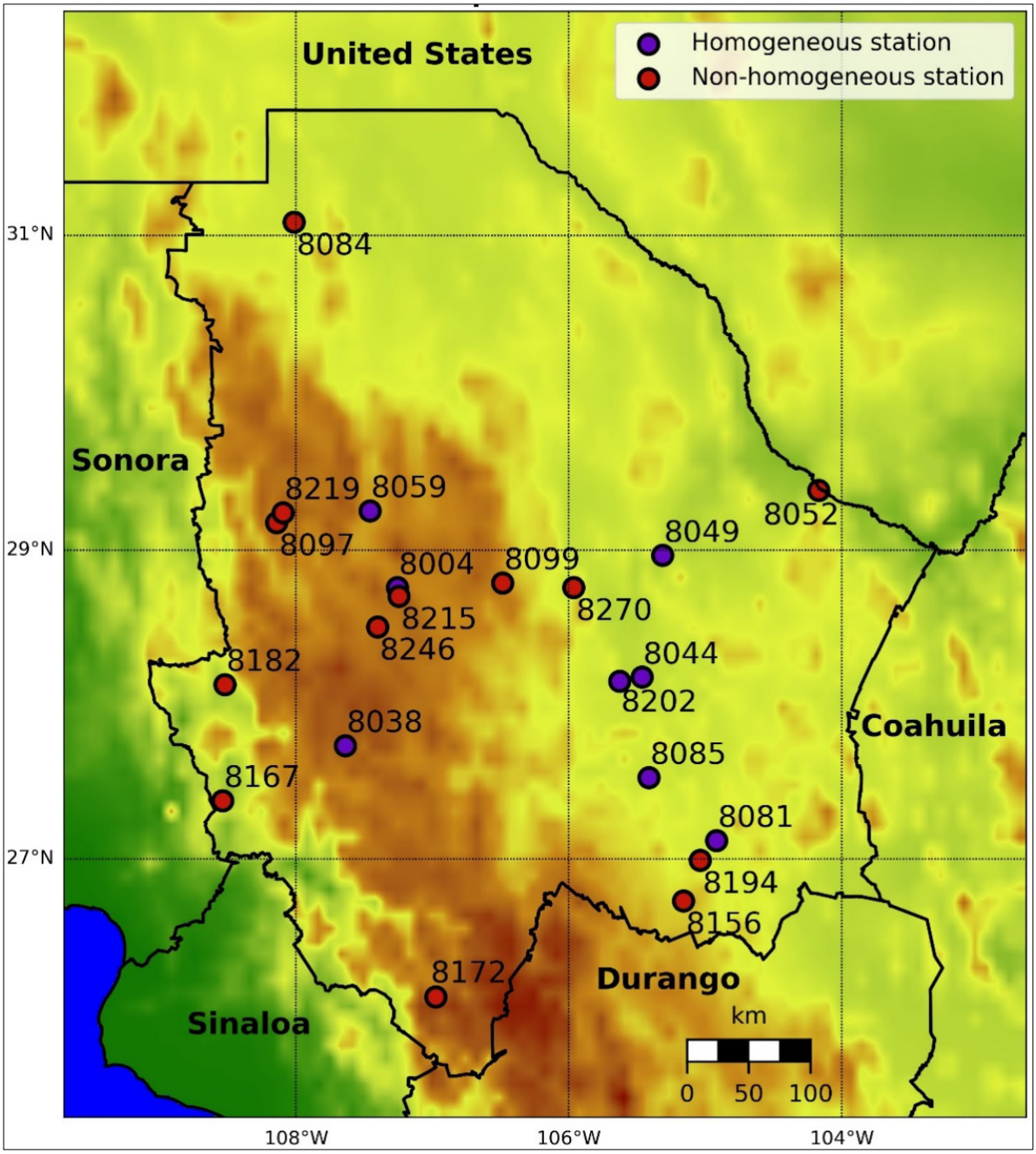

Figure 2. Geographical location of the climatological stations of the state of Chihuahua with at least 80% data and in operation.

4.2. Rainfall Climatology

Tables 7, 8, and 9 summarize the climatological normals of annual and monthly precipitation for the periods 1961-1990, 1981-2010, and 1961-2012. The difference in the state average of rainfall between the periods 1961-1990 and 1981-2010 shows a considerable decrease in the annual precipitation regime, with values of 389.06 and 371.96 mm, respectively, a loss of 17.01 mm corresponding to 4.40%. This decrease is accentuated in September, with an average variation of 17.25 mm between both periods. Figure 3 illustrates the distribution and evolution of monthly mean precipitation using the histogram and mass curve graph.

Table 7. Climatological precipitation normals for the period 1961-1990.

Month/Station	8004	8038	8044	8049	8059	8081	8085	8202	State average
January	12.87	39.34	8.05	7.36	11.51	7.64	6.92	6.51	12.53
February	6.07	29.24	5.01	3.79	6.15	6.09	6.09	4.07	8.31
March	6.82	17.53	3.58	3.41	4.37	2.67	3.41	3.18	5.62
April	5.47	12.92	11.17	6.84	7.66	5.72	6.97	8.79	8.19
May	9.11	15.18	12.61	12.16	8.64	13.16	11.92	10.90	11.71
June	40.09	70.75	33.75	35.44	21.38	43.66	35.91	32.79	39.22
July	118.99	164.64	66.33	60.48	83.30	76.98	74.44	70.12	89.41
August	123.96	128.60	67.76	77.61	88.16	75.12	75.35	78.81	89.42
September	82.96	103.51	65.92	56.98	65.95	64.91	75.59	73.63	73.68
October	24.62	41.88	21.48	24.92	23.17	24.35	20.37	25.99	25.85
November	8.16	26.25	5.85	8.09	8.22	6.88	6.35	6.44	9.53
December	16.10	52.25	8.46	10.95	11.06	7.12	9.78	8.95	15.58
Annual	**455.22**	**702.09**	**309.94**	**308.03**	**339.57**	**334.31**	**333.10**	**330.18**	**389.06**

Table 8. Climatological precipitation normals for the period 1981-2010.

Month/Station	8004	8038	8044	8049	8059	8081	8085	8202	State average
January	14.96	36.41	10.90	10.67	11.01	7.23	6.34	10.25	13.47
February	7.23	35.02	6.26	6.45	9.44	4.09	3.36	4.85	9.59
March	7.04	26.14	3.93	5.47	5.61	4.51	2.81	3.90	7.43
April	7.23	23.08	7.92	7.42	9.10	5.89	6.86	6.50	9.25
May	7.05	19.33	13.72	14.24	8.99	16.20	12.92	12.32	13.10
June	30.47	60.48	34.74	34.91	22.97	42.31	33.57	27.69	35.89
July	109.99	133.36	69.46	68.96	86.45	72.45	78.04	70.64	86.17
August	121.93	129.64	72.26	69.69	89.67	77.02	67.13	70.84	87.27
September	62.33	89.06	48.77	37.89	50.81	61.58	49.94	51.03	56.43
October	21.73	46.63	20.75	35.68	18.92	23.54	17.86	26.26	26.42
November	5.66	28.23	8.84	10.62	8.97	7.28	7.83	8.24	10.71
December	11.86	54.09	10.33	10.04	15.15	9.87	9.50	9.15	16.25
Annual	**407.47**	**681.46**	**307.86**	**312.03**	**337.08**	**331.97**	**296.16**	**301.68**	**371.96**

Table 9. Climatological precipitation normals for the period 1961-2012.

Month/Station	8004	8038	8044	8049	8059	8081	8085	8202	State average
January	13.45	36.78	8.25	8.80	10.90	5.87	6.53	8.16	12.34
February	6.53	31.19	6.02	4.98	7.64	5.35	4.74	4.40	8.86
March	6.73	21.13	3.59	4.31	4.92	3.66	3.08	3.53	6.37
April	6.34	17.42	7.95	7.27	8.11	5.06	7.03	7.63	8.35
May	7.81	16.70	13.22	13.14	8.66	14.11	12.18	11.27	12.14
June	34.53	64.04	32.82	34.17	21.49	40.67	34.37	29.29	36.42
July	114.23	149.54	67.44	63.68	84.94	73.33	76.23	70.40	87.47
August	121.43	128.31	67.63	72.23	88.83	72.99	71.59	73.12	87.02
September	72.21	95.25	56.52	46.90	58.30	65.57	62.83	61.93	64.94
October	25.57	43.49	20.98	29.58	20.46	23.69	19.40	25.61	26.10
November	7.11	27.34	7.33	9.18	8.45	7.37	6.93	7.55	10.16
December	13.51	51.62	9.11	10.14	12.68	8.26	9.48	8.81	15.45
Annual	**429.46**	**682.81**	**300.87**	**304.38**	**335.38**	**325.93**	**314.38**	**311.65**	**375.61**

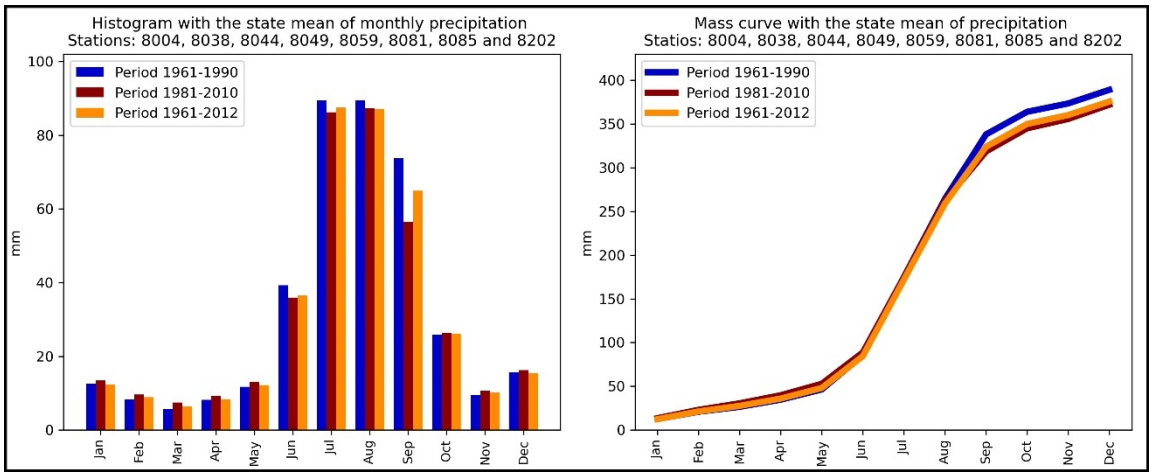

Figure 3. Histogram with the monthly mean of precipitation (left) and mass curve with the mean of precipitation (right) for the periods 1961-1990, 1981-2010 and 1961-2012. The values correspond to tables 7, 8 and 9.

Regarding the maximum precipitation values for the period 1961-2012, these were observed at station 8038, installed in the municipality of Bocoyna, in the southeast of the state, with an annual average of 682.81 mm; while the minimum annual accumulated were obtained in station 8044, installed in the municipality of Delicias, in the east of the state, with an annual average of 300.87 mm. It should be noted that the highest rainfall was obtained in the climatological stations closest to the western coastline of Mexico, specifically in the mountainous area of the Great Plateau and Chihuahuan Canyons, and as it moves further into the continental zone, towards the plains and dunes of the north, there is a considerable decrease in precipitation patterns. This is because the rainfall in Chihuahua is mainly induced by orographic forcing and is strongly influenced by cyclonic activity from the Pacific Ocean. Although the trajectories of tropical cyclones are interrupted by friction with the continental topography, strong winds and extreme rains can have effects in some states in the interior of the country, such as the state of Chihuahua (Rosengaus-Moshinsky *et al.*, 2014).

4.3. Precipitation trend

The precipitation trend was calculated using the *pymannkendall* library (Hussain *et al.*, 2019), precisely, the *seasonal_test* function, which corresponds to the Mann Kendall Seasonal test (Hirsch *et al.*, 1982), this variant eliminates the effect of seasonality. It was used as a level of significance $\alpha = 0.05$ and a seasonal period of 12 months. The test returns the statistical trend values (*trend*), p-value of significance test (*Valor P*), the normalized test statistic (*Z*), Kendall Tau (*Tau*), Mann Kendall score (*S*), Theil-Sen slope (*slope*), and Kendall-Theil Robust Line interception (*interception*).

The results determined that, for the study period, in seven of the eight data series analyzed, a negative trend persists in the accumulated annual precipitation, but only at stations 8038 and 8085, located in the southern and southeastern part of the state, the existing trend is considered significantly decreasing with a slope of -66.56 and -35.25 mm respectively. On the opposite side, only station 8049, located in the northwest, presents a positive trend in increasing precipitation, with a slope of 4.56 mm. In the remaining five stations, a negative but not significant trend is maintained (Table 10).

Table 10. Statistical values of the Mann Kendall test for the six weather stations.

Station ID	Trend	p-value	Z	Tau	S	Slope	Interception
8004	NSDT	0.27	-1.12	-0.16	-14	-18.81	452.09
8038	SDT	0.05	-1.97	-0.27	-24	-66.56	803.65
8044	NSDT	0.93	-0.09	-0.02	-2	-1.72	278.72
8049	SIT	0.80	0.26	0.05	4	4.56	253.22
8059	NSDT	0.67	-0.43	-0.07	-6	-9.41	349.20
8081	NSDT	0.78	-0.27	-0.05	-4	-1.52	310.82
8085	SDT	0.02	-2.32	-0.32	-28	-35.25	370.83
8202	NSDT	0.44	-0.77	-0.11	-10	-10.66	315.35

Note. The abbreviation of the trend corresponds to the meaning of Table 1.

In Figure 4 the map of Chihuahua is presented with the geographical distribution of the precipitation trend by the climatological station. On the other hand, Figure 5 shows the interannual variability of rainfall and the Mann Kendall test's slope line for the period 1961-2012 by the weather station.

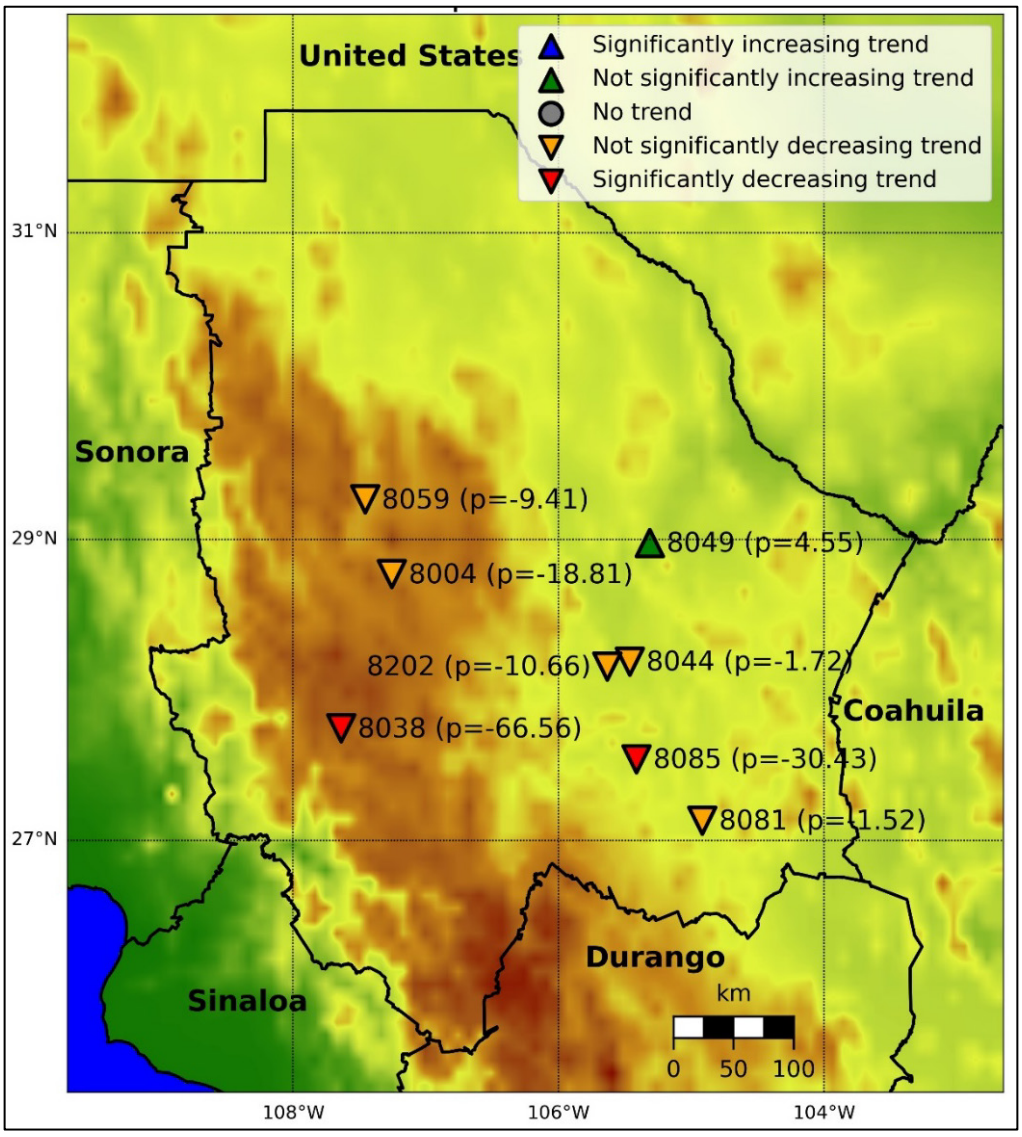

Figure 4. Geographical distribution of the precipitation trend according to the Mann Kendall test for the period 1961-2012.

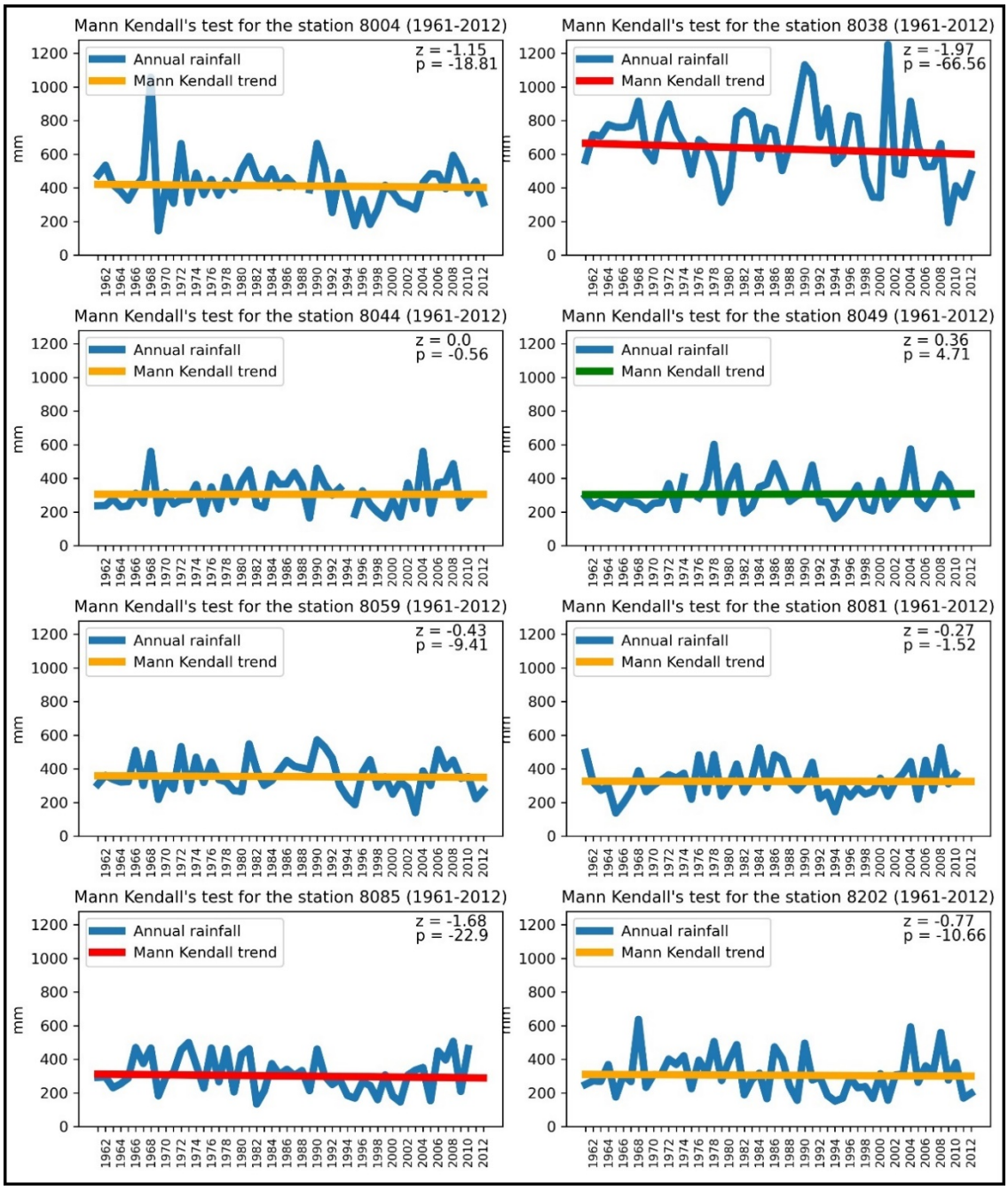

Figure 5. Rainfall trend with the Mann Kendall´s test by climatological station for the period 1961-2012. Not significantly increasing trend (green line), not significantly decreasing trend (orange line) and significantly decreasing trend (red line).

4.4. Climatic extremes indices of precipitation

The results obtained with the ten climatic extremes indices of rainfall events, showed a slight alteration in the precipitation regimes in Chihuahua. With respect to consecutive dry days (CDD), an increase of close to one day was observed in stations 8004 and 8038, with a slope of 0.71 and 0.96 respectively; a decrease of 1.73 and 3.47 mm in the annual precipitation of wet days (PRCTOT) in stations 8004 and 8038, respectively; increase in annual precipitation of very humid days (R95P) in stations 8044 and 8049, with values of 0.85 and 1.06 respectively; and an increase in the annual precipitation of extremely humid days (R99P) in stations 8004, 8038, and 8044, with values of 0.9, 0.4 and 0.80 respectively. In summary, the climate change indices proposed by the ETCCDI indicate a

decrease in the days and in the annual amount of precipitation, but in contrast, a slight increase in the intensity of extreme storms in the state of Chihuahua (Table 11). The geographic distribution of trends by indices is illustrated in Figures 6 through 8.

Table 11. Trend values in the 10 indices of climatic extremes of precipitation.

Station ID	CDD (Days)	CWD (Days)	PRCTOT (mm)	R10MM (Days)	R20MM (Days)	R95P (Days)	R99P (Days)	RX1DAY (mm)	RX5DAY (mm)	SDII (mm)
8004	0.71	-0.07	-1.73	-0.08	-0.06	-0.13	0.90	0.27	-0.05	-0.01
8038	0.96	0.04	-3.47	-0.10	-0.01	0.24	0.40	0.13	0.16	0.03
8044	0.06	-0.02	-0.25	-0.03	0.01	0.85	0.80	0.23	0.17	0.01
8049	-0.13	-0.09	0.82	0.09	0.06	1.06	-0.22	0.17	0.20	0.05
8059	-0.25	-0.05	-0.45	-0.01	0.02	0.26	0.13	0.11	0.05	0.02
8081	-1.16	-0.01	-0.09	-0.02	0.01	-0.42	-0.18	-0.21	-0.28	-0.06
8085	-0.16	0.01	-0.92	-0.04	-0.03	0.02	0.29	-0.13	-0.08	-0.01
8202	0.46	-0.01	-0.62	-0.02	-0.02	-0.20	-0.20	-0.10	-0.30	0.00

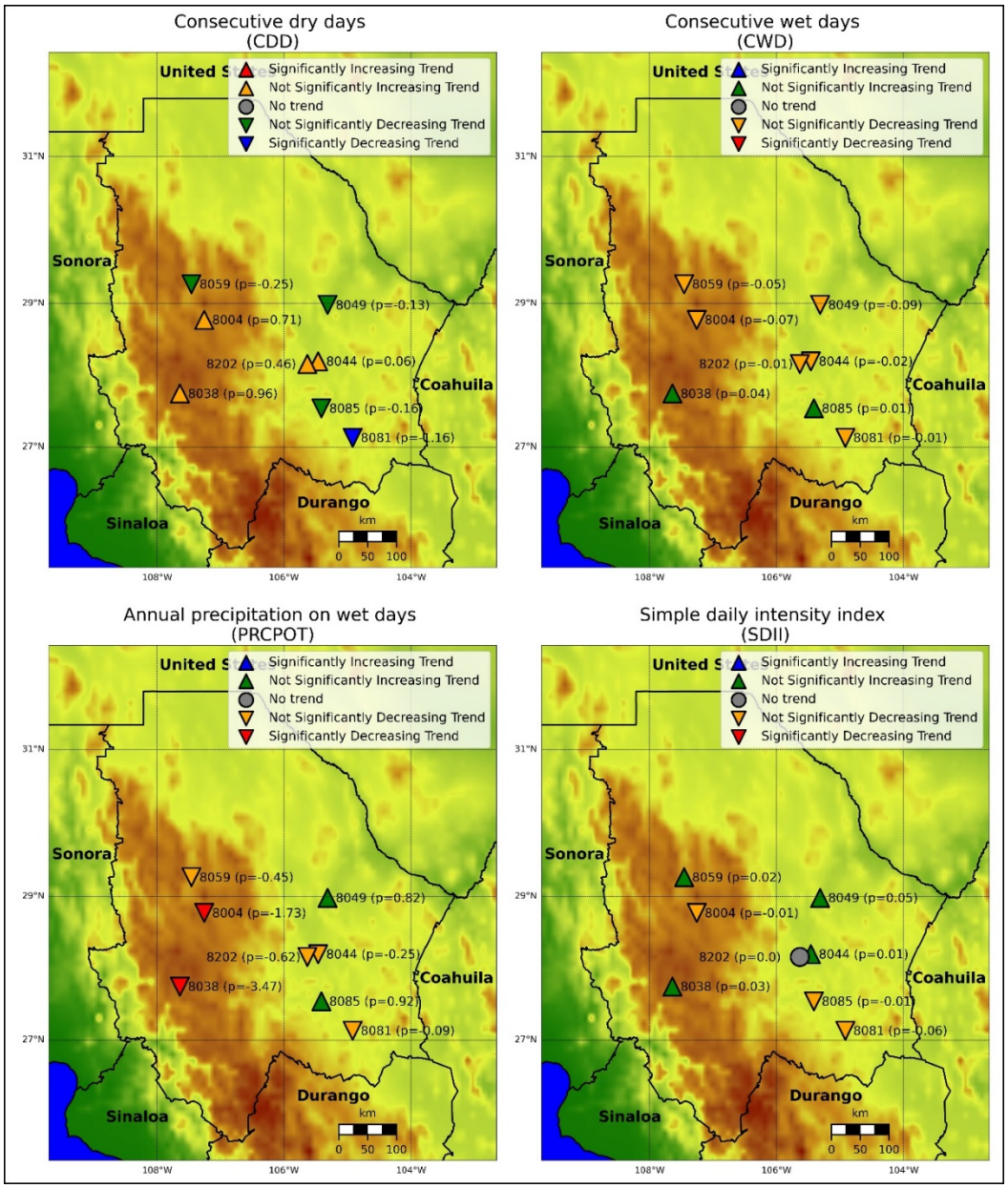

Figure 6. Geographical distribution of the trend for the CDD, CWD, PRCTOT and SDII indices.

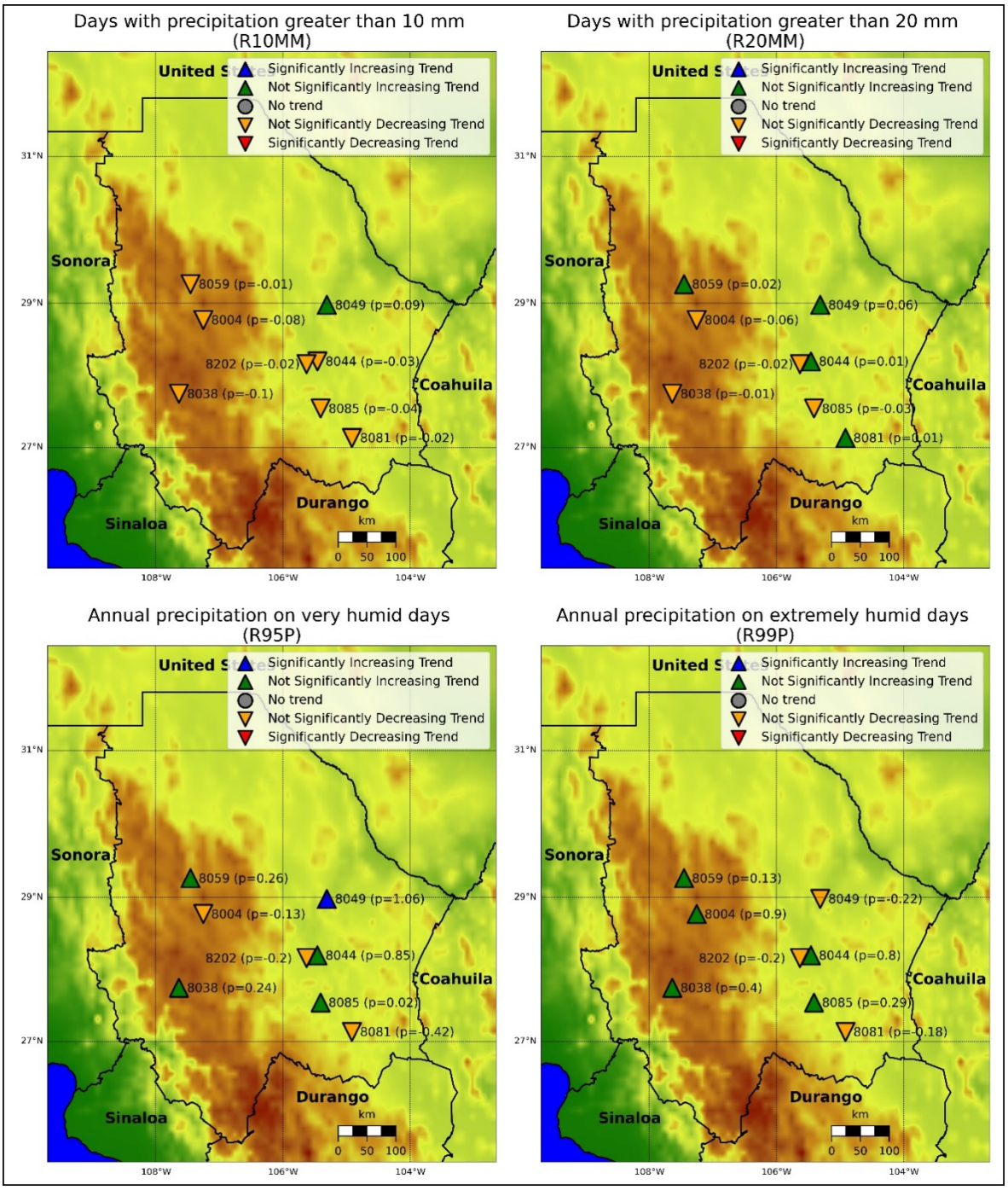

Figure 7. Geographical distribution of the trend for the R10MM, R20MM, R95P and R99P indices.

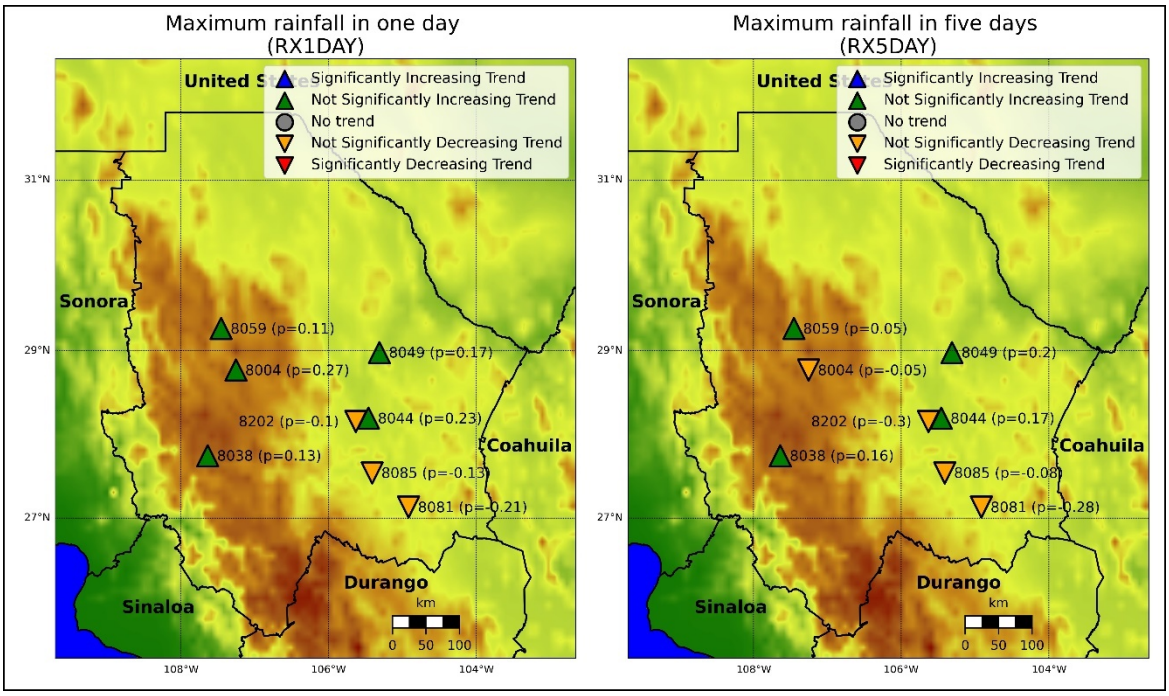

Figure 8. Geographical distribution of the trend for the RX1DAY and RX5DAY indices.

5. Discussion

In this work, the fluctuations in precipitation that occurred in the state of Chihuahua over 52 years, from 1961 to 2012, were analyzed. Of the 279 weather stations located in the state of Chihuahua, only eight exceeded the quality control and homogeneity criteria applied in this study. It should be noted that 226 stations, corresponding to 81%, present as out of service status, and the remaining ones, which are operating, have considerable information gaps. In addition, the similarity between the Pettitt and SNHT homogeneity tests was notorious. Both approved and rejected the same data series. This is in agreement with what was stated by Buishand (1982), who determined that there are minor differences between the different homogeneity tests to reject or accept the data series. No adjustments were applied to the data series identified as non-homogeneous, since this type of correction requires a clear identification of the reasons causing the breakdown before any action can be taken (Ahmed *et al.*, 2013). Otherwise erroneous results may be obtained.

The behavior of precipitation patterns is a highly complicated task since it is a chaotic phenomenon that fluctuates in time and space (Rousseau-Figueroa *et al.*, 2016; Haro *et al.*, 2016), and the high levels of dispersion presented by micro and mesoscale factors that generate it (Peña, 2004; Montoya *et al.*, 2005). However, through the selection of reliable data series and the application of validated statistical tests, it was possible to identify the existence of changes in the precipitation regimes in the study area in this work.

The surface of Chihuahua's state is located in a region that presents a natural scarcity of water, with average annual rainfall in the climatological stations analyzed of 389.06 mm for the period 1961-1990 and 371.96 mm for the period 1981-2010. The discrepancy between the annual and monthly average of state precipitation obtained in this work, with only eight stations, concerning the climatological normals for the state of Chihuahua from other sources of information (Breña-Puyol, 2004; Esparza, 2014), is associated with the calculation period, the number of weather stations considered and their spatial coverage.

The alteration in precipitation regimes, added to the growing demand for water resources, mainly for the agricultural activity that consumes 80% of the available water, demands public policies

for sustainable management and responsible use by users. Otherwise, there is a risk of experiencing adverse effects and a decrease in water availability in Chihuahua's state for the near future, not only for resource users but also for the environment. Because the aggravated effects of droughts and water scarcity are presented by natural causes and social factors where management policies and sustainable use of water reserves are relevant (FAO, 2013).

6. Conclusions

The results obtained with the Mann Kendall trend test indicate an alteration of the rainfall regime in the state of Chihuahua with a significantly decreasing trend in the southern and southeastern part of the state, mainly during September, and a not considerably increasing trend in the northwest. This fact makes it possible to determine that the droughts of recent years are a consequence of Climate Change rather than a natural variability of the climate. On the other hand, three of the extreme climatic precipitation indices proposed by the ETCCDI determined that the increase in the intensities of extraordinary storms can be attributed to Climate Change, according to the annual precipitation indices of extremely humid days (R99P), maximum precipitation in one day (RX1DAY) and maximum precipitation in five days (RX5DAY). In addition, the annual precipitation index for very humid days (PRCPTOT), in correspondence with the Mann Kendall test, indicates a decrease in annual precipitation in the south of the state.

Faced with the alteration of the rainfall regime in the state of Chihuahua, it is imperative to maintain constant monitoring of the variable's behavior, which leads to the rehabilitation of weather stations that are out of operation even to implement new automatic weather stations that provide greater detail.

Likewise, the changes in the frequency and intensity of rainfall in the state of Chihuahua demand the development and application of a plan for adaptation to Climate Change in the main socio-economic activities, which allow adjusting the demands of water resources sustainably.

References

AENOR (Asociación Española de Normalización y Certificación). 2004. Redes de estaciones meteorológicas automáticas: Directrices para la validación de registros meteorológicos procedentes de redes de estaciones automáticas. Madrid, España: Asociación Española de Normalización y Certificación (AENOR), 7 p.

Ahmed, N.H., Deni, S.M. 2013. Homogeneity Test on Daily Rainfall Series for Malaysia. *Matematika*, 29(1c), 141-150. http://doi.org/10.11113/MATEMATIKA.V29.N.586

Alexandersson, H. 1986. A homogeneity test applied to precipitation data. *International Journal of Climatology*, 6, 661-675. https://doi.org/10.1002/joc.3370060607

Alexandersson, H., Moberg, A. 1997. Homogenization of Swedish temperature data. Part I: homogeneity test for linear trends. *International Journal of Climatology*, 17, 25-34. https://doi.org/10.1002/(SICI)1097-0088(199701)17:1<25::AID-JOC103>3.0.CO;2-J

Alencar de Silva-Alves, K.M., Silva-Nóbrega, R. 2017. Tendencias pluviométricas y concentración estacional de precipitación en la cuenca hidrográfica del río Moxotó-Pernamcuco-Brasil. *Revista Geográfica de América Central*, 1(58), 295-313. https://doi.org/10.15359/rgac.58-1.12

Alves, T.L.B., Azevedo, P.V., Farias, A.A. 2015. Comportamento da precipitação pluvial e sua relação com o relevo nas microrregiões do Cariri Oriental e Ocidental do estado da Paraíba. *Revista Brasileira de Geografia Física*, 8(6), 1601-1614. https://doi.org/10.5935/1984-2295.20150090

Benavides-Ballesteros, H.O., León-Aristizabal, G.E. 2007. Información técnica sobre gases de efecto invernadero y el cambio climático. Colombia: IDEAM - Instituto de Hidrología, Meteorología y Estudios Ambientales, nota técnica IDEAM-METEO/008-2007, 99 p.

Berger, A. 1986. Annual and seasonal climatic variations the northern hemisphere and Europe during the last century. *Annales Geophysicae*, 4 (4), 385-400.

Breña-Puyol, A.F. 2004. Precipitación y recursos hidráulicos en México. México: Universidad Autónoma Metropolitana, 316 p.

Buishand, T.A. 1982. Some methods for testing the homogeneity of rainfall records. *Journal of hydrology*, 58(1-2), 11-27. https://doi.org/10.1016/0022-1694(82)90066-X

Caballero, M., Lozano-García, S., Vázquez-Selem, L., Ortega, B. 2010. Evidencias de cambio climático y ambiental en registros glaciales y en cuencas lacustres del centro de México durante el último máximo glacial. *Boletín de la Sociedad Geológica Mexicana*, 62(3), 359-377.

Cervera-Gómez, L.E., Cervantes-Rendón E. [Coordinadores]. 2018. Indicadores del agua en Chihuahua: Geografía del gua en el ordenamiento territorial del estado de Chihuahua. El Colegio de Chihuahua, Laboratorio de Geomática, reporte técnico, 97 p. https://doi.org/10.13140/RG.2.2.25564.69766

Esparza, M. 2014. La sequía y la escasez de agua en México: Situación actual y perspectivas futuras. *Secuencia*, 89, 195-219.

FAO (Food and Agriculture Organization). 2013. Tackling Water Scarcity: A Framework for Agriculture and Food Security. Rome, Italy: Food and Agriculture Organization of the United Nations, 78 p.

Ferrelli, F., Brendel, A.S., Piccolo, M.C., Perillo, G.M.E. 2020. Tendencia actual y futura de la precipitación en el sur de la región Pampeana (Argentina). *Investigaciones Geográficas*, 102, 1-17. https://doi.org/10.14350/rig.59919

Flores-Campaña, L.M., Arzola-González, J.F., Ramírez-Soto, M., Osorio-Pérez, A. 2012. Repercusiones del cambio climático global en el estado de Sinaloa, México. *Cuadernos de Geografía*, 21(1), 115-129. ISSN 2256-5442.

Greenpeace. 2018. Imágenes y datos: Así nos afecta el cambio climático. España: Greenpeace, 66 p.

Gobierno del Estado de Chihuahua. 2005. Plan Estatal de Desarrollo 2004-2010. Chihuahua, México: Gobierno del Estado, 165 p.

Guajardo-Panes, R.A., Granados-Ramírez, G.R., Sánchez-Cohen, I., Díaz-Padilla, G., Barbosa-Moreno, F. 2017. Validación espacial de datos climatológicos y pruebas de homogeneidad: caso Veracruz, México. *Tecnología y Ciencias del Agua*, 8(5), 157-177. https://doi.org/10.24850/j-tyca-2017-05-11

Haro, A.X., Limaico, C.T., Llosas, Y.E. 2016. Predicción de datos meteorológicos en cortos intervalos de tiempo en la ciudad de Riobamba usando la teoría del caos. *Sistemas, Cibernética e Informática*, 13(1), 34-41. ISSN: 1690-8627.

Hirsch, R.M., Slack, J.R., Smith, R.A. 1982. Techniques of trend analysis for monthly water quality data. *Water resources research*, 18(1), 107-121. https://doi.org/10.1029/WR018i001p00107

Hussain, M., Mahmud, I. 2019. pyMannKendall: a python package for non-parametric Mann Kendall family of trends tests. *The Journal of Open Source Software*, 4(39), 1556. DOI: https://doi.org/10.21105/joss.01556

INEGI (Instituto Nacional de Estadística y Geografía). 2013. Conociendo Chihuahua. México: Instituto Nacional de Estadística y Geografía, 36 p.

IPCC (Grupo Intergubernamental de Expertos sobre el Cambio Climático). 2014. Cambio climático 2014: Informe de síntesis. Contribución de los Grupos de trabajo I, II y III al Quinto Informe de Evaluación del Grupo Intergubernamental de Expertos sobre el Cambio Climático [Equipo principal de redacción, R.K, Pachauri y Meyer, L.A. (eds.)]. IPCC, Ginebra, Suiza, 157 p.

Karl, T.R., Easterling, D.R. 1999. Climate extremes: selected review and future research directions. *Climatic Change*, 42, 309-325. https://doi.org/10.1023/A:1005436904097

Kendall, M.G. 1975. Rank correlation methods. London, England: Charles Griffin, 202 p.

Khosravi, H., Sajedi-Hosseini, F., Nasrollahi, M., Gharechaei, H.R. 2017. Trend analysis and detection of precipitation fluctuations in arid and semi-arid regions. *Desert*, 22(1), 77-84. https://doi.org/10.22059/jdesert.2017.62173

Kundzewicz, Z.W., Robson, A. [Editors]. 2000. Detecting trend and other changes in hydrological data. Geneva, Suiza: World Meteorological Organization, WMO/TD-No. 113, 158 p.

Loyola-Martínez, E., Medellín-Milán, P., Avalos-Lozano, J.A., Aguilar-Robledo, M. 2011. Cambio climático y variabilidad en la dinámica de los ecosistemas de Wirikuta, municipio de Catorce (1950-2010). *Revista Geográfica de América Central*, 2, 1-19. ISSN-2115-2563.

Mallakpour, I., Villarini, G. 2016. A simulation study to examine the sensivity of the Pettit test to detect abrupt changes in mean. *Hydrological Sciences Journal*, 61(2), 245-254. https://doi.org/10.1080/02626667.2015.1008482

Mann, H.B. 1945. Nonparametric tests against trend. *Econometrica*, 13, 245-259.

Miller, G.T. 2007. Ciencia ambiental: Desarrollo sostenible, un enfoque integral. México: Editores Internacional Thomson, 8va Edición, 120 p.

Monterroso, A.I. 2012. Contribución al estudio de la vulnerabilidad al cambio climático en México [Tesis de Doctorado]. Universidad Nacional Autónoma de México, México.

Montoya, G., Palomino, R. 2005. Sistemas pluviogenéticos en Colombia: influencia de frentes fríos del hemisferio norte. *Meteorología Colombiana*, 9, 75-82. ISSN-0124-6984.

Pacheco, G.A.B., Hernández, R. 2019. Cambio climático algunos aspectos a considerar para la supervivencia del ser vivo: revisión sistemática de la literatura. *Revista cuidarte*, 10(3), 1-13. https://doi.org/10.15649/cuidarte.v10i3.664

Palaniswami, S., Muthih, K. 2018. Change point detection and trend analysis of rainfall and temperature series over the Vellar river basin. *Polish Journal of Environmental Studies*, 27(4), 1673-1681. https://doi.org/10.15244/pjoes/77080

Peña, A. 2004. Modelación de celdas lluviosas para la estimación de precipitación en una región interandina tropical [Tesis de Maestría]. Universidad Nacional de Colombia, Colombia.

Peña-Quiñones, A.J., Arce-Barboza, B.A., Ayarda-Moreno, M.A., Lascano-Aguilar, C.E. 2010. Simulación de los requerimientos hídricos de pasturas en un escenario de cambios climáticos generados con análisis espectral singular. *Acta Agronómica*, 59(1), 1-8.

Pérez-Palmar, E. 2017. El cambio climático, ¿ficción o realidad?... una percepción desde la comunidad internacional. *Revista Geográfica Venezolana*, 58(1), 198-213.

Peterson, T.C., Zhang, X., Brunet-India, M., Vázquez-Aguirre, J.L. 2008. Changes in North American extremes derived from daily weather data. *Journal of Geographical Research*, 113(D07113), 1-9. https://doi.org/10.1029/2007JD009453

Pettitt, A.N. 1979. A Non-Parametric Approach to the Change-Point Problem. *Journal of the Royal Statistical Society*, 28(2), 126-135. https://doi.org/10.2307/2346729

Rosengaus-Moshinsky, M., Jiménez-Espinosa, M., Vázquez-Conde, M.T. 2014. Atlas climatológico de ciclones tropicales en México. México: Centro Nacional de Prevención de Desastres, 106 p. ISBN: 970-628-633-0.

Rousseau-Figueroa, P.A., Ramírez-Hernández, J., Infante-Prieto, S.O., Villa-Angulo, R., Hallack-Alegría, M. 2016. La influencia del efecto del borde en el pronóstico de precipitaciones utilizando DWT diádica, MODWT, ANN y ANFIS. *Ciencia y Tecnología del Agua*, 7(3), 93-113.

Sánchez-Cohen, I., Díaz-Padilla, G., Cavazos-Pérez, M.T., Granados-Ramírez, G.R., Gómez-Reyes, E. 2011. Elementos para entender el cambio climático y sus impactos. México: Medio Ambiente y Ecología, 167 p.

Serrano-Vincenti, S., Ruiz, J.C. and Bersona, F. 2017. Heavy rainfall and temperature projections in a climate change scenario over Quito, Ecuador. *La Granja: Revista de Ciencias de la Vida*, 25(1), 16-32. https://doi.org/10.17163/lgr.n25.2017.02

Stock Informático. 2012. Cartografía de uso de suelo y vegetación del estado de Chihuahua. Chihuahua: Gobierno del Estado de Chihuahua/Secretaria de Desarrollo Rural/Dirección de Desarrollo Forestal, 97 p.

Useros-Fernández, J.L. 2013. El cambio climático: sus causas y efectos medioambientales. *Anales de la Real Academia de Medicina y Cirugía de Valladolid*, 50, 71-98.

Yozgatligil, C., Yazici, C. 2015. Comparison of homogeneity tests for temperature using simulation study. *International Journal of Climatology*, 36(1), 62-81. https://doi.org/10.1002/joc.4329

UACJ (Universidad Autónoma de Ciudad Juárez). 2019. Programa Estatal de Cambio Climático Chihuahua 2019. Universidad Autónoma de Ciudad Juárez. Gobierno del estado de Chihuahua, 198 p.

Watkiss, P., Downing, T., Handley, C., Butterfield, R. 2005. The Impacts and Costs of Climate Change: Final Report September 2005. Oxford, England: AEA Technology Environment/Stockholm Environment Institute, 77 p.

WMO (World Meteorological Organization). 1986. CLICOM project: climate data management system. Geneva, Switzerland: World Meteorological Organization, 33 p.

WMO (World Meteorological Organization). 2007. Role of climatological normals in a changing climate. Geneva, Switzerland: World Meteorological Organization, WMO-TD N. 1377, 43 p.

WMO (World Meteorological Organization). 2018. Guide to Instruments and Methods of Meteorological Observation: volume V - Quality assurance and management of observing systems. Geneva, Switzerland: World Meteorological Organization, WMO-No. 8, 2018 edition, 133 p.

Zarenistanak, M., Dhorde, A.G., Kripalani, R.H. 2014. Trend analysis and change point detection of annual and seasonal precipitation and temperature series over southwest Iran. *Journal of Earth System Science*, 123(2), 281-295. https://doi.org/10.1007/s12040-013-0395-7

Zhang, X., Yang, F., Chan, R. 2018. Introduction to RClimDex v1.9. Ontario, Canada: Climate Research Division/Environment Canada, 26 p.

Cuadernos de Investigación Geográfica *Geographical Research Letters*	2022	Nº 48	pp. 133-156	EISSN 1697-9540

http://doi.org/10.18172/cig.5062

ESTRATEGIAS DE ADAPTACIÓN AL CAMBIO CLIMÁTICO EN EL VIÑEDO DE LA CUENCA MEDITERRÁNEA: EL CASO DEL RIOJA

TEODORO LASANTA[1], CARLOS BAROJA-SÁENZ[1, 2], MELANI CORTIJOS-LÓPEZ[1]*, ESTELA NADAL-ROMERO[1], IGNACIO MARTÍN[3], ENRIQUE GARCÍA-ESCUDERO[3]

[1] Instituto Pirenaico de Ecología (IPE, CSIC), Campus de Aula Dei, Avda. Montañana, 177, 50080 Zaragoza, España.

[2] Instituto Geográfico Nacional (IGN), C/ General Ibáñez de Ibero, 3, 28003 Madrid, España.

[3] Instituto de Ciencias de la Vid y del Vino (ICVV) (CSIC, Universidad de La Rioja, Gobierno de La Rioja), Servicio de Investigación Agraria y Sanidad Vegetal del Gobierno de La Rioja, Finca La Grajera, España.

RESUMEN. El cambio climático está imponiendo condiciones cada vez más cálidas y secas en los viñedos de la cuenca mediterránea, que afectan tanto a la fisiología y fenología de la vid, como a la producción y a la calidad de la uva. En este contexto, se hacen necesarias medidas de adaptación y mitigación frente al cambio climático para mantener vinos de alta calidad y tipicidad varietal, así como para responder a las demandas del mercado. El objetivo de este trabajo es mostrar estrategias de adaptación que están llevando a cabo o están considerando los viticultores de la Denominación de Origen Calificada Rioja (DOCa Rioja). Entre las estrategias destacan: i) los cambios de localización del viñedo, bien hacia áreas con posibilidades de riego y suelos muy fértiles (terrazas bajas, principalmente), o bien hacia zonas de mayor altitud (glacis altos, fundamentalmente), con lo que se trata de evitar los efectos del estrés hídrico y del incremento de las temperaturas; y ii) las modificaciones en el sistema de conducción de la cepa, sustituyendo en muchas ocasiones la conducción en vaso por la de espaldera, con el fin de hacer coincidir un mayor grado de mecanización de las tareas agronómicas y la mejora del microclima de la cepa, especialmente en las nuevas plantaciones sobre suelos muy fértiles. Estas estrategias serán cada vez más relevantes, teniendo en cuenta el previsible incremento de las temperaturas y de las sequías en los futuros escenarios climáticos. No obstante, se plantea la duda de si serán suficientes o se necesitará eliminar restricciones actuales impuestas por la DOCa Rioja, como ampliar el área de cultivo del viñedo en zonas de montaña o introducir nuevas variedades.

Strategies for adaptation to climate change in vineyards in the Mediterranean basin: the case of the DOCa Rioja

ABSTRACT. Climate change is promoting increasingly hot and dry conditions in the vineyards of the Mediterranean basin, affecting both the physiology and phenology of the vine, as well as the production and quality of the grape. In this context, adaptation and mitigation measurements against climate change are necessary to maintain high quality wines and varietal typicity, as well as to respond to market demands. The objective of this study is to show adaptation strategies that are being carried out or considered by winegrowers of the Denomination of Origin Qualified Rioja (DOCa Rioja). Among the strategies, the following should be highlighted: changes in the location of the vineyard, either towards areas with irrigation possibilities and very fertile soils (mainly low terraces), or towards higher altitude areas (mainly high glacis), thus trying to avoid the effects of water stress and increased temperatures; and (ii) modifications in the strain conduction system, often replacing the vessel

conduction with the trellis conduction, in order to match a greater degree of mechanization of the agronomic tasks and the improvement of the improvement of the vine's microclimate, especially in the new plantations in very fertile soils. These strategies will be increasingly relevant, taking into account the foreseeable increase in temperatures and droughts in the future climate scenarios. However, the question arises as to whether these strategies will be sufficient or whether it will be necessary to eliminate current restrictions imposed by DOCa Rioja, such as expanding the vineyard in mountain areas or introducing new varieties.

Palabras clave: Viticultura, regadío, viñedos de altitud, gestión de viñedos, Denominación de Origen.

Key words: Viticulture, irrigation, high altitude vineyards, vineyard management, "terroir".

Recibido: 10 Marzo 2021

Aceptado: 27 Abril 2021

*Correspondencia: Melani Cortijos López, Instituto Pirenaico de Ecología (IPE, CSIC), Campus Aula Dei, Avda. Montañana, 177, 50080 Zaragoza, España. E-mail address: melani@ipe.csic.es

1. Introducción

El sector vitivinícola es especialmente vulnerable al cambio climático (CC), por su elevada dependencia de las condiciones climáticas y ambientales (Carroquino *et al.,* 2020). Especialmente, el incremento de las temperaturas y el estrés hídrico asociados al CC tienen efectos sobre la fisiología y fenología de la vid, los rendimientos y la calidad de la uva (Iglesias *et al.,* 2010; Jones y Alves, 2012; Fraga *et al.,* 2016a; Ramos, 2017).

En los últimos años, se han realizado diversos estudios a escala mundial y regional para evaluar y predecir cómo afecta el CC a la viticultura en la actualidad, y cómo afectará en las próximas décadas (López-Bustíns *et al.,* 2014; Mills-Novoa *et al.,* 2016; Ramos, 2017; van Leeuwen y Destrac-Irvine, 2017; Irimia *et al.,* 2018; Biasi *et al.,* 2019; Del Pozo *et al.,* 2019, entre otros). Los estudios realizados identifican tres efectos del CC especialmente sensibles para la viticultura: i) el aumento de las temperaturas; ii) la modificación de los patrones de lluvia, con un reparto irregular a escala anual e interanual de las precipitaciones, con la existencia de periodos de sequía más frecuentes, intensos y duraderos, junto con episodios de lluvias muy intensas que ocasionan graves problemas de erosión en el suelo; y iii) el incremento de la radiación solar, en particular de los rayos UV-B.

Los estudios climáticos señalan que, durante el siglo XX, la temperatura se ha incrementado entre 0,5 y 1ºC (IPCC, 2014), y que esta tendencia continuará durante el siglo XXI con incrementos entre 1 y 4ºC, en función de la cantidad de las emisiones de gases de efecto invernadero (IPCC, 2014). El incremento de la temperatura implica un adelanto de las etapas fenológicas de la vid (brotación, floración, envero y maduración), lo que lleva a una cosecha más temprana (Ramos, 2017; van Leeuwen y Destrac-Irvine, 2017; Santillan *et al.,* 2019). Jones (2006) señala que la cosecha de la uva se ha adelantado entre seis y veinticinco días en Europa, reflejando la fuerte relación entre calentamiento y fenología de la vid. En el hemisferio norte, la madurez de la uva, es decir, la composición óptima para que el vino sea de buena y adecuada calidad, se debe alcanzar entre el 10 de septiembre y el 10 de octubre, cuando las temperaturas comienzan a disminuir (van Leeuwen y Seguin, 2006). Si la maduración transcurre con temperaturas elevadas, el resultado supondrá uvas con características desequilibradas, con altos niveles de azúcar y, por tanto, un grado alcohólico elevado del vino, y baja concentración de ácidos orgánicos, lo que reduce la capacidad para el envejecimiento del vino, con un pH alto y escasa complejidad aromática (van Leeuwen y Destrac-Irvine, 2017; Carroquino *et al.,* 2020).

Los cambios en la precipitación no son tan claros ni tan uniformes como en el caso de las temperaturas (IPCC, 2014). En la cuenca mediterránea, la precipitación anual no muestra una tendencia clara (Peña-Angulo *et al.,* 2020). Sin embargo, se ha observado la disminución de la precipitación en primavera y la mayor frecuencia e intensidad de las sequías, generando en la vid de secano periodos más acusados de estrés hídrico (De Luis *et al.,* 2009; Domínguez-Castro *et al.,* 2019). El estrés hídrico provoca la senescencia prematura de las hojas, lo que dificulta la correcta maduración de la uva y reduce los rendimientos, ya que condiciona el número de racimos y las bayas alcanzan menor peso (Romero *et al.,* 2015; Del Pozo *et al.,* 2019). Por otro lado, los escenarios futuros inciden en que el estrés hídrico se incrementará debido a la mayor demanda de agua por un aumento de la evapotranspiración (Iglesias *et al.,* 2011; Domínguez-Castro *et al.,* 2019). Otro aspecto del CC que influye en la fenología de la vid es el incremento de la radiación solar, especialmente de los rayos UV-B (Schultz, 2000), lo que puede ser positivo en determinadas circunstancias para los compuestos fenólicos del hollejo de la uva, pero negativo en otras para los aromas y el color, especialmente si la radiación es muy elevada (Van Leeuwen y Darriet, 2016).

Así las cosas, el CC está imponiendo condiciones cada vez más cálidas y secas en los viñedos, por lo que la calidad y los rendimientos se están viendo afectados. Aún lo estarán más en el futuro de continuar la actual tendencia climática (van Leeuwen *et al.,* 2019).

La globalización en la vitivinicultura es una realidad mucho más evidente que en otros cultivos y productos agroalimentarios. Alrededor de un tercio de la producción mundial de vino se exporta a los mercados internacionales, que son extremadamente competitivos (Albisu, 2014). Hay que tener en cuenta que el consumo de vino retrocede desde los años setenta del pasado siglo: en el quinquenio 1976-80 el consumo medio anual era de 285,7 millones de hectólitros (M/hl), mientras que para el periodo 2011-2015 lo fue de 241,8 M/hl. Sin embargo, la producción cada vez es mayor por la incorporación de nuevos países productores al mercado mundial, de tal modo que la producción supera claramente a la demanda, suponiendo en ese mismo quinquenio de 2011-2015 una producción de 271,4 M/hl/año (Barco Royo, 2018). Son los vinos de calidad, con características específicas ligadas a un territorio, los que mejor se comercializan en los mercados internacionales del vino y mayor rentabilidad aportan a las regiones productoras (Albisu, 2014; Constantini *et al.,* 2016).

En este contexto, normalmente cada vino se presenta en el mercado con una etiqueta de Denominación de Origen (D.O.) concreta, identificándose de algún modo con el concepto de "*Terroir*", es decir, conjunto de factores naturales y humanos que interactúan para producir un vino específico (Vaudour, 2002; van Leeuwen y Seguin, 2006; Hinnewinkel, 2010). Estos factores incluyen el clima, el suelo, la topografía, el sistema de cultivo de la vid y las prácticas vitícolas y enológicas; juntos crean características únicas y distintivas en el vino de un lugar dado, lo que es percibido y reconocible por los consumidores y expertos (Costantini *et al.,* 2016; Vaudour *et al.,* 2015; Priori *et al.,* 2019).

Es cierto que se puede cultivar la vid en climas muy diversos, pero no es menos cierto que la viticultura de calidad sólo es posible en un estrecho rango de condiciones climáticas fuera del cual se puede producir vino, pero por lo general de una calidad muy inferior (Mills-Novoa *et al.,* 2016). Para muchas regiones vitícolas mediterráneas, con vinos muy reconocidos y valorados en los mercados, tiene especial interés mantener la calidad y tipicidad de la uva, con el fin de no perder mercados o sufrir la bajada de los precios que los consumidores están dispuestos a pagar (van Leeuwen *et al.,* 2019).

Las áreas mediterráneas tienen una gran diversidad de condiciones ambientales, como consecuencia de un relieve complejo, que genera una elevada heterogeneidad topográfica y topoclimática (Nogués-Bravo, 2006; Serra *et al.,* 2008; García-Ruiz *et al.,* 2011). Por otro lado, cuentan con infraestructuras de riego y elevados conocimientos sobre el manejo del agua, lo que facilita dotar de riego a cultivos tradicionalmente de secano, como el viñedo (Lasanta, 2009; Jlassi *et al.,* 2016). Nuestra hipótesis es que la diversidad de ambientes y su conocimiento, así como el riego, ofrecen oportunidades de adaptación local a la viticultura mediterránea, lo que puede ayudar a mitigar el cambio

climático y a mantener un sector socioeconómico fundamental para muchas regiones vitivinícolas (Lehmann *et al.,* 2013; Delay *et al.,* 2015).

El cambio climático es una realidad, por lo que es necesario explorar la capacidad de los viticultores para aprovechar su medio ambiente y gestionar un correcto manejo de las prácticas agrícolas que permiten adaptarse al CC. El objetivo de este trabajo pasa por aportar información sobre las primeras medidas de adaptación al CC que se están realizando en los viñedos de la Denominación de Origen Calificada Rioja (DOCa Rioja, en adelante). En concreto, se estudian: i) los cambios en la localización del viñedo entre 1977 y 2017, y ii) los cambios en las prácticas agronómicas relacionadas con el sistema de conducción de las cepas. Mostrar estos cambios tiene un elevado interés práctico para la propia región de la DOCa Rioja, donde el sector vitivinícola basado en el vino de calidad constituye uno de los motores fundamentales de la economía regional, y para otras áreas mediterráneas en las que la producción de vino de alta calidad ofrece beneficios económicos, sociales y ambientales, además de generar empleo y constituir un factor de sostenibilidad (Iglesias *et al.,* 2011; Burge *et al.,* 2015; Santillan *et al.,* 2019).

2. Materiales y métodos

2.1. Área de estudio

En este estudio se trabaja a tres escalas espaciales (regional, comarcal y municipal), en función de la información disponible y del tipo de cambio estudiado.

2.1.1. Escala regional: El territorio de La Rioja

El vino de Rioja (España) procede de viñedos localizados en tres provincias: La Rioja (que aporta el 68,7% de la superficie), Álava (20,5%) y Navarra (10,7%) (Fig. 1). En este artículo, hablamos de Rioja para el conjunto de la DOCa Rioja, y nos referimos en otras ocasiones exclusivamente al territorio de La Rioja como provincia. A escala de la provincia de La Rioja, el sector vitivinícola tiene un destacado peso socioeconómico. Basta señalar que en 2017 el viñedo ocupaba 46.876 ha, es decir el 30% del espacio agrícola, siendo el segundo cultivo en extensión, después de los cereales con 50.674 ha, y un 32,4% de la superficie cultivada (Gobierno de La Rioja, 2020). Es el primero en aportación económica dentro del sector agrario, con un montante de 320,2 M. de euros en 2017, lo que equivale al 45,6% de la Producción Final Agraria. La producción de vino aportó, en la misma fecha, 692,3 millones de euros y 2.396 empleos (el 10,2% del empleo industrial). En conjunto, el sector vitivinícola representó el 12,3% del Producto Interior Bruto de La Rioja. La aportación económica fue aún mayor en las comarcas de Álava y Navarra, amparadas bajo en la DOCa Rioja, ya que la vitivinicultura es su pilar económico, en algunos municipios casi único (Lasanta, 2018).

El viñedo de Rioja se localiza en las llanuras de la Depresión del río Ebro, caracterizadas por una suave topografía y altitudes comprendidas entre 300 y 600 m s.n.m. (Fig. 1). En este sector, el relieve se resuelve en varios niveles de glacis y terrazas, que alternan con restos de plataformas estructurales (Gonzalo Moreno, 1981). Los glacis están formados por un sustrato rocoso de areniscas y margas terciarias, cubiertos por acumulaciones cuaternarias, donde la presencia de cantos es frecuente, especialmente en los niveles más altos. Las terrazas poseen suelos más profundos y fértiles que los glacis, si bien las más antiguas cuentan con abundantes cantos. Al norte y al sur del área de localización del viñedo, aparecen un conjunto de sierras incluidas en la Cordillera Cantábrica y el Sistema Ibérico, respectivamente, con altitudes superiores a los 800 m s.n.m. De cara al desarrollo de la vid y de la calidad del vino, los materiales de los suelos de La Rioja pueden clasificarse en tres órdenes: Alfisoles, Mollisoles e Inceptisoles, según la clasificación de la Soil Taxonomy (Martínez Vidaurre, 2017).

El clima de la DOCa Rioja es muy variado, con influencias atlánticas en el sector occidental y mediterráneas en el oriental, a lo que hay que unir los contrastes que crea el relieve, lo que origina un

mosaico de regímenes climáticos (Cuadrat y Vicente-Serrano, 2008). En el sector occidental, las precipitaciones superan los 500 mm, alcanzando su máximo en invierno y primavera. El balance hídrico es favorable y son pocos los meses con déficit de agua. Las temperaturas resultan suaves, con amplitud térmica moderada. En el sector oriental, las precipitaciones no alcanzan los 400 mm en la mayor parte de los observatorios, registrándose los máximos en otoño y primavera. Las temperaturas son más elevadas, con mayor oscilación térmica que en el sector más occidental, mostrando un carácter más continental. El déficit hídrico y la evapotranspiración potencial alcanzan valores elevados (Cuadrat y Vicente-Serrano, 2008). Tonietto y Carbonneau (2004) reconocen en el viñedo de Rioja unas condiciones climáticas especialmente adecuadas para la viticultura de calidad, con un nivel aceptable en restricciones climáticas, así como unas condiciones más ventajosas que en otros territorios vitivinícolas (Zhu *et al.,* 2014). Las proyecciones de diferentes escenarios de cambio climático en la región indican que las temperaturas se van a incrementar en torno a 4ºC a finales del siglo XXI y las precipitaciones se reducirían alrededor de un 15%, considerando en ambos casos el escenario de emisiones de gases de efecto invernadero (RCP8.5) (http://escenarios.adaptecca.es/). Estos cambios suponen condiciones de mayor aridez climática, con un notable aumento de la frecuencia y severidad de los eventos de sequía (García-Valdecasas *et al.,* 2020).

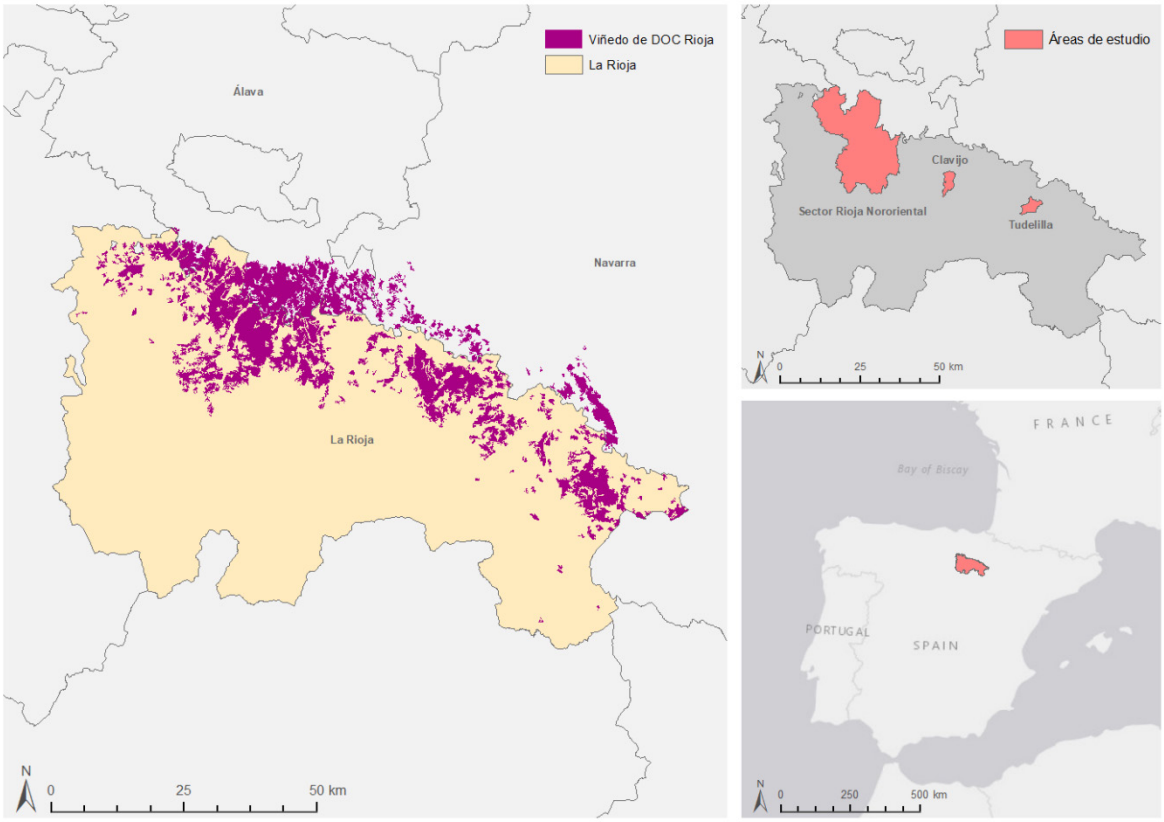

Figura 1. Área de estudio.

2.1.2. Escala comarcal: La Rioja Alta y los municipios de Clavijo y Tudelilla

Para conocer los cambios en la distribución espacial del viñedo, se trabajó a dos escalas: comarcal y municipal. A escala comarcal, se seleccionó un sector de la Rioja Alta (Fig. 1), donde el viñedo ha constituido, desde hace más de un siglo, la matriz del paisaje (Galilea-Salvador, 2010). En este sector, el río Ebro recorre el área de estudio de Oeste a Este, recibiendo por su margen derecha las aguas de sus afluentes Oja-Tirón y Najerilla, mientras que por la izquierda desaguan una serie de barrancos de corto recorrido que descienden de la Sierra de Cantabria (Ollero Ojeda, 1996), por lo que

dominan glacis y terrazas como formas de relieve, con una topografía de suaves pendientes y formas ligeramente alomadas o llanas (Gonzalo Moreno, 1981). El clima es de tipo mediterráneo con influencia atlántica, con una precipitación media de 500-600 mm y valores máximos en primavera e invierno. La temperatura media anual oscila entre los 12-13ºC, registrándose una moderada amplitud térmica: 4-6ºC en diciembre-enero y 20-21ºC en julio-agosto (Cuadrat y Vicente-Serrano, 2008). Los suelos predominantes son Calcisoles, con textura franca y arenosa (Gómez Miguel, 2006).

Por otro lado, para conocer los cambios del viñedo en altitud, se trabajó en dos municipios: Clavijo y Tudelilla (Fig. 1). Se eligieron estos dos municipios por: i) su localización en el sector central de La Rioja (clima de transición entre las condiciones más oceánicas del sector occidental y más mediterráneas del sector oriental); ii) ser municipios con marcado carácter de secano, por lo que los viñedos no pueden beneficiarse fácilmente del agua de riego y iii) ser representativos del piedemonte o somontano, lo que implica importantes diferencias de altitud entre las cotas extremas de ambos municipios. Además, uno de los municipios (Clavijo) tiene escasa tradición vitícola, mientras que el otro (Tudelilla) ha tenido el cultivo de la vid como principal actividad económica, al menos desde mediados del siglo XX.

2.1.3. El vino de Rioja

La diversidad de condiciones climáticas y edáficas da lugar a una gama de vinos muy amplia y variada, con buena aceptación en mercados diversos, en los que progresivamente ha ido adquiriendo nuevas cuotas de reconocimiento y posicionamiento. Así, en el quinquenio 1979-83 se comercializó una media de 99,24 Mlitros/año, de los que el 71,7% se destinó al comercio interior y el resto al comercio exterior. En el quinquenio 2013-17, se vendió una media de 281,75 Mlitros/año, de los que el 62,6% fue al mercado nacional y el resto se exportó a países de los cinco continentes, siendo Reino Unido, Alemania y EE.UU. los principales consumidores (Lasanta, 2018).

La producción de vino de Rioja está regulada y controlada desde 1926 por el Consejo Regulador (C.R.) de la DOCa Rioja, cuya misión es: i) delimitar el territorio del Rioja; ii) controlar el cultivo y las exigencias de elaboración para la obtención de un vino de calidad, haciendo uso del contenido de su Reglamento y de las Normas de Campaña; y iii) promocionar la imagen del Rioja y ayudar a los agentes del sector a buscar nuevos mercados. De cara a los objetivos de este trabajo conviene resaltar algunas cuestiones reguladas por el C.R. de la DOCa Rioja:

1. En 2018, el 90,85% del viñedo de Rioja (59.819 ha) eran variedades tintas y el 9,15% (6.022 ha) variedades blancas. Entre las variedades tintas, las más importantes son el *Tempranillo* (79,7% de la superficie total del viñedo) y la *Garnacha tinta* (6,9%). Otras variedades tintas están permitidas: *Graciano* (1,9%), *Mazuelo* (1,9%) y *Maturana Tinta*. Entre las variedades blancas, la más representativa es la *Viura* (6,3%). Recientemente, se han incluido otras variedades blancas: *Maturana Blanca, Tempranillo Blanco, Turruntés, Verdejo, Chardonnay y Sauvignon Blanc*, que están teniendo una buena acogida por parte de los viticultores, pero dada su reciente implantación todavía ocupan muy poca superficie en el conjunto de la DOCa Rioja. En definitiva, el Rioja presenta escasa diversidad varietal, ya que las tres variedades principales ocupan el 96,8% del viñedo de Rioja (C.R. de la DOCa Rioja, 2019).
2. Desde el año 2000 el C.R. de la DOCa Rioja limitó los rendimientos con el fin de ajustar la oferta a la demanda y mantener la calidad. En uvas tintas, el rendimiento máximo es de 6500 kg/ha y en blancas de 9000 Kg/ha, pudiéndose incrementar (o disminuir en su caso) un 10% más en función de las circunstancias de cada año.
3. En su momento y con los criterios de entonces, la Ley 25/1970, de 2 de diciembre, del Estatuto de la Viña, del Vino y de los Alcoholes prohibió el riego del viñedo para evitar la sobreproducción de vino, lo que plantearía problemas de comercialización en los mercados y la

pérdida de calidad ligada a la menor graduación alcohólica. Sin embargo, las frecuentes e intensas sequías durante los años noventa, aconsejaron suprimir dicha ley para asegurar las cosechas y en su caso una correcta maduración de la uva. A partir de la Ley 24/2003, de 10 de julio, de la Viña y del Vino, los viñedos pueden recibir riegos de apoyo durante el ciclo de cultivo, generalmente riego localizado por goteo, en las fechas y condiciones que la DOCa Rioja determina (Lasanta *et al.*, 2016).

4. El sistema tradicional de poda de la cepa ha sido el vaso. No obstante, desde 1991 el CR de la DOCa Rioja admitió el sistema de conducción apoyado en espaldera, manteniéndose de forma similar los criterios de densidad de plantación que regían para el sistema de poda en vaso. La admisión del sistema en espaldera obedece, entre otras cuestiones, a dos objetivos: i) aumentar el grado de mecanización de las explotaciones vitícolas, y ii) favorecer la instalación del riego localizado, con el apoyo de las estructuras de conducción del viñedo en espaldera, lo que puede contribuir a facilitar la instalación del riego y, en algunos casos, a economizar el gasto de agua (Rodríguez Rodrigo, 2000).

2.2. Fuentes de información y métodos

2.2.1. Cartografía del viñedo en La Rioja Alta y su relación con las formas de relieve

A escala comarcal, se estudió la evolución de la localización del viñedo entre 1977 y 2017 en la Rioja Alta. La metodología se apoyó en las fotografías aéreas de 1977 y de 2017. Se escanearon los fotogramas con la máxima resolución, se georreferenciaron y se cartografiaron con detalle las parcelas de viñedos, con la ayuda de un software SIG (Arc View). Las imágenes utilizadas cubrieron un total de 517,37 km^2. Una vez generados los mapas, los datos se exportaron a un software SIG raster (ArcGis 10.5), con el objetivo de poder analizar y visualizar los datos espacialmente. Para relacionar la distribución del viñedo, en ambas fechas, con un documento de síntesis de las condiciones ambientales, se utilizó un mapa geomorfológico, elaborado por Galilea-Salvador (2010), que incluye tanto formas de sedimentación (glacis y terrazas) como de vertientes (vertientes regularizadas) y áreas de erosión (badlands y rills).

2.2.2. Cartografía del viñedo y su relación con la altitud en Clavijo y Tudelilla

En el mismo sentido, se cartografió la distribución del viñedo en 1977 y en 2017 en Clavijo y Tudelilla. Como primer paso para elaborar la cartografía, se descargó la información disponible en la sede del catastro (https://www.sedecatastro.gob.es). Esta información, de tipo vectorial en formato *shapefile*, sirvió de base para determinar mediante técnicas de fotointerpretación las parcelas de viñedo. La información vectorial se modificó para ajustar los polígonos de las parcelas a la superficie cubierta por vid, ya que en algunos casos las parcelas cuentan con cultivos diferentes. Una vez identificadas todas las parcelas de interés, se exportó como una nueva capa vectorial, y se creó un campo en la tabla de atributos en el que se calculó la superficie de los polígonos (*Calculate Geometry*).

Para derivar la información de altitud y pendiente nos servimos del Modelo Digital del Terreno (MDT05) con paso de malla de 5 metros, disponible en el Centro de Descargas del Instituto Geográfico Nacional (https://centrodedescargas.cnig.es/CentroDescargas). Los límites municipales de Tudelilla y Clavijo se obtuvieron de la Infraestructura de Datos Espaciales de La Rioja (IDE Rioja: www.larioja.org). Para ajustar el MDT05 a los límites municipales, se generó un buffer espacial de 200 metros con el perímetro de los municipios, y esa nueva capa sirvió para cortar el MDT. Posteriormente, se aplicó una paleta de color adecuada para la visualización de los sectores con mayor y menor altitud, medida sobre el nivel del mar.

Para conocer la altitud de las parcelas se optó por un proceso en varios pasos: (1) crear los centroides de cada parcela de viñedo – *Feature to point*, (2) superponer esta información con el modelo digital del terreno y extraer la información de la altitud en dichos centroides – *Extract Multivalues to points*, y (3) unir la información resultante con el archivo vectorial de las parcelas – *Join*.

Con el proceso descrito, se obtuvo una tabla de atributos de las parcelas de viñedo, con información sobre superficie y altitud en el centro de la parcela. La tabla de atributos constituyó la base de datos que puede exportarse en formato de texto para realizar los análisis y los gráficos oportunos.

2.2.3. Información sobre superficie de viñedo en regadío y sistema de conducción en La Rioja

La información sobre la evolución de la superficie de viñedo en La Rioja (periodo 1990-2018) se obtuvo del C.R. de la DOCa Rioja. Su distribución en secano y regadío, así como la información sobre la superficie reconvertida y reestructurada con subvención oficial para transformar la conducción de las cepas (periodo 2001-2015), se recopilaron del Registro Vitivinícola del Gobierno de La Rioja (RVGLR). Se trata de dos fuentes de información totalmente fiables, ya que se trabaja a escala de parcela y los técnicos del Gobierno de La Rioja comprueban en el campo la verosimilitud de la información.

3. Resultados

3.1. La distribución del viñedo en La Rioja Alta (1977-2017) en relación con las formas de relieve

La Tabla 1 incluye información sobre las formas de relieve en un sector de la Rioja Alta. El conjunto del área de estudio ocupa 517,2 Km^2, donde dominan los glacis (170,3 Km^2) y las terrazas aluviales (192,1 Km^2), que constituyen formas de sedimentación muy favorables para el uso agrícola, al poseer suelos profundos, con frecuencia fértiles, de escasa pendiente, buen drenaje y abundancia de cantos rodados con matriz arenosa, cualidades muy positivas para el cultivo de viñedos (Tabla 1). Los cursos fluviales que recorren el área de estudio han generado un sistema de terrazas amplio, que incluye hasta 9 niveles. Los glacis, que ponen en contacto los bordes montañosos circundantes (Cordillera Cantábrica y Sistema Ibérico) con los fondos de valle, fueron originados por la acción erosiva de los cursos torrenciales no encauzados, que depositaron sus sedimentos en las zonas más deprimidas de los pies de la montaña. Presentan una pendiente relativamente suave (por debajo del 5%, generalmente), pudiendo identificarse en algunos sectores hasta 12 niveles (Galilea-Salvador, 2010). Algunos viñedos también ocupan otras formas de relieve: paleocanales, valles en cuna y vertientes regularizadas, mientras que el 28,4% del territorio, que hemos agrupado con el nombre genérico de dominios geológicos, no cuentan con viñedos (Tabla 1).

La Figura 2 muestra la distribución del viñedo en 1977 y en 2017 en la zona seleccionada de Rioja Alta. En los cuarenta años transcurridos entre ambas fechas, el viñedo se ha expandido de forma muy importante, pasando de ocupar 11.490 ha en 1977 (el 22,2% del área estudiada) a 18.961 ha en 2017 (el 36,6% del área estudiada), lo que representa un incremento del 65%. Todas las formas de relieve con viñedos han visto incrementada su superficie entre ambas fechas, si bien las terrazas medias y los glacis altos son las áreas que registraron un mayor incremento proporcional, con un 126% y 168,8%, respectivamente. En este sentido, es muy destacable el incremento que ha registrado el viñedo en los glacis altos: en 1977 ocupaba el 23,4% de la superficie cubierta por esta forma de relieve, y en 2017 el 63%. Esta evolución se observa también en los glacis medios, donde el viñedo ha pasado de ocupar el 38% en 1977 al 63,2% en 2017, en la Terraza 1, del 17,2% en 1977 al 28,6% en 2017, y en las terrazas bajas, del 22,7% en 1977 al 43,2% en 2017.

Tabla 1. Superficie ocupada por las formas de relieve en el sector estudiado de La Rioja Alta.

Formas de relieve	Superficie (Km^2)	% sobre el total
Formas con viñedos		
Terrazas altas (6-9)	36	7
Terrazas medias (4-5)	23,4	4,5
Terrazas bajas (2-3)	58,6	11,3
Terraza holocena y lecho de inundación (1)	74,1	14,3
Glacis altos (6-12)	8,8	1,7
Glacis medios (4-5)	64,7	12,5
Glacis bajos (2-3)	71	13,7
Glacis y conos holocenos (1)	25,8	5
Paleocanales y valles en cuna	2,5	0,5
Vertientes regularizadas	4,2	0,8
Rills y badlands	1,2	0,2
Formas sin viñedos		
Dominios geológicos	146,9	28,4
Total	517,2	100

Elaboración propia a partir de Galilea-Salvador (2010).

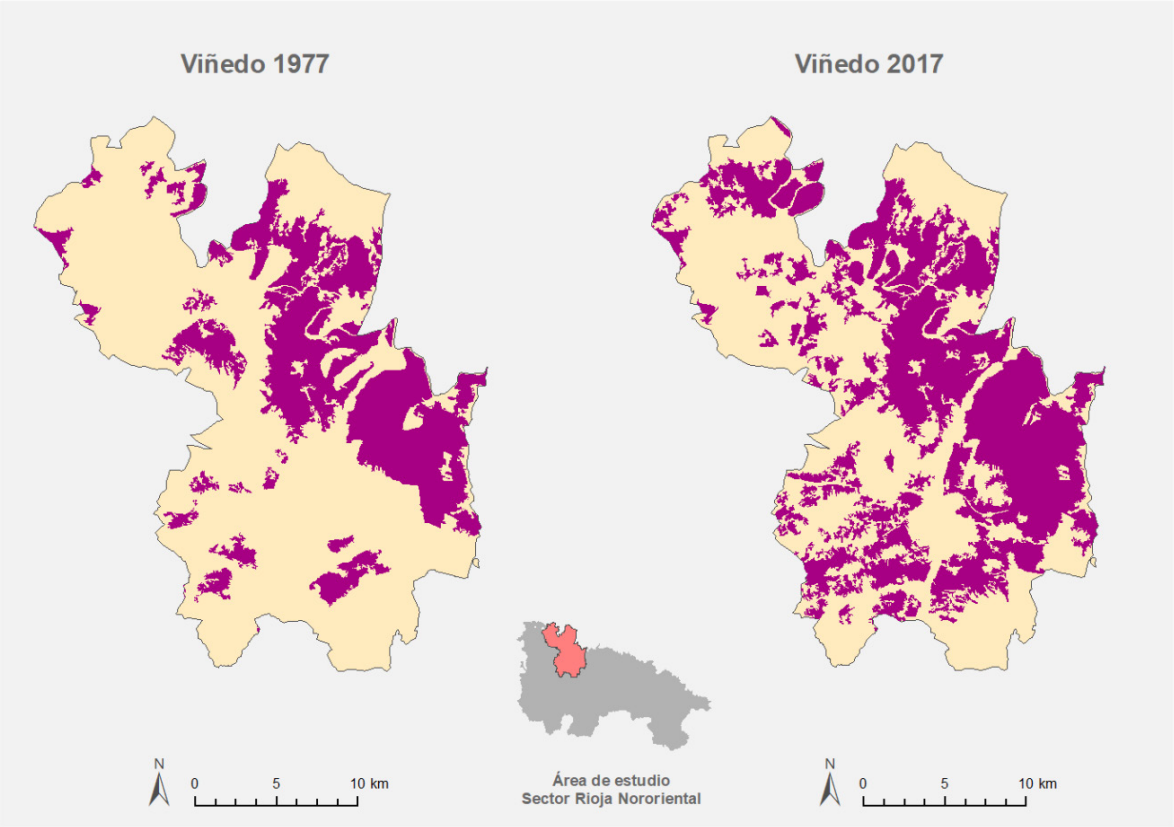

Figura 2. Cambios en la localización del viñedo en La Rioja Alta (1977-2017).

La Figura 3 recoge dos imágenes de viñedos junto al cauce del río Ebro. Tradicionalmente las terrazas y glacis bajos se dedicaron al cultivo de frutales, hortalizas, maíz, alfalfa, patatas y remolacha. Sin embargo, en las últimas décadas muchas de las huertas tradicionales han sido sustituidas por viñedos, aprovechando las infraestructuras de riego, al ser actualmente un cultivo más rentable que los anteriores.

Figura 3. Viñedos junto al río Ebro. a) San Asensio; b) El Cortijo.

3.2. El ascenso en altitud del viñedo en Clavijo y Tudelilla

La Figura 4 incluye la distribución del viñedo en los municipios de Clavijo y Tudelilla, en 1977 y en 2017. En Clavijo, el cultivo de la vid ocupaba muy poca extensión en 1977: 53 ha. En Tudelilla, por el contrario, el viñedo tenía mayor presencia, con 490 ha. Entre 1977 y 2017, los dos municipios registran la expansión del viñedo, alcanzando Clavijo 220 ha (se multiplica por cuatro respecto a 1977) y Tudelilla 800 ha (un incremento del 63%). Estos datos muestran cómo el viñedo se ha incrementado en Clavijo desde el 2,7% de su superficie en 1977 al 11,2% en 2017. Mientras tanto, en Tudelilla la ocupación del viñedo registra una evolución que va desde el 27,7% en 1977 al 42% en 2017.

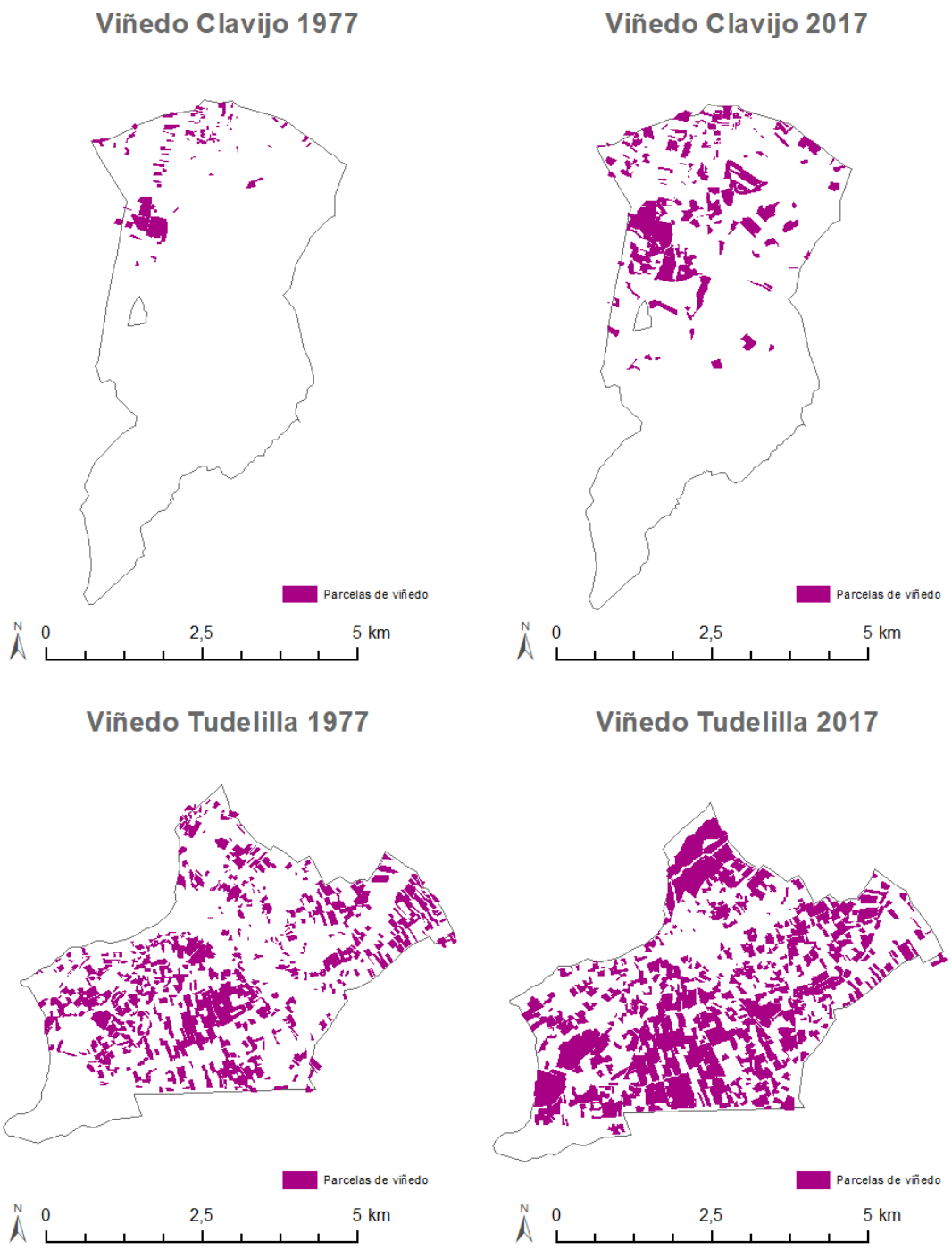

Figura 4. Localización del viñedo en Clavijo y Tudelilla (1977-2017).

La expansión superficial del viñedo implica que en ambos municipios el viñedo ocupe más superficie, en cualquier rango de altitud, en 2017 que en 1977 (Fig. 5). No obstante, se observa que en 1977 en Clavijo no había viñedos por encima de los 650 m s.n.m., mientras que en 2017 los hay en 12 ha (el 5,45% de la superficie del viñedo). Por otro lado, es en el rango de 601 a los 650 ms.n.m. donde el incremento ha sido mayor, pasando de 24 ha a 88 ha, es decir, se ha visto multiplicado por 3,6. En Tudelilla, el viñedo por encima de 600 m s.n.m. ha pasado de representar el 21,4% en 1977 al 24,3% en 2017.

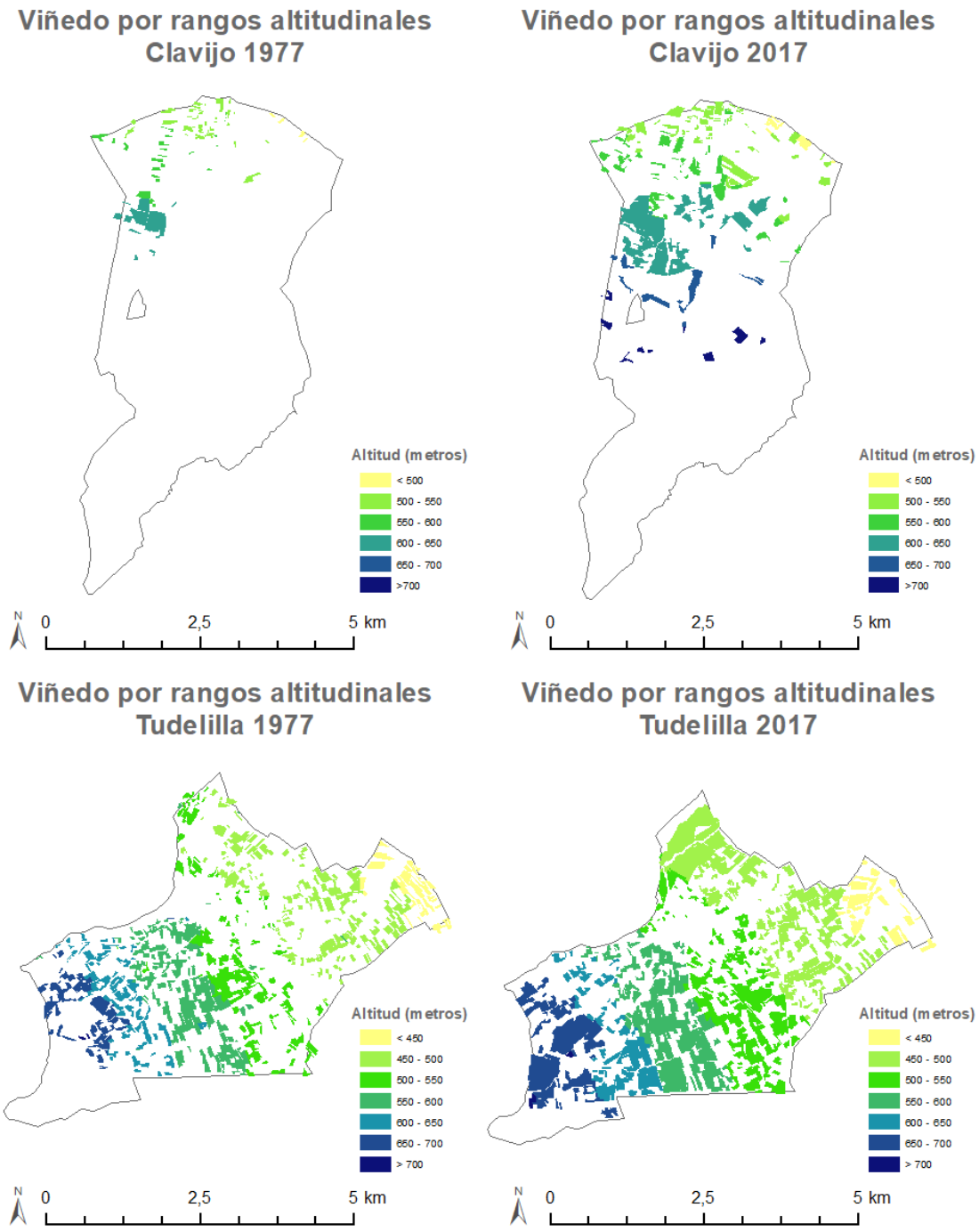

Figura 5. Superficie de viñedo por rangos altitudinales en Clavijo y Tudelilla (1977-2017).

La Figura 6 aporta dos imágenes de viñedos jóvenes plantados en cotas elevadas. La imagen 6a hace referencia a viñedos en Clavijo, donde una bodega ha recuperado campos abandonados cubiertos por matorrales (*Tymus vulgaris*, *Rosmarinus officinalis*, *Genista scorpius, Rosa sp., Buxus sempervirens, Crataegus monogyna, Juniperus communis*,…) para llevar a cabo la plantación de vid. La recuperación trata de mantener el paisaje, conservando los bosquetes y árboles aislados en los márgenes de los campos (*Quercus ilex sp. Ballota* y *Quercus pyrenaica*, fundamentalmente), así como los antiguos bancales y los límites de los campos. El viñedo llega a alcanzar cotas superiores a los 850 m s.n.m. La imagen 6b corresponde a viñedos de altitud en Tudelilla. En este caso, se ha desmontado parcialmente un bosque de carrascas con suelos muy pedregosos para la plantación de los viñedos.

Figura 6. Viñedos de altitud. a) viñedos en antiguos campos abandonados en Clavijo. b) Viñedos entre carrascas en Tudelilla.

3.3. El incremento del viñedo en regadío en La Rioja

La Figura 7 revela que la superficie de viñedo en regadío se ha visto incrementada considerablemente en los últimos 28 años. Aunque el riego estuvo prohibido hasta 2003, las viñas no desaparecieron totalmente de los polígonos de regadío, si bien no se regaban, al menos legalmente hablando. En 1991, el viñedo en regadío ocupaba 1.319 ha (el 3,7% de la superficie total), iniciando un ascenso moderado hasta 2002 (4.060 ha). A partir de esta fecha, la superficie de viñedo en regadío se ha multiplicado por 3,5, hasta ocupar 14.324 ha en 2018 (el 30,3% de la superficie total), mientras que el de secano se contraía el 15,7%, pasando de 39.019 ha en 2003, a 32.836 ha en 2018. Estos cambios en la distribución espacial y en el manejo del riego del viñedo, han contribuido al incremento de los rendimientos y de la producción de uva. No obstante, la variabilidad interanual de la producción es elevada, circunstancia directamente ligada a la variabilidad climática (heladas, sequías, tormentas), que influye en la productividad y en el estado sanitario del viñedo. En el periodo 1990-2018, el rendimiento medio en regadío fue de 8.084 Kg de uva por hectárea, con un valor máximo de 11.362 kg/ha y un mínimo de 6.499 kg/ha, mientras que los rendimientos medios en secano fueron en el mismo periodo de 6.319 kg/ha, situándose en una horquilla de 9.562 kg/ha y 4.213 kg/ha, lo que representa un 22% menos que en regadío.

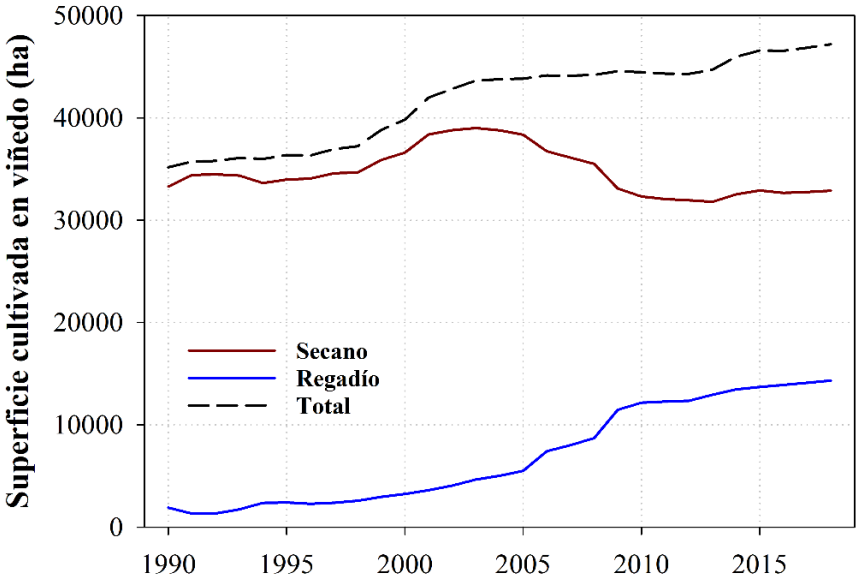

Figura 7. Distribución del viñedo en secano y regadío en La Rioja (1990-2018).

3.4. Modificaciones en el sistema de conducción: El incremento del viñedo en espaldera

Se considera que el sistema de conducción del viñedo es un agente modulador del bioclima de la cepa, habida cuenta de su influencia en el microclima de la cepa y en su fisiología. El sistema de conducción engloba, en sentido amplio, la densidad de plantación, el marco de plantación, la altura del tronco, la distribución de la vegetación anual, el tipo de poda, la carga y su distribución, así como el conjunto de operaciones en verde. De todos estos aspectos, el cambio reciente de mayor relieve registrado en la DOCa Rioja tiene que ver con el sistema de conducción, con una evolución de las formas libres a las apoyadas. Hasta finales del pasado siglo, la mayor parte de los viñedos se cultivaban con el sistema de conducción en vaso. Sin embargo, desde el año 2000, las nuevas plantaciones se dirigen a espaldera. Incluso, ha sido frecuente la transformación de cepas conducidas en vaso a la espaldera. Entre 2000 y 2015, la superficie transformada con ayudas públicas fue de 12.065 ha (el 28,8% del viñedo de La Rioja), lo que supuso una subvención total de más de 66 millones de euros. A esta superficie hay que añadir el viñedo transformado por los viticultores con financiación propia, estimándose que más del 50% del viñedo de La Rioja se cultiva en la actualidad en espaldera (RVGLR, 2016; Lasanta *et al.,* 2016).

La Figura 8a muestra un viñedo joven conducido en espaldera y con riego localizado. Muchas parcelas cultivadas tradicionalmente con frutales, localizadas en glacis y terrazas bajas, se cultivan hoy con viñedo. En su caso, el riego tradicional se aplicaba por gravedad, con todos los inconvenientes que esta modalidad de riego conlleva. Actualmente, una parte importante del viñedo riojano utiliza el riego localizado, apoyándose para ello en la estructura de postes y alambres que conducen la cepa. La Figura 8b corresponde a un viñedo antiguo, localizado en un glacis medio, conducido antes en vaso y ahora en espaldera, al que se le ha dotado recientemente de riego.

Figura 8. Ejemplos de cambios en la conducción del viñedo como medidas de adaptación al cambio climático.

El uso del riego y la implantación del viñedo en suelos muy fértiles (terrazas y glacis bajos) implica un elevado desarrollo vegetativo de las cepas, del crecimiento de la masa foliar y de la productividad del viñedo, asociado por lo general a una mayor carga y, por tanto, de un mayor número de racimos, más pesados y con bayas de mayor volumen, lo que sin duda representa una amenaza potencial para la calidad de la uva, y supone un mayor riesgo de ataque de enfermedades. Ante esta tesitura, el viticultor trata de superar tales inconvenientes jugando adecuadamente con los factores que determinan el sistema de conducción en su conjunto (Fig. 8a y b), decantándose progresivamente por la conducción en espaldera, viéndose más limitado el uso del tradicional en vaso (Fig. 8c). Con esta decisión, el viticultor habrá de elegir razonablemente la estructura de la espaldera y realizar un manejo de la vegetación que le permita acceder a un adecuado microclima de hojas y racimos. En algunos viñedos se busca una mejora del microclima con la eliminación tardía de las hojas basales, ya senescentes, para incrementar la insolación, si bien controlando que no se produzca una sobreexplotación de los racimos (Fig. 8d).

Por otro lado, y sobre todo en suelos fértiles, cada vez es mayor el número de viñedos en los que se emplea una cubierta vegetal (sembrada o espontánea), como alternativa al laboreo tradicional (Fig. 9). No obstante, entre las consecuencias de la cubierta vegetal se incluye la competencia con las cepas por el agua y los nutrientes, especialmente por el nitrógeno, reduciendo su disponibilidad, el vigor y la superficie foliar total y expuesta de la planta, lo que afecta a la capacidad fotosintética y a la composición y calidad de la uva (Martín *et al.,* 2018).

Figura 9. Imágenes de viñedos con cubierta vegetal.

4. Discusión

El incremento de las temperaturas y el estrés hídrico, derivados del cambio climático, influyen de forma determinante en el desarrollo y actividad de la vid: menor rendimiento, contención del crecimiento vegetativo y de la superficie foliar, así como en la activación de procesos de senescencia prematura de las hojas. Por otro lado, se modifica la actividad fisiológica dando lugar a un incremento de la respiración y a la disminución de la fotosíntesis, como consecuencia del aumento de la evapotranspiración y del estrés hídrico. Todo ello contribuye a crear un microclima de la cepa desfavorable para la calidad de la uva (color, aroma, azúcares, acidez…), por el exceso de exposición de los racimos a los rayos solares (Iglesias *et al.,* 2010; Ramos, 2017; García-Escudero, 2018). Por lo tanto, la calidad de la uva y del vino pueden verse comprometidos, afectando especialmente al atributo de tipicidad, ligado al *Terroir* y, consecuentemente, al mercado del vino (van Leeuwen y Seguin, 2006; Bernetti *et al.,* 2012; Mozell y Thach, 2014; Delay *et al.,* 2015).

Para combatir los efectos del CC en la vid, los viticultores de diferentes regiones del mundo están poniendo en marcha distintas medidas de adaptación. Parte de la estrategia a seguir pasa por cambios en el material vegetal (portainjertos, variedades de uva y clones) y en los sistemas de conducción de la cepa, con medidas tales como la elevación de la altura del tronco, el mantenimiento de una adecuada relación entre el área de la hojas y la carga de cosecha o el retraso del momento de la poda…, todo ello con el fin de que no se adelante o se acorte la fenología de la vid y que la cosecha de la uva se realice en el periodo óptimo de maduración para cada entorno vitícola, lo que se sitúa con frecuencia a finales de septiembre o principios de octubre en la cuenca mediterránea. Si se adelanta la fecha de la vendimia, para evitar un grado alcohólico elevado y disminuir la acidez, se corre el riesgo de no alcanzar niveles suficientes de color y aroma. Si, por el contrario, se retrasa la vendimia es muy posible que haya un exceso de azúcar (alto grado alcohólico del vino) y escasa acidez (problemas para envejecer el vino). Además, es muy probable que se incrementen los problemas fitosanitarios de la uva (García-Escudero, 2018).

Contra la sequía, se trata de luchar utilizando material vegetal más resistente o tolerante al déficit hídrico y con mayor eficiencia en el uso del agua, disminuyendo en su caso la densidad de cepas, trasladando los viñedos a suelos con mayor capacidad de retención de agua y con posibilidades de riego. Frente a la mayor radiación solar y a los riesgos de sobreexposición, se busca que la cepa ofrezca mayor protección de las hojas y de los racimos, incrementando su densidad (manteniéndose a la vez porosa), cambiando la exposición de las cepas y, por lo general, con una buena gestión en conjunto de los sistemas de conducción (van Leeuwen y Destrac-Irvine, 2017; van Leeuwen *et al.,* 2019; Del Pozo *et al.,* 2019).

Los efectos acumulativos de las adaptaciones señaladas pueden ser suficientes hasta mediados del siglo XXI (Brison y Levraut, 2010), pero a partir de la segunda mitad del siglo XXI es posible que se requieran cambios más profundos, como la introducción de variedades no locales y buscar nuevas áreas para el viñedo que retrasen la maduración (van Leeuwen y Destrac-Irvine, 2017). Ello puede llevar a la aparición de nuevas regiones vitícolas, mientras que las actuales, incluso las que podríamos considerar históricas, podrían volverse inadecuadas (Fraga *et al.,* 2016b). Jones *et al.* (2005) estudiaron veintisiete regiones vinícolas de alta calidad, comprobando un aumento de las temperaturas de 1,3ºC en invierno y de 1,4ºC en verano desde 1950. Por otro lado, los escenarios de CC indican que las regiones vitivinícolas se deberán extender hacia los polos y hacia altitudes más elevadas, para intentar mantener las actuales características de sus vinos (Moriondo *et al.,* 2013; Irimia *et al.,* 2018). Investigaciones recientes señalan que las zonas vitícolas se desplazarán de 150 a 300 km hacia el polo para 2049, y unos 12 a 25 Km más para 2099, en un escenario medio de emisiones de gases efecto invernadero (Mills-Novoa *et al.,* 2016). Hannah *et al.* (2013) señalan que en las cinco regiones más importantes en producción de vino, el área adecuada para producir vino de calidad se reducirá entre el 25% y el 73% para 2050. En regiones vitivinícolas en las que las restricciones de cultivo y de elaboración de vino son

importantes, como es el caso de la estricta reglamentación de la DOCa Rioja, mantener la calidad y especificidad del vino no será tarea sencilla si las condiciones ambientales cambian.

Frente al escenario del cambio climático, los viticultores de la DOCa Rioja en su momento tendrán, si cabe, la opción de adaptarse cambiando la localización de los viñedos, el sistema de conducción de la cepa y utilizando el riego entre otras medidas paliativas que puedan garantizar unas vendimias similares. En este trabajo, hemos comprobado que los viticultores siguen principalmente dos estrategias, en función de los condicionantes ambientales locales. Con el objetivo de cambiar la localización del viñedo: i) desplazar viñedos hacia zonas de regadío, y ii) ubicarlos a mayor altitud. En el sector estudiado de la Rioja Alta, el viñedo ocupaba 2.605 ha en las terrazas 1, 2 y 3 en 1977, mientras que lo hacía con 4.652 ha en 2017, es decir, un incremento del 78,6%. Llama la atención la expansión incluso en la terraza 1 (1.277 ha en 1977 y 2.122 ha en 2017), donde los viñedos están expuestos a inundaciones periódicas y a una humedad edáfica elevada, de forma permanente. Es en las terrazas bajas y glacis bajos donde el viñedo aprovecha las infraestructuras de riego. De hecho, en La Rioja este tipo de viñedo ha pasado de ocupar 1.893 ha a 14.324 ha entre 1990 y 2018, para asegurar las producciones y mitigar el estrés hídrico. Galilea *et al.* (2015) señalan que el mayor atractivo económico del viñedo en las últimas décadas ha supuesto que muchos viñedos se hayan instalado en áreas de regadío, utilizando suelos muy fértiles, ocupados anteriormente por frutales, hortalizas, maíz y alfalfa, haciendo que estos cultivos experimenten un fuerte retroceso desde los años ochenta del pasado siglo (Lasanta, 2010), por lo que han dejado de ser la base económica de muchas explotaciones. Sin embargo, en el actual contexto de CC, el riego del viñedo comienza a ser necesario para estabilizar el rendimiento y mantener el vino de calidad (Fraga *et al.,* 2018; Wenter *et al.,* 2018).

Sin embargo, la expansión por tierras fértiles y de regadío plantea algunos problemas, como el mayor riesgo de heladas en días con inversión térmica, el incremento de la productividad por unidad de superficie, con una posible pérdida de la calidad de la uva, un mayor desarrollo vegetativo, induciendo una mayor densidad de vegetación en la cepa, lo que favorece la aparición de enfermedades, que a su vez exigen tratamientos fitosanitarios más frecuentes, y compromete la maduración de la uva (Teixeira *et al.,* 2013; Ponti *et al.,* 2018; Sgubin *et al.,* 2018; Carroquino *et al.,* 2020). Los inconvenientes planteados por el cultivo del viñedo en suelos fértiles y de regadío trata de superarlos el viticultor con la elección del sistema de conducción del viñedo más adecuado, destacando como ya se ha indicado una tendencia a la conducción en espaldera, donde busca aunar ventajas culturales, calidad y adaptación al CC. Con financiación privada o pública, más del 50% del viñedo de La Rioja se cultiva en la actualidad mediante el sistema en espaldera, mientras que antes del año 2000 la mayoría del viñedo se disponía en vaso. Con la espaldera se busca, además de un incremento de la producción y de un mayor rendimiento económico, mecanizar determinados trabajos de cultivo, procurar modular el microclima de la cepa, mejorando una adecuada recepción de la radiación solar, lo que contribuye a la maduración y mejora de la calidad de la uva (van Leeuwen y Darriet, 2016). Sin embargo, algunos autores sostienen que es más eficaz la poda en vaso (*gobelet*) que la conducción en espaldera para combatir la sequía, ya que la poda en vaso favorece una superficie de hoja moderadamente baja, lo que reduce la transpiración de la vid (Santesteban *et al.,* 2017; van Leeuwen y Destrac-Irvine, 2017).

Por otro lado, el laboreo tradicional del suelo se está sustituyendo por el cultivo con cubierta vegetal (natural o sembrada) en las calles, incluso a nivel de la fila. Con ello, el viticultor trata de limitar el crecimiento de las vides, que resulta excesivo en muchos nuevos viñedos plantados en suelos fértiles, como los de las terrazas y glacis bajos. La cubierta vegetal tiene, además, otras ventajas desde una perspectiva de agricultura sostenible: disminuye la erosión del suelo y la transferencia de agroquímicos a las aguas, e incrementa la captura de CO_2 y la biodiversidad (Lasanta y Sobrón, 1988; Biddoccu *et al.,* 2015). Además, las cubiertas vegetales contribuyen a mejorar las interacciones de la agricultura con el medio ambiente, limitando el uso de herbicidas y plaguicidas, compitiendo por los nutrientes con el viñedo, mejorando la estructura del suelo y el contenido de materia orgánica, a la vez que mejora el color de los vinos (Ibáñez-Pascual *et al.,* 2011; Martín *et al.,* 2018). Desde una perspectiva paisajística contribuye en primavera a aumentar los contrastes con los viñedos próximos, cuando el verde de las

herbáceas alterna con el marrón o los colores rojizos de la tierra arada (Lasanta y Ruiz-Flaño, 2014). De cualquier modo, es importante el manejo racional de las cubiertas vegetales, jugando con su intensidad de cobertura, con las especies que la conforman y con su temporalidad, para así no impactar negativamente en el desarrollo normal del cultivo (Martín *et al.,* 2018).

Otros viñedos, por el contrario, se han desplazado hacia los glacis medios y altos. Concretamente, 4.644 ha en 2017 frente a 2.665 ha en 1977 en La Rioja Alta, buscando los beneficios de la altitud y poner más terrenos en explotación en un periodo de expansión de la vid. En este sentido, en Clavijo y Tudelilla los viñedos más altos no superaban los 600 m s.n.m. de altitud en 1977, mientras que en 2017 llegan a cotas próximas a los 900 m. El desplazamiento hacia espacios más elevados implica volver a cultivar viñedos en áreas vitícolas tradicionales, cuando el vino era un producto alimenticio más, y cuando se reservaba para el viñedo los terrenos más pobres, donde otros cultivos más exigentes encontraban serias limitaciones, bien por ausencia de agua, o bien por pendientes elevadas o presencia de abundantes piedras (Arnáez *et al.,* 2006). Galilea *et al.* (2015) señalan que el 15% del viñedo, del sector de La Rioja Alta considerado en este trabajo, ya se cultivaba por encima de los 600 m s.n.m. de altitud en 1956. La plantación de viñedos en cotas altas se ha convertido en un aval de calidad y en una respuesta al CC, con el fin de evitar el adelanto de la maduración, los niveles elevados de alcohol y la disminución de la acidez, características con las que los vinos pierden frescura y capacidad de envejecimiento (Teixeira *et al.,* 2013; Carroquino *et al.,* 2020). Por otro lado, los viñedos sufren menos estrés térmico e hídrico, un menor acoso de enfermedades y plagas y la maduración de la uva es más pausada (Jones, 2006; Ramos, 2017). Los viñedos en altitud dan lugar a vinos con menos graduación, mayor carga aromática, color más estable y mayor acidez, que los posiciona más cerca de los vinos tradicionales de calidad, con tipicidad propia ligada a un determinado *Terroir*, a partir de lo cual entrarían en un nicho determinado de mercado (van Leeuwen y Seguin, 2006; Hinnewinkel, 2010; Delay *et al.,* 2015).

Hasta muy recientemente, se consideraba que las áreas de montaña presentaban fuertes desventajas para el cultivo del viñedo, por sus limitaciones ambientales (heladas tardías, tormentas frecuentes, laderas muy pendientes, ciclos insuficientes…). Sin embargo, en el actual contexto de cambio climático es obligado preguntarse si será la montaña mediterránea una solución de adaptación de la viticultura para producir uva de calidad. En este sentido, Vigl *et al.* (2018) señalan que algunas regiones de los Alpes se consideran cada vez más como una solución prometedora para el cultivo de viñedos. Delay *et al.* (2015) sugieren que la montaña puede ser un activo para que el viñedo se adapte al cambio climático, ya que, junto a la complejidad local de ambientes, capaz de acoger una amplia gama de variedades, se suma el menor estrés térmico que el registrado en altitudes más bajas. La viticultura podría ser, además, una alternativa económica en zonas de media montaña mediterránea, que se añadiría a las pocas vías de futuro que hay en la actualidad (ganadería extensiva y producción de madera), dadas sus escasas aptitudes para actividades industriales y turísticas frente a las montañas alpinas (Conti & Fagarazzi, 2005; Sancho-Reinoso, 2013; Lasanta *et al.,* 2019).

No obstante, hay algunas cuestiones a considerar: i) los modelos climáticos pronostican una fuerte variabilidad interanual y eventos extremos más frecuentes, cuestiones que probablemente sean más acusadas en áreas de montaña (Caffarra y Eccell, 2011; Sherrer*et al.,* 2016; Vigl*et al.,* 2018; Wenter *et al.,* 2018); y ii) la conservación del suelo y su manejo es un parámetro importante para la sostenibilidad de los viñedos, ya que es el uso agrícola que causa mayor pérdida de suelo (Tropeano, 1984; Tarolli *et al.,* 2015; Galilea Salvador, 2015). Por ello, es esencial aplicar medidas de conservación del suelo y del agua, entre las que destaca el cultivo en terrazas, ya que éstas favorecen la infiltración, disminuyen la escorrentía y la erosión del suelo (Cots-Folch *et al.,* 2006, 2009; Tarolli *et al.,* 2015; Arnáez *et al.,* 2015; Rodrigo-Comino, 2018). En uno de los municipios estudiados (Clavijo), se aprovechan antiguos bancales para la instalación de los nuevos viñedos, manteniéndose además las encinas en los márgenes de los campos y los pequeños bosquetes próximos. Los viticultores deben, por tanto, tener en cuenta estas limitaciones ambientales de la montaña, además de considerar las exigencias del mercado y las expectativas del consumidor por productos específicos y de fuerte tipicidad. En

cualquier caso, en la DOCa Rioja esta posibilidad no existe en la actualidad, ya que la montaña queda excluida de las áreas amparadas bajo dicha denominación. En este sentido, la iniciativa privada está tratando de ampliar la delimitación de la DOCa Rioja, o bien que se les permita establecer otro sello o marca de calidad.

5. Conclusiones

Este trabajo intenta proporcionar información sobre estrategias adecuadas que los viticultores de la DOCa Rioja pueden desarrollar para adaptarse al cambio climático, mitigando los efectos en las vides del aumento de las temperaturas y de los periodos de sequía. Se ha señalado que en la Rioja Alta el viñedo se ha expandido entre 1977 y 2017 por todas las formas de relieve, al tratarse de un cultivo económicamente muy rentable en las últimas décadas, y por su buena aceptación en mercados exigentes en vinos de elevada calidad. En este contexto, los glacis altos y las terrazas bajas, incluida la T1, registran incrementos notables en la superficie ocupada por viñedos. En los glacis altos, los nuevos viñedos buscan las ventajas bioclimáticas que proporciona su mayor altitud respecto a otras formas de relieve. Hacia las terrazas bajas se han desplazado los viñedos buscando las infraestructuras de riego, que hasta los años ochenta se utilizaron para el cultivo de frutales y hortalizas. Lo cierto es que la superficie de viñedo en regadío se ha multiplicado por 3,5 en La Rioja entre 2003 y 2018, mientras que en secano se contraía el 15,7% entre ambas fechas. En los municipios de piedemonte estudiados (Clavijo y Tudelilla), los nuevos viñedos ascienden en altitud, superando los 700 m s.n.m., una cota impensable hace tres décadas. Por otro lado, los cambios también se han dirigido hacia el sistema de conducción, sustituyendo progresivamente el sistema en espaldera al de vaso. Antes del año 2000, casi todo el viñedo de la DOCa Rioja se conducía en vaso, mientras que en la actualidad se estima que más del 50% se dirige en espaldera. Con ello, y estableciendo actuaciones que mejoren el microclima de hojas y racimos, se puede alcanzar una correcta maduración de la uva, se reducen costes de cultivo, y se facilitan y mejoran muchas faenas de cultivo, así como las aplicaciones fitosanitarias.

Los cambios señalados en el cultivo del viñedo deben hacernos reflexionar sobre los límites o conceptos agronómicos que se asumían como inmutables, considerando cuáles tienen vigencia hoy y/o tendrán en el futuro. Los nuevos escenarios, como consecuencia del CC, están dando lugar a nuevos retos a los que el viticultor, el agrónomo y el enólogo deben enfrentarse. Para ello, ha de pensarse en soluciones como la búsqueda de material vegetal adaptado, diferentes sistemas de cultivo, u opciones, como las señaladas en este trabajo: los cambios de localización del viñedo (plantación en altitud y en suelos de regadío) para evitar el estrés hídrico y térmico, y los cambios de conducción. Del mismo modo, debe contemplarse la modificación o flexibilización de la normativa vitivinícola, que permita el encaje de soluciones que en estos momentos no se contemplan. En este sentido, la reglamentación de la DOCa Rioja, por lo general muy estricta y comprometida con la calidad, puede plantearse de cara al futuro la introducción de nuevos materiales vegetales, ya sean nuevas variedades o clones de variedades ya autorizadas, así como la apertura a nuevas localizaciones del viñedo.

La capacidad de los productores para adaptarse a un clima cambiante es limitada por las circunstancias sociales, económicas y políticas, incluyendo el capital económico, la educación, los arreglos institucionales y las capacidades de organización. Es necesario abordar estas circunstancias para que los productores se adapten eficazmente en el futuro.

Agradecimientos

Este trabajo ha contado con el apoyo financiero del proyecto LIFE MIDMACC (LIFE18 CCA/ES/001099), financiado por la Unión Europea, y MANMOUNT (PID2019-105983RB-I00/AEI/10.13039/501100011033), financiado por la Agencia Estatal de Investigación. Ha contado, además, con la ayuda del grupo de investigación "Procesos Geoambientales y Cambio Global"

(E02_17R), financiado por el Gobierno de Aragón y la Fundación Social Europea. Agradecemos también las enseñanzas recibidas y la ayuda permanente de Rubén Sáenz (Depadre, viñedos de montaña S.L), Aritz Espinosa y Luis Ángel García (Bodegas Vivanco).

Referencias

Albisu, L.M. 2014. Reflexiones en torno a la dinámica innovadora del sector del vino. *Cuadernos de Estudios Agroalimentarios* 6, 141-152.

Arnáez, J., Ortigosa, L.M., Ruiz-Flaño, P., Lasanta, T. 2006. Distribución espacial del viñedo en la Comunidad Autónoma de La Rioja: influencia de la topografía y las formas de relieve. *Polígonos. Revista de Geografía* 16, 11-34. https://doi.org/10.18002/pol.v0i16.409

Arnáez, J., Lana-Renault, N., Lasanta, T., Ruiz-Flaño, P., Castroviejo, J. 2015. Effects of farming terraces on hydrological and geomorphological processes. A review. *Catena* 128, 122-134. https://doi.org/10.1016/j.catena.2015.01.021

Barco Royo, E. 2018. *Análisis de un sector: Rioja 4.0*. Gobierno de La Rioja, Logroño, 443 pp.

Bernetti, I., Menghini, S., Marinelli, N., Sacchelli, S., Alampi Sottini, V. 2012. Assessment of climate change impact on viticulture: economic evaluations and adaptation strategies analysis for the Tuscan wine sector. *Wine Economics and Policy* 1, 73-86. http://doi.org/10.1016/j.wep.2012.11.002

Biasi, R., Brunori, E., Ferrara, C., Salvati, L. 2019. Assessing impacts of climate change on phenology and quality traits of *Vitis vinífera* L.: The contribution of local Knowledge. *Plants* 8, 121. https://doi.org/10.3390/plants8050121

Biddoccu, M., Ferraris, E., Opsi, F., Cavallo, E. 2015. Effects of soil management on long-term runoff and soil erosion rates in sloping vineyards. In: G. Lollino, A. Manconi, J. Clague, W. Shan, M. Chiarle (Eds.), *Engineering Geology for Society and Territory*. Springer, Cham, vol. 1, pp. 159-163. https://doi.org/10.1007/978-3-319-09300-0_30

Brison, N., Levrault, F. 2010. *Le Livre Vert du project CLIMATOR*. Ademe, 334 pp.

Burge, M., Hsiang, S.M., Miguel, E. 2015. Global non-linear effect of temperature on economic production. *Nature* 527, 235-239.https://doi.org/10.1038/nature15725

Caffarra, A., Eccel, E. 2011. Projecting the impacts of climate change on the phenology of grapevine in a mountain area. *Australian Journal Grape Wine Research* 17, 52-61. http://doi.org/10.1111/j.1755-0238.2010.00118.X

Carroquino, J., García-Casarejos, N., Gargallo, P. 2020. Classification of Spanish wineries according to their adoption of measures against climate change. *Journal of Clearer Production* 244, 118874. https://doi.org/10.1016/j.jclepro.2019.118874

Constantini, E.A.C., Lorenzetti, R., Malorgio, G. 2016. A multivariate approach for the study of environmental drivers of wine economic structure. *Land Use Policy* 57, 53-63. https://doi.org/10.1016/j.landusepol.2016.05.015

Conti, G., Fagarazzi, L. 2005. Forest expansion in mountain ecosystems: "environmentalist's dream" or societal nightmare? *Planum* 11, 1-20.

Cots-Folch, R., Martínez-Casasnovas, J.A., Ramos, M.C. 2006. Land terracing for new vineyard plantations in the north-western Spanish Mediterranean region: landscape effects of the EU Council Regulation policy for vineyards' restructuring. *Agriculture, Ecosystems and Environment* 115, 88-96. https://doi.org/10.1016/j.agee.2005.11.030

Cots-Folch, R., Martínez-Casasnovas, J.A., Ramos, M.C. 2009. Agricultural trajectories in a Mediterranean mountain region (Priorat, NE Spain) as a consequence of vineyard conversion plants. *Land Degradation and Development* 20, 1-13. https://doi.org/10.1002/ldr.856

C.R. de la DOCa Rioja, 2019. *Estadísticas 2018. El Rioja en cifras*.www.riojawine.com

Cuadrat, J.M., Vicente-Serrano, S.M. 2008. Características espaciales del clima en La Rioja modelizadas a partir de Sistemas de Información Geográfica y técnicas de regresión espacial. *Zubía. Monográfico* 20, 119-142.

Delay, E., Piou, C., Querol, H. 2015. The mountain environment, a driver for adaptation to climate change. *Land Use Policy* 48, 51-62. http://doi.org/10.1016/j.landusepol.2015.05.08

De Luis, M., González-Hidalgo, J.C., Longares, L.A., Stepanék, P. 2009. Seasonal precipitation trends in the Mediterranean Iberian Peninsula in second half of 20th century. *International Journal of Climatology* 29, 1312-1323. http://doi.org/10.1002/joc.1778.

Del Pozo, A., Brund-Saldias, N., Engler, A., Ortega-Farías, S., Acevedo-Opazo, C., Lobos, G.A., Jara-Rojas, R., Molina-Montenegro, M.A. 2019. Climate change impacts and adaptation strategies of agriculture climate regions (MCRs). *Sustainability* 11, 2769. https://doi.org/10.3390/su11102769

Domínguez-Castro, F., Vicente-Serrano, S.M., Tomás-Burguera, M., Peña-Gallardo, M., Beguería, S., El Kenawi, A., Luna, Y., Morata, A. 2019. High spatial resolution climatology of drought events for Spain: 1961-2014. *Journal of Climatology* 39, 5046-5062. https://doi.org/10.1002/joc.6126

Fraga, H., Santos, J.A., Moutinho-Pereira, J., Carlos, C., Silvestre, J., Eiras-Dias, J., Mota, T., Marheiro, A.C. 2016a. Statistical modelling on grapevine phenology in Portuguese wine regions: observed trends and climate change projection. *Journal Agriculture Science* 154(5), 795-816. https://doi.org/10.1017/S0021859615000933

Fraga, H., García de Cortazar Atauri, I., Malheiro, A.C., Santos, J.A. 2016b. Modelling climate change impacts on viticultural yield, phenology and stress conditions in Europe. *Global Change Biology* 22, 3774-3788. https://doi.org/10.1111/gcb.13382

Fraga, H., García de Cortázar Atauri, I., Santos, J.A. 2018. Viticultural irrigations demands under climate change scenarios in Portugal. *Agricultural Water Management* 196, 66-74. https://doi.org/10.1016/j.agwat.2017.10.023

Galilea, I., Arnáez, J., Lasanta, T., Ortigosa, L. 2015. Evolución y desfragmentación del paisaje del viñedo en La Rioja Alta (España) en el periodo 1956-2000. *Boletín de la Asociación de Geógrafos Españoles* 69, 315-331. https://doi.org/10.21138/10.21138/bage.1899

Galilea Salvador, I. 2010. *Evolución del paisaje del viñedo en el sector nororiental de La Rioja Alta (1956-2000)*. Universidad de La Rioja, 137 pp.

Galilea-Salvador, I. 2015. *Erosión de suelos y laderas en el espacio agrícola de La Rioja. Aplicación y cartografía del modelo RUSLE*. Tesis Doctoral, Universidad de La Rioja, 405 pp., Logroño.

García-Escudero, E. 2018. Consideraciones sobre el cambio climático y la viticultura. *Vida Rural* 449, 38-44.

García-Ruiz, J.M., López-Moreno, J.I., Vicente-Serrano, S., Lasanta, T., Beguería, S. 2011. Mediterranean water resources in a Global Change scenario. *Earth Science Reviews* 105 (3-4), 121-139. https://doi.org/10.1016/j.earscirev.2011.01.006

García-Valdecasas Ojeda, M., Yeste, P., Gámiz-Fortis, S.R., Castro-Díez, Y., Esteban-Parra, M.J. 2020. Future changes in land and atmospheric variables: An analysis of their couplings in the Iberian Peninsula. *Science of the Total Environment* 722, 137902. https://doi.org/10.1016/j.scitotenv.2020.137902

Gobierno de La Rioja. 2020. Estadística Agraria Regional, 2017. Gobierno de La Rioja, 118 pp., Logroño. www.larioja.org

Gómez Miguel, V. 2006. Mapa de unidades taxonómicas principales de la denominación de origen calificada La Rioja (escala 1:50.000). *Atlas Nacional de España: geología, geomorfología y edafología* (Sánchez-Ortiz Rodríguez, M.P., Coord.). Centro Nacional de Información Geográfica, 195 pp., Madrid.

Gonzalo Moreno, A.N. 1981. *El relieve de La Rioja. Análisis de Geomorfología estructural*. Instituto de Estudios Riojanos, 2 vols., Logroño.

Hannah, L., Roehrdanz, P., Ikegami, M., Shepherd, A.V., Shaw, M.R., Tabor, G., Xhi, L., Marquet, P., Hijmans, R. 2013. Climate change, wine, and conservation. *Proceedings of the National Academy of Sciences* 110 (17), 6907–12. https://doi.org/10.1073/pnas.1210127110

Hinnewinkel, J.C. 2010. *Faire vivre le terroir*. Centre d' Études et de Recherche sur la Vigne et le Vin - Université de Bordeaux, 231 pp.

Ibáñez-Pascual, S., Pérez, J.L., Peregrina, F., Chávarri, J.B., García-Escudero, E. 2011. Cubierta vegetal en viñedo. Un sistema de mantenimiento del suelo capaz de mejorar el color de los vinos. *Cuaderno de Campo* 47, 30-34.

Iglesias, A., Mougou, R., Moneo, M. 2011. Towards adaptation of agriculture to climate change in the Mediterranean. *Regional Environmental Change* 11, 159-166. https://doi.org/10.1007/s10113-010-0187-4

Iglesias, A., Quiroga, S., Schlickenrieder, J. 2010. Climate change and agricultural adaptations: assessing management uncertainty for four crop types in Spain. *Climate Research* 44 (1), 83-94. http://dx.doi.org/10.3354/cr00921

IPCC. 2014. Climate Change 2014, synthesis report. Contribution of working groups I, II and III to the fifth assessment report of the Intergovernmental Panel on Climate Change. Core writing team R. Pachauri and L. Meyer Eds. IPCC, Geneva, Switzerland, 151 p.

Irimia, L.M., Latiche, C.V., Quenol, H., Sfica, L. 2018. Shifts in climate suitability for wine production as a result of climate change in a temperature climate wine region of Romania. *Theoretical Applied Climatology* 131, 1069-1081. https://doi.org/10.1007/s00704-017-2033-9

Jlassi, W., Nadal-Romero, E., García-Ruiz, J.M. 2016. Modernization of new irrigated lands in a scenario of increasing water scarcity: from large reservoirs to small ponds. *Cuadernos de Investigación Geográfica* 42 (1), 233-259. https://doi.org/10.18172/cig.2918

Jones G.V. 2006. Climate and terroir: impacts of climate variability and change on wine. In: Macqueen R.W., Meinert L.D. (eds) *Fine wine and terroir-the geoscience perspective*. Geoscience Canada reprint series no. 9, Geological Association of Canada. St. John's, Newfoundland, 247p.

Jones, G.V., White, M.A., Cooper, O.R., Storchmann, K. 2005. Climate change and global wine quality. *Climatic Change* 73 (3), 319-343. https://doi.org/10.1007/s10584-005-4704-2

Jones, G.V., Alves, F. 2012. Impact of climate change on wine production: a global overwiew and regional assessment in the Douro valley of Portugal. *International Journal Global Warming* 4, 383-406. https://doi.org/10.1504/IJGW.2012.049448

Lasanta, T. 2009. Functional changes in the irrigation at the Ebro basin: a survey of the role of irrigation through time. *Boletín de la Asociación de Geógrafos Españoles* 50, 385-388.

Lasanta, T. 2010. Evolución regional y dinámica del paisaje en La Rioja (1950-2010). *Zubía* 28, 49-88.

Lasanta, T. 2018. El Rioja: cambios locales para acceder a un mercado global. En: *Sistemas productivos con anclaje territorial*. Juan Antonio Márquez Domínguez (Director Edición). Editorial: Universidad de Huelva, 137-152 pp. ISBN: 978-84-17288-97-6

Lasanta, T., Inarejos, V.C., Arnáez, J., Pascual-Bellido, N.E., Ruiz-Flaño, P. 2016. Evolución del paisaje vitícola en La Rioja (2000-2015). Un análisis del papel de los programas de reconversión y reestructuración del viñedo. *Investigaciones Geográficas* 66, 9-25. https://doi.org/10.14198/INGEO2016.66.01

Lasanta, T., Nadal-Romero, E., García-Ruiz, J.M. 2019. Clearing shrubland as a strategy to encourage extensive livestock farming in the Mediterranean mountains. *Cuadernos de Investigación Geográfica* 45 (2), 487-513. http://doi.org/10.18172/cig.3616

Lasanta, T., Ruiz-Flaño, P. 2014. Los paisajes del viñedo en La Rioja: tradición y renovación. *Berceo* 167, 13-38.

Lasanta, T., Sobrón, I. 1988. Influencia de las prácticas de laboreo en la evolución hidromorfológica de suelos cultivados con viñedo. *Cuadernos de Investigación Geográfica* 14, 81-97. https://doi.org/10.18172/cig.966

Lehmann, N., Briner, S., Finger, R. 2013. The impact of climate and price risks on agricultural land use and crop management decisions. *Land Use Policy* 35, 119-130. http://doi.org/10.1016/j.landusepol.2013.05.008

López-Bustins, J.A., Pla, E., Nadal, M., de Herralde, F., Savé, R. 2014. Global change and viticulture in the Mediterranean region: a case study in north-eastern Spain. *Spanish Journal of Agricultural Research* 12 (1), 78-88. https://doi.org/10.5424/sjar/2014121-4808

Martín, I., Martínez, J., Domínguez, N., López, D., García-Escudero, E. 2018. Influencia del viñedo en la cubierta vegetal espontánea. *Vida Rural* 449, 30-37.

Martínez Vidaurre, J.M. 2017. *Influencia del tipo de suelo en el estado nutricional de la vid, el desarrollo vegetativo, la producción, la composición de la uva y de los vinos de la variedad Tempranillo tinto* (Vitis vinífera L.) *en el ámbito de la D.O.Ca Rioja*. Tesis Doctoral, Universidad de la Rioja.

Mills-Novoa, M., Pszcólkowski, P., Meza, F. 2016. The impact of climate change on the viticultural suitability of Maipo Valley, Chile. *The Professional Geographer* 68(4), 561-573. https://doi.org/1080/00330124.2015.1124788

Moriondo, M., Jones, G.V., Bois, B., Dibari, C., Ferrise, R., Trombi, G., Bindi, M. 2013. Projected shifts of wine regions in response to climate change. *Climate Change* 119 (3), 825-839. https://doi.org/10.1007/s10584-013-0739-y

Mozell, M.R., Thach, L. 2014. The impact of climate change on the global wine industry: challenges & solutions. *Wine Economics and Policy* 3, 81-89. https://doi.org/10.1016/j.wep.2014.08.001

Nogués-Bravo, D. 2006. Assessing the effects of environmental and anthropogenic factors in land cover diversity in a Mediterranean mountain environment. *Area* 38 (4), 432-444. https://doi.org/10.1111/j.1475-4762.2006.00709.x

Ollero Ojeda, A. 1996. Las riberas naturales del Ebro en La Rioja. *Zubía. Monográfico* 8, 123-136.

Peña-Angulo, D., Vicente-Serrano, S.M., Domínguez-Castro, F., Murphy, C., Reig, F., Tramblay, Y., Trigo, R.M., Luna, M.Y., Turco, M., Noguera, I., Aznárez-Balta, M., García-Herrera, R., Tomás-Burguera, M., El Kenawi, A. 2020. Long-term precipitation in southwestern Europe reveals no clear trend attributable to anthropogenic forcing. *Environmental Research Letters* 15 (9), 094070. https://doi.org/10.1088/1748-9326/ab9c4f

Ponti, L., Gutiérrez, A., Boggia, A., Neteler, M. 2018. Analysis of grape production in the face of climate change. *Climate* 6, 20. https://doi.org/10.3390/cli6020020

Priori, S., Pellegrini, S., Perria, R., Puccioni, S., Storchi, P., Valboa, G., Costantini, E.A.C. 2019. Scale effect of terroir under three contrasting vintages in the Chianti Classico area (Tuscany, Italy). *Geoderma* 334, 99-112. https://doi.org/10.1016/j.geoderma.2018.07.048

Ramos, M.C. 2017. Projection of phenology response to climate change in rainfed vineyards in north-east Spain. *Agricultural and Forest Meteorology* 247, 104-115. https://doi.org/10.1016/j.agrformet.2017.07.022

Rodríguez Rodrigo, C., 2000. *El sistema de conducción del viñedo. Análisis ecofisiológico, agronómico y económico de cinco sistemas de conducción*. Universidad de La Rioja, Logroño, 208 pp.

Rodrigo-Comino, J. 2018. Five decades of soil erosion research in "terroir". The state-of the-art. *Earth-Science Reviews* 179, 436-447. https://doi.org/10.1016/j.earscirev.2018.02.014

Romero, P., Gil-Muñoz, R., Fernández-Fernández, J.L., del Amor, F.M., Martínez-Cutillas, A., García-García, J. 2015. Improvement of yield and grape and wine composition in field-grown *Monastrell* grapevines by partial root zone irrigation, in comparison with regulated deficit irrigation. *Agriculture Water Management* 149, 55-73. https://doi.org/10.1016/j.agwat.2014.10.018

RVGLR. 2016. Reconversiones de viñedo y reestructuraciones con espaldera (2001-2015). Gobierno de La Rioja. Informe.

Sancho-Reinoso, A. 2013. Land abandonment and the dynamics of agricultural landscapes in Mediterranean mountain environments: The case of Ribagorça (Spanish Pyrenees). *Erdkunde* 67 (4), 289-308. https://doi.org/10.3112/erdkunde.2013.04.01

Santesteban, L.G., Miranda, C., Urrestarazu, J., Loidi, M., Royo, J.B. 2017. Severe trimming and enhanced competition of laterals as a tool to delay ripening in Tempranillo vineyards unded semiarid conditions. *OENO ONE: Journal International des Sciences de la Vigne et du Vin* 51 (2), 191-203. https://doi.org/10.20870/oeno-one.2017.51.2.1583

Santillan, D., Iglesias, A., La Jeunesse, I., Garrotte, L., Sotés, V. 2019. Vineyard in transition: A global assessment of the adaptation needs of grape producing regions under climate change. *Science of the Total Environment* 657, 839-852. https://doi.org/10.1016/j.scitotenv.2018.12079

Schultz, H. 2000. Climate change and vitiviniculture: a European perspective on climatology, carbon dioxide and UV-B effects. *Australian Journal Grape Wine Research* 6, 2-12. https://doi.org/10.1111/j.1755-0238.2000.tb00156.x

Serra, P., Pons, X., Saurí, D. 2008. Land-cover and land-use change in a Mediterranean landscape: a spatial analysis of driving forces integrating biophysical and human factors. *Applied Geography* 28 (3), 189-209. http://doi.org/10.1016/j.apgeog.2008.02.001

Sgubin, G., Swingendouw, D., Dayon, G., García de Cortázar-Atauri, I., Ollart, N., Pagé, C., van Leeuwen, C. 2018. The risk of tardive frost damage in French vineyards in a changing climate. *Agricultural and Forest Meteorology* 250 (251), 226-242. https://doi.org/10.1016/J.AGRFORMET.2017.12.253

Sherrer, S.C., Fischer, E.M., Rosself, R., Liniger, M.A., Groci-Maspoli, M., Knutti, R. 2016. Emerging trends in heavy precipitation and hot temperature extremes in Switzerland. *Journal Geophysical Research: Atmosphere* 121, 2626-2637. https://doi.org/10.1002/2015JD024634

Tarolli, P., Sofia, G., Galligaro, S., Prostocimi, M., Preti, F., Dalla Fontana, G. 2015. Vineyards in terraced landscapes: new opportunities from Lidar data. *Land Degradation and Development* 26, 92-102. https://doi.org/10.1002/ldr.2311

Teixeira, A., Eiras-Dias, J., Castellarin, S.D., Gerós, H. 2013. Berry phenolics of grapevine under challenging environments. *International Journal of Molecular Sciences* 14, 18711-18739. https://doi.org/10.3390/ijms140918711

Tonietto, J., Carbonneau, A. 2004. A multicriteria climatic classification system for grape-growing worldwide. *Agricultural and Forest Meteorology* 24, 81-97. https://doi.org/10.1016/j.agrformet.2003.06.001

Tropeano, D. 1984. Rate of soil erosion processes on vineyards in central Piedmont (NW Italy). *Earth Surface Processes and Landforms* 9, 253-266. https://doi.org/10.1002/esp.3290090305

Van Leeuwen, C., Darriet, P. 2016. Impact of climate change on viticulture and wine quality. *Journal Wine Economics* 11, 150-167. https://doi.org/10.1017/jwe.2015.21

Van Leeuwen, C., Destrac-Irvine, A. 2017. Modified grape composition under climate change conditions requires adaptations in the vineyard. *Oeno One* 51 (2), 147-154. https://doi.org/10.20870/oeno-one.2017.51.2.1647

Van Leeuwen, C., Destrac-Irvine, A., Dubznet, M., Duchêne, E., Gowdy, M., Marguerit, E., Pieri, P., Parker, A., de Rességuier, L., Ollat, N. 2019. An update on the impact of climate change in viticulture and potential adaptations. *Agronomy* 9, 514. https://doi.org/10.3390/agronomy9090514

Van Leeuwen, C., Seguin, G. 2006. The concept of terroir in viticulture. *Journal Wine Research* 17 (1), 1-10. https://doi.org/10.1080/09571260600633135

Vaudour, E. 2002. The quality of grapes and wine in relation to geography: notions of terroir at various scales. *Journal Wine Research* 13, 117-141. https://doi.org/10.1080/0957126022000017981

Vaudour, E., Constantini, E.A.C., Jones, G.V., Mocali, S. 2015. An overview of the recent approaches to terroir functional modelling, footprinting and zoning. *Soil* 1, 287-312. https://doi.org/10.5194/soil-1-287-2015

Wenter, A., Zanotelli, D., Montagnani, L., Tagliavini, M., Andreotti, C. 2018. Effect of different timings and intensities of water stress on yield and berry composition of grapevine (Cv Sauvignon blanc) in a mountain environment. *Scientia Horticulturae* 236, 137-145. https://doi.org/10.1016/j.scienta.2018.03.037

Vigl, L.E., Schmid, A., Moser, F., Balotti, A., Gartner, E., Katz, H., Quendier, S., Ventura, S., Raifer, B. 2018. Upward shifts in elevation -a winning strategy for mountain viticulture in the context of climate change? E35 Web of Conferences 50.02006 (2018). *XX Congreso Internacional Terroir*. https://doi.org/10.1051/e3sconf/20185002006

Zhu, X., Moriondo. M., Lerland van, E.C., Trombi, M. 2014. A model-based assessment of adaptation options for Chianti wine production in Tuscany (Italy) under climate change. *Regional Environmental Change* 16, 86-96. http://doi.org/10.1007/s10113-04-0622-2

Cuadernos de Investigación Geográfica *Geographical Research Letters*	2022	Nº 48	pp. 157-174	EISSN 1697-9540

http://doi.org/10.18172/cig.5044

CLIMATIC CHANGES AND DISTRIBUTION OF PLANT FORMATIONS IN THE STATE OF PARAIBA, BRAZIL

RAFAEL CÁMARA ARTIGAS[1]*, BARTOLOMEU ISRAEL DE SOUZA[2], RAQUEL PORTO DE LIMA[3]

[1]*University of Seville, Department of Physical Geography and Regional Geographic Analysis, C/ Maria de Padilla s/n, 41004 Seville, Spain.*

[2]*Federal University of Paraíba, Campus I, Cidade Universitária, João Pessoa, PB, 58051-900, Brazil.*

[3]*State University of Paraíba, R. Baraúnas, 351, Universitário, Campina Grande, PB, 58429-500, Brazil.*

ABSTRACT. The state of Paraíba in northeast Brazil contains four of the seven biomes present in the country: Mata Atlântica, Cerrado, Caatinga and Matas Serranas. On the other hand, Amazônia, Pantanal and Pampa were not found in this area. This special situation allows us to analyse changes in the distribution of these four large Brazilian biomes according to bioclimatic conditions, using the methodology of bioclimatic regime types. Based on the analysis of variables from periods of hydric and thermal vegetation stagnation, obtained from hydric and bioclimatic balances, average monthly temperature and rainfall, that methodology enables us to establish a typology of 27 types of bioclimatic regimes and 243 bioclimatic regime subtypes with the 9 Thornthwaite ombrothermal levels. In Paraíba 4 types of bioclimatic regimes are currently identified (mesophyllo, tropophyllo, xerophyllo and eurythermophilous) and 9 subtypes according to ombrothermal levels. In order to analyse the changes, extreme change situations were chosen: a past scenario with the Last Glacial Maximum (40 ky); and an RCP 8.5 climate change scenario for the CMSS 4.0 model for the year 2070. This enabled 3 bioclimatic regime maps of each of the 3 aforementioned situations to be obtained, providing a map of potential distribution of the plant formations of Paraíba state according to the specific field knowledge and bioclimatic mapping obtained for the present. This paper concludes that a retrocession of the Mata Atlântica can be seen from the Last Glacial Maximum up to the present, losing its optimal bioclimatic conditions and therefore remaining in a highly fragile relict situation in the face of anthropic pressure (sugarcane cultivation and urban expansion); an advance toward 2070 of the Caatinga in its shrub form as a predominant formation is indicated by the projection of climate change in 2070 for the analysed situation, specifically resulting from anthropic pressure, in this case due to livestock activities which have affected this biome in Paraíba since the mid-19th century.

Cambios climáticos y distribución de las formaciones vegetales en el Estado de Paraiba, Brasil

RESUMEN. El estado de Paraiba en el nordeste del país, recoge cuatro de los siete biomas presentes en Brasil: la Mata Atlántica, el Cerrado, la Caatinga y las Matas Serranas. Por otro lado, Amazonia, Pantanal y Pampa no se encontraron en esta área. Esta situación especial nos permite hacer un análisis de los cambios en la distribución de estos cuatro grandes biomas brasileños en función de las condiciones bioclimáticas con el uso de la metodología de tipos regímenes bioclimáticos. Dicha metodología, a partir del análisis de las variables de los periodos de paralización vegetativa hídrica y térmica, obtenidos de los balances hídricos y bioclimáticos, la precipitación y la temperatura media mensual, nos permite establecer una tipología de 27 tipos de regímenes bioclimáticos y 243 subtipos de regímenes bioclimáticos con los 9 niveles ombrotérmicos de Thornthwaite. Se identifican actualmente

para Paraiba 4 tipos de regímenes bioclimáticos (mesophyllo, tropophyllo, xerophyllo y euritermophyllo) y 9 subtipos en función de los niveles ombrotérmicos. Para poder hacer un análisis de cambios se han elegido situaciones extremas de cambio: por un lado, un escenario del pasado con el Ultimo Máximo Glaciar (40 ky), y por otro un escenario de cambio climático RCP 8.5 para el modelo CMSS 4.0 para el año 2070. Se obtienen así 3 cartografías de regímenes bioclimáticos de cada una de las tres situaciones citadas y se aporta una cartografía de la distribución potencial de las formaciones vegetales del estado de Paraiba en función de los propios conocimientos de campo y de la cartografía bioclimática que se ha obtenido para la actualidad. Como conclusión de este trabajo se puede ver un retroceso de la Mata Atlántica desde el Ultimo máximo Glaciar hasta la actualidad, perdiendo son condiciones bioclimáticas óptimas y quedando por lo tanto en una situación relicta de alta fragilidad ante la presión antrópica (cultivos de caña de azúcar y expansión urbana) y un avance hacia el 2070 de la caatinga en su forma arbustiva como formación predominante según marca la proyección del cambio climático en el 2070 para el escenario analizado, y como resultado de la propio acción antrópica, en este caso con actividades ganaderas, que se viene ejerciendo sobre este bioma en Paraiba desde mediados del siglo XIX.

Key words: Bioclimatic regimes, climate change, Caatinga, Mata Atlântica, Paraíba.

Palabras clave: Regímenes bioclimáticos, cambio climático, Caatinga, Mata Atlântica, Paraíba.

Received: 22 February 2021

Accepted: 20 June 2021

*Corresponding author: Rafael Camara Artigas. University of Seville, Department of Physical Geography and Regional Geographic Analysis. C/ Maria de Padilla s/n 41004 Seville, Spain. E-mail address: rcamara@us.es

1.Introduction

The idea of potential vegetation is based on the existence of non-restrictive bioclimatic values of field capacity at a given temperature and precipitation for the respective place. We do not include the climax concept of Clements (1916), whereby each climate zone presents a single possible climax community, though the state of maturity implies an edaphic evolution which in turn interacts on the vegetation itself, and all this considering that the climate conditions remain stable over time, something which, as is known, does not happen. It is currently accepted that mature plant formations change as a result of climate change and are continually subject to changes in factors which could be defined as disruptive (such as anthropic management) or naturals.

Potential vegetation enables us to establish what the specific and structural vertical and horizontal composition and state of the plant formations are for some given bioclimatic conditions, without considering the textural soil conditions which mark the field capacity and hence the availability of subsurface water (Mather and Yoshioka, 1966; Tuhkanen, 1980). In other words, in optimal conditions: dense or open forest, shrub and grassland formations.

Using data from inventories of vegetation and current vegetation coverage in those places as anthropically unchanged as possible, to obtain, based on potential conditions, significant interpretations and results, which are fundamental in order to undertake more scientifically precise interventions for conservation, preservation and recovery of degraded areas.

Numerous vegetation and bioclimatic classifications exist in scientific literature, though none of them establish a direct relationship between the bioclimatic variables of thermal and hydric vegetation stagnation and the type of corresponding plant formation.

This paper presents the application of new methodology developed by Cámara *et al.* (2020) in which those variables are considered and applied to the state of Paraíba, Brazil. Its aim is to establish a potential bioclimatic framework so that, based on it, analogies can be drawn between some vegetation inventories done in that state and to thereby attain and identify distribution patterns according to bioclimatic variables, ultimately determining just how far local conditions of the physical environment and anthropisation have influenced that distribution. But it also allows, based on continuous climate data, the evolution or dynamics of the potential vegetation to be established from the past up to the present, along with the respective projection into the future, depending on the climate change scenarios. This can help raise society's awareness about the value of those plant formations and their conservation, and about humankind's own natural living resources. The most characteristic plant formations of the State of Paraiba range from very humid situations (ombrophyllas) with the Atlantic Forest on the coast, to extreme arid situations such as the caatinga xerophylla in the continental interior.

2.Materials and methods

To carry out this work, the methodology of Cámara (1997) and Cámara *et al.* (2020) was used, based on the completion of 1,500 bioclimatic diagrams of North America, South America, Central America, the Caribbean, Europe, Africa and Asia, identifying the bioclimatic indicators to establish the bioclimatic regime conditions for each plant formation in its corresponding bioclimatic zone. This is a geo-botanic research method based on analysis of parametric data, expressed by means of two graphs showing the hydric balance of (HB) of Thornthwaite (Thornthwaite *et al.,* 1956, 1957) and the bioclimatic balance (BB) of Montero de Burgos and González Rebollar (Montero and González, 1974).

It is grounded on the combination of information about the texture of the geomorphologic surface formations (expressed by means of field capacity or water available for plants until soil saturation), with the vegetation coverage/root depth. The monthly value obtained for runoff in the HB is used to correct the monthly useful precipitation (p) value for plants in the BB. With this contribution the balances are mutually related to each other and in turn to the surface formations that sustain the vegetation and the specific vegetation type in the respective vertical and horizontal structure.

When the bioclimatic limits and values (precipitation, temperature and thermal and hydric vegetation stagnation) of the plant formations and their distribution are related to the bioclimatic ranges, an environmental description is obtained, adjusted to seasonal time factors (months of the year): temperature/rainfall (mean T and monthly P), edaphic/sediment (field capacity) and spatial (vegetation distribution). We call this environmental description the bioclimatic regime. Each of these bioclimatic regimes can be subject to further nuances as the edaphic/sediment factor is more precisely detailed, along with the scale in which it is considered; this enables multi-scale application of this method. On small continental or regional (1:1,000,000-1:200,000) scale and also medium (1:50,000) scale, the potential values are considered, i.e., with no restriction by field capacity or vegetation coverage (FC = 400 mm). If we work at a detailed scale (1:10,000-1:5,000), the real coverage and field capacity values are considered.

The edaphologic factor is not considered in this paper due to its scale of detail and treatment; the altitudes are reflected in the data obtained in the Worldclim continuous climate database (http://worldclim.org/version2) (Fick y Hijmans, 2017), from which mean annual and monthly temperature values and monthly and annual precipitation values were extracted.

Depending on the thermal conditions, vegetation situated in a place according to thermal limitation is defined in the classification based on the postulates of Schimper (1903), Warming (1909) and Huguet del Villar (1929) in Cámara *et al.* (2020):

- Thermophyllo: located in places with no thermal restrictions and with reduced annual thermal range. Hydric vegetation stagnation may exist;

- Eurythermophyllo: substantial thermal variation during the year and in each month, but without thermal vegetation stagnation occurring;
- Criophyllo: presents when there is short to medium thermal stagnation lasting from 1 to 5 months, with deciduous species predominating;
- Mesocriophyllo: presents in places where thermal stagnation lasts from 6 to 9 months, conditioning the distribution of broadleaf vegetation;
- Hypercriophyllo: limiting the development of woody species, with from 10 to 12 months of thermal vegetation stagnation.

As with temperature, depending on the limitation imposed by the lack of water in a space, different situations will present (Cámara *et al.,* 2020), also following the above postulates:

- Ombrophyllo, presenting in places where there is no water deficit throughout the year (precipitation is more than 60 mm in all months);
- Mesophyllo, more hydric scarcity but without that leading to vegetation stagnation. Some months may present a hydric deficit in the soil;
- Tropophyllo, when there is an edaphic hydric deficit that gives way to vegetation stagnation, as long as it lasts from 1 to 4 months. In the case of the tropics, this concerns tropical deciduous forests, which may present thorns;
- Xerophyllo, if the hydric conditions lead to a longer vegetation stagnation, lasting from 5 to 8 months. Thorny *crassulaceae* and shrubs predominate;
- Hyperxerophyllo, with 9 to 12 months of hydric vegetation stagnation, with shrub vegetation and open *crassulaceae*, very dispersed, or practically without it.

For the procedure of calculating and obtaining the mapping of Paraíba's climate regimes the Worldclim database was used (Fick and Hijmans, 2017); the mapping algebra in the ArcGis software was employed to obtain the different bioclimatic regimes present in the state's territory. To do so, the mapping of months with hydric and thermal vegetation stagnation, total precipitation, potential evapotranspiration and average monthly temperature were used as variables. Based on those variables, algorithms were used to establish each type of bioclimatic regime (Cámara *et al.,* 2020).

In accordance with the presented characteristics, 5 major macro-scale zonal categories were identified, along with 27 meso-scale 'bioclimatic regime' types. Likewise, based on the ombrothermal index of Thornthwaite and crossing it with the 27 BRTs, 162 subtypes are obtained (of the 243 possible). This is a typology that closely represents the distribution of the large groups of biomes: tundra, boreal coniferous forests, mixed forests, deciduous forests, cold prairies, warm steppes, subtropical forests and humid and dry tropical forests (Table 1).

Using this methodology, three maps of the study area were developed: one of the Last Glacial Maximum (22 ky), with a pixel size of 4.61 km, and two others with a pixel size of 0.92 km, showing the present and the RCP 8.5 scenario for the CCSM4.0 coupled climate change model, to simulate the climate system of the Earth. It is a cooperative effort between climate researchers from the USA, supported by the National Science Foundation (NSF) and centred at the National Centre for Atmospheric Research (NCAR), comprising five separate models which simultaneously simulate the Earth's atmosphere, ocean, land, terrestrial ice and sea ice, plus a central coupling component. The CCSM enables researchers to conduct fundamental studies about past, present and future states of the Earth's climate.

Table 1. Bioclimatic regimes related to terrestrial biomes. Months of hydric vegetation stagnation (first column) and months of hydric vegetation stagnation (first row). Own production.

PVH/ PVT	**0**	**0**	**1 to 4**	**5 to 8**	**9 to 12**
0	OMBROPHYLLO Rainforest	MESOPHYLLO Semi-deciduous forest	TROPOPHYLLO Dry forest	XEROPHYLLO Thorny scrub	HIPERXEROPHYLLO Warm desert
0	EURITERMO OMBROPHYLLO Laurisilva forest	EURITERMO MESOPHYLLO Subtropical deciduous forest	EURITERMO TROPOPHYLLO Subtropical sclerophyllous forest	EURITERMO XEROPHYLLO Subtropical sclerophyllous shrubland	EURITERMO HIPERXEROPHYLLO Warm steppe
1 to 5	CRIO OMBROPHYLLO Broadleaf deciduous forest	CRIO MESOPHYLLO Mixed broadleaf deciduous and coniferous forest	CRIO TROPOPHYLLO Mixed coniferous and broadleaf deciduous forest	CRIO XEROPHYLLO Conifer shrubs	CRIO HIPERXEROPHYLLO Cold steppe
6 to 9	MESOCRIO OMBROPHYLLO coniferous forest (firs)	MESOCRIO MESOPHYLLO Mixed coniferous forest	MESOCRIO TROPOPHYLLO Deciduous coniferous and coniferous forest	MESOCRIO XEROPHYLLO *Ericaceae* scrub	MESOCRIO HIPERXEROPHYLLO Cold desert
10 to 12	HIPERCRIO OMBROPHYLLO Tundra Open shrub coniferous	HIPERCRIO MESOPHYLLO Tundra (deciduous shrub)	HIPERCRIO TROPOPHYLLO Tundra (*Ericaceae* and *Cyperaceae*)	HIPERCRIO XEROPHYLLO Tundra (lichens and bush willow)	HIPERCRIO HIPERXEROPHYLLO tundra/ice

3. Study area

The state of Paraíba is situated in the northeast of the Federated Republic of Brazil, with an area of 56,585 km^2 (Fig. 1). It stretches from east to west from the Atlantic Ocean to the interior of the Brazilian Shield, presenting ecosystems that gradually change from the Mata Atlântica and Cerrado de Tabuleiro by the coast to the Caatinga in the inland sector. The Caatinga biome dominates much of its territory and is associated to a tropophyllo bioclimatic regime, and in more arid conditions to the xerophyllo regime. In coastal areas where the Mata Atlântica and Cerrado are found, they are only present in mesophyllo bioclimatic regimes, even though the Atlantic forest is actually a refuge of an ombrophyllo forest developed in other more humid past climate conditions (Fig. 2). This methodology allows to establish which are the changes in the bioclimatic regimes and their relationship with the plant formations, which also implies changes in the anthropic agricultural uses of the territory. Xerification, for example, not only affects natural vegetation, but also soil uses that are practiced in that territory. In intertropical environments these changes in soil use can be very important, because they change economic relations. It also can lead, in less developed countries, to food crises.

Paraíba's relief is formed by four large units (Carvalho, 1982) that condition the state's bioclimatic features and hence the distribution of plant formations:

- the littoral unit with the Low Coastal Plain and the table-like relief of the Tabuleiro;
- the Brazilian Shield, which with its levels of pediplanation in this sector forms the Boroborema highlands (400 to 600 m altitude), mainly drained by the basin of the Paraíba River, which flows into the Atlantic;
- the Sertão depression (200 to 400 m altitude) in the western part, also on the Brazilian Shield, drained by the Piranhas River;
- the mountain reliefs south of the Sertão and the Cariri, which reach 1,000 m altitude, and the Areia range in the Agreste, where the bioclimatic conditions become more humid.

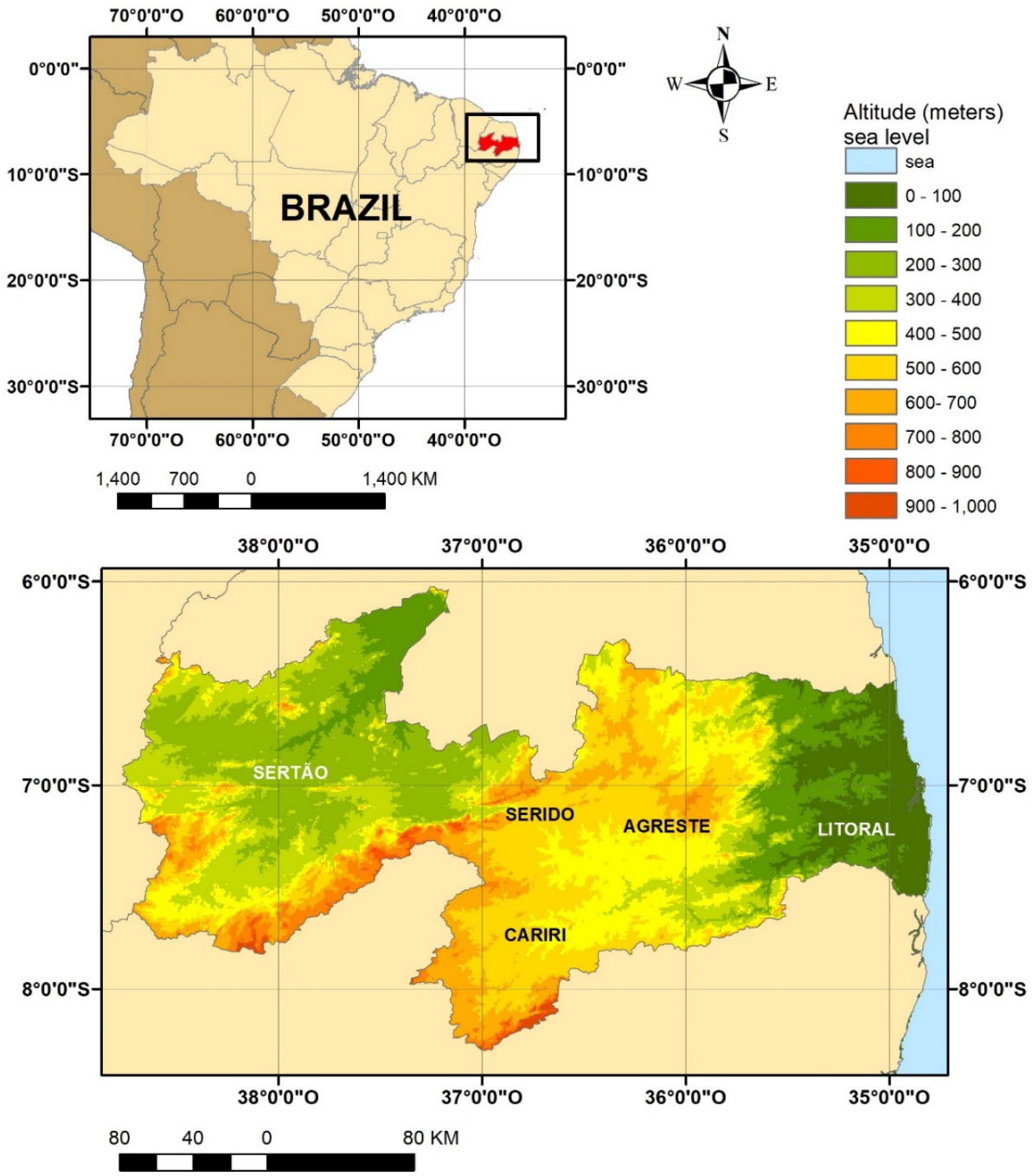

Figure 1. Location of the state of Paraíba in the Federative Republic of Brazil and its physiography. Own production based on SRTM 30 ascseg of the United States Geological Survey.

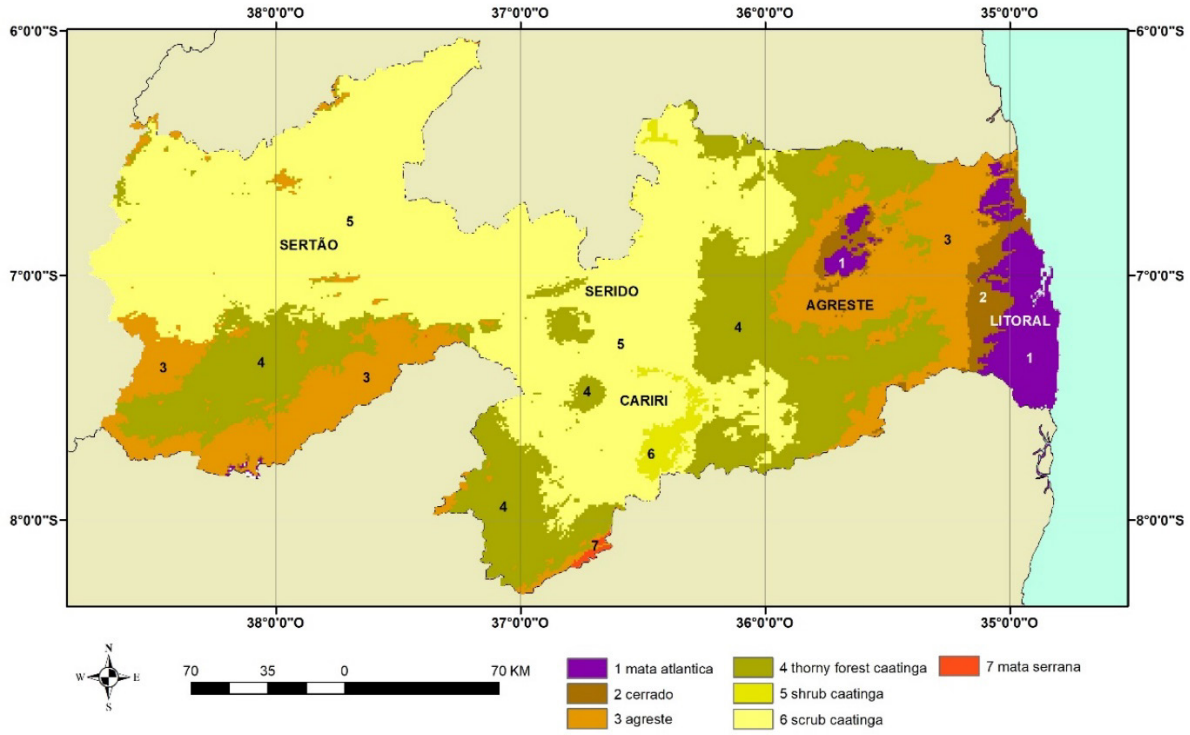

Figure 2. Distribution of plant formations in Paraíba state according to bioclimatic conditions. Own production.

The Mata Atlântica is a humid forest situated along the coast of Brazil, extending southward from the state of Rio Grande do Norte as far as Paraguay and Argentina (Misiones province) (Peres *et al.,* 2020; Morellato *et al.,* 2000; Mori *et al.,* 1981) in an inferior humid to subhumid-humid mesophyllo bioclimatic regime. It is highly threatened and very fragmented by anthropic action, especially sugarcane cultivation. In Paraíba state the impact is very high and only fragments remain (Ranta *et al.,* 1998; Thomas, 2008; Oliveira, 1993), which in the capital João Pessoa have been absorbed by urban sprawl, remaining as islands in the middle of the city (Mata do Buraquinho) (Paladini and Cámara, 2015; Paladini, 2016) (Fig. 3).

The vegetation inventory plots done in this area (Paladini, 2016) identified the following dominant species: *Ephedranthus pisocarpus, Campomanesia dichotoma, Blepharocalyx salicifolius* and *Cupania revolute*; the most abundant families were *Myrtaceae* and *Sapindaceae*, typical of the Mata Atlântica, though there were also Cerrado species, with *Eugenia punicifolia, Hancornia speciosa, Maytenus obtusifolia* and *Anacardium occidentale* standing out, with the families *Apocynaceae, Myrtaceae, Celastraceae* and *Malpigiaceae* the most abundant.

The Agreste is a transition plant formation between the Mata Atlântica and the Caatinga, with a predominance of deciduous species, mainly from the Caatinga. It is distributed as a narrow fringe parallel to the coast in the Brazilian states of Bahía, Sergipe, Alagoas, Pernambuco (Rodrigues de Lira *et al.,* 2010), Paraíba (Rodrigues *et al,* 2014) and Rio Grande do Norte (Fig. 4), in conditions of subhumid-dry tropophyllo bioclimatic regime.

Figure 3. Interior of the Mata Atlântica forest in Mata do Buraquinho (João Pessoa) in the coastal zone of Paraíba. July 2015. Photo by R. Cámara.

Figure 4. Vegetation of the Agreste in an area of inselbergs (Araruna Municipality) and 'savannization' of forest for livestock grazing. July 2020. Photo by B. Israel de Souza.

The Cerrado de Tabuleiro (Rizzini, 1992) is a plant formation related to the Cerrado biome which mainly occurs in the central/western region of Brazil (Cole, 1986; Furley y Ratter, 1988; Riou, 1995) but which also develops on the geomorphic formation of the Tabuleiro, formed by silts and sands from the Barreiras Formation (Pliocene) (Silva *et al.,* 2015) on the coast of northeast Brazil (Freire *et al.,* 2011). This plant formation presents species typical of the Cerrado; although found in subhumid-dry mesophyllo regime bioclimatic conditions, the substrate of sands and silts of the Barreiras Formation favours situations of edaphic xericity, enabling this formation to develop instead of the Mata Atlântica (Paladini, 2016). Collapse erosion has occurred over this geologic formation, caused by major storms and very fast subsurface circulation through erosion pipes, called *voçorocas*, with species from the Mata Atlântica situated at the bottom due to the concentrated humidity (Paladini, 2016) (Fig. 5).

Figure 5. Cerrado de Tabulerio in Conde Municipality (Paraíba coast). January 2020. Photo by B. Israel de Souza.

Until the 1960s there was very little agricultural use due to the acid and nutrient-poor soils where it is located. The vegetation was therefore largely preserved. That situation changed starting in the 1970s, due to the National Alcohol Programme (Pró-Alcool) and the federal government's incentives for fuel production using plant biomass derived from sugarcane to reduce dependence on petroleum imports (Moreira and Targino, 1997; Paladini, 2016).

There is a disjunction in the subhumid-dry tropophyllo bioclimatic regime found in two specific points of the state: northeast of the city of Campina Grande in Areia municipality in the Borborema highlands. Between 600 and 750 m, in windward conditions that permit rain with an average of up to 1,200 mm/year, where a humid and subhumid tropical forest is distributed, regionally known in this part of Brazil as Brejo de Altitude (Tabarelli and Santos, 2004; Ab'Saber, 2003).

The Caatinga is the dominant plant formation in the interior of Paraíba state in the Planalto da Borborema and the Sertão. It presents three different structures according to the bioclimatic regime and humidity conditions. In semiarid tropophyllo regime bioclimatic conditions thorny forest formations predominate (Fig. 6). In the municipalities of São João do Tigre and Caturité, on the surface of the Cariris Velhos range between 600 and 750 m, the dominant species are *Mimosa ophthalmocentra, Capparis flexuosa, Anadenanthera colubrina, Aspidosperma pyrifolium, Ziziphus joazeiro* and *Commiphora leptophloeos* (Porto de Lima, 2012).

Figure 6. Area with preserved Caatinga forest coverage in the municipality of São João do Tigre. September 2017. Photo by B. Israel de Souza,

In situations of greater anthropic disruption or more xericity in semiarid xerophyllo biocomiatic regime high and closed scrub formations develop. The inventories done in Coxixola municipality show that the dominant species are *Croton sonderianus* and *Myracrodruon urundeuva*.

In the Cariri range, close to the municipality of São Domingos do Cariri, there is a more xeric region with an arid xerophyllo bioclimatic regime and open bush and low thorny deciduous formations (Porto de Lima, 2012), with *Poincianella pyramidalis* and numerous cacti such as *Pilosocereus catingicola*, *Pilosocereus polygonus* (xique-xique) and bromeliaceae (*Bromelia laciniosa*) densely covering the ground.

In the work developed by Souza *et al.* (2015) in the municipality of São Domingos do Cariri, in a landscape notable for the few individuals and the low diversity of plant species, *Poincianella pyramidalis* was one of those that stood out with respect to the others, a common feature in this part of Paraíba, according to Barbosa *et al.* (2007). Alongside *Croton sonderianus* and *Aspidosperma pyrifolium*, *Poincianella pyramidalis* presents as dominant in most of the phyto-sociological survey work done in the Caatinga (Sampaio, 1996).

Unlike the situation we have in the Paraíba highlands and in the Sertão, the data from the Serra do Paulo, southwest of the Paraíba River basin in the Cariri, show the importance of mountainous areas in the Caatinga biome. In these situations, there is generally a higher average amount of rain and lower temperatures compared to areas at lower altitude, which favours the presence of more vegetation with greater diversity (Sampaio, 2010), known as Matas Serranas, which correspond to a subhumid-dry eurythermophilous bioclimatic regime. Furthermore, the abrupt topography of some hillsides hampers the presence of more human usage in various localities; this is therefore a decisive factor in the presence of vegetation coverage that is still relatively preserved (Fig. 7).

In the case of the region of Areia municipality and its surroundings, there is a disjunction of the Mata Atlântica in the state's interior, in humid mountains, known as Brejos de Altitude. They were largely substituted in the past, not just by sugarcane to produce cachaça and rapadura (unrefined whole cane sugar), but also by coffee cultivation and, starting in the second half of the 20th century, by cattle pastureland (Moreira and Targino, 1997).

Figure 7. Interior of the State Park of Mata do Pau-Ferro (Areia municipality), with Brejos de Altitude vegetation. Photo by Joel Maciel Pereira Cordeiro, September de 2017.

4. Results

Three bioclimatic maps were obtained using the aforementioned methodology, based on the continuous Worldclim databases. First, a map of the current bioclimatic situation, which enabled us to reference the bioclimatic regimes identified with the current plant formations, based on our field experience in the study area (Fig. 8). We used it to produce Tables 2 and 3, which show the extent of the bioclimatic regime types and the plant formations described in the previous section.

In Paraíba state it is possible to identify the thermophilous regime, located in places without thermal limitations and with a low annual thermal range. The eurythermophilous regime is occasionally found, with significant thermal variation during the course of the year and in each month, though without any vegetation stagnation due to thermal causes. In the resulting map of Paraíba state, 4 of the 27 types of bioclimatic regimes were obtained: mesophyllo, tropophyllo, xerophyllo and eurythermal tropophyllo. Figure 8 and Table 2 shows the large area (28,246 km^2) occupied by the xerophyllo (semiarid and arid) bioclimatic regime in western and central Paraíba. Based on the combination with the ombrotypes of Thornthwaite (1956), we obtain the 9 subtypes that appear in Figure 8.

This means that the potentially most extensive plant formation at present in Paraíba state (Table 3) would be Scrub Caatinga (26,612 km^2) and Thorny Forest Caatinga (14,760 km^2). The Caatinga as a whole is the biome most represented in the state (43,006 km^2), followed by Agreste (9,620 km^2) and Mata Atlântica (2,394 km^2).

Second, a map was produced to show the bioclimatic conditions for the Last Glacial Maximum (40 ky). Based on the bioclimatic results, we were able to project the extent of the plant formations at that time, which are shown in Figure 9 and Tables 2 and 3.

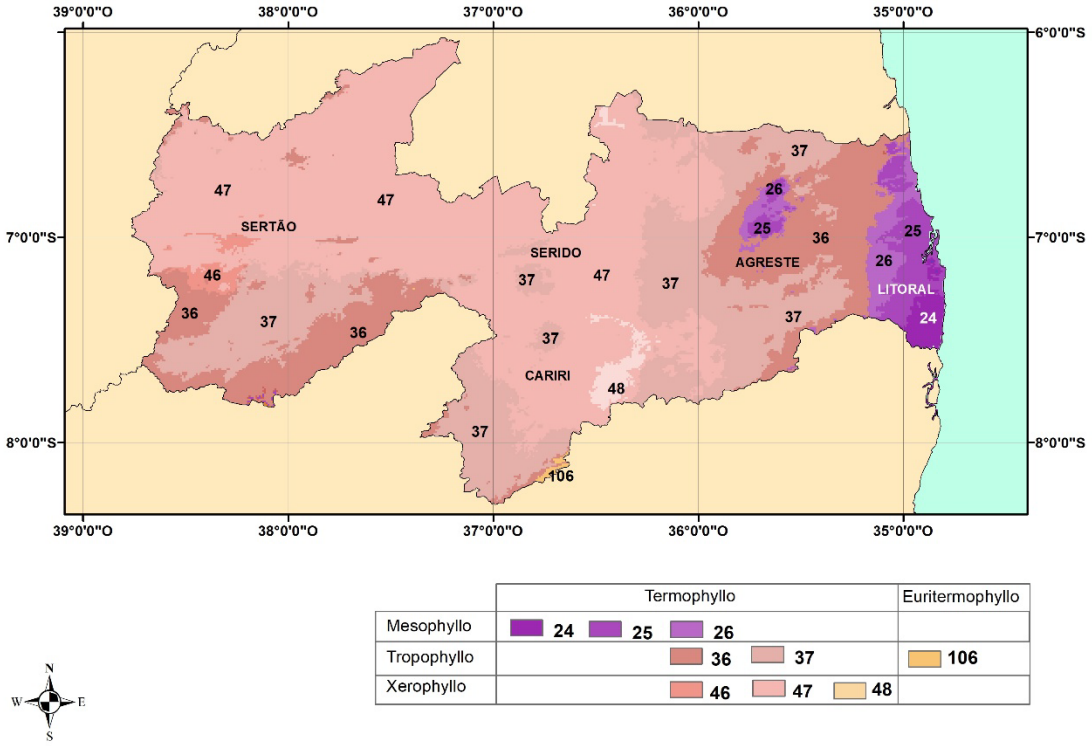

Figure 8. Map of the current situation of the bioclimatic regimes of Paraíba state: inferior humid (24), humid-subhumid (25) and subhumid-dry (26) mesophyllo; subhumid-dry (36) and semiarid (37) tropophyllo; subhumid-dry (46), semiarid (47) and arid (48) xerophyllo; subhumid-dry eurithermophyllo tropophyllo (106). Source: own production.

Table 2. Area in km² of the bioclimatic regime types in Paraíba state at the Last Glacial Maximum, at present (2021) and for the RCP 8.5 scenario of the CCMS 4.0 climate change model.

Bioclimatic regime subtype	Last Glacial Maximum	2021	CCMS4.0 2070 RCP8.5
Ombrophyllo	4698.57	2.56	0.00
Mesophyllo	7611.26	3801.62	0.00
Tropophyllo	17008.40	24402.13	7139.76
Xerophyllo	7504.96	28246.36	46740.72
Hyperxerophyllo	0.00	0.00	2649.72
Eurythermal mesophyllo	1785.88	11.93	0.00
Eurythermal tropophyllo	19495.88	72.42	0.00
Eurythermal xerophyllo	3231.60	0.00	0.00

Table 3. Area in km² of potential plant formations in Paraíba state at the Last Glacial Maximum, at present (2021) and for the RCP 8.5 scenario of the CCMS 4.0 climate change model.

	Last Glacial Maximum	2021	CCMS4.0 2070 RCP8.5
Mata Atlântica	9801.09	2394.97	0.00
Cerrado	2508.74	1430.51	0.00
Agreste	12373.61	9620.78	0.00
Thorny Forest Caatinga	4634.79	14760.05	7139.76
Scrub Caatinga	7504.96	27612.47	0.00
Shrub Caatinga	0.00	633.89	49390.44
Brejo	1785.88	11.93	0.00
Mata Serrana	19495.88	72.42	0.00
Mata Serrana Shrub	3231.60	0.00	0.00

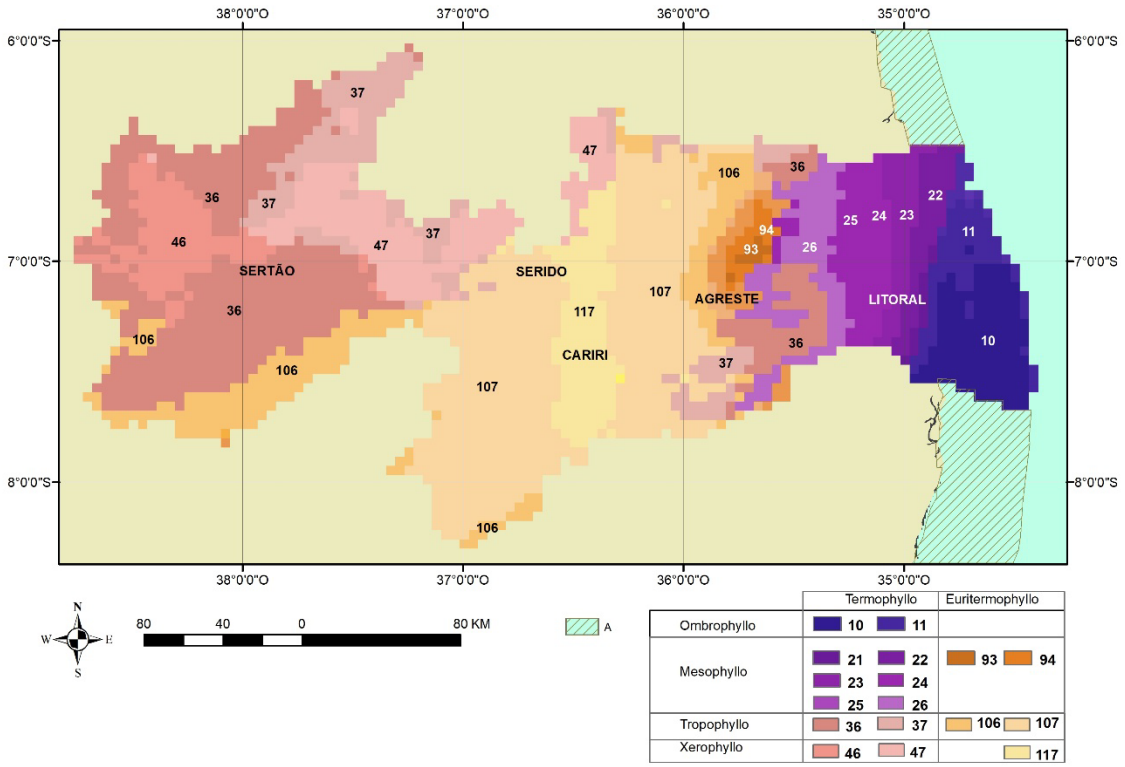

Figure 9. Map of the bioclimatic regimes of Paraíba state at the Last Glacial Maximum (40 ky) with: hyper-humid (10), superlative humid (11) ombrophyllo; superlative humid (21), superior humid (22), medium humid (23), inferior humid (24), humid-subhumid (25), subhumid-dry (26) mesophyllo; subhumid-dry (36), semiarid (37) tropophyllo; subhumid-dry (46), semiarid (47) xerophyllo; medium humid (93), inferior humid (94) eurithermophyllo mesophyllo; subhumid-dry (106), semiarid (107) eurithermophyllo tropophyllo; semiarid eurithermophyllo xerophyllo (117). Source: own production.

Compared to the current area, the Mata Atlântica area was clearly 7,406 km^2 larger, extending over the now submerged continental shelf; a hyper-humid to superlative humid ombrophyllo bioclimatic regime covered an area of 4,698 km^2 that is virtually non-existent today. This leads us to suggest that the Mata Atlântica present nowadays in humid-subhumid mesophyllo bioclimatic conditions comprises relicts of that previous situation. The rising sea level since the Last Glacial Maximum and the receding coast (Tabuleiro cliffs on the Paraíba coast) (Peulvast *et al.,* 2004) left the Mata Atlântica restricted to its current positions. The area covered by eurythermal bioclimatic conditions is also more important, from eurythermal mesophyllo to xerophyllo, with 24,513 km^2 versus the current 83 km^2, mainly distributed in the Cariri, in areas nowadays occupied by the Caatinga.

The tropophyllo and xerophyllo bioclimatic conditions resembling the current ones, with Caatinga, are limited to the Sertão, with situations similar to those found today.

Finally, a third map was produced, showing the situation of the state projected to the year 2070 in the RCP 8.5 scenario according to the CMSS 4.0 coupled climate change model (Fig. 10). In this situation the ombrophyllo, mesophyllo and eurythermophilous bioclimatic regime conditions disappear; only tropophyllo and xerophyllo bioclimatic regimes are still represented, with the hyperxerophyllo appearing in the Seridó. The more humid conditions are reduced to an arid tropophyllo regime in the mountains and in the Agreste, and semiarid along the coast, implying the disappearance of the bioclimatic conditions for all the current plant formations except the thorny forest Caatinga (7,139 km^2) in the tropophyllo conditions and the shrub Caatinga (49,390 km^2) for the rest of the state, with desert conditions in the Seridó.

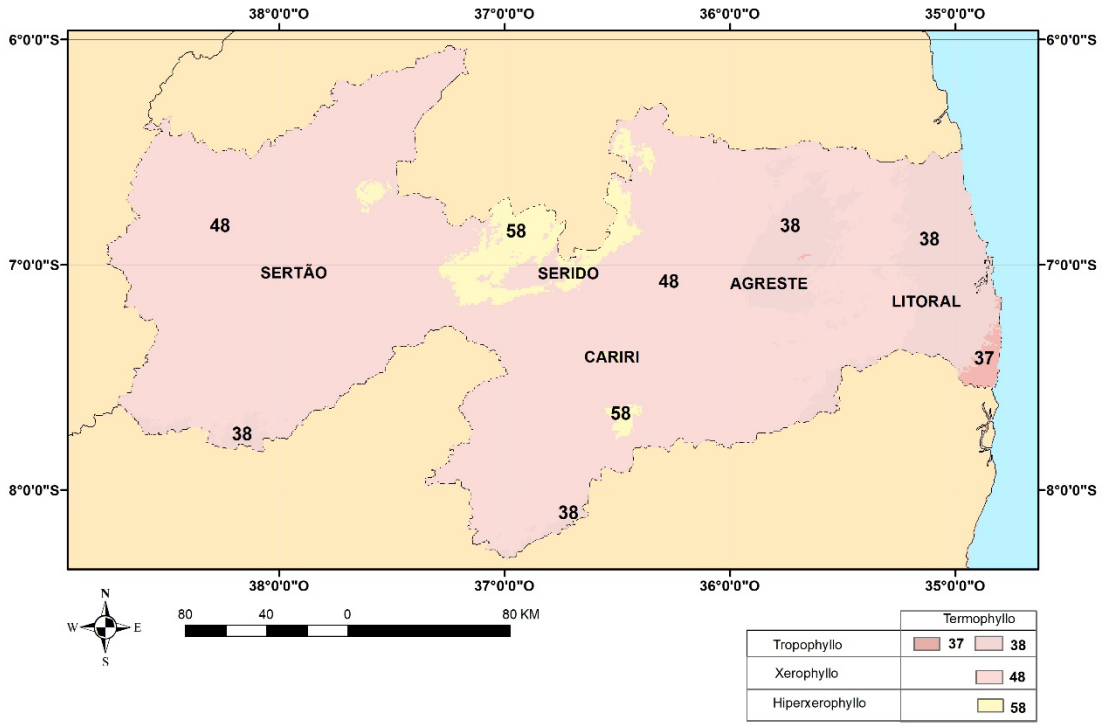

Figure 10. Map of the bioclimatic regimes in Paraíba state for the RCP 8.5 year 2070 scenario of the CMSS 4.0 model with: semiarid (37) and arid (38) tropophyllo; arid xerophyllo (48); and arid hyperxerophyllo (58). Source: own production.

5. Discussion and conclusions

The application of the methodology proposed by Cámara *et al.* (2020) allows the bioclimatic regimes to be associated to the plant formations, based on the current situation. The results of past bioclimatic situations can then be seen, such as the case of the Last Glacial Maximum, as well as future ones with the RCP 8.5 year 2070 scenario for the CMSS 4.0 model. We compared these results with existing publications for the past and for the future of Paraíba state.

For past situations we looked to the most recent one with the greatest contrast – the Last Glacial Maximum. In the respective map, what is most relevant is the exposed continental shelf, nowadays submerged (Peulvast *et al.,* 2004), and the expanded presence on it of the Mata Atlântica. Marine pollen data gathered in northeast Brazil indicate the presence of Caatinga in the interior between the periods of the Last Glacial and the early Holocene (42,000 BP to 9,400 BP), most of the time reflecting semiarid conditions. The longest and most humid period was between 18,500 and 12,800 years BP, enabling the expansion of humid forests, as indicated by the expansion of tropical forest and humid mountain forests (Ruiz Pesenda *et al.,* 2010), with a return to drier climatic conditions during the early Holocene (Behling *et al.,* 2000). It is possible that during the Last Glacial period some of the current humid forests in the mountains (Andrade-Lima, 1982; Ab'Saber, 1997) were connected, forming a larger area during the colder and more humid climatic conditions. Gu *et al.* (2017) thus hold that the Atlantic forest expanded after the Last Glacial in the lowlands along Brazil's coast, including the continental shelf still exposed during that period, before the rising post-glacial sea level flooded the continental shelf.

We considered the extreme situation for 2070 in a scenario with a very high level of greenhouse gas emissions, with radiative forcing of 8.5 W/m^2 (RCP 8.5) with rising trend, and 936 ppm of CO_2 in the atmosphere. Hausfather and Peters (2020) indicate that RCP 8.5 was based on what ended up being an overestimate of projected carbon production, as for 2070 such resources will be almost exhausted, unable to produce more greenhouse gas emissions because they will have been replaced by clean energy alternatives such as solar or wind power. They assert that this makes the RCP 8.5 scenario increasingly

implausible with each year that passes. Since the Fifth IPCC Report this situation has been considered very unlikely, though still possible, because the feedbacks are not well understood (Ward *et al.,* 2012).

As seen in Table 4, the projection for 2070 of RCP 8.5 is 2ºC on average. The central aim of the Paris Agreement was to boost the global response to climate change, keeping global temperature increase in this century under 2ºC higher than preindustrial levels.

Table 4. Projections of increased global warming (°C) (Fifth IPCC Report).

	2046-2065	2081-2100
Scenario	*Avg. and probable range*	*Avg. and probable range*
RCP 2.6	1.0 (0.4 to 1.6)	1.0 (0.3 to 1.7)
RCP 4.5	1.4 (0.9 to 2.0)	1.8 (1.1 to 2.6)
RCP 6	1.3 (0.8 to 1.8)	2.2 (1.4 to 3.1)
RCP 8.5	2.0 (1.4 to 2.6)	3.7 (2.6 to 4.8)

The work of Steffena *et al*. (2018) nevertheless detected a threshold in which temperatures can increase between 4 and 5ºC over preindustrial levels, taking climate system feedback mechanisms into account, which would vouch for the 2ºC situation for an RCP 8.5 in 2070. That would imply an average sea-level rise of 0.30 m for 2070 and 0.63 m for 2100 (Table 5).

Table 5. Projections of increase of average global sea level (meters) (Fifth IPCC Report).

	2046-2065	2081–2100
Scenario	*Avg. and probable range*	*Avg. and probable range*
RCP 2.6	0.24 (0.17 to 0.32)	0.40 (0.26 to 0.55)
RCP 4.5	0.26 (0.19 to 0.33)	0,47 (0,32 to 0,63)
RCP 6	0.25 (0.18 to 0.32)	0.48 (0.33 to 0.63)
RCP 8.5	0.30 (0.22 to 0.38)	0.63 (0.45 to 0.82)

Based on the inventories and the results of the bioclimatic variables, we can establish a relationship between the bioclimatic regimes and the distribution of plant formations, identifying spatial distribution patterns of those formations and the respective species according to those bioclimatic variables, within the framework of each bioclimatic regime type or subtype (with the ombroclimate) – average temperature, annual precipitation, potential evapotranspiration and hydric vegetation stagnation (in the case of Paraíba) – as well as the indexes for real and potential bioclimatic intensity derived from the bioclimatic balances (BBs) of Montero de Burgos and González Rebollar (1974). It is thus an effective method to relate the distribution of plant formations and bioclimatic regime types; we can therefore make forward and backward projections, showing variation of the distribution of plant formations according to the bioclimatic regimes in the considered situations.

This paper shows the possibility of recognizing the presence of relict plant formations in the current conditions, such as the case of the Mata Atlântica, and explains the presence of species requiring less humidity within that formation. On the other hand, the 2070 projection warns that the xerification process may take place if the barrier of a 2ºC increase in the planet's average temperature compared to the preindustrial era is surpassed, leading to disappearance of the bioclimatic conditions that would enable conservation of the Mata Atlântica itself or the dry thorny forests of the Caatinga, with shrub forms expanding in the Sertão and in the Cariri down to the coast or even desert conditions in the Seridó.

Beyond this potential bioclimatic framework, the processes involved in the use of plant resources and soils have over time replaced the original coverage of flora, producing extensive degradation and establishing a situation, with respect to the Caatinga, which may be leading a large part of Paraíba to worrisome levels of desertification.

Acknowledgments

The knowledge about these plant formations derives from our field experience in joint research projects between the University of Seville and the Federal University of Paraíba (main campus in João Pessoa). These projects have resulted in research articles, two master degree theses and two doctoral theses. Based on the fieldwork, it was possible to profile the extent of the plant formations and comprehensively map them with the bioclimatic regimes obtained for the state of Paraíba: *Recursos y manejo del territorio y del agua en la cuenca hidrografica del rio Paraiba: disponibilidad y uso para el desarrollo de las comunidades locales*. Programa de Cooperación Internacional (Acciones Integradas), Ministerio de Educación y Ciencia-AECID. D/024312/09 (2010-2012) y *Conservación y valorización socio-ambiental de los recursos naturales del litoral de Paraiba.* Programa de Cooperación Internacional (acciones integradas), Ministerio de Educación y Ciencia-AECID. A/017075/08 (2008-2009)

References

Ab'Saber, A.N. 1977. Problemática da desertificação e da savanização no Brasil intertropical. *Geomorfologia* 53, 1-19.

Andrade-Lima, D. 1982. Present-day forest refuges in northeastern Brazil. En: G.T. Prance, (Ed.), *Biological Diversication in the Tropics*. Colombia University Press, New York, pp. 245-251.

Barbosa, M.R.V., Lima, I.B., Lima, J.R., Cunha, J.P., Agra, M.F., Thomas, W.W. 2007. Vegetação e flora no Cariri Paraibano. *Oecologia Brasiliensis* 11 (3), 313-322.

Behling, H., Arz, H.W., Patzold, J., Wefer, G. 2000. Late Quaternary vegetational and climate dynamics in northeastern Brazil, inferences from marine core GeoB3104-1. *Quaternary Science Reviews* 19 (10), 981-994. https://doi.org/10.1016/S0277-3791(99)00046-3

Cámara, R. 1997. *República Dominicana: dinámica del medio físico en la región Caribe (Geografía Física, Sabanas y Litoral) Aportación al conocimiento de la tropicalidad insular*. Tesis doctoral. Universidad de Sevilla. https://idus.us.es/handle/11441/85112

Cámara, R., Díaz del Olmo, F., Martínez, J.R. 2020. TBRs, a methodology for the multi-scalar cartographic analysis of the distribution of plant formations. *Boletín de la Asociación de Geógrafos Españoles* 85, 1–38. https://doi.org/10.21138/bage.2915

Carvalho, M.G.R F. 1982. *Estado da Paraiba. Classificaçao Geomorfológica*. Editora universitária da Universidad Federal da Paraiba. Joao Pessoa.

Cole, M. 1986. *The Savannas. Biogeography and Geobotany*. Academic Press. London.

Fick, S.E., Hijmans, R.J. 2017. Worldclim 2: New 1-km spatial resolution climate surfaces for global land areas. *International Journal of Climatology* 37 (12), 4302-4315. https://doi.org/10.1002/joc.5086.

Freire, M., Farias A.S., Soares de Araujo, F. 2011. Composição florística e estrutura de um fragmento de vegetação savânica sobre os tabuleiros pré-litorâneos na zona urbana de Fortaleza, Ceará. *Rodriguésia* 62 (2), 407-423.

Furley, P.A, Ratter J.Á. 1988. Soil resources and plant communities of the central Brazilian cerrado and their development. *Journal of Biogeography* 15, 97-108. https://doi.org/10.2307/2845050

Gu, F., Karin, A.F., Zonneveld, K.A.F., Chiessi, C.M., Arz, H.W., Pätzold, J., Behlinga, H. 2017. Long-term vegetation, climate and ocean dynamics inferred from a 73,500 years old marine sediment core (GeoB2107-3) off southern Brazil. *Quaternary Science Reviews* 172 (15), 55-71 https://doi.org/10.1016/j.quascirev.2017.06.028

Hausfather, Z., Peters, G. 2020. Emissions–the 'business as usual' story is misleading. *Nature* 577 (7792), 618-20. https://doi.org/10.1038/d41586-020-00177-3

Huget del Villar, E. 1929. *Geobotánica.* Colección Labor, Sección XII, Ciencias Naturales, nº 199-200, Barcelona.

Montero de Burgos, J.L., González, J.L.R. 1974. *Diagramas bioclimáticos.* ICONA/Ministerio de Agricultura, Madrid.

Moreira, E., Targino, I. 1997. *Capítulos de Geografia Agrária da Paraíba*. Ed. UFPB, Joao Pessoa.

Morellato, L.P., Talora, D.C., Takahasi, A., Bencke, C.C., Romera, E.C., Zipparro, V.B. 2000. Phenology of Atlantic Rain Forest tres: a comparative study. *Biotropica Special Issue: The Brazilian Atlantic Forest* (32) 4b, 811-823. https://doi.org/10.1111/j.1744-7429.2000.tb00620.x

Mori, S.A., Boom, B.M., Prance, G.T. 1981., Distribution patterns and conservation of Eastern Brazilian Coastal Forest Tree Species. *Brittonia* 33 (2), 233-245.

Oliveira P. 1993. The Brazilian Atlantic Rain Forest: An ecological tragedy for Humankind. *Global Ecology and Biogeography Letters* (39) 1, 30-31.

Paladini, B., Cámara, R. 2015. Retroceso de la mata atlántica en el entorno de Joao Pessoa (Estado de Paraiba, Brasil). Análisis de la Biodiversidad. In: *Análisis Espacial y representación geográfica: innovación y aplicación*. Departamento de Geografia y Ordenacion del Territorio, pp. 1563-1570, Zaragoza.

Paladini, B. 2016. *Deforestación de la Mata Atlántica en el litoral del Estado de Paraíba (Brasil). Cambios ambientales y riesgos geomorfológicos: voçorocas.* Tesis Doctorado en Geografía. Universidad de Sevilla, Sevilla.

Peres, E.A., Pinto-da-Rocha, R., Lohmann, L.G., Michelangeli, F.A., Miyaki, C.Y., Carnaval, A.C. 2020. Patterns of Species and Lineage Diversity in the Atlantic Rainforest of Brazil. *Neotropical Diversification: Patterns and Processes*, pp 415-447.

Peulvast, J.N., Claudino Sales, V. 2004. Stepped surfaces and palaeolandforms in the northern Brazilian «Nordeste»: Constraints on models of morphotectonic evolution. *Geomorphology* 62 (1), 89-122. http://doi.org/10.1016/j.geomorph.2004.02.006

Porto de Lima, V.R. 2012. *Caracterización biogeográfica del bioma de Caatinga en el sector semiárido de la cuenca del río Paraiba, Noreste de Brasil: propuesta de ordenación y gestión de un medio semiárido tropical***.** Tesis Doctorado en Geografía. Universidad de Sevilla, Sevilla.

Ranta, P., Blom, T., Miemela, J., Joemsuu, E., Siitonen, M. 1998. The fragmented Atlantic rain forest of Brazil: size, shape and distribution of forest fragments. *Biodiversity and Conservation* 7, 385-403.

Rodrigues, J.S., Castelo Branco J.S., Miranda de Melo, J.I. 2014. Flora de um inselberg na mesorregião agreste do estado da Paraíba-Brasil. *Polibotánica* 37, 47-61.

Rodrigues de Lira, D., Bezerra de Araujo, M.S., Sa Baretto, E.V., Alves da Silva H. 2010. Mapeamento e Quantificação da Cobertura Vegetal do Agreste Central de Pernambuco Utilizando o NDVI. *Revista Brasileira de Geografia Física* (3), 157-162.

Riou, G. 1995. *Savanes. L'herbe, l'arbre et l'homme en terres tropicales*. Masson. Paris.

Rizzini, C.T. 1992. *Tratado de Biogeografia do Brasil: aspectos ecológicos, sociológicos e florísticos*. Ambito Cultural Edições. Rio de Janeiro.

Ruiz Pessenda, L.C., Marques Gouveia, S. E., Souza Ribeiro A., Oliveira P. E., Aravena R. 2010. Late Pleistocene and Holocene vegetation changes in northeastern Brazil determined from carbon isotopes and charcoal records in soils. *Palaeogeography, Palaeoclimatology, Palaeoecology* 297 (3–4), 597-608. https://doi.org/10.1016/j.palaeo.2010.12.026

Sampaio, E.V.S.B. 2010. Características e potencialidades. En: M. A Gariglio, E. V. S. B. Sampaio, L. A. Cestaro, P. Y. Kageyama (ed.). *Uso sustentável e conservação dos recursos florestais da caatinga*. Ministerio do Meio Ambiente, pp. 29-48, Brasília.

Schimper, A.F.W. 1903. *Plant-Geography upon a physiological basis.* Clarendon Press, Oxford.

Silva, T., Torres, L.M., Furrier, M. 2015. Caracterización geológica y geomorfológica del Municipio de Joao Pessoa, PB. Brasil. *Revista Geográfica de América Central* 54, 113-134. http://doi.org/10.15359/rgac.1-54.5

Souza, B.I., Cámara, R., Lima, E.R.V. 2015. Caatinga e desertificação. *Mercator* 14 (1), 131-150. http://doi.org/10.4215/RM2015.1401.0009

Steffena, W., Rockströma J., Richardson K., Lentond T.M., Folkea, C., Livermanf, D., Summerhayesg, C.P., Barnoskyh, A.D., Cornella S.E., Crucifixi, M., Dongesa, J.F., Fetzera, I., Ladea, S.J., Scheffer, M., Winkelmannk, R., Schellnhubera, H.J. 2018. Trajectories of the Earth System in the Anthropocene. *PNAS* 115 (33), 8252-8259. https://doi.org/10.1073/pnas.1810141115

Tabarelli, M., Santos, A.M.M. 2004. Uma breve descrição sobre a História Natural dos Brejos nordestinos. In: K. C. Porto, J. P. Cabral, M. Tabarelli (ed.). *Brejos de altitude em Pernambuco e Paraíba: história natural, ecologia e conservação.* Ministério do Meio Ambiente. Série Biodiversidade, 9. Brasília.

Thomas, W.W. 2008. *The Atlantic Coastal Forest of Northeastern Brazil.* The New York Botanical Garden Press. New York.

Thornthwaite, C.W., Mather, J.R. 1956. *The Water Balance*. Drexel Institute of Technology, Laboratory of Climatology 8, 1-104.

Thornthwaite, C.W., Mather, J.R. 1957. Instructions and Tables for Computing Potential Evapotranspiration and the Water Balance. *Climatology* 10, 181-311.

Tuhkanen, S. 1980. Climatic parameters and indices in plant geography. *Acta Phytogeographica Suecica* 67, 1-108.

Ward, J.D., Mohr, S.H., Myers, B.R., Nel, W.P. 2012. High estimates of supply constrained emissions scenarios for long-term climate risk assessment. *Energy Policy* 51, 598-604. https://doi.org/10.1016/j.enpol.2012.09.003

Warming, E. 1909. *Oecology of plants*. *An Introduction to the Study of Plant Communities.* Oxford University Press, London.

Cuadernos de Investigación Geográfica *Geographical Research Letters*	2022	Nº 48	pp. 175-196	EISSN 1697-9540

http://doi.org/10.18172/cig.4908

LAND COVER CHANGES IN COFFEE CULTURAL LANDSCAPES OF PEREIRA (COLOMBIA) BETWEEN 1997 AND 2014

BEATRIZ E. MURILLO LÓPEZ[1]*, ALEXANDER FEIJOO MARTÍNEZ[1], ANDRÉS F. CARVAJAL[2]

[1]*Universidad Tecnológica de Pereira, Facultad de Ciencias Ambientales, Vereda La Julita, A.A. 097, Pereira, Colombia.*

[2]*Faculty of Environmental and Civil Engineering, Universidad Antonio Nariño, Bogotá D.C., Colombia.*

ABSTRACT. Understanding how and what land cover changes and transitions have occurred in a territory is crucial to planning and managing high-demand surfaces. At the landscape level, the challenge is determining the allocation and management of various land cover options. Therefore, for natural resources planning and management, a study characterizing and analysing the territory of interest should be included. This work aimed to analyse the changes and land cover patterns in the city of Pereira, Colombia, within the framework of the Colombian Coffee Cultural Landscape. The evaluated period was between 1997 and 2014, and a Geographic Information System, ENVI 4.8 programme and QGIS programme were used for multitemporal analysis. To describe the land cover transitions, two temporal moments were analysed with Landsat satellite images: one moment was for the year 1997, which was taken in August (Landsat 5), and the other moment was for the year 2014, which was taken in July (Landsat 8). At level 1 of CORINE (Coordination of information on the environment), the areas of land cover corresponding to agricultural areas, forests and semi-natural areas decreased most in the analysis period, while artificial surfaces increased. At level 3, the cover with the greatest decrease in territory was coffee crops, which showed a negative annual loss rate of -3.97%, followed by permanent crops (-2.67%). The continuous and discontinuous urban fabric showed the greatest growth with a positive annual rate of 4.14%. In conclusion, the land cover that lost the most territory was coffee crop, mainly due to political-economic factors, such as the dissolution of the International Coffee Agreement and the National Federation of Coffee Growers that discouraged coffee cultivation and permanent crops. Likewise, sociocultural factors, such as smallholder farmers have guided the changes in land cover and have stimulated productive styles to adapt and remain, increasing heterogeneous agricultural areas.

Cambios en la cubierta del suelo en los paisajes culturales del café (Colombia) entre 1997 y 2014

RESUMEN. Comprender cómo y qué cambios y transiciones de las cubiertas del suelo se han dado en un territorio es clave para la planificación y gestión de las superficies con alta demanda. A nivel del paisaje, el desafío es cómo decidir la asignación y gestión de opciones de coberturas del terreno. Por lo tanto, para la planificación y manejo de los recursos naturales se debe incluir un estudio de caracterización y análisis del territorio. Este trabajo tiene como objetivo analizar los cambios y los patrones de cubierta del suelo en la ciudad de Pereira, Colombia, en el marco del Paisaje Cultural Cafetero de Colombia. El período evaluado se estableció entre 1997 y 2014, se trabajó con Sistemas de Información Geográfica y se emplearon los programas ENVI 4.8 y QGIS para el análisis multitemporal. Para describir las transiciones de coberturas, se propuso un análisis en dos momentos con imágenes del satélite Landsat, una para el año 1997 tomada en agosto (Landsat 5) y la otra para el año 2014 del mes de Julio (Landsat 8). Se encontró en el primer nivel de Corine que las cubiertas de territorios agrícolas, bosques y áreas seminaturales fueron las áreas que porcentualmente más han disminuido en el período de análisis mientras que han

aumentado las zonas artificales; también se halló para el tercer nivel de Corine que la cubierta que más territorio ha cedido fueron los cultivos de café con una tasa negativa por año de -3,97%, seguido de los cultivos permanentes (-2,67%); mientras que, el tejido urbano continuo y discontinuo presentó el mayor crecimiento con una tasa positiva por año de 4,14%. En conclusión, la cubierta del suelo que más perdió territorio fue el cultivo de café, principalmente por factores político-económicos, como la disolución del Convenio Internacional del Café y la Federación Nacional de Cafeteros que desestimularon el cultivo de café y los cultivos permanentes. Así mismo, factores socioculturales, como el minifundio, han orientado los cambios en las cubiertas del suelo y han estimulado los estilos productivos para adaptarse y permanecer, aumentando las áreas agrícolas heterogéneas.

Keywords: Multitemporal analysis, Landsat, land cover transition, rural-urban change.

Palabras claves: Análisis multitemporal, Landsat, transición de coberturas, cambio rural-urbano.

Received: 15 October 2020

Accepted: 2 June 2021

*Corresponding author: Beatriz Elena Murillo López, Research Group in Andean Tropical Agroecosystems, Universidad Tecnológica de Pereira, Facultad de Ciencias Ambientales, Vereda La Julita, A.A. 097, Pereira, Colombia. E-mail address: betymu@utp.edu.co

1. Introduction

In the processes related to human occupation of the territory, there are several changes that require the understanding and research about the elements that motivate local, regional and global changes. This approach requires information integration from social, natural and geographic sciences (Rindfuss *et al.,* 2004; Turner *et al.,* 2007), to understand the factors that influence land covers, site diversity and interpret dramatic changes in the transformation of land use, mainly impacting rural areas, such as cultivated land is diminishing (Boudet *et al.,* 2020; Chen *et al.,* 2020; D'Amour *et al.,* 2017; Xia *et al.,* 2020), which lead to the loss of food security of human communities at local scales. This reduction in land for agricultural production affects the long-term economic development, food security and ecological security of regions, as well as the livelihoods of farmers and rural residents' wellbeing (Xia *et al*., 2020).

The rapid expansion of cities is showing and it is also affecting the biodiversity of ecosystems and reducing the areas providing high-value ecosystem services (Narducci *et al.,* 2019). Landscape changes over time reflect the management of natural resources, cultural practices (van der Ploeg and Ventura, 2014) and priorities in land use planning (Verburg *et al.,* 2009). Classifying the terrain allows us to assess and identify changes in the use and cover of inhabited spaces and to understand the interactions and relationships with communities in that territory. This spatial social construction enables assessment of land use planning scenarios to integrate the environmental component in the decision-making process for plans and programmes, which can have significant effects on the environment and communities (Loiseau *et al.,* 2012; Sanhouse-Garcia *et al.,* 2017; Ashiagbor *et al.,* 2020; Chen *et al.,* 2020).

Modification of the landscape is a product of agrarian activity and the physiographic transformations derived from settlement types (Rivera, 2014, Xia *et al.,* 2020) and national or regional policies. A comparative analysis study that shows the state of land management due to anthropogenic changes is necessary (Zúñiga *et al.,* 2003; Carvajal, *et al.,* 2009; Murillo-López, 2010; Sanhouse-Garcia *et al.,* 2017), accompanied by multitemporal analyses to identify the changes in land cover and uses

(Turner II *et al.,* 2007; Napieralski *et al.,* 2013), to provide primary source of data that represents the terrain and spatial analyses.

In the processes of human occupation and transformation of the landscape, territories have been configured that are the result of adaptation processes, which developed from the introduction of the great richness and conservation of coffee variety seeds, biodiversity and the provision of ecosystem services, located in landscapes in the north of the Andes mountain range, with regions of medium mountains (1000 to 1900 m.a.s.l.) and with an average climate (precipitation between 1200 and 2300 mm, temperature between 17 and 24°C). The regions with these characteristics were denominated Coffee Cultural Landscape of Colombia (CCL), where the culture and economy were developed around the coffee crop in small plots (0.5-3 ha), in which the distances between plants and the combination with other species of trees created symmetrical figures with multiple forms in the vegetation arrangements. The plots are part of small farms (average 5.3 ha) in which management practices, decision making and administration are carried out by the family, with its members educated and employed in a traditional way in daily tasks and learning about the environment, which is preserved in memory and inherited from generation to generation (Fernandez *et al.,* 2010; UNESCO, 2021; PCC, 2021).

This panorama of the Coffee Cultural Landscape of Colombia led to its declaration in 2011 as a World Heritage Site by the United Nations Educational, Scientific and Cultural Organization (UNESCO), as it is considered as a scenario that should be prioritized for the preservation of the tangible (type of architecture in housing and crops, introduction of biodiversity-friendly systems and benefits in the generation of ecosystem services) (Ruiz-Cobo *et al.,* 2010; Botero-Arango *et al.,* 2020, Rojas-Cano *et al.,* 2021) and the intangible (culture, rootedness, sense of place, heritage and identity) and, because of the risk in the destruction of its unique characteristics, in which man with his ingenuity has managed to modify the landscapes.

In Colombia, the area occupied by rural areas is distributed among forests and semi-natural areas (56.7%), agricultural areas (38.6%), non-agricultural (2.2%) and other (includes non-agricultural infrastructure and other land uses) (2.5%) (DANE, 2016); and the management, administration and sustainable use of covers and land uses is not clearly incorporated into the issue of rural development; the territory occupied by rural areas is still unknown (cover, uses, variables, resources and distribution), and it is still unclear which uses generate greater pressure and how the dynamics of human activities have changed and fragmented the landscape. The CCL's richness is being transformed, which has been poorly studied for the change in land cover and land use caused by the introduction of agro-industrial systems of coffee, banana, avocado, pastures and the expansion of the urban frontier of the cities (Nieto *et al.,* 2016; Molina-Rico *et al.,* 2019). In the case of the department of Risaralda, the agricultural area went from 78.5% in 1970 to 50% in 2014 (DANE, 1970; DANE, 2016), with changes leading to the loss of land for agriculture and occupation of condominiums for human dwelling.

The above emphasizes the need to consider the territory as an important concept in policymaking (INCODER and Misión Rural, 2013) and the need for a multitemporal analysis that shows ground cover changes. Therefore, it is necessary to evaluate the consequences of urban expansion on farmland to determine possible areas of conflict, as well as strategies to create more sustainable forms of urban expansion and understand cultural landscapes as the results of long-term biological and social relationships (Lindholm and Ekblom, 2019). Therefore, we propose the following questions: (i) How have land covers changed between 1997 and 2014 in Pereira? and (ii) What were the main changes in the CCL of the city of Pereira? In addition, if the CCL is undergoing different changes, it is expected to find empirical evidence of how, and on what scale, these regions are responding to human-induced changes over time. To answer this question, it was necessary to approach it practically, using geospatial information at two moments in time (1997 and 2014); further, this work aimed at analysing the multitemporal changes in land cover and its transitions in the coffee cultural landscape of the municipality of Pereira.

2. Study area

The research was carried out between 2017 and 2018 in the city of Pereira, Colombia. The territory is located on the western slope of the central mountain range (three mountain ranges cross the Colombian territory from south to north). Pereira has an area of 607 km^2 and is located between 4º 43' 4.8" North and 75º 50' 38.4" West; and 4º 52' 15.6" North and 75º 36' 18" West in the central-western part of the country. The urban area has an average annual temperature of 21.6 °C, and the average annual precipitation is 2354.3 mm (IDEAM, 2014).

The study area is mountainous, so it presents a variety of climates and the elevation ranges between 900 and 5,200 m.a.s.l. (Fig. 1). The coffee cultural landscape (CCL) was classified into six zones, Pereira belongs to zone C with rural areas located in the central mountain range of the Andes and with an altitude that ranges for coffee cultivation between 1,500 and 1,900 m.a.s.l. Other crops such as corn, beans, plantain, and other subsistence products are grown in the landscape, but coffee is, of course, the dominant crop covering 57% of the total area of the coffee farms (Fernandez Retamoso *et al.,* 2010; PCC, 2021).

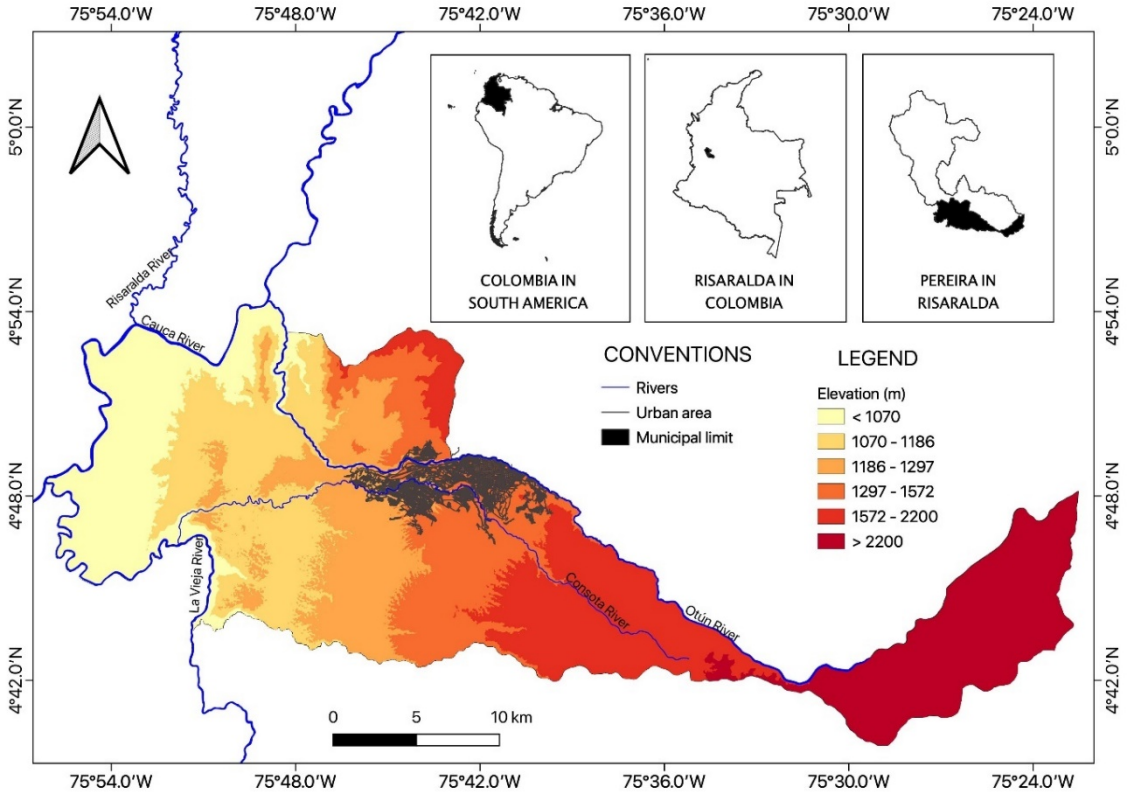

Figure 1. Municipality of Pereira showing elevational differences.

According to the 2018 census, Pereira has an approximate population of 467,269 inhabitants, of which 81,432 (17.4%) are inhabitants of the rural zone (DANE, 2019). Pereira has a history associated with agricultural production, from the pre-Columbian population of Quimbaya and the indigenous Zerrillos, who supported themselves through agriculture; by the mid-nineteenth century, the Cauca colonies built estates for the production of sugarcane and cocoa towards the flatter areas between Pereira and Cartago, while the colonies from Antioquia, Caldas and Tolima developed subsistence crops on the western slopes of the central mountain range between the Otún and Consota Rivers (Rivera, 2014).

Pereira emerged from two contradictory cultures, the grand hacienda with colonial identity and slavery towards the areas with lower slopes (between the *corregimiento* of Cerritos and Cartago) and

the displaced landless peasants of Antioquia, Valle del Cauca, Tolima and Caldas, who settled with smallholdings in the steepest areas between the Consota and Otún Rivers. Currently, the type of farm in Pereira continues to have similar characteristics as those of the settlers in the early nineteenth century. According to the 2016-2019 Municipal Development Plan, the rural sector has been categorized into four zones, where the greatest presence of farms with areas between two and four hectares is highlighted. These farms are mainly located east of the city of Pereira in the territory between the Consota and Otún Rivers (smallholdings), while the western area of the municipality has fewer farms but with an average area of 25.9 ha. This territorial distribution shows permanence in the type of occupancy of the rural territory of Pereira (Table 1 and Fig. 1).

Table 1. Distribution characteristics by rural territory zone in Pereira.

Zone	*Veredas*	*Corregimientos*	Area of Zone (ha)	Farm (number)	Cover	Mean area per farm (ha)
1	38	La Florida, La Bella, Tribunas Corcega, eastern part of Arabia	4,617	2,264	Coffee crop (CC); heterogeneous agricultural areas (HAA); rotation crop (RC)	2.04
2	34	Morelia (not including Los Planes), Altagracia, la Estrella; La Palmilla and the western part of Arabia	8,642	2,187	CC; heterogeneous agricultural areas (HAA); permanent crop (PC)	3.95
3	24	Combia Alta and Combia Baja	4,967	1,368	CC; heterogeneous agricultural areas (HAA); permanent crop (PC)	3.63
4	10	Caimalito, Puerto Caldas, Cerritos and the Planes de Morelia	19,726	762	Permanent crop (PC); pasture (Ps)	25.89

Adapted from the Pereira City Council, 2016. Technical support document for the 2016-2019 Municipal Development Plan "Pereira, Capital del Eje" (*Pereira, Capital of the Axis*), Pereira. *Vereda and Corregimiento: it's political-administrative local level division*

3. Material and methods

3.1. Data (Landsat)

The Landsat satellite images were selected and downloaded from the server of the Earth Resources Observation and Science Center (EROS), United States Geological Survey (USGS); the search for available images included the study area and images that contained the least amount of interference (clouds and flaws) (https://earthexplorer.usgs.gov/). Two images were chosen: one image was for the year 1997, which was taken in August (Landsat 5), and the other image was for the year 2014, which was taken in July (Landsat 8) (Table 2). Since the years selected depended on the availability and quality of the satellite images, as well as avoiding interference by cloudiness, dry-season months were chosen for the study area.

Table 2. Characteristics of the Landsat images used in the supervised classification for the analysis period.

Date	**Time**	**Path/Row**	**Sensor**	**Spatial resolution of bands used (m)**
1997/8/21	14:50:36.921	009/057	LANDSAT 5	30
2014/7/19	15:18:48.190	009/057	LANDSAT 8	30

3.2. Methodological approach

The research aimed to analyse land cover transitions in the city of Pereira between 1997 and 2014 and answer the following questions: (i) How have land covers changed between 1997 and 2014 in Pereira? and (ii) What were the main changes in the CCL of the city of Pereira? The theorical approach was based on Rindfuss *et al.,* (2004), and we used remote sensing and addressed the CORINE land cover classification categories for Colombia. In this way, biophysical changes were evaluated at two points in time and the socio-economic analysis was framed in the statistics provided by the National Administrative Department of Statistics (DANE).

To this end, a supervised classification of the land cover in both periods was proposed; initially, Landsat satellite images were used to classify the cover based on the nomenclatures proposed by CORINE Land Cover and adapted for Colombia. Subsequently, processing of the information to calculate the net areas of each cover type for each year was carried out; then, the multitemporal analysis was performed to determine the rates of change for each cover type; and finally, change patterns analysis and accuracy assessment were performed to identify transitions by cover, which land cover have changed and to which classes (cross tabulation matrix) and where it was located (land cover transitions map). The proposed scheme homogenized the analysis categories for comparing the same territory in two different moments and thus interpret the primary cover information for Pereira.

3.3. Land cover classification

Land cover classification was performed using Landsat images, which have several spectral bands, and depending on their band combination, a colour was assigned to the image; each spectral band was associated with the specified ground cover. For the image with Landsat 8, RGB (red, green and blue) colour bands 5, 6 and 4 were used, while for the Landsat 5 image, RGB bands 4, 5 and 3 were used. For the supervised classification, training areas (ROIs, regions of interest) were selected that were the basis for classification. The ROI was selected based on information available in Google Earth images, Bing maps and from field work. A total of 15 characteristics were assigned to land cover: dense forest (DF), gallery and/or riparian forest (GRF), plantation forest (PF), bamboo forest (BF), stover (S), paramo (P), coffee crop (CC), permanent crop (PC), rotation crop (RC), heterogeneous agricultural area (HAA), pasture (Ps), glacier and perpetual snow (GS), bare rock (BR), water surface (WS) and urban fabric (UF).

The cover categories were based on CORINE Land Cover (CLC) adapted for Colombia. Four cover classes of the five CLCs were used for the first level: *i. Artificial Surfaces* are lands that comprise the areas of cities, towns and peripheral areas that are being incorporated into urban zones; *ii. Agricultural Areas* are mainly dedicated to the production of food, fibres and other industrial raw materials, including crops and pastures; *iii. Forests and semi-natural areas* comprise wooded, scrub and herbaceous vegetation cover with little or no anthropic intervention and also includes bare soils and rocky and sandy outcrops; and finally, *iv. Water surfaces,* which includes permanent, intermittent and seasonal bodies and canals (Table 3) (IDEAM *et al.,* 2008).

Table 3. Nomenclature of land cover units according to the CORINE Land Cover methodology adapted for Colombia.

CORINE Land Cover Colombia	
1. ARTIFICIAL SURFACES	**3. FOREST SAND SEMI-NATURAL AREAS**
1.1. Urban fabric	*3.1. Forest*
1.1.1. Continuous urban fabric	3.1.1. Dense natural forest
1.1.2. Discontinuous urban fabric	3.1.2. Fragmented natural forest
2. AGRICULTURAL AREAS	3.1.3. Gallery and/or riparian forest
2.1 Annual or rotation crops	3.1.4 Mangrove forest
2.1.1 Other annual or rotation crops	3.1.5 Plantation forest
2.2 Permanent crops	*3.2. Shrub and/or herbaceous vegetation associations*
2.2.1 Other permanent crops	3.2.1 Natural grasslands and savannas
2.2.2 Sugar cane	3.2.2 Shrubs and bushes
2.2.3 Panela cane sugar	3.2.3 Sclerophyllous and/or thorny vegetation
2.2.4 Banana and plantain	3.2.4 Paramo and subparamo vegetation
2.2.5 Coffee	3.2.5 Rupicolous vegetation
2.2.6 Cacao	*3.3. Open spaces with little or no vegetation*
2.2.7 Oil palm	3.3.1 Beaches, dunes, sands
2.2.8 Fruit trees and berry plantations	3.3.2 Bare rock
2.2.9 Greenhouse crops	3.3.3 Sparsely vegetated or degraded areas
2.3 Pasture	3.3.4 Burned areas
2.3.1 Clean pasture	3.3.5 Glaciers and perpetual snow
2.3.2 Wooded pasture	**5. WATER SURFACES**
2.3.3 Weedy or shrubby pasture	*5.1. Inland waters*
2.4 Heterogeneous agricultural areas	5.1.1 Rivers (50 m)
2.4.1 Crop mosaic	5.1.2 Natural lagoons, lakes and marshes
2.4.2 Pasture and crop mosaic	5.1.3 Canals
2.4.3 Crop, pasture and natural spaces mosaic	5.1.4 Reservoirs and water bodies
2.4.4 Pasture and natural spaces mosaic	

Source: IDEAM *et al.,* 2008. Magdalena-Cauca Basin Land Cover Map: CORINE Land Cover Methodology adapted for Colombia at a scale of 1:100,000. Institute of Hydrology, Meteorology and Environmental Studies, Agustín Codazzi Geographical Institute and Regional Autonomous Corporation of the Magdalena River. Bogotá, DC, 200p.

3.4. Information processing

Landsat satellite images were used as the basis for processing information, in which each spectral band was combined to define and calculate image attributes. After adjusting the image, the ENVI 4.8 programme was used to extract the features, which consisted of a supervised or rule-based classification of the covers assigned by the CORINE nomenclature (ENVI, 2008; IDEAM *et al.,* 2008). Next, each image was clipped with the Pereira shapefile, and the area information was extracted by cover type. Georeferencing the images (1997 and 2014) and map was carried out using the WGS84 reference system (World Geodetic System, 1984) and the UTM projection (Universal Transverse Mercator) zone 18 N for Colombia.

Subsequently, for manipulating, extracting and analysing the image information as shapefiles, the programme QGIS version 2.1.6 was used, which is an Open Source Geographic Information System (GIS), which enables working with various formats and functionalities of vector and raster data, also supporting different types of databases (Sanhouse-Garcia *et al.,* 2017; Santiago, 2014). In this study,

this tool was used for the treatment of vectors, georeferencing, improving information and the geographical presentation of land cover.

3.5. Multitemporal analysis

A comparison of previously classified images was performed independently; then, the areas for each type of land use were calculated with the ENVI programme. The requirement was to create the same thematic legend for the two moments so that they were comparable. The analysis had two parts: determining the total change by use with the net exchange (gain or loss) and the annual rate of change, which was estimated according to the equation proposed by (Puyravaud, 2003). This rate (r) was calculated as follows:

$$r = (1/(t_2 - t_1)) \times \ln(A_2/A_1)$$

where $(t_2 - t_1)$: study period; A_1: land area at the beginning of the period; A_2: land area at the end of the period

Subsequently, a table was generated with the annual rate of change for the 1997-2014 study period, showing the transitions that occurred, which allowed for determination of the uses with the greatest gain or loss (net change) for the municipality of Pereira and the proportion by use of the annual change.

3.6. Change patterns analysis and accuracy assessment

Change patterns analysis and accuracy assessment were performed to identify transitions by cover, which land cover have changed and to which classes. A cross-tabulation matrix was constructed that allowed observing the transitions of the different classes evaluated, detecting changes and making an analysis of the real patterns that these changes entail (Rojas-Briceño *et al,* 2019). The matrix contains a vertical and horizontal axis with the classes for each moment in time (1997-2014). The data on the main diagonal represent the area of each cover without change during the time evaluated; those areas outside the diagonal show the changes between the two dates for each of the covers. The matrix was read by interpreting the columns as the increase in areas in hectares and the rows as the decrease in areas in hectares.

To identify where the principal transitions were located we made a map showing land cover transition. We used the cross-tabulation matrix and identified the changes of each cover and towards which class; for the map we selected the changes that were greater than 200 ha, allowing the spatial location of the changes.

The accuracy of the classification output was assessed by generating a confusion matrix with the ENVI programme. To generate the confusion matrix, the 34,666-validation pixel (observed class) were overlayed on the final classified image and the observed class points compared to the coinciding classified pixel (Ashiagbor *et al.,* 2020). Kappa coefficient of agreement and overall accuracies were calculated from the confusion matrix.

4. Results

4.1. Net change in land covers for 1997 and 2014 in Pereira, CORINE Levels 1, 2 and 3

The level 1 cover analysis showed an overview that the agricultural areas for 1997 and 2014 were the dominant cover, with 60.7% and 59.4%, respectively, followed by forests and semi-natural areas (34.3% and 31.9%); artificial surfaces had corresponding areas of 3.7% for 1997 and 7.6% for

2014 of the total area of Pereira; finally, water surfaces were evident in 1.2% of the total area for both years (Table 4 and Fig. 2).

Table 4. Classification of cover area for CORINE Level 1.

COVER	Year 1997		Year 2014	
	Area (ha)	Area (%)	Area (ha)	Area (%)
Agricultural areas	36,876.33	60.7 %	36,045.72	59.4 %
Forests and semi-natural areas	20,847.87	34.3 %	19,356.03	31.9 %
Artificial surfaces	2,276.73	3.7 %	4,599.45	7.6 %
Water surfaces	715.32	1.2 %	715.05	1.2 %
Total surface	60,716.25	100 %	60,716.25	100 %

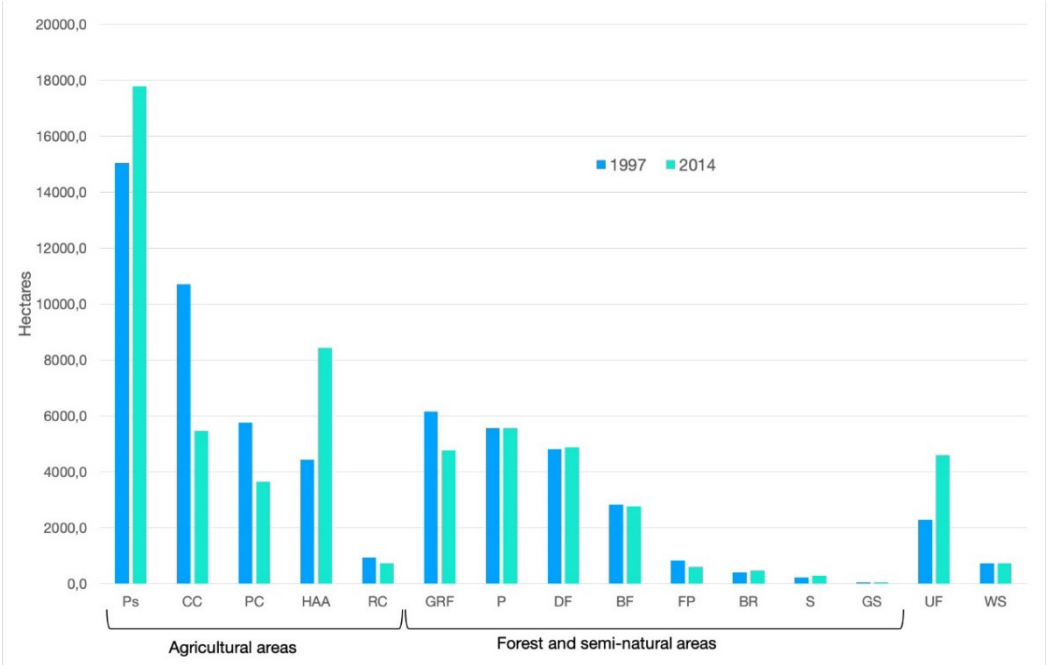

Figure 2. Net cover in hectares for the years 1997 and 2014 in the municipality of Pereira.

The natural and semi-natural surfaces for Pereira in 1997 were mainly distributed as follows: Gallery and riparian forest (GRF) encompassed 6,145.7 ha (10.12%) with patches distributed throughout the municipality; paramo (P) encompassed 5,573.6 ha (9.2%) belonging to the Los Nevados National Natural Park (NNP) (high elevation zone and east of the municipality); dense forest (DF) encompassed 4,804.6 ha (7.9%) of the territory and was mainly located in the upper area of the Otún River basin and east of the city of Pereira; and bamboo forest (BF) encompassed 2,824.9 ha (4.6%). To a lesser extent the following land covers were also present: water surfaces (WS), associated with natural lagoons, lakes and surface water courses; bare rock (BR), mainly in the high elevation area of the Los Nevados NNP east of the municipality; stover (S), near the urban area; and finally, glaciers and perpetual snow (GS) (Fig. 2 and 3).

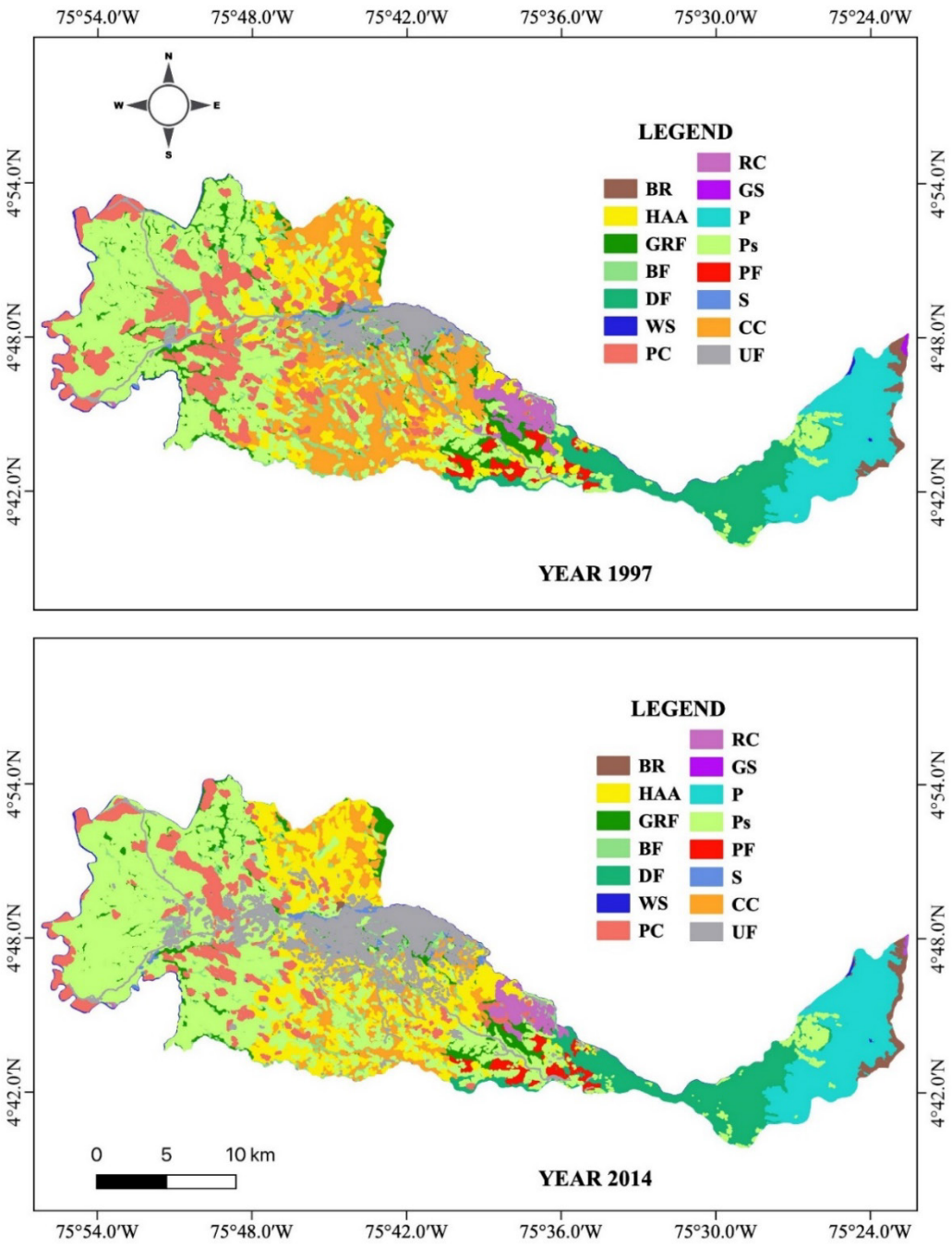

Figure 3. Land cover of the municipality of Pereira for the years 1997 and 2014.

The area dedicated to agricultural land in 1997 in Pereira is described as follows from largest to smallest cover area: (9) Pasture (Ps) comprised the largest use in the municipality, with 15,047 ha (24.8% of the total area) and was mainly found west of the municipality and in the lowest altitude areas; (*10*) heterogeneous agricultural areas (HAA) comprised 4,438.9 ha (7.3%); (*11*) CC comprised 10,706 ha (17.6%), and both cover classes (10 and 11) were observed mainly in the centre of the municipality from north to south; (*12*) permanent crops (PC) comprised 5,747 ha (9.5%) and were mostly concentrated in the west in the low elevation zone; (*13*) rotation crops (RC) covered 937 ha (1.5%); (*14*) FP covered 821.1 ha (1.3%) and were located mainly east of the urban fabric; and finally, (*15*) continuous and discontinuous urban fabric (UF) comprised 2,276 ha (3.7%) of the total surface of Pereira (Fig. 2 and 3).

For 2014, the natural and semi-natural territory for Pereira was distributed as follows: paramo (P) comprised 5,558.7 ha (9.2%) of land cover and belonged to the Los Nevados NNP (high elevation and east of the municipality); dense forest (DF) comprised 4,877.6 ha (8%) of the territory and was found mainly towards the east of the municipality; the cover for gallery and riparian forest (GRF) was 4,757.7 ha (7.8%) with patches distributed throughout the territory of the municipality; bamboo forest (BF) comprised 2,765 ha (4.5%); and finally, water surfaces (WS), bare rock (BR), stover (S) and glaciers and perpetual snow (GS) comprised the smallest areas in terms of cover (Fig. 2 and 3).

The net areas of the agricultural lands in Pereira for the year 2014 were identified and the following characteristics were determined: (*9*) pasture (Ps) continued to be the largest land cover in the municipality with 17,788 ha (29.3% of the total area) and was mainly concentrated in the western zone of the municipality; (*10*) heterogeneous agricultural area (HAA) increased to 8,433 ha (13.9%); (*11*) CC comprised 5,454 ha (9%), occurring in the central zone between the north and south of the municipality; (*12*) permanent crop (PC) covered 3,647 ha (6%) with patches distributed towards the lower elevation zone west of Pereira; (*13*) rotation crop (RC) comprised 722.8 ha (1.2%); (*14*) FP covered 603.6 ha (1%) and was concentrated in the middle basin of the Otún River towards the area east of the municipality; and finally, (*15*) continuous and discontinuous urban fabric (UF) comprised 4,599 ha (7.6%) of the total surface of Pereira (Fig. 2 and 3).

4.2. Changes in land cover for the 1997-2014 period (annual rate of change)

The covers in CORINE Level 1 showed the following changes: three of the four covers presented annual decreases in area, with forest and semi-natural areas having the greatest change (-0.38%), followed by agricultural areas (-0.16%) and to a lesser extent water surfaces (-0.002); artificial surfaces showed an annual growth of 4.14% (Table 5).

Table 5. Annual rate of change in cover classes between 1997-2014 in Pereira.

COVER	Period		Net change	Year	Rate of change (r)	Rate (%)
	1997 Area (ha)	2014 Area (ha)				
Agricultural areas	36,876.33	36,045.72	-830.61	17	-0.00134	-0.1340
Forests and semi-natural areas	20,847.87	19,356.03	-1,491.84	17	-0.00437	-0.4367
Artificial surfaces	2,276.73	4,599.45	2,322.72	17	0.04136	4.1365
Water surfaces	715.32	715.05	-0.27	17	-0.00002	-0.0022

The annual rates of change between 1997 and 2014 showed losses and gains among the land covers analysed. The cover that lost the most territory was CC, with a negative rate per year of -3.97%, followed by permanent crop (PC) (-2.67%), PF (-1.81%), rotation crop (RC) (-1.53%), gallery and riparian forest (GRF) (-1.51%), glacier and perpetual snow (GS) (-1.34%) and to a lesser extent, bamboo forest (BF), paramo (P) and water surface (WS) also decreased (Table 6).

The covers that gained surface area included the continuous and discontinuous urban fabric (UF), with the highest annual change rate of 4.14%, which was followed by heterogeneous agricultural areas (HAA) (3.77%), stover (S) (1.61%), pasture (Ps) (0.98%), bare rock (BR) (0.77%) and dense forest (DF) (0.09%) (Table 6).

Table 6. Annual rate of change in land cover classes between 1997 and 2014 in Pereira.

Use	Period				Net change	Year	Rate of change (r)	Rate (%)
	1997 Area (ha)	1997 (%)	2014 Area (ha)	2014 (%)				
WS	715.32	1.18	715.05	1.18	-0.27	17	-0.0000	-0.002
DF	4,804.56	7.91	4,877.64	8.03	73.08	17	0.0009	0.089
GRF	6,145.74	10.12	4,757.67	7.84	-1,388.07	17	-0.0151	-1.506
PF	821.07	1.35	603.63	0.99	-217.44	17	-0.0181	-1.810
CC	10,706.04	17.63	5,454.63	8.98	-5,251.41	17	-0.0397	-3.967
BF	2,824.92	4.65	2,765.34	4.55	-59.58	17	-0.0013	-0.125
HAA	4,438.89	7.31	8,433.27	13.89	3,994.38	17	0.0378	3.775
GS	51.93	0.09	41.31	0.07	-10.62	17	-0.0135	-1.346
P	5,573.61	9.18	5,558.67	9.16	-14.94	17	-0.0002	-0.016
Ps	15,047.28	24.78	17,788.05	29.30	2,740.77	17	0.0098	0.984
PC	5,747.13	9.47	3,646.98	6.01	-2,100.15	17	-0.0268	-2.675
S	220.05	0.36	289.17	0.48	69.12	17	0.0161	1.607
BR	405.99	0.67	462.60	0.76	56.61	17	0.0077	0.768
RC	936.99	1.54	722.79	1.19	-214.20	17	-0.0153	-1.527
UF	2,276.73	3.75	4,599.45	7.58	2,322.72	17	0.0414	4.136

4.3. *Change patterns analysis and accuracy assessment*

The net changes and annual rates of change for each cover generally show growth or decrease in their surface areas and the trends of change for the period studied; by going deeper into the patterns of change it is possible to show which covers are gaining areas and at whose expense. It was found that the greatest changes were observed in the western zone of Pereira and between the north and the south, close to the urban area (Fig. 4). For the 1997 classification it was estimated that an overall accuracy of 96.1% and a Kappa coefficient of 0.96; while for 2014, the following were evaluated an overall accuracy of 84.1% and Kappa coefficient equal to 0.81 (Table 7).

In land cover change matrix was found that the pasture (Ps) was the cover that more surface obtained, the acquired territory was transferred mainly from permanent crops (PC) (2,405.5 ha), coffee crops (CC) (1,173.3 ha) and gallery and riparian forest (GRF) (850.1 ha). The urban fabric (UF) was the cover with the highest rate of positive change and acquired this area mainly from CC (836.5 ha), Ps (509.9 ha), heterogeneous agricultural areas (HAA) (365.9 ha), PC (282.9 ha) and, to a lesser extent, GRF (189.1 ha) and bamboo forest (BF) (106.1 ha). The HAA obtained territory essentially from coffee crops (3,641.3 ha) and pasture (1,039.9 ha) (Table 7 and Fig. 4).

Drastic changes were evident in the covers that decreased the most in their surface areas, such as coffee crops and permanent crops (Fig. 4); both gave way to HAA (3,641.3 ha and 315.5 ha respectively) and pasture (1,173.3 and 2,405.5 ha). In order to, the forest and semi-natural areas were moved where the movement of the agricultural frontier was evident; the areas with dense forest (DF), galery and riparian forest (GRF) and bamboo forest (BF) were affected by the increase in covers such as coffee crops, HAA, permanent crops, transitory crops and pastures (Table 7).

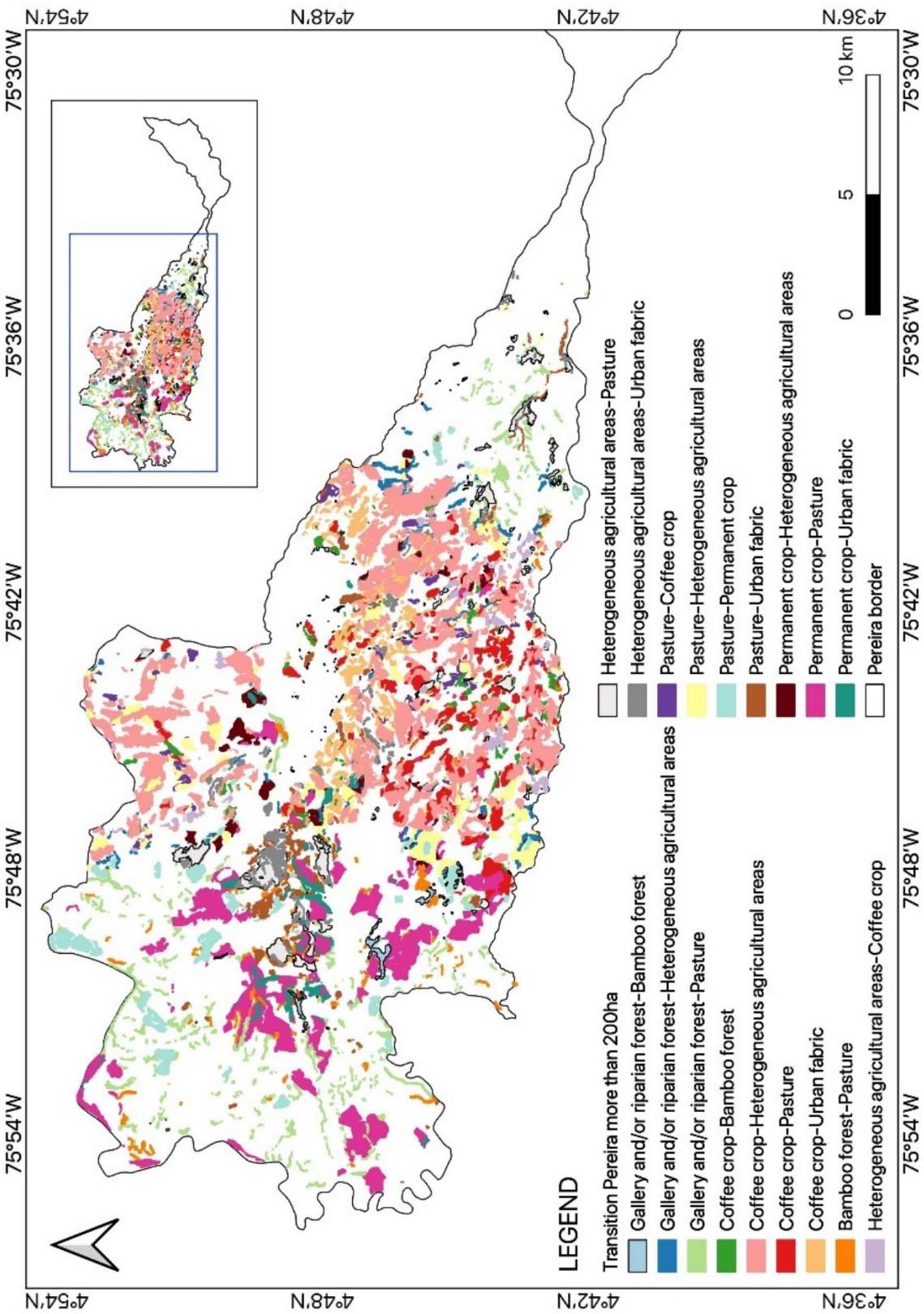

Figure 4. Land cover transitions in Pereira between 1997-2014.

		Year 2014 (Overall Accuracy: 84.1%; Kappa coefficient: 0.81)																
Year 1997 (Overall Accuracy: 96.1%; Kappa Coefficient: 0.96)		WS	DF	GRF	PF	CC	BF	HAA	GS	P	Ps	PC	S	BR	RC	UF	T97	%
	WS	**690.9**	0.9	1.3			0.8			10.1	2.7	6.3		2.3		0.1	715.3	1.2
	DF		**4,560.4**	4.3	69.4	5.0	0.9	32.6		19.5	102.0	1.4			4.0	5.1	4,804.6	7.9
	GRF	1.1	6.0	**4,122.2**	92.3	178.4	208.4	263.4			850.1	148.5	44.9	0.5	40.1	189.8	6,145.7	10.1
	PF		106.6	150.7	**349.8**	22.6	1.9	14.9			167.1	3.7			0.5	3.3	821.1	1.4
	CC	0.1		82.4	0.1	**4,483.9**	238.3	3,641.3			1,173.3	162.3	83.4	4.2	0.1	836.6	10,706.0	17.6
	BF		2.1	29.3	1.4	101.0	**2,134.4**	126.8			283.1	24.5	8.1		8.2	106.1	2,824.9	4.7
	HAA	0.1	26.7	136.4	59.7	219.0	15.4	**2,876.9**			687.3	51.4		0.2		365.9	4,438.9	7.3
	GS								**41.3**					10.6			51.9	0.1
	P	3.9	14.4							**5,434.9**	9.3			111.2			5,573.6	9.2
	Ps	12.9	159.1	133.7	29.0	278.7	47.6	1,039.9		20.0	**12,000.5**	728.5	19.7		67.9	509.9	15,047.3	24.8
	PC	6.1		43.5		111.4	95.5	315.5			2,405.5	**2,483.2**	0.8	2.2	0.6	282.9	5,747.1	9.5
	S			5.1			2.1				10.4		**131.8**			70.7	220.1	0.4
	BR									74.2			0.4	**331.5**			406.0	0.7
	RC		0.1	40.4	0.7	52.2	16.1	99.7			64.2	34.6			**600.7**	28.4	937.0	1.5
	UF		1.4	8.5	1.3	2.4	4.0	22.4			32.6	2.8	0.1		0.8	**2,200.6**	2,276.7	3.7
	T14	715.1	4,877.6	4,757.7	603.6	5,454.6	2,765.3	8,433.3	41.3	5,558.7	17,788.1	3,647.0	289.2	462.6	722.8	4,599.5	**60,716.3**	
	%	1.2	8.0	7.8	1.0	9.0	4.6	13.9	0.1	9.2	29.3	6.0	0.5	0.8	1.2	7.6		

Table 7. Land cover change matrix in Pereira between 1997-2014 (area in hectares).

5. Discussion

The study and analysis of land cover change and spatial patterns requires an interdisciplinary science that involves i.) biophysical aspects through remote sensing and ii.) the human aspect as the decision makers who can determine the change in the territory (Rindfuss *et al.,* 2004; Turner II *et al.,* 2007). Some international, national and regional politics was crucial in land cover changes in Pereira for the analysis period, in addition, the practices and cultural heritage have preserved some covers, demonstrating the change dynamics in the territory.

5.1. Analysis of land cover change in Pereira for the 1997-2014 period

The struggles for territory in present-day Pereira during the colonial period refer to conflicts over territorial power between groups of Spaniards, creole heirs and indigenous American peasantry (Quimbaya peasantry). Between 1850 and 1950, Pereira began to grow due to the high levels of poverty and exclusion of the landless peasant population of Caldas, Antioquia and northern Valle (Palacios, 1979; Rivera, 2014). The violence and displacement of the population in the allocation of land tenure to new landowners triggered the growth of new smallholder populations in the central-western area of the country.

The highest slopes are in the eastern area of Pereira (Fig. 1), and in this territory, there is the National Natural Parks of Colombia with the Los Nevados NNP, which contributes to the conservation of important ecosystems worldwide, such as three of the remaining glaciers in the country (Nevado del Ruíz, Nevado de Santa Isabel and Nevado del Tolima), Super-Paramo and Paramo ecosystems, High Andean Wetlands and High Andean Forests and Andean Forests (PNN, 2020). The covers identified in this area of the municipality show the specialized management of this territory by the system of protected areas (SINAP: Sistema Nacional de Áreas Protegidas -SIDAP: Sistema Departamental de Áreas Protegidas). These covers maintain their net areas, and the changes seen could be related to the climate changes in which the changes in snow (GS) surface lead to decreases and increases in bare rock (BR).

The forests in Latin America have been reduced by more than 50% of the original cover in 2000; countries such as Brazil, Mexico and Costa Rica showed the most significant changes (Sanhouse-Garcia *et al.,* 2017). In Colombia, loss of forest between 1990 and 2014 was 6,095,312 ha with a rate of change of -0.41 ha for that period (Galindo *et al.,* 2014); in contrast, for the municipality of Pereira, the dense forest (DF) occurring in the upper middle zone of the Otún River basin and the paramo (P) were maintained for the study period (1997-2014). These measures taken by national institutions and regional companies have allowed for conservation and management in the protection of these forest covers and semi-natural areas.

Contrary to what occurred with the dense forest (DF), gallery and riparian forests (GRF) showed decreased surface areas during the course of the study (81.65 ha/year), since this type of cover is scattered over the territory of Pereira. It is believed that these forests have mainly been converted to pasture (Ps), expanding the agricultural frontier and maintaining animal access to the protected water in these areas. Something similar occurred in the mountainous area of Spain between 1990 and 2006, where the area occupied by forest became pasture and bush due to deforestation and fires (Martínez-Vega *et al.,* 2017).

The agricultural territory comprises the largest surface area for 1997 and 2014 (62.1% and 60.4%, respectively), but there is evidence of a change in the land cover type. For 1997, CC encompassed 10,706 ha, corresponding to 17.6% of the agricultural area of Pereira, while for 2014, this cover was 5,454 ha (9%); meanwhile, the heterogeneous agricultural area (HAA) increased in the analysis period from 4,438.9 ha (7.3%) to 8,433 ha (13.9%) (Fig. 2 and 3). This change could be explained by the coffee crisis experienced in Colombia in the 1990s; however, the beginning of this cultivation in the region dates back to the beginning of the 20th century, in which coffee began to emerge

as a prosperous business in Antioquia and the landless peasants who arrived in Pereira arrived with the idea of colonizing land for this crop (Rivera, 2014). From 1930 to 1980, an economic boom occurred in Colombia due to the cultivation of coffee, which became the most significant product for the economic and social development of the country in the 20th century and it was supported by the National Federation of Coffee Growers (Toro Zuluaga, 2005; Rettberg, 2010). This period of prosperity was cut short in 1989, when the International Coffee Agreement for the members of the International Coffee Organization (ICO) ended. The suspension of export quotas and the decrease in the international price of coffee led coffee growers to generate new strategies to boost agricultural production on farms, diminishing the size of coffee growing areas, which were replaced with other types of crops.

Prior to 1997, coffee production intensification occurred, guided by the demand of the international market and institutions, such as the National Federation of Coffee Growers of Colombia. Coffee growing in Colombia was and continues to be mainly a smallholder farmer activity, and peasant families have influenced the reproduction and geographical spread of coffee (Palacios, 1979; Guhl, 2004; Toro Zuluaga, 2005; Barón, 2010). Agricultural families in the region converted subsistence crops into coffee production (Guhl, 2008). Coffee cultivation had an impact on the societies and landscape of Pereira and coffee plantations (Toro Zuluaga, 2005). However, with the collapse of the agreement in 1989, there was a slowdown in the demand for this product, thus, in 1997, the Federation generated policies aimed at reducing the areas intended for coffee cultivation, which initially resulted in changes in land cover. Smallholder farmers consolidated local power structures, which allowed for a faster response in adjusting the demands for agricultural products, and quick landscape changes.

The continuous and discontinuous urban fabric (UF) showed the highest growth in the area and study period from 2,276 ha (3.7%) in 1997 to 4,599 ha (7.6%) in 2014, doubling the occupied surface with an annual growth rate of 4.1%. This information is close to that found by (Carvajal, 2017) in the La Vieja River basin for the analysis period of 1989-2000, where he identified an annual growth of 4.7%. This growth is linked to the pressure exerted on other land uses, generating change in the ecosystems. These changes are associated with growth of the urban population (urbanization), expansion of the built area (urban growth) and low-density dispersed urban development in the urban-rural perimeter (urban sprawl) (Nelson, 2005). These processes are observed in the maps of cover transitions in the city of Pereira, mainly the discontinuous growth in the 2014 map compared with the 1997map, showing the pressure on CC and gallery and riparian forest (GRF).

The urban-rural relationship in China has experienced a process from binary opposition and segmentation to overall planning and integration (Chen *et al.,* 2020). Therefore, promoting sustainable development in the territory requires consideration of the relationships among urban-rural areas to augment agricultural cover and forests and semi-natural areas, promote stewardship of nature and improve social aspects, such as employment and food security. The growth of urbanized territory should be integrated with other land covers through planning, government incentives and academic knowledge.

5.2. Annual rate of change

The lost area that corresponded to agricultural territory and forest and semi-natural areas represented 136 ha per year, which was translated to artificial areas. Forest cover (dense forest, gallery forest, bamboo, stover and paramo) of Pereira for 1997 (32.2%) and for 2014 (30.1%) was lower with respect to the departmental average (37%) and the national average (51.6%) (IDEAM, 2017). This finding indicated the strong pressure exerted by the population, urban growth and agricultural uses over time. According to (Chen *et al.,* 2020), it is necessary to consider the potential, capacity and requirements of rural development, which will improve the social function of rural territories, such as employment, food and agricultural goods supply, and the promotion of biodiversity.

In this study, pasture (clean, weedy, and wooded pasture) was the largest cover area for both 1997 and 2014 (with 24.8% and 29.3% of the total area for both years) and gained 0.98% per year

(161.22 ha per year); however, when comparing the area reached in 2014 (17,788 ha) with the area estimated by the Secretariat of Agricultural Development of Risaralda (2015), which states 22,490 ha for the same year, there are 4,702 ha unaccounted for. Therefore, it is likely that in the heterogeneous agricultural area (HAA), some pasture areas are hidden; these pastures are mixed with other uses that make their detection difficult from satellite images. Likewise, the fragmentation of some surfaces is evident, where mixed covers occur. Similar results were found by Ellis *et al.* (2010) in a marginal coffee growing region of Mexico, where annual rate of change for pasture was positive and the vast majority of land reported previous land cover for coffee production.

Heterogeneous agricultural areas (HAA) with an annual growth rate of 3.77% are the result of fragmentation and different management practices; the spatial and temporal configuration of this mosaic is the consequence of diverse coexisting agricultural uses and of activities, such as industry and tourism (Guhl, 2008). This finding shows that the area of CC for the year 1997 was converted into farms by 2014 with various types of crops and subsequently urbanized.

5.3. Dynamics of coffee production and export and changes in land cover

CC lost the most surface area in the municipality of Pereira in the study period, with an annual loss rate of -3.97%. The coffee axis was one of leading coffee exporters in the twentieth century and with the crisis of 1989, there was a change in land cover in the region. However, the metric tons of coffee produced for export between 1992 and 2018 show no major changes, producing an average of 605 thousand tons per year. However, the country's share of coffee in global exports declined; 19.6% in total exports in 1997, and 4.5% in 2014 (Fig. 5). A different behaviour was found by Ambinakudige and Choi (2009) in India, where conversion of rice paddies (the land for subsistence farming) to coffee was a result of increased coffee prices in the early 1990s, immediately after the Indian Coffee Board's control of the coffee market was removed. By the end of the 1990s, most of the land allotted by the government for coffee cultivation had already been converted to that crop.

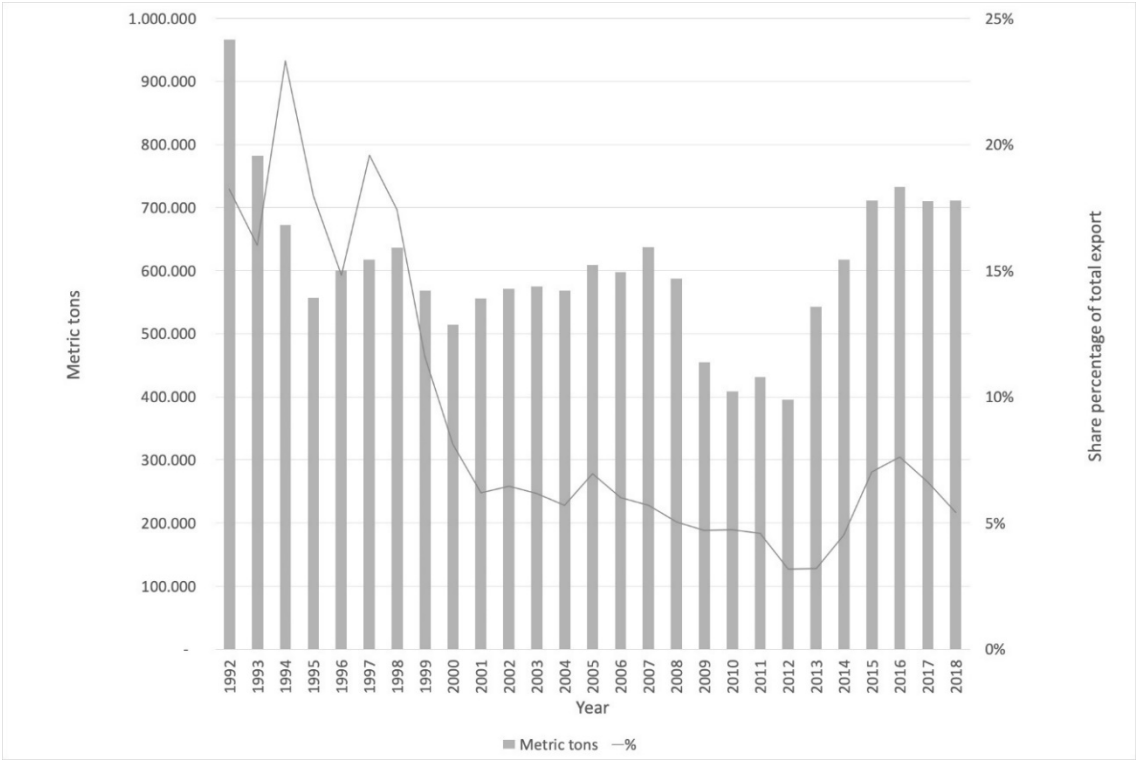

Figure 5. Coffee exports by share percentages and metric tons between 1992 and 2018.

With the collapse of the International Coffee Agreement in 1989, there was an international decrease in the price of this product, which generated a progressive decrease in cultivated area. CC between 1997 and 2014 showed an annual decrease rate of -3.97% in Pereira, while this decrease generated a change in the landscape and although the region is still culturally known as the coffee axis and remains on the UNESCO's World Heritage list as a Coffee Cultural Landscape - CCL, there has been a profound loss of that type of land cover (Table 7 and Fig. 4). Although some farmers abandoned this type of cultivation and sold farms, others reduced the area used for CCs but remained through time and through constant price crises. According to Guhl (2008), those persistent producers revitalize the surface of their farms, changing from pasture to coffee and from coffee to pasture or mixing with other types of agricultural products, which has allowed them to maintain themselves. Farmers have styles or forms of agriculture that are firmly rooted in a stock of cultural knowledge (Van der Ploeg and Ventura, 2014). Those styles comprise ways of organizing and reorganizing the internal and external requirements of the farms, which allow farmers to remain in the territory, as well as contributing to the heterogeneity of the agricultural systems in the cultural coffee landscape of Colombia.

The land cover has changed in the last 17 years for the study area, due mainly to the coffee crisis, that was particularly hard on the small Colombian coffee producers, who were less able to adapt to the new circumstances because of financial constraints: Prices paid to producers decreased by a third (32.6 percent) between January 1985 and December 2004 (Rettberg, 2010). Traditional and modernized CCs were eradicated to plant plantains, avocado, citrus and grass, mainly African grasses, to produce meat and milk (Carvajal *et al.,* 2013). These changes, in addition to mismanagement of the territory by government entities, have introduced problems, such as the displacement of the rural population, decreased food supply for both urban and rural populations, and problems of pollution and erosion of natural resources. Likewise, when the costs of production or the cost of being there are very high, the production of marketable goods that are generated in that territory to cover the costs is not enough, leading to possible changes in both the use of the territory and the type of owners who can acquire the land and use it under other conditions.

Although the decrease in the area dedicated to coffee cultivation in the municipality of Pereira is evident, there are regions in Colombia where this crop has become important and other zones of the coffee axis still maintain coffee productivity. The dynamics of the territory, the changes in the landscape and the production of agricultural goods are dynamized by geographic conditions, the quality of production and disease control, the price of products in the market, the type of productive systems, the land market and other variables not considered in this study.

These multitemporal analyses of land cover change demonstrate spatial arrangements and aid in understanding the dynamism of socioecological systems such as the CCL and how human processes guide such changes in the land. The importance of this type of work is to understand the transitions in land cover because they are a mirror reflecting the stage of socio-economic development (Chen *et al.,* 2020). In consequence it is going to help make better decisions for resources management and access to these resources, in addition to supporting and preserving rural communities and cultural practices that promote the security of society (food supply, job generation in rural areas and promotion of natural environments).

The interesting and dynamic nature of the dual human-environment system that creates changes in the landscape is one of the challenges presented by this type of multi-temporal analysis. Nevertheless, observation and monitoring with emphasis on the local and regional generates a detailed classification of the land for the evaluation of changes directed at specific problems. These studies detail biophysical changes and are an important source of primary information for planning. This research highlights the territories and covers that have undergone the greatest change, suggesting that local authorities should take up this work in their planning to recognize the zones that need to be intervened; that is, if the CCL is to be preserved, the zones that have changed towards coffee cultivation should be highlighted and promoted, and those zones that have lost area to other types of land covers should be intervened in.

6. Conclusions

Agricultural areas were dominant in Coffee Cultural Landscapes of Pereira and they were the land covers that changed the most in the 1997-2014 period. The land cover that lost the most territory was coffee crop, with a negative rate per year of -3.97%, mainly due to political-economic factors, such as the dissolution of the International Coffee Agreement and the National Federation of Coffee Growers that discouraged coffee cultivation and permanent crops. Likewise, sociocultural factors, such as smallholder farmers have guided the changes in land cover and have stimulated productive styles to adapt and remain, increasing heterogeneous agricultural areas.

Forest and semi-natural areas were replaced where the movement of the agricultural frontier was evident and they were affected by increase in land covers such as coffee crops, heterogeneous agricultural areas, permanent crops, transitory crops and pastures. The last transformed 850 ha of galery and riparian forest, 283 ha of bamboo forest and 102 ha of dense forest.

Livestock activities changed representative areas of Coffee Cultural Landscapes of Pereira between 1997 and 2014, consequently, pasture was the land cover that more area obtained, and the acquired territory was transferred mainly from permanent crops (2,405.5 ha), coffee crops (1,173.3 ha) and gallery and riparian forest (850.1 ha).

Related to rural-urban changes it was found that continuous and discontinuous urban fabric was the land cover with the highest positive annual change rate (4.14%), showing a growth from 2,276 ha in 1997 to 4,599 ha in 2014. These changes are associated with growth of the urban population (urbanization), expansion of the built area (urban growth) and low-density dispersed urban development in the urban-rural perimeter (urban sprawl), due to city-level planning policies that promoted rural parcelling for the expansion of artificial surfaces.

Acknowledgements

This publication is part of the doctoral thesis in Environmental Sciences of the first author in the Graduate Programme of the Faculty of Environmental Sciences of the Technological University of Pereira. The doctoral thesis was supported by the internal convocation of the Vice-Rectory of Research of the Technological University of Pereira, Colombia (E2-18-2). The first author had a forgivable loan scholarship from COLCIENCIA-COLFUTURO for her doctoral studies (647), Colombia. Likewise, the translation of this document was supported by the graduate school of the Faculty of Environmental Sciences. Finally, the authors appreciate the participation and support provided by the research group Management in Tropical Andean Agroecosystems (GATA) and the research seedbed Socioecological Landscape Planning.

References

Ambinakudige, S., Choi, J. 2009. Global coffee market influence on land-use and land-cover change in the Western Ghats Of India. *Land Degrad. Dev.* 20, 327-335. https://doi.org/10.1002/ldr.921

Ashiagbor, G., Forkuo, E.K., Asante, W.A., Acheampong, E., Quaye-Ballard, J.A., Boamah, P., Mohammed, Y., Foli, E. 2020. Pixel-based and object-oriented approaches in segregating cocoa from forest in the Juabeso-Bia landscape of Ghana. *Remote Sensing Applications: Society and Environment* 19, 100349. https://doi.org/10.1016/j.rsase.2020.100349

Barón, J.D. 2010. Geografía, café y prosperidad en los Andes Occidentales de Colombia. *Revista de Economía Del Rosario* 13, 117–190.

Botero-Arango, A.J., Feijoo-Martínez, A., Molina-Rico, L.J., Quintero Vargas, H. 2020. Mapeo y caracterización de servicios ecosistémicos en fincas cultivadas con plátano, Quindío, Colombia. *Scientia et Technica 25*, 584–594. https://doi.org/https://doi.org/10.22517/23447214.22731

Boudet, F., MacDonald, G.K., Robinson, B.E., Samberg, L.H. 2020. Rural-urban connectivity and agricultural land management across the Global South. *Global Environmental Change* 60, 101982. https://doi.org/10.1016/j.gloenvcha.2019.101982

Carvajal, A.F., Feijoo, A., Quintero, H., Rondón, M.A. 2009. Soil organic carbon in different land uses of colombian andean landscapes. *Revista de La Ciencia Del Suelo y Nutrición Vegetal* 9 (3), 222–235.

Carvajal, A.F., Feijoo, A., Quintero, H., Rondón, M.A. 2013. Soil organic carbon storage and dynamics after C3-C4 and C4-C3 vegetation changes in sub-Andean landscapes of Colombia. *Chilean Journal of Agricultural Research* 73 (4), 391–398. https://doi.org/10.4067/S0718-58392013000400010

Carvajal, A.F. 2017. *Impactos del cambio en las coberturas de la superficie terrestre, sobre el almacenamiento de carbono y la regulación climática en la cuenca del río La Vieja, Colombia*. Universidad Nacional de Colombia.

Chen, K., Long, H., Liao, L., Tu, S., Li, T. 2020. Land use transitions and urban-rural integrated development: Theoretical framework and China's evidence. *Land Use Policy* 92, 104465. https://doi.org/10.1016/j.landusepol.2020.104465

DANE (Departamento Administrativo Nacional de Estadística), 1970. *Censo nacional agropecuario.https://www.dane.gov.co/files/investigaciones/agropecuario/CNA_1970/CALDAS_QUINDIO_RISARALDA.PDF*

DANE (Departamento Administrativo Nacional de Estadística), 2016. *Tercer Censo Nacional Agropecuario*. https://www.dane.gov.co/files/images/foros/foro-de-entre-ga-de-resultados-y-cierre-3-censo-nacional-agropecuario/CNATomo2-Resultados.pdf

DANE (Departamento Administrativo Nacional de Estadística), 2019. *Resultados Censo Nacional de Población y Vivienda 2018*. Pereira, Risaralda, 27.

D'Amour, C.B., Reitsma, F., Baiocchi, G., Barthel, S., Güneralp, B., Erb, K H., Haberl, Creutzig, F., Seto, K.C. 2017. Future urban land expansion and implications for global croplands. *Proceedings of the National Academy of Sciences of the United States of America* 114 (34), 8939–8944. https://doi.org/10.1073/pnas.1606036114

Ellis, E.A., Baerenklau, K.A., Marcos-Martínez, R., Chavez, E. 2010. Land use/land cover change dynamics and drivers in a low-grade marginal coffee growing region of Veracruz, Mexico. *Agroforest Syst* 80, 61–84. https://doi.org/10.1007/s10457-010-9339-2

ENVI, 2008. ENVI feature extraction module user's guide. *Computing*, 78.

Fernández Retamoso, M.P., Rincón Jaime, C., Isaza Londoño, J.L., Nieto González, C.E., CRECE (Centro de Estudios Regionales Cafeteros y Empresariales), 2010. *Coffee Cultural Landscape. An exceptional fusion of nature, collective human effort and culture*. C. y Estrategias, Ed., Bogotá, Colombia.

Galindo, G., Espejo, O.J., Ramírez, J.P., Forero, C., Valbuena, C.A., Rubiano, J.C., Lozano, R.H., Vargas, K.M., Palacios, A., Palacios, S., Franco, C.A., Granados, E.I., Vergara, L.K., Cabrera, E. 2014. *Memoria técnica de la cuantificación de la superficie de bosque natural y deforestación a nivel nacional. Actualización periodo 2012-2013.* Instituto de Hidrología, Meteorología y Estudios Ambientales, Bogotá D.C., Colombia.

Guhl, A. 2004. Café y cambio de paisaje en la zona cafetera colombiana entre 1970 y 1997. *Cenicafé* 55 (1), 29–44. http://biblioteca.cenicafe.org/handle/10778/102

Guhl, A. 2008. Café y cambio de paisaje en Colombia, 1970- 2005. *Fondo Editorial Universidad EAFIT - Banco de La República.*

IDEAM (Instituto de Hidrología, Meteorología y Estudios Ambientales), 2014. *Sistema de Información Hidrológica y Meteorológica -SISDHIM*. http://www.ideam.gov.co/web/tiempo-y-clima/seguimiento-tiempo

IDEAM (Instituto de Hidrología, Meteorología y Estudios Ambientales), 2017. *Proyecto Sistema de Monitoreo de Bosques y Carbono (SMBYC)*. http://www.ideam.gov.co/web/ecosistemas/bosques-recurso-forestal

IDEAM (Instituto de Hidrología, Meteorología y Estudios Ambientales), IGAG (Instituto Geográfico Agustín Codazzi), CORMAGDALENA (Corporación Autónoma Regional del Río Grande del Magdalena), 2008. *Mapa de Cobertura de la Tierra Cuenca Magdalena-Cauca: Metodología CORINE Land Cover adaptada para Colombia a escala 1:100.000.*

INCODER (Instituto Colombiano de Desarrollo Rural), Misión Rural, 2013. *Territorio Vivo, Del enfoque territorial a la gestión territorial en el marco del desarrollo rural colombiano* (Vol. 53). Bogotá, Colombia. https://doi.org/10.1017/CBO9781107415324.004

Lindholm, K.J., Ekblom, A. 2019. A framework for exploring and managing biocultural heritage. *Anthropocene* 25, 100195. https://doi.org/10.1016/j.ancene.2019.100195

Loiseau, E., Junqua, G., Roux, P., Bellon-Maurel, V. 2012. Environmental assessment of a territory: An overview of existing tools and methods. *Journal of Environmental Management* 112, 213–225. https://doi.org/10.1016/j.jenvman.2012.07.024

Martínez-Vega, J., Díaz, A., Nava, J.M., Gallardo, M., Echavarría, P. 2017. Assessing Land Use-Cover Changes and Modelling Change Scenarios in Two Mountain Spanish National Parks. *Environments* 4 (4), 79. https://doi.org/10.3390/environments4040079

Molina-Rico, L.J., Correa-Valencia, J.A., Feijoo-Martínez, A. 2019. Transformaciones territoriales, mudanzas y cambios en servicios ecosistémicos, Armenia, Colombia. *Revista Colombiana de Ciencias Sociales* 10 (1), 93-118. https://doi.org/10.21501/22161201.3061

Murillo-López, B.E. 2010. *Disponibilidad de recursos y tipos de sistemas de cultivo de café y plano en la cuenca del río La Vieja, Colombia.* Proyecto de Maestría. Universidad Tecnológica de Pereira.

Napieralski, J., Barr, I., Kamp, U., Kervyn, M. 2013. *Remote Sensing and GIScience in Geomorphological Mapping*. *Treatise on Geomorphology* (Vol. 3). Elsevier Ltd. https://doi.org/10.1016/B978-0-12-374739-6.00050-6

Narducci, J., Quintas-Soriano, C., Castro, A., Som-Castellano, R., Brandt, J. S. 2019. Implications of urban growth and farmland loss for ecosystem services in the western United States. *Land Use Policy* 86, 1–11. https://doi.org/10.1016/j.landusepol.2019.04.029

Nelson, G. 2005. Drivers of ecosystem change: summary chapter. Ecosystems and Human Well-being: Current State and Trends. *The Millennium Ecosystem Assessment Series*, *1*, 73–76.

Nieto C.O.A., Jiménez N.L.F., Nieto R.M. 2016. Variación de coberturas forestales y ocupación del territorio en el municipio de Armenia 1939-1999. *Revista Luna Azul* 42, 319 - 340. https://revistasojs.ucaldas.edu.co/index.php/lunazul/article/view/1621

Palacios, M. 1979. *El café en Colombia (1850 - 1970) Una historia económica, social y política* (Presencia). Bogotá, Colombia.

PCC (Paisaje Cultural Cafetero), 2021. *Paisaje Cultural Cafetero.* http://paisajecultural cafetero.org.co

PNN (Parque Nacional Natural), 2020. Parque Nacional Natural Los Nevados. https://www.parquesnacionales.gov.co/portal/es/ecoturismo/region-andina/parque-nacional-natural-los-nevados/

Puyravaud, J.P. 2003. Standardizing the calculation of the annual rate of deforestation. *Forest Ecology and Management* 177, 593–596. https://doi.org/10.1016/S0378-1127(02)00335-3

Rettberg, A. 2010. Global Markets, Local Conflict. Violence in the Colombian Coffee Region after the Breakdown of the International Coffee Agreement. *Latin American Perspectives* 37 (2), 111-132. https://doi.org/10.1177/0094582X09356961

Rindfuss, R.R., Walsh, S.J., Turner, B.L., Fox, J., Mishra, V. 2004. Developing a science of land change: Challenges and methodological issues. *Proceedings of the National Academy of Sciences of the United States of America* 101 (39), 13976–13981. https://doi.org/10.1073/pnas.0401545101

Rivera Pabón J.A. 2014. Del período precolombino al mito fundacional de Pereira: Cien siglos de historia previa. *Revista de Antropología y Sociología: Virajes* 16 (2), 67-102. https://revistasojs.ucaldas.edu.co/index.php/virajes/article/view/924

Rojas Briceño, N B., Barboza Castillo, E., Maicelo Quintana, J.L., Oliva Cruz, S.M., Salas López, R. 2019. Deforestación en la Amazonía peruana: Índices de cambios de cobertura y uso del suelo basado en SIG. *Boletín de la Asociación de Geógrafos Españoles* 81. https://doi.org/10.21138/bage.2538a

Rojas-Cano, A., Feijoo-Martínez, A., Molina-Rico, L.J., Zúñiga-Torres, M.C., Quintero Vargas, H. 2021. Caracterización de agricultores y estrategias conducentes a políticas públicas en el eje cafetero. *Rev. Colomb. Cienc. Soc* 12 (1), 2216–1201. https://doi.org/10.21501/22161201.3476

Ruiz-Cobo, D.H., Feijoo, A., Rodríguez, C. 2010. Comunidades de marcoinvertebrados edáficos en diferentes sistemas de uso del terreno en la cuenca del Río Otún, Colombia. *Acta Zoológica Mexicana* 2, 165-178.

Sanhouse-Garcia, A.J., Bustos-Terrones, Y., Rangel-Peraza, J.G., Quevedo-Castro, A., Pacheco, C. 2017. Multi-temporal analysis for land use and land cover changes in an agricultural region using open source tools. *Remote Sensing Applications: Society and Environment* 8, 278–290. https://doi.org/10.1016/j.rsase.2016.11.002

Santiago, I. 2014. *Tutorial Quantum GIS*, 2.6 versión Brighton.

Toro Zuluaga, G. 2005. Eje Cafetero colombiano. *Revista de Ciencias Humanas* 35, 127–149.

Turner II, B., Lambin, E.F., Reenberg, A. 2007. The emergence of land change science for global environmental change and sustainability. *PNAS 104* (52), 20666–20671. https://doi.org/10.1073/pnas.0704119104

UNESCO, 2021. *Coffee Cultural Landscape of Colombia*. https://whc.unesco.org/en/list/1121/

Van der Ploeg, J.D., Ventura, F. 2014. Heterogeneity reconsidered. *Current Opinion in Environmental Sustainability* 8, 23–28. https://doi.org/10.1016/j.cosust.2014.07.001

Verburg, P.H., van de Steeg, J., Veldkamp, A., Willemen, L. 2009. From land cover change to land function dynamics: A major challenge to improve land characterization. *Journal of Environmental Management* 90(3), 1327–1335. https://doi.org/10.1016/j.jenvman.2008.08.005

Xia, M., Zhang, Y., Zhang, Z., Liu, J., Ou, W., Zou, W. 2020. Modeling agricultural land use change in a rapid urbanizing town: Linking the decisions of government, peasant households and enterprises. *Land Use Policy* 90, 104266. https://doi.org/10.1016/j.landusepol.2019.104266

Zuñiga, M.C., Feijoo, A., Quintero, H. 2003. Trayectoria de los sistemas campesinos de cría en un área del piedemonte de Alcalá, Valle del Cauca. *Scientia et Technica* 23, 81–86. https://doi.org/10.22517/23447214.7395

Cuadernos de Investigación Geográfica *Geographical Research Letters*	2022	Nº 48	pp. 197-213	EISSN 1697-9540

http://doi.org/10.18172/cig.5143

QGIS A CONSTANTLY GROWING FREE AND OPEN-SOURCE GEOSPATIAL SOFTWARE CONTRIBUTING TO SCIENTIFIC DEVELOPMENT

MARCELA ROSAS-CHAVOYA[1], JOSÉ LUIS GALLARDO-SALAZAR[2]*, PABLITO MARCELO LÓPEZ-SERRANO[3], PEDRO CAMILO ALCÁNTARA-CONCEPCIÓN[4], ANA KAREN LEÓN-MIRANDA[5]

[1]Programa Institucional de Doctorado en Ciencias Agropecuarias y Forestales, Universidad Juárez del Estado de Durango, México.

[2]Facultad de Ciencias Forestales. Universidad Juárez del Estado de Durango, México.

[3]Instituto de Silvicultura e Industria de la Madera. Universidad Juárez del Estado de Durango, México.

[4]Dep. de Ingeniería Geomática e Hidráulica, División de Ingenierías. Universidad de Guanajuato, México.

[5]Copter Log Services GmbH, Klagenfurt am Wörthersee, Austria.

ABSTRACT. QGIS is the most popular free geospatial software in the world. QGIS belongs to the Open-Source Geospatial Foundation (OSGeo). Among the main strengths of this Geographic Information Systems are: the incorporation of tools via plugins, and a community of users and developers in constant growth. Despite the importance on the use of QGIS on the scientific community, to date there are no systematic studies indicating how the acceptance of this software has evolved through time. Therefore, the objective of this research was to characterize the scientific production and extent where QGIS has been used as their main geospatial tool. We conducted a bibliometric analysis of documents published in Scopus from 2005 to 2020 (931 manuscripts). The annual rate of publications increase was 40.3%. We found strong and positive correlations regarding the number of contributing code programmers ($r=0.66$, $p<0.005$); and the total income of the QGIS project ($r=0.88$, $p<0.001$). Seventy-two percent of the publications were included in six fields of study, being Earth and Planetary Sciences the most representative. Italy was the country with larger scientific production, while the USA was the most influential country (being the first, regarding the number of citations). In terms of the countries, the larger number of papers found were from Portugal, Italy, Brazil, and France. The International Archives of the Photogrammetry Remote Sensing and Spatial Information Sciences - ISPRS Archives stands among journals with the largest number of publications (47). In terms of collaborative networks among countries, we found strong links between authors from Germany, Switzerland, Greece, and Spain. Author network analysis showed three solid networks in different fields of study. We observed a favorable trend in the acceptance of QGIS across the world and a widespread development of collaborative networks. The present paper allowed increase the knowledge of geographic information systems, especially the development of scientific production using QGIS.

QGIS un software libre geospacial en constantemente crecimiento que contribuye al desarrollo científico

RESUMEN. QGIS es el software libre geoespacial más popular del mundo perteneciente a la Open Source Geospatial Foundation (OSGeo). Entre sus principales fortalezas se encuentran: la incorporación de herramientas vía plugins, y una comunidad de usuarios y desarrolladores en constante crecimiento. A pesar de la importancia que tiene el uso de QGIS en la comunidad científica, a la fecha no existen estudios sistemáticos que indiquen cómo ha evolucionado la

aceptación de este software a través del tiempo. Por lo tanto, el objetivo de esta investigación fue caracterizar la producción científica y la magnitud en la que QGIS se ha utilizado como principal herramienta geoespacial. Realizamos un análisis bibliométrico de los documentos publicados en Scopus de 2005 a 2020 (931 manuscritos). La tasa anual de incremento de publicaciones fue del 40,3%. Encontramos correlaciones fuertes y positivas con respecto al número de desarrolladores de código (r = 0,66, p <0,005); y los ingresos totales del proyecto QGIS (r = 0.88, p <0.001). El setenta y dos por ciento de las publicaciones se incluyeron en seis campos de estudio, siendo las Ciencias de la Tierra y Planetarias la más representativa. Italia fue el país con mayor producción científica, mientras que Estados Unidos fue el país más influyente (el primer lugar en número de citas). En cuanto a los países, el mayor número de artículos encontrados fueron de Portugal, Italia, Brasil y Francia. La International Archives of the Photogrammetry Remote Sensing and Spatial Information Sciences - ISPRS Archives se encuentra entre las revistas con más publicaciones (47). En términos de redes de colaboración entre países, encontramos fuertes vínculos entre autores de Alemania, Suiza, Grecia y España. El análisis de redes de colaboración entre autores identificó tres redes sólidas en diferentes campos de estudio. Observamos una tendencia favorable en la aceptación de QGIS en todo el mundo y un desarrollo generalizado de redes colaborativas. El presente trabajo permitió incrementar el conocimiento de los sistemas de información geográfica, especialmente el desarrollo de la producción científica utilizando QGIS.

Key words: Open-source software, QGIS, collaborative network, geospatial science, scientific contributions.

Palabras clave: software libre y de código abierto, QGIS, redes de colaboración, ciencias geoespaciales, contribuciones científicas.

Received: 17 July 2021

Accepted: 2 November 2021

*Corresponding author: José Luis Gallardo-Salazar, Facultad de Ciencias Forestales, Universidad Juárez del Estado de Durango, Durango 34239, México. E-mail address: 1107805@alumnos.ujed.mx

1. Introduction

Free software allows us to know and adapt its source code to the needs of each user and gives the freedom to reproduce and distribute copies for the benefit of society (Stallman, 2015). Science is closely related with the Free Software concept. The fact that one of the most important aspects of science is reproducibility, a feature which allows anyone to test data, hypothesis, and methods, makes free software an ideal framework for the scientific work. In this context, the use of free software has been consolidated in our societies in a gradual and constant way (Robles *et al.*, 2019). Consequently, in the last decade, this philosophy has been further developed and permeated all scientific fields, including the geospatial sciences (Brovelli *et al.*, 2017; Coetzee *et al.*, 2020; Conrad *et al.*, 2015; Minghini *et al.*, 2020; Neteler *et al.*, 2012).

Free software focused on geospatial sciences had already a tradition on science right from the beginning of the free software, but it did not have an impact on geosciences until several individual projects gathered and decided to integrate a unique community. The creation and evolution of these projects is based on crowdsourcing, which is supported by large communities (project leaders, users, developers, translators, educational and research institutions, etc.) from all over the world (Sarı *et al.*, 2019; See *et al.*, 2016). Over the years, this resulted in interesting but dispersed software packages with lack of direction. It was not until 2006, when first FOSS4G project leaders joined forces to create the Open Source Geospatial Foundation (OSGeo) (www.osgeo.org) (Moreno-Sanchez, 2012). To date, this type of software has been called FOSS4G (Free and Open-Source Software for Geospatial Applications).

OSGeo is a non-profit organization with the mission to support the collaborative development of open geospatial technologies and promote their use (Franceschi *et al.*, 2019).

One of the most popular OSGeo projects in recent years is QGIS (Graser and Olaya, 2015; István, 2012; Jaya and Fajar, 2019; Sandhya, 2020; Vázquez-Rodríguez, 2018). This software was born in 2002 under the name of Quantum GIS and developed by Gary Sherman, his main aim was to show an interface to visualize geospatial data (Hugentobler, 2008; Moyroud and Portet, 2018). Although it was developed in Qt toolkit and C++, an Application Programming Interface (API) of Python was incorporated in 2007, extending its functionality and increasing the number of developers who collaborate with the improvements in the code (Graser and Olaya, 2015). It currently consists of approximately 2 million lines of code (https://www.openhub.net/p/qgis/analyses/latest/languages_summary) and is used by thousands of users around the world (https://trends.google.es/trends/explore?date=all&q=%2Fm%2F0ct9z5).

The process of incorporating developers and adding code (https://vimeo.com/431673684) has allowed QGIS to move from being just a spatial information viewer to become a powerful Geographic Information System (GIS) tool used by a wide variety of users, not only to view, but also to edit and perform complex spatial analysis (Moyroud and Portet, 2018).One of the indicators of consolidation of QGIS is the more than 16 meetings of developers held biannually since 2009, which are events organized by volunteers with the aim of bringing together the developers of the QGIS project from around the world, often within a university campus. These events are of great importance for work planning, strengthening links in the community and serving to address relevant issues on project improvements and needs (https://qgis.org/en/site/getinvolved/meetings/index.html).

Furthermore, the growing interest in this software is reflected in the structuring of 31 user groups from different countries, recognized by the QGIS project (revised in December 2020). These groups have the purpose of organizing local user meetings, participating in voting on various issues in the eyes of the international QGIS community and in some cases raise funds to contribute to the continuity of the project (https://www.qgis.org/en/site/forusers/usergroups.html).

Since its creation, FOSS4G has been a strong community and many studies have been done looking at their developments. For instance, Neteler *et al.* (2012) described the history and functionality of the more than 400 GRASS (Geographical Resources Analysis Support System) modules, free software pioneer in geosciences. In addition, Conrad *et al.* (2015) analyzed architecture, functionality, development status and implementation of SAGA (System for Automated Geoscientific Analysis), highlighting its wide spectrum of scientific applications. In terms of comparative studies, Steiniger and Bocher (2009) listed the different desktop GIS software projects and discussed the advantages and disadvantages with emphasis on research and education; István (2012) did a review on the most popular software in the field of landscape ecology; Vázquez-Rodríguez (2018) analyzed the characteristics for the estimation of statistics in raster layers; Sandhya (2020) evaluated the open source GIS software based on economic criteria, functions and abilities compared to software under commercial licenses and concludes that QGIS is the most popular user friendly leading free software. While the popularity and leadership of QGIS is perceptible, to our knowledge, there are no scientific studies addressing the role of this software in academia and research.

In that sense, scientific publications are a fundamental element in the process of dissemination of advances, knowledge generation and application and measurement of the impact on the environment of some topic or tool (Rueda-Clausen *et al.*, 2005). On the other hand, the importance of such kind of studies yields light on the directions and possibilities on the near future for the Geographic Information Systems field and, in general, for the geospatial sciences. Even more, to know current impacts of QGIS would get further developments on the programming community, since it can represent an opportunity and an exciting field to work on. In fact, studies like the present analysis could serve to bring the scientific community closer to the QGIS project, since most of the early developers and first professional users of QGIS were not academics but software developers and people working for governments. Even

today, development is driven by professional user needs more than research groups. This is a significant difference to e.g. SAGA GIS project which is driven by research groups (Conrad *et al.*, 2015).

The documentary method called bibliometric analysis has the potential to statistically study scientific production, growth, and distribution. This method is important because it is a transparent, reproducible and systematic review process with the aim of evaluating scientific activity and its impact on society (Broadus, 1987; Pritchard, 1969). Therefore, the aim of this study was to characterize the scientific production where the QGIS software was the central instrument, under the following research questions:

1) Is there a relationship over time between the number of articles that use QGIS and the increase in code contributors and income?
2) In which fields of study is most frequently the use of QGIS?
3) Which are the general characteristics of research over time, differentiated by authors, journals and countries?
4) What have been the most influential articles and authors according to number of citations?
5) What are the most important collaboration networks of countries and authors?

2. Materials and methods

A literature search was conducted using the Scopus database (https://www.scopus.com) on 15th May 2021. Scopus was chosen among scientific databases because several authors report advantages such as a larger number of journals, documents and citations reported, compared to other scientific databases (AlRyalat *et al.*, 2019; Granda-Orive *et al.*, 2013).

The word "QGIS" was used in the search process and concentrated on the title, abstract and keywords, that is, if word QGIS appeared in one of these the paper was select. The search period covered exclusively scientific contributions published from 2002 (emergence of QGIS) to 2020 (Moyroud and Portet, 2018). The query code was as follows: TITLE-ABS-KEY (QGIS) AND PUBYEAR > 2002 AND (EXCLUDE (PUBYEAR, 2021).

A dataset was built including Year, H-Index, authors, and title from each publication. A review process was carried out over the Scopus dataset to exclude publications that were not directly related to the objective of the present study. Additionally, all authors and journals names were standardized to avoid duplications and/or incorrect classification. The final dataset was the starting point for the analysis. The analysis was carried out in the free software R (R Development Core Team 2020), using the "bibliometrix" package (Aria and Cuccurullo, 2017). Total citations (TC) were calculated per publication.

Furthermore, we captured the number of QGIS code contributors (who write, develop and debug the code of program) and the total income of the QGIS project (https://www.openhub.net/p/qgis/contributors/summary; https://qgis.org/en/site/getinvolved/governance/finance/index.html). Both data were included on the dataset to understand awareness of the community and their interests, in terms of income by project. Both variables were correlated with the number of documents published over time using the Pearson's correlation algorithm.

An analysis over publications by field of study, countries, top cited manuscripts, sources, scientific collaboration networks, and coauthorships was made.

3. Results and discusión

3.1. Publication dynamics

The search on Scopus resulted in a final database with 931 scientific documents using the QGIS software as their main GIS tool (see supplementary material https://cutt.ly/6RUvGe1). It is important to note that although the search filter was set starting on 2002 (when the emergence of QGIS is reported, Moyroud and Portet, 2018), no published documents were found until 2005. Those 931 scientific manuscripts from the period 2005-2020 were included in 524 different journals, books, or conference papers. The papers were written by a total of 2,755 authors (0.29 documents per author) and until 2020 there was reported an average of 3.81 citations in Scopus (Table 1).

Table 1. Summary of the database.

Description	
Documents	931
Period	2005-2020
Average documents per year	62.06
Sources (Journals, Books, etc.)	524
Document types:	
Article	559
Conference paper	313
Book chapter	*34*
Review	*15*
Book	*4*
Conference review	*2*
Note	*4*
Keywords	2624
Average citations per document	3.81
Authors	2755
Authors per document	3.5
Documents per Author	0.29
Authors of single-authored document	79
Authors of multi-authored documents	3178

Figure 1 shows the chronological distribution of documents published in the referred period. Annual growth rate was 40.3% with an exponential behavior. The number of documents published shows a positive correlation with the number of code contributors ($r=0.66$, $p<0.005$) (Figure 2a). This is likely to make the software more attractive and robust to respond to research needs and questions and gain reputation with the scientific community (Sandhya, 2020). Conrad *et al.* (2015) mention that a rapidly growing community of users and code contributors around the world are key to the success of the software with QGIS features.

According to financial reports, total income of the project shows a significant growth from 2014 to 2020 from 28.7 k€ to 236.7 k€ respectively (Figure 1). For the period 2014 to 2020, the number of documents published had a strong and positive correlation with the total income of the QGIS project ($r=0.88$, $p<0.001$) (Figure 2b). However, the financial reports of QGIS webpage includes only the incomes of donations and payment of sponsors members. It does not include the projects which were fund by public and private institutions, neither the projects which were funding by crowdfunding.

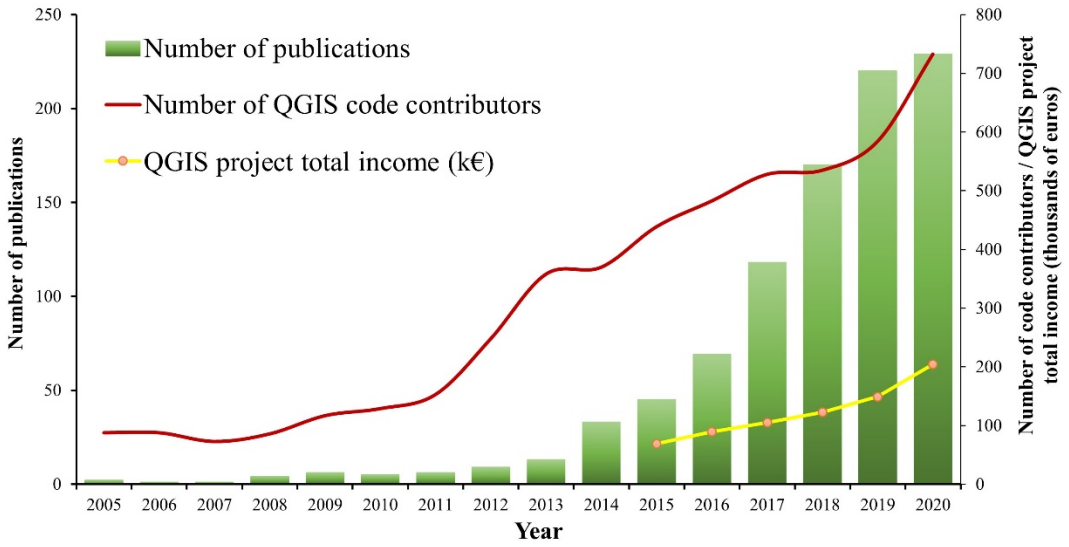

Figure 1. QGIS evolution (2005-2020) regarding number of publications (green bars), code contributors' frequency (red line) and total income by QGIS project (thousands of euros) (orange dots over a yellow line).

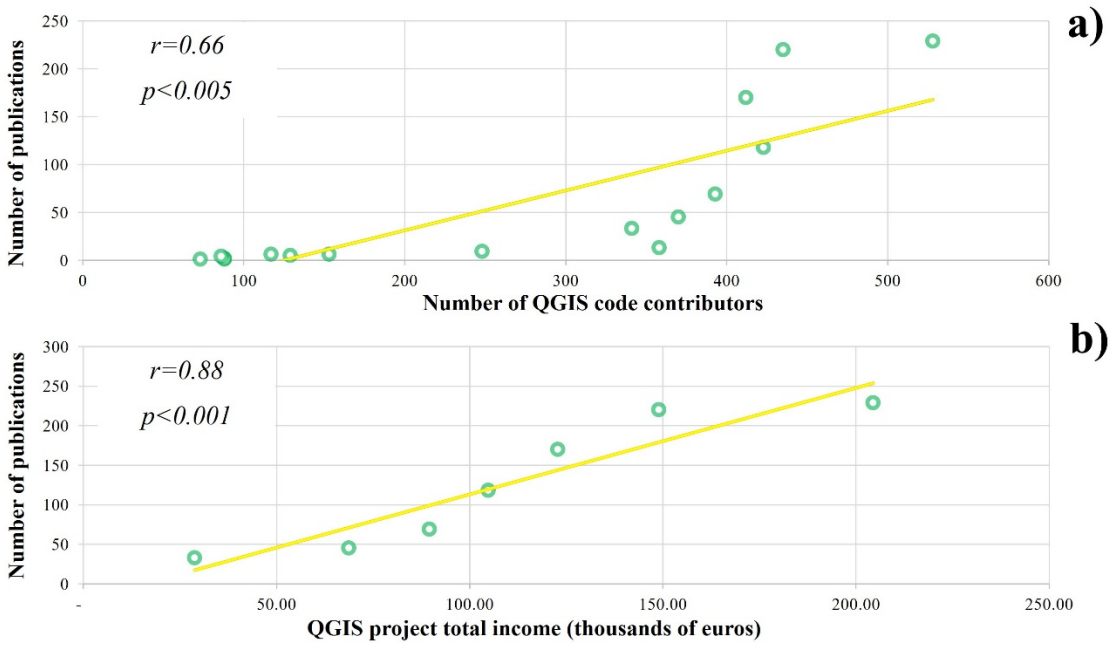

Figure 2. Pearson's correlations. a) publications vs. code contributors; b) publications vs. total income.

3.2. Publication according to the field of study

The chronological distribution of publications was analyzed according to the field of study and discipline. As illustrated in Figure 3, Earth and Planetary Sciences, Environmental Science, Computer Science, Social Sciences, Engineering and Agricultural and Biological Sciences, represent 72% of the total scientific contributions (668 documents) with 143, 132, 133, 115, 83 and 62 scientific contributions respectively. The origins of GIS are closely related to forest management or urban planning, nevertheless, at the last decades many other disciplines have incorporated the software GIS as tool (Foresman, 1998; Lünen and Travis, 2012). The interest of scientists to develop research using QGIS in these fields of study could be related to the development of the new functions and plugins.

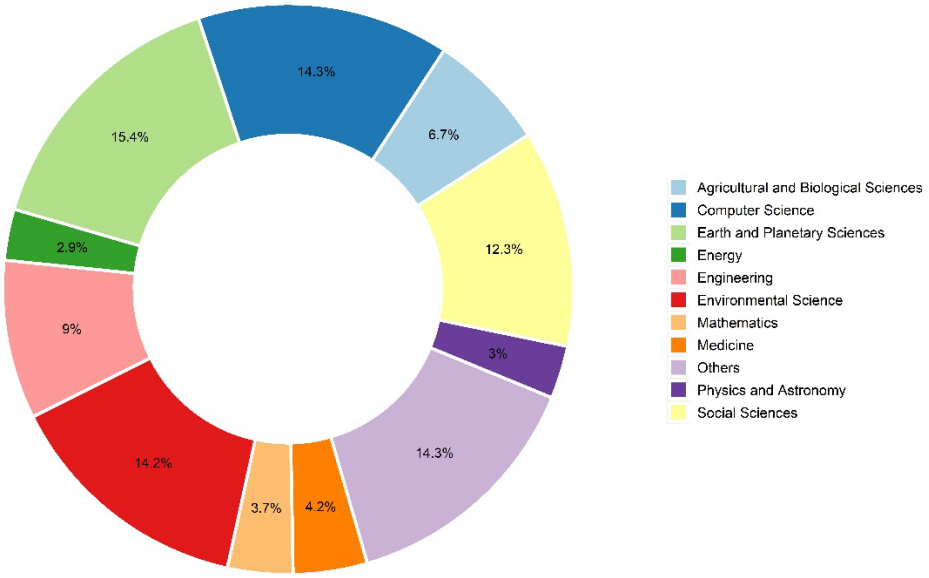

Figure 3. Chronological distribution of the 931 publications per field of study.

With respect to Earth and Planetary Sciences: Minin *et al.* (2019) used QGIS as a platform to close the gap between GIS and a virtual planetary observatory. Wolfe *et al.* (2020) developed an open source, semi-automated, QGIS-based graphical user interface (GUI) for fault-slide estimation and noted that free applications provide greater access and functionality for scientific computing and for displaying and analyzing spatial data sets. With respect to the categories Environmental Science, the application of QGIS is very varied. It has been used to assess soil erosion risk (Duarte *et al.*, 2016b), develop comprehensive GIS-based environmental management systems and specific tools for geovisual analysis (Bernasocchi *et al.*, 2012; Teodoro *et al.*, 2015), study vegetation characteristics using remote sensing (Duarte *et al.*, 2014a), analyze land use changes (Saputra *et al.*, 2020) and simulate hydrological effects (Bittner *et al.*, 2020). QGIS has been used in Social Sciences to study emotions of the population after a natural disaster (Gruebner *et al.*, 2017), geovisualization of tourists in Indonisia with Instagram data (Rofi'i *et al.*, 2019) and some other spatial data analysis with social networks (Sabah and Şimşek, 2017; Sowkhya *et al.*, 2018).

3.3. The most productive countries of corresponding authors

Overall, 75 countries published scientific contributions on the QGIS software. Italy was the country with the highest number of publications, followed by India and Brazil. Figure 4 shows the top ten of most productive countries in terms of the number of documents, and number of citations received per country. Together, these 10 countries contributed to the 30% of the total number of publications. It is important to note that five countries are in Europe, three in Asia and two in America. This indicates that, in addition to the proliferation of research using QGIS in Europe, this software has gained a reputation with the scientific community worldwide (Franceschi *et al.*, 2019). This trend could be explained by synergies of efforts such as the Open source software strategy defined and adopted by the European Commission since 2000 (Li *et al.*). This seemed to be the case in countries like Italy, which in 2010 the Constitutional Court approved the Rules on the adoption and dissemination of free software in the public administration (Corte costituzionale della Repubblica Italiana: Sentenza N. 122 2010 ("Corte costituzionale della Repubblica Italiana: Sentenza N. 122.," 2010). In South America, several efforts have been made to promote the use of free geospatial software in public administration and academia (Quinn, 2020).

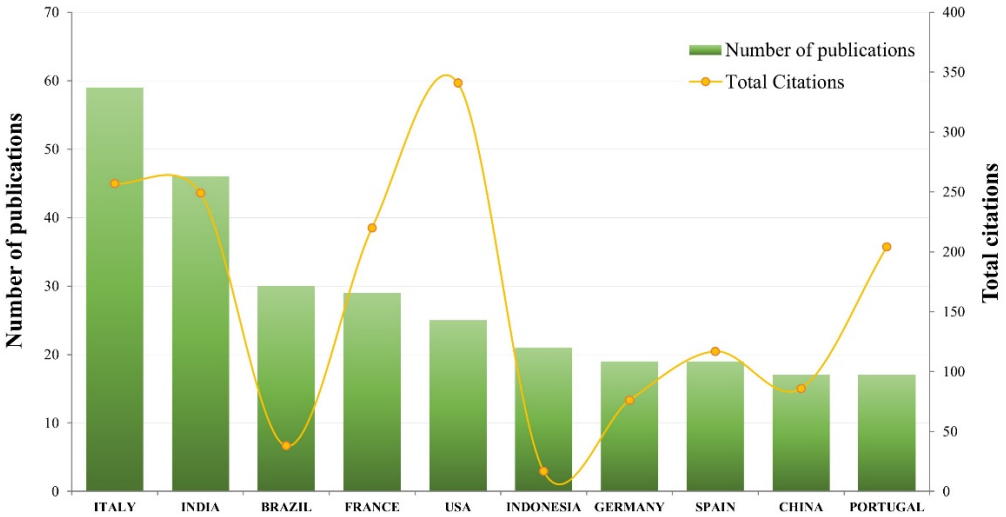

Figure 4. Number of papers and total citations received per country.

On average, these countries were cited 58 times, and while it is quite common for the countries with the highest number of publications to be those with the highest number of citations, this is not always the case. It is interesting to note the situation of Italy, India, Brazil and France. Although these four countries were the ones with the larger number of publications, the United States was the most influential country, reporting 341 total citations, almost three times more than the average per country. This may make sense due to the number of journals specialized in GIS with a high impact factor whose editorials were sitting over this country. In addition, the language of publication could be an important factor for the citation rate, often the non-English-speaking scientist decides to publish scientific articles in their first language, which makes their article less accessible to the international audience (Bitetti and Ferreras, 2017).

3.4. Top authors per number of publications

Contributions of the top 10 authors represented 9% of the total number of papers in the database. We found researchers from 5 countries: Portugal, Brazil, France, Italy and Switzerland. H-index is shown, which measures and compares productivity and impact taking into account the number of papers published and the number of citations (Jacsó, 2011). The author with the largest H-index is Zribi M. (50) who has participated in many publications about applications of QGIS (Baghdadi *et al.*, 2018a, 2018b), sometimes more than one on the same journal or book. An example of this case was the book titled "QGIS and Applications in water and risks", where Zribi M. participated as co-editor and co-author of a chapter. The aim of this book was to update knowledge of research geomatics teams, students of various levels, and engineers involved in the management of water and territory (Baghdadi *et al.*, 2018a), that exhibited the community interest to move from technical and scientific workflow to QGIS environment.

On the other hand, Teodoro A. C., Duarte L. and Rossetto R. were the authors with the largest number of papers published, with 20, 17 and 8, respectively. Teodoro A.C. and Duarte L. belonged to the University of Porto, Teodoro has published papers on risk maps and forest fire assessment (Teodoro and Amaral, 2017; Teodoro and Duarte, 2013), and participated in papers as co-author with Duarte, on developing maps for monitoring groundwater pollution vulnerability (Duarte *et al.*, 2015), as well as the development and publication of plugins for QGIS (Correia *et al.*, 2018; Duarte *et al.*, 2019; Duarte *et al.*, 2016a; Duarte *et al.*, 2018; Duarte *et al.*, 2014a; Duarte *et al.*, 2014b). It is interesting to note that a large pro-portion of papers published by Duarte are on the development of plugins, i.e. the generation

of specific functions within QGIS. This is possible thanks to the characteristics of free software that give the possibility of modifying and adapting the code to the needs of each user (Stallman, 2015).

Likewise, Rosseto R. was the main author of the development effort of the FREEWAT, plugin of QGIS, a tool for groundwater and surface water management with a module for rural water management (Rossetto *et al.*, 2018). FREEWAT was a project financed by the HORIZON 2020 programme of the European Union (Rossetto *et al.*, 2015). Since the development of FREEWAT several papers have had derivatives on its applications and improvements. For instance, De Filippis *et al.* (2020) described the supplies and workflow for using FREEWAT, also showing 13 examples from different countries. Furthermore, Criollo *et al.* (2019) introduced the ArkvaGIS module incorporated to FREEWAT that helps to store, manage and visualize the results of hydrochemical and hydrogeological analyzes.

The two authors with the largest number of contributions (Teodoro and Duarte) have produced papers from 2013 to 2019; being 2018 their most productive year. Meanwhile, Rossetto published his work from 2016 to 2020. All three authors with the largest publication numbers using QGIS have research lines on Earth and Planetary Science and Enviromental Science (Table 2).

Table 2. Most productive authors and affiliation.

Authors	ORCiD	Affiliation	Country	No. of publications	H-index
Teodoro A.C.	http://orcid.org/0000-0002-8043-6431	University of Porto	Portugal	20	16
Duarte L.	http://orcid.org/0000-0002-8043-6431	University of Porto	Portugal	17	8
Rossetto R.	http://orcid.org/0000-0003-2072-3241	Scuola Superiore Sant'Anna	Italy	8	12
Filho A.C.P.	http://orcid.org/0000-0002-9838-5337	Universidad de Federal de Mato Grosso do Sul	Brazil	7	17
Baghdadi N.	https://orcid.org/0000-0002-9461-4120	Universidad de Montpellier	France	6	49
Cannata M.	https://orcid.org/0000-0003-2527-1416	University of Applied Sciences and Arts of Southern Switzerland	Switzerland	6	11
Foti G.	https://orcid.org/0000-0001-8257-0602	University of Reggio Calabria	Italy	6	11
Mioto C.L.	https://orcid.org/0000-0002-6951-9527	Universidad de Federal de Mato Grosso do Sul	Brazil	6	8
Zribi M.	https://orcid.org/0000-0001-6141-8222	Université de Toulouse	France	6	50
Borsi I.	-	TEA SISTEMI S.p.A	Italy	5	12

3.5. Top manuscripts per number of citations

Table 3 shows the most cited papers. TC was accumulative number over time, i.e. previously published papers have cumulative advantages. Therefore, a column with citations per year is shown to put into perspective the number of citations for each paper regardless of the year of publication. Studying the number of citations of papers allows us to know the interesting topics and characteristics that confer projection among the scientific community (Patience *et al.*, 2017).

Table 3. Top Manuscripts per citations.

Manuscripts	DOI	Total Citations (TC)	TC per Year
Ilayaraja and Ambica (2015), Nat Environ Pollut Technol	-	145	20.7
Boschmann and Cubbon (2014), Prof Geogr	10.1080/00330124.2013.781490	89	11.1
Grinand *et al.* (2013),Remote Sens Environ	10.1016/j.rse.2013.07.008	83	9.2
Kaya *et al.* (2019), Hum Ecol Risk Assess	10.1080/10807039.2018.1470896	71	23.7
Dile *et al.* (2016), Environ Model Softw	10.1016/j.envsoft.2016.08.004	69	11.5
Lindberg *et al.* (2018), Environ Model Softw	10.1016/j.envsoft.2017.09.020	59	14.7
Kim *et al.* (2014), Plos One	10.1371/journal.pone.0098043	59	7.4
Chen *et al*. (2010), J Hydro-Environ Res	10.1016/j.jher.2010.04.017	49	4.1
Thiele *et al.* (2017), Soild Earth	10.5194/se-8-1241-2017	46	9.2
Jung (2016), Ecol Informatics	10.1016/j.ecoinf.2015.11.006	44	7.3

The paper with the highest number of citations was that by Ilayaraja and Ambica (2015) with 20.7 citations per year. This manuscript was published in the Nature Environment and Pollution Technology journal. This research consists in an interpolation analysis on a river using QGIS with the aim of describing water quality across the India´s river. On the other hand, in 2013 Boschman and Cubbon used QGIS to illustrate the use of maps in social research as a resource for qualitative interviews and community mapping (Boschmann and Cubbon, 2014). Boschman and Cubbon highlighted the use of QGIS in both, natural and social sciences.

In addition, Grinand *et al.* (2013) made a multitemporal analysis over the dry forest of Madagascar. The lost forest area was estimated from 2000 to 2010, through the use of remote sensing techniques and open-source software (R, GRASS y QGIS). Likewise, Kaya *et al.* (2019) published in the Journal Human and Ecological Risk Assessment: An International Journal with the title "Spatial data analysis with R programming for environment". Kaya et al included the use of QGIS, coupled with the R software in order to conduct a water quality spatially explicit assessment. These papers highlighted the capacity for integration between visualization and analysis processes of QGIS and other open-source software such as R, SAGA GIS, GRASS GIS, among others (Lush and Lush, 2014; Muenchow *et al.*, 2017; Passy and Théry, 2018).

A significant proportion (30%) of the most cited papers aimed to raise awareness of the development of plugins within the QGIS environment (Dile *et al.*, 2016; Jung, 2016; Lindberg *et al.*, 2018; Teodoro and Duarte, 2013). This can be explained if we take into account that one of the most relevant features of QGIS is that it has a Python API, which represents an advantage in terms of speed and ease in the development of new features (Graser and Olaya, 2015), allowing more interested people around the world to actively participate in the development of the software (Sarı *et al.*, 2019).

3.6. Most relevant sources

An analysis of the journals with the larger number of publications (Table 4) showed that 19.6% of publications were found in only 10 of the 524 total journals. In particular, two journals stood up: The International Archives of Photogrammetry, Remote Sensing and Spatial Information Sciences - ISPRS Archives (47) and the IOP Conference Series: Earth and Environmental Science (28). The journal with the larger impact factor was Environmental Modelling and Software with 4.55; the fact that this journal had the larger number of papers could be due to the preference of the authors to publish in journals that guarantee high projection among the scientific community.

Table 4. Top journals.

Sources	Total Publications	Impact Factor
International Archives of the Photogrammetry Remote Sensing and Spatial Information Sciences - ISPRS Archives	47	0.93
IOP Conference Series: Earth and Environmental Science	28	0.45
International Multidisciplinary Scientific Geoconference Surveying Geology and Mining Ecology Management SGEM	19	0.24
Proceedings of SPIE - The International Society for Optical Engineering	17	0.56
Anuario Do Instituto De Geociencias	15	0.23
Remote Sensing	14	4.51
Environmental Modelling and Software	13	4.55
ISPRS International Journal of Geo-Information	12	2.24
Lecture Notes in Computer Science	10	1.17
ISPRS Annals of The Photogrammetry Remote Sensing and Spatial Information Sciences	8	-

3.7. Analysis over scientific collaboration networks

3.7.1. Countries' collaboration

Another important topic for analysis, in addition to quantity indicators, was to analyze the existing networks of scientific collaboration. Figure 5 illustrates the links between each of the countries. The network was built taking into account the number of citations between documents, i.e. the number of citations of documents from another country that contain a document from a particular country. It is important to note that isolated nodes were removed; therefore, the network of collaborating countries consisted of 21 nodes and 45 links between 2005 and 2020.

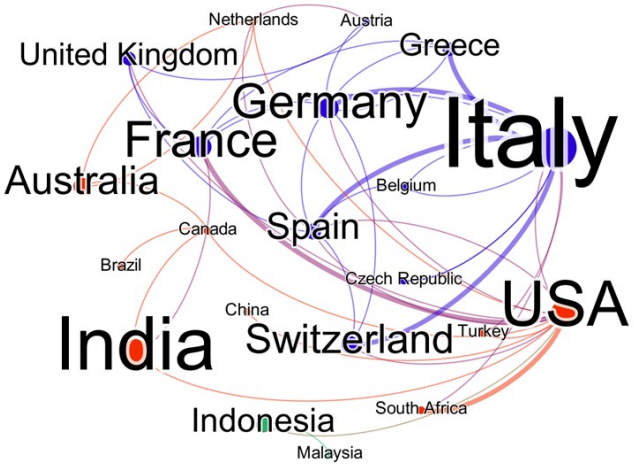

Figure 5. Countries' collaboration network.

Figure 5 indicates how strong the collaboration networks are between countries. USA, Italy, and India have larger circles than other countries, indicating that they are more productive in this area of research, which is consistent with the information in Figure 4. The arrows suggest strong links among authors from the USA with France, and USA with South Africa. Italy's strongest relationships are with Germany, Switzerland, Greece, and Spain. It is important to note that the thinness of links implies a low level of cooperation. It should be noted that Brazil, although it is the third country with the highest number of articles published, is one of the ones with the fewest collaboration links. This suggests that international collaborative networks are extremely important; however, there are countries with strong internal scientific production networks.

3.7.2. Authors' collaboration

The relationship of co-authorship in the scientific contributions contained in Scopus allows us to analyze to some extent the structure of collaboration within an academic community. In this study, with the information obtained from the authors, the productivity and collaboration network of authors who have published some work using the QGIS software as a central tool was built.

The science of our time is done in collaboration in different fields of knowledge. In the scientific work on QGIS it was observed that there is little collaboration. Figure 6 shows the relationships of scientific collaboration between authors who have published some work in the information sources consulted. Isolated nodes were removed resulting in a collaborative network with 19 authors and 31 collaborative links. The circles represent the authors, and the lines indicate the collaborations between them. The size of the circles indicates greater or lower number of studies carried out by an author. Five well-defined groups of collaboration were found, the largest was the group formed by the collaboration of seven authors, followed by the group formed by five authors, a third group is formed by three authors,

and finally two groups with two authors, suggesting developing networks of collaboration. The network formed by Duarte I, Teodoro AC and Gonçalves JA works in monitoring of natural resources topic. Rossetto R, Foglia I, Borsi I, Pouliaris C, De Filippis G, Cannata M and Kallioras A form a network specialized in water resources management. While, Korzun VA, Orgilbayar I, Tsogbadrakh N., Tserennorov D and Balakhonov SV use QGIS for epidemiological analyzes. That showed there are collaboration networks in several disciplines which use QGIS.

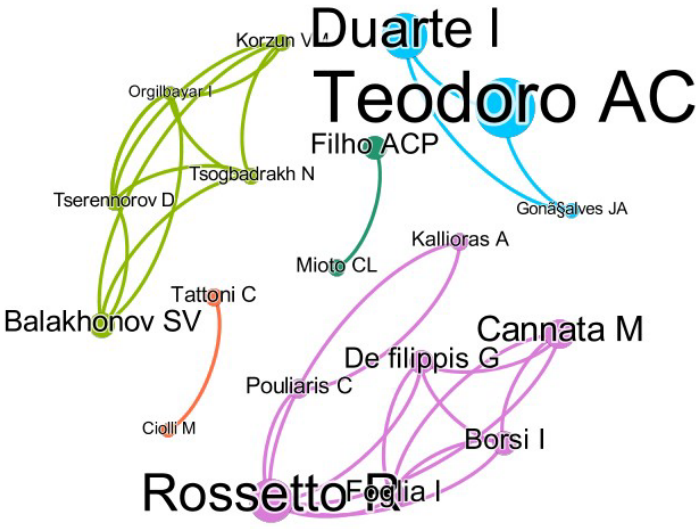

Figure 6. Authors' collaboration network.

4. Conclusions

QGIS constitutes a strong, wide, and diverse software who reflects the interest of the scientific community regarding geospatial sciences. The use of bibliometric techniques allowed us to have an overall view of the interest from the scientific community over the spatially explicit free software, and, in specific, over QGIS software.

We can conclude as well that there is a growing acceptance of QGIS by the scientific community as a tool in the development and analysis of research. Its success has been largely influenced by the extensibility of the software, and the dissemination of scientific studies on development of plugins and applications in various areas of knowledge. The present study contributes to answer the starting questions at the following highlights:

1) There is a relationship between the number of articles and the number of programmers who contributed to the code ($r = 0.66$), also with respect to the income of the QGIS project ($r = 0.88$). This indicates that the acceptance of QGIS into scientific community grows with respect to the people involved in the project. It could be interesting analyzing the income of specialized plugins and crowdfunding projects instead just the information of financial reports.

2) QGIS is used in several fields of study. The fields of study with more publications are Earth and Planetary Sciences (15.4%), Environmental Science (14.2%), Computer Science (14.3%), and social sciences (12.3%).

3) Scientific production has been on a growing trend since 2005, with an annual increase rate of 40.3%. The sources with the most publications on the subject were International Archives of Spatial Information Sciences and Remote Photogrammetry Sensing - ISPRS Archives and IOP Lecture Series: Earth and Environmental Sciences. Meanwhile, the most productive authors were Teodoro AC and

Duarte L, both authors attached to the University of Porto. Researchers from 75 countries have published articles related to QGIS, Italy and India being the most prolific countries.

4) The articles most cited in the period studied (2005-2020) were Ilayaraja and Ambica (2015) y Boschmann and Cubbon (2014), from Earth and Planetary Sciences and social sciences respectively. In addition, the most frequent fields of study were: Earth and Planetary Sciences (15.4%), Enviromental Sciencie (14.2%), Computer Science (14.3%), and social sciences (12.3%).

5) The most important country collaboration network is conformed for Italy, Germany, Switzerland, Greece and Spain. Author network analysis showed three solid networks in different fields of study.

The bibliometric analysis carried out with the contributions recorded in Scopus databases proved to be ideal for finding out characteristics and evolution of scientific production, where QGIS was used as the main tool. It is remarkable that every day more countries are added to the list of free software users. However, it is necessary to develop multiple studies highlighting advantages in order to promote and strengthen this culture; and thus, provide intellectual and scientific tools based on free software. In future research, it could compare trends and collaboration networks in the use of QGIS with commercial GIS software. It will also be interesting to analyze the potential of other scientific repositories.

Acknowledgments

The authors are grateful to the Mexican National Science and Technology Council (CONACYT) for supporting the studies of the first author and corresponding author.

References

AlRyalat, S.A.S., Malkawi, L.W., Momani, S.M. 2019. Comparing Bibliometric Analysis Using PubMed, Scopus, and Web of Science Databases. *JoVE* (152), e58494. https://doi.org/10.3791/58494

Aria, M., Cuccurullo, C. 2017. Bibliometrix: An R-tool for comprehensive science mapping analysis. *Journal of Informetrics,* 11(4), 959-975. 10.1016/j.joi.2017.08.007

Baghdadi, N., Mallet, C., Zribi, M. 2018a. Mapping of Drought. In *QGIS and Applications in Water and Risks*. Hoboken, NJ, USA.

Baghdadi, N., Mallet, C., Zribi, M. 2018b. *QGIS and Generic Tools* (Vol. 1): Wiley Online.

Baroni, C., Carton, A., Seppi, R. 2004. Distribution and Behaviour of Rock Glaciers in the Adamello-Presanella Massif (Italian Alps). *Permafrost and Periglacial Processses* 15, 243-259. https://doi.org/10.1002/ppp.497

Bernasocchi, M., Coltekin, A., Gruber, S. 2012. An open source geovisual analytics toolbox for multivariate spatio-temporal data in environmental change modelling. ISPRS Ann. Photogramm. Remote Sens. *Spatial Inf. Sci.*, I-2, 123-128. https://doi.org/10.5194/isprsannals-I-2-123-2012

Bittner, D., Rychlik, A., Klöffel, T., Leuteritz, A., Disse, M., Chiogna, G. 2020. A GIS-based model for simulating the hydrological effects of land use changes on karst systems – The integration of the LuKARS model into FREEWAT. *Environmental Modelling & Software*, 127, 104682. https://doi.org/10.1016/j.envsoft.2020.104682

Bitetti, M.S., Ferreras, J.A. 2017. Publish (in English) or perish: The effect on citation rate of using languages other than English in scientific publications. *Ambio*, 46(1), 121-127. https://doi.org/10.1007/s13280-016-0820-7

Boschmann, E., Cubbon, E. 2014. Sketch Maps and Qualitative GIS: Using Cartographies of Individual Spatial Narratives in Geographic Research. *The Professional Geographer*, 66(2), 236-248. https://doi.org/10.1080/00330124.2013.781490

Broadus, R.N. 1987. Toward a definition of "bibliometrics". *Scientometrics,* 12(5), 373-379. https://doi.org/10.1007/BF02016680

Brovelli, M.A., Minghini, M., Moreno-Sanchez, R., Oliveira, R. 2017. Free and open source software for geospatial applications (FOSS4G) to support Future Earth. *International Journal of Digital Earth*, 10(4), 386-404. https://doi.org/10.1080/17538947.2016.1196505

Chen, D., Shams, S., Carmona-Moreno, C., Leone, A. 2010. Assessment of open source GIS software for water resources management in developing countries. *Journal of Hydro-environment Research*, 4(3), 253-264. https://doi.org/10.1016/j.jher.2010.04.017

Coetzee, S., Ivánová, I., Mitasova, H., Brovelli, M.A. 2020. Open Geospatial Software and Data: A Review of the Current State and A Perspective into the Future. ISPRS International Journal of Geo-Information, 9(2). https://doi.org/10.3390/ijgi9020090

Conrad, O., Bechtel, B., Bock, M., Dietrich, H., Fischer, E., Gerlitz, L., Wehberg, J., Wichmann, V., Böhner, J. 2015. System for Automated Geoscientific Analyses (SAGA) v. 2.1.4. *Geosci. Model Dev.*, 8(7), 1991-2007. https://doi.org/10.5194/gmd-8-1991-2015

Correia, R., Duarte, L., Teodoro, A.C., Monteiro, A. 2018. Processing Image to Geographical Information Systems (PI2GIS)—A Learning Tool for QGIS. *Education Sciences*, 8(2). https://doi.org/10.3390/educsci8020083

Corte costituzionale della Repubblica Italiana: Sentenza N. 122. 2010. Retrieved from https://www.cortecostituzionale.it/actionSchedaPronuncia.do?anno=2010&numero=122

Criollo, R., Velasco, V., Nardi, A., Manuel de Vries, L., Riera, C., Scheiber, L., Jurado, A., Brouyère, S., Pujades, E., Rossetto, R., Vázquez-Suñé, E. 2019. AkvaGIS: An open source tool for water quantity and quality management. *Computers & Geosciences*, 127, 123-132. https://doi.org/10.1016/j.cageo.2018.10.012

De Filippis, G., Pouliaris, C., Kahuda, D., Vasile, T. A., Manea, V.A., Zaun, F., Panteleit, B., Dadaser-Celik, F., Positano, P., Nannucci, M.S., Grodzynskyi, M., Marandi, A., Sapiano, M., Kopač, I., Kallioras, A., Cannata, M., Filiali-Meknassi, Y., Foglia, L., Borsi, I., Rossetto, R. 2020. Spatial Data Management and Numerical Modelling: Demonstrating the Application of the QGIS-Integrated FREEWAT Platform at 13 Case Studies for Tackling Groundwater Resource Management. *Water*, 12(1). https://doi.org/10.3390/w12010041

Dile, Y.T., Daggupati, P., George, C., Srinivasan, R., Arnold, J. 2016. Introducing a new open source GIS user interface for the SWAT model. *Environmental Modelling & Software*, 85, 129-138. https://doi.org/10.1016/j.envsoft.2016.08.004

Duarte, L., Espinha-Marques, J., Teodoro, A.C. 2019. An Open Source GIS-Based Application for the Assessment of Groundwater Vulnerability to Pollution. *Environments*, 6(7). https://doi.org/10.3390/environments6070086

Duarte, L., Moutinho, O., Teodoro, A. 2016a. MicMac GIS application: free open source. *Proc.SPIE*, 10005. https://doi.org/10.1117/12.2240196

Duarte, L., Silva, P., Teodoro, A.C. 2018. Development of a QGIS Plugin to Obtain Parameters and Elements of Plantation Trees and Vineyards with Aerial Photographs. *ISPRS International Journal of Geo-Information*, 7(3). https://doi.org/10.3390/ijgi7030109

Duarte, L., Teodoro, A., Gonçalves, H. 2014a. Deriving phenological metrics from NDVI through an open source tool developed in QGIS. *Proc.SPIE,* 9245. https://doi.org/10.1117/12.2066136

Duarte, L., Teodoro, A.C., Gonçalves, H., Dias, A., Espinha-Marques, J. 2014b. Assessing groundwater vulnerability to pollution through the DRASTIC method, A GIS open source application (Vol. 101).

Duarte, L., Teodoro, A.C., Gonçalves, J. A., Guerner Dias, A.J., Espinha Marques, J. 2015. A dynamic map application for the assessment of groundwater vulnerability to pollution. *Environmental Earth Sciences,* 74(3), 2315-2327. https://doi.org/10.1007/s12665-015-4222-0

Duarte, L., Teodoro, A.C., Gonçalves, J.A., Soares, D., Cunha, M. 2016b. Assessing soil erosion risk using RUSLE through a GIS open source desktop and web application. *Environmental Monitoring and Assessment*, 188(6), 351. https://doi.org/10.1007/s10661-016-5349-5

Foresman, T. (1998). *The history of geographic information systems: perspectives from the pioneers*. Prentice-Hall.

Franceschi, S., Adoch, K., Kang, H.K., Hupy, C., Coetzee, S., Brovelli, M.A. 2019. OSGEO un Committee Educational Challenge: a use case of sharing software and experience from all over the world. Int. Arch. Photogramm. *Remote Sens. Spatial Inf. Sci*., XLII-4/W14, 49-55. https://doi.org/10.5194/isprs-archives-XLII-4-W14-49-2019

Granda-Orive, J.I., Alonso-Arroyo, A., García-Río, F., Solano-Reina, S., Jiménez-Ruiz, C.A., Aleixandre-Benavent, R. 2013. Ciertas ventajas de Scopus sobre Web of Science en un análisis bibliométrico sobre tabaquismo. *Revista española de Documentación Científica*; 36 (2). https://doi.org/10.3989/redc.2013.2.941

Graser, A., Olaya, V. 2015. Processing: A Python Framework for the Seamless Integration of Geoprocessing Tools in QGIS. *ISPRS International Journal of Geo-Information*, 4(4), 2219-2245. https://doi.org/10.3390/ijgi4042219

Grinand, C., Rakotomalala, F., Gond, V., Vaudry, R., Bernoux, M., Vieilledent, G. 2013. Estimating deforestation in tropical humid and dry forests in Madagascar from 2000 to 2010 using multi-date Landsat satellite images and the random forests classifier. *Remote Sensing of Environmen*t, 139, 68-80. https://doi.org/10.1016/j.rse.2013.07.008

Gruebner, O., Lowe, S.R., Sykora, M., Shankardass, K., Subramanian, S.V., Galea, S. 2017. A novel surveillance approach for disaster mental health. *Plos One*, 12(7), e0181233. https://doi.org/10.1371/journal.pone.0181233

Hugentobler, M. 2008. Quantum GIS. In S. Shekhar & H. Xiong (Eds.), *Encyclopedia of GIS* (pp. 171-188). New York: Springer Science & Business Media.

Ilayaraja, K., Ambica, A. 2015. Spatial Distribution of Groundwater Quality Between Injambakkam-Thiruvanmyiur Areas, South East Coast of India. N*ature Enviroment and Pollution Tecnology*, 14, 771-776.

István, S. 2012. Comparison of the most popular open-source GIS software in the field of landscape ecology. Acta Geographica Debrecina. *Landscape & Environment Series*, 6, 76-92.

Jacsó, P. 2011. The h-index, h-core citation rate and the bibliometric profile of the Scopus database. *Online Information Review*, 35(3), 492-501. https://doi.org/10.1108/14684521111151487

Jaya, M., Fajar, A. (2019). *Analysis of the implementation quantum GIS: comparative effect and user performance*.

Jung, M. 2016. LecoS — A python plugin for automated landscape ecology analysis. *Ecological Informatics*, 31, 18-21. https://doi.org/10.1016/j.ecoinf.2015.11.006

Kaya, E., Agca, M., Adiguzel, F., Cetin, M. 2019. Spatial data analysis with R programming for environment. *Human and Ecological Risk Assessment: An International Journal*, 25(6), 1521-1530. https://doi.org/10.1080/10807039.2018.1470896

Kim, H.-A., Shin, J.-Y., Kim, M.-H., Park, B.-J. 2014. Prevalence and Predictors of Polypharmacy among Korean Elderly. *Plos One*, 9(6), e98043. https://doi.org/10.1371/journal.pone.0098043

Li, Y., Zhao, M., Mildrexler, D. J., Motesharrei, S., Mu, Q., Kalnay, E., Zhao, F., Li, S., Wang, K. 2016. Potential and Actual impacts of deforestation and afforestation on land surface temperature. *Journal of Geophysical Research: Atmospheres*, 121(24), 372-314,386. http://doi.org/10.1002/2016JD024969

Lindberg, F., Grimmond, C.S.B., Gabey, A., Huang, B., Kent, C. W., Sun, T., Theeuwes, N.E., Järvi, L., Ward, H.C., Capel-Timms, I., Chang, Y., Jonsson, P., Krave, N., Liu, D., Meyer, D., Olofson, K.F.G., Tan, J., Wästberg, D., Xue, L., Zhang, Z. 2018. Urban Multi-scale Environmental Predictor (UMEP): An integrated tool for city-based climate services. *Environmental Modelling & Software*, 99, 70-87. https://doi.org/10.1016/j.envsoft.2017.09.020

Lünen, A., Travis, C. 2012. History and GIS: Epistemologies, considerations and reflections.Springer.

Lush, C., Lush, M. 2014. QGIS Suitability Assessment. *JNCC Report*, No 542.

Minghini, M., Mobasheri, A., Rautenbach, V., Brovelli, M.A. 2020. Geospatial openness: from software to standards & data. Open Geospatial Data, Software and Standards, 5(1), 1. https://doi.org/10.1186/s40965-020-0074-y

Minin, M., Rossi, A.P., Marco Figuera, R., Unnithan, V., Marmo, C., Walter, S.H.G., Demleitner, M., Le Sidaner, P., Cecconi, B., Erard, S., Hare, T.M. 2019. Bridging the Gap Between Geographical Information Systems and Planetary Virtual Observatory. 6(3), 515-526. https://doi.org/10.1029/2018EA000405

Moreno-Sanchez, R. 2012. Free and Open Source Software for Geospatial Applications (FOSS4G): A Mature Alternative in the Geospatial Technologies Arena. Transactions in GIS, 16(2), 81-88. https://doi.org/10.1111/j.1467-9671.2012.01314.x

Moyroud, N., Portet, F. 2018. Introduction to QGIS. In N. Baghdadi, C. Mallet, & M. Zribi (Eds.), QGIS and Generic Tools (pp. 1-17): https://doi.org/10.1002/9781119457091.ch1

Muenchow, J., Schratz, P., Brenning, A. 2017. RQGIS: Integrating R with QGIS for Statistical Geocomputing R. *The R Journal*, 9(2), 409-428. https://doi.org/10.32614/RJ-2017-067

Neteler, M., Bowman, M.H., Landa, M., Metz, M. 2012. GRASS GIS: A multi-purpose open source GIS. *Environmental Modelling & Software*, 31, 124-130. https://doi.org/10.1016/j.envsoft.2011.11.014

Passy, P., Théry, S. 2018. The Use of SAGA GIS Modules in QGIS. In *QGIS and Generic Tools* (pp. 107-149). Wiley & Sons.

Patience, G.S., Patience, C.A., Blais, B., Bertrand, F. 2017. Citation analysis of scientific categories. *Heliyon*, 3(5), e00300. https://doi.org/10.1016/j.heliyon.2017.e00300

Pritchard, A. 1969. Statistical Bibliography or Bibliometrics. *Journal of Documentation*, 25, 348-349.

Quinn, S. 2020. Free and open source GIS in South America: political inroads and local advocacy. International *Journal of Geographical Information Science*, 34(3), 464-483. https://doi.org/10.1080/13658816.2019.1665672

Robles, G., Steinmacher, I., Adams, P., Treude, C. 2019. Twenty Years of Open Source Software: From Skepticism to Mainstream. *IEEE Software*, 36(6), 12-15. https://doi.org/10.1109/MS.2019.2933672

Rofi'i, A., Wibowo, T.W., Sudaryatno, Farda, N.M. 2019. Tourists geovisualization analysis utilizing Instagram data in central java province and special region of Yogyakarta. Int. Arch. Photogramm. *Remote Sens. Spatial Inf. Sci.*, XLII-4/W16, 535-542. https://doi.org/10.5194/isprs-archives-XLII-4-W16-535-2019

Rossetto, R., Borsi, I., Foglia, L. 2015. FREEWAT: FREE and open source software tools for WATer resource management. *Rendiconti online della Società Geologica Italiana*, 35, 252–255. https://doi.org/10.3301/ROL.2015.113

Rossetto, R., De Filippis, G., Borsi, I., Foglia, L., Cannata, M., Criollo, R., Vázquez-Suñé, E. 2018. Integrating free and open source tools and distributed odelling codes in GIS environment for data-based groundwater management. *Environmental Modelling & Software*, 107, 210-230. https://doi.org/10.1016/j.envsoft.2018.06.007

Rueda-Clausen, C.F., Villa-Roel, C., Rueda-Clausen, C.E. 2005. Indicadores bibliométricos: origen, aplicación, contradicción y nuevas propuestas. *MedUNAB*, 8, 29-36.

Sabah, L., Şimşek, M. 2017. Investigation of spatial data with open source social network analysis and Geographic Information Systems applications. *Int. Arch. Photogramm. Remote Sens. Spatial Inf. Sci.*, XLII-4/W6, 81-83. https://doi.org/10.5194/isprs-archives-XLII-4-W6-81-2017

Sandhya, C. 2020. Exploring Opportunities with Open Source GIS. *International Journal of Engineering Research and Technology*, 9(5). https://doi.org/10.17577/IJERTV9IS050545

Saputra, A.W.W., Azazi Zakaria, N., Ngai Weng, C. 2020. Changes in Land Use in the Lombok River Basin and Their Impacts on River Basin Management Sustainability. *IOP Conference Series: Earth and Environmental Science*, 437, 012036. https://doi.org/10.1088/1755-1315/437/1/012036

Sarı, A., Tosun, A., Alptekin, G. I. 2019. A systematic literature review on crowdsourcing in software engineering. *Journal of Systems and Software*, 153, 200-219. https://doi.org/10.1016/j.jss.2019.04.027

See, L., Mooney, P., Foody, G., Bastin, L., Comber, A., Estima, J., Fritz, S., Kerle, N., Jiang, B., Laakso, M., Liu, H.-Y., Milčinski, G., Nikšič, M., Painho, M., Pődör, A., Olteanu-Raimond, A.-M., Rutzinger, M. 2016. Crowdsourcing, Citizen Science or Volunteered Geographic Information? *The Current State of Crowdsourced Geographic Information*, 5(5), 55. https://doi.org/10.3390/ijgi5050055

Sowkhya, B., Amaduzzi, S., Raawal, D. 2018. Visualization and analysis of cellular & Twitter data using QGIS. *Int. Arch. Photogramm. Remote Sens. Spatial Inf. Sci.*, XLII-4/W8, 199-209. https://doi.org/10.5194/isprs-archives-XLII-4-W8-199-2018

Stallman, R. 2015. *Free hardware and free hardware designs.* GNU.org.

Steiniger, S., Bocher, E. 2009. An overview on current free and open source desktop GIS developments. *International Journal of Geographical Information Science*, 23(10), 1345-1370. https://doi.org/10.1080/13658810802634956

Teodoro, A.C., Amaral, A. 2017. Evaluation of forest fires in Portugal Mainland during 2016 summer considering different satellite datasets. *Proc.SPIE*, 10421. https://doi.org/10.1117/12.2278262

Teodoro, A.C., Duarte, L. 2013. Forest fire risk maps: a GIS open source application – a case study in Norwest of Portugal. *International Journal of Geographical Information Science*, 27(4), 699-720. https://doi.org/10.1080/13658816.2012.721554

Teodoro, A.C., Duarte, L., Sillero, N., Gonçalves, J.A., Fonte, J., Gonçalves-Seco, L., Pinheiro da Luz, L.M., dos Santos Beja, N.M.R. (2015). An integrated and open source GIS environmental management system for a protected area in the south of Portugal. Paper presented at the *Proc.SPIE*.

Thiele, S.T., Grose, L., Samsu, A., Micklethwaite, S., Vollgger, S.A., Cruden, A.R. 2017. Rapid, semi-automatic fracture and contact mapping for point clouds, images and geophysical data. *Solid Earth*, 8(6), 1241-1253. https://doi.org/10.5194/se-8-1241-2017

Vázquez-Rodríguez, R. 2018. Uso de sistemas de información geográfica libres para la protección del medio ambiente. Caso de estudio: manipulación de mapas ráster con datos. *Revista Universidad y Sociedad*, 10, 158-164.

Wolfe, F.D., Stahl, T.A., Villamor, P., Lukovic, B. 2020. Short communication: A semiautomated method for bulk fault slip analysis from topographic scarp profiles. *Earth Surf. Dynam.*, 8(1), 211-219. https://doi.org/10.5194/esurf-8-211-2020

CUADERNOS DE INVESTIGACIÓN GEOGRÁFICA
GEOGRAPHICAL RESEARCH LETTERS
Guide for authors

Cuadernos de Investigación Geográfica (*Geographical Research Letters*) publishes scientific, unedited, peer-reviewed works. These should normally not exceed 7500 words, although articles of major dimension can be published if the Editor approves it. Notes and chronicles should not exceed 2500 words.

Submission to this journal proceeds totally online via http://publicaciones.unirioja.es/revistas/cig.

Preparation

Manuscripts should preferably be written in English. Authors who are not fluent in English should have their manuscript checked by someone proficient in the language. Manuscripts in which the English is difficult to understand may be returned to the author for revision before scientific review.

Manuscripts must necessarily incorporate the following information:

Cover letter. The authors should send the Editor a presentation letter of the manuscript highlighting the most outstanding aspects of the work. Five experts in the subject (name, institution and email), who could act as referees, will be suggested in this letter. These experts will have no direct link with the authors.

Title. This should be concise and informative.

Author names and affiliations. Please clearly indicate the given name(s) and family name(s) of each author and check that all names are accurately spelled. Present the authors' affiliation address: institution, mailing address, country and email.

Corresponding author. Indicate who will handle correspondence at all stages of refereeing and publication, also postpublication. Ensure that the e-mail address is given.

Abstract. It is necessary to include an abstract (300-400 words). The abstract should state briefly the purpose of the research, the principal results and major conclusions. If the article is published in Spanish, an English abstract must be included.

Keywords. Immediately after the abstract, provide a maximum of 5 keywords. These keywords will be used for indexing purposes.

Acknowledgements. Include acknowledgements in a separate section, at the end of the article, before the references. If you want to add research funding, you must add the project title (number), funding organization and country.

Article structure

Divide your article into clearly defined and numbered sections. Sections and Subsections should be numbered 1.1 (then 1.1.1, 1.1.2, ...), 1.2, etc. In any case, the manuscript must include introduction, study area, methods and materials, results, discussion and conclusions. Subsections may have a short heading.

Number consecutively the equations that are displayed in the text.

In the papers written in English, decimals will be separated by a point (e.g., 27.3). A comma will be used for the thousands separator (e.g., 24,237). In the papers written in Spanish, decimals will be separated by comma (e.g., 27,3). A point will be used for the thousands separator (e.g., 24.237).

Tables

Please submit tables as editable text and not as images. Tables can be placed inside the text, or on separate page(s) at the end. Number tables consecutively in accordance with their appearance in the text and place the table heading.

Figures

Illustrations (figures, maps and photographs) should be submitted as separate files and numbered according to the sequence in the text. The files should be sent together in one or several compressed files (.zip, .rar) not exceeding 4Mb. Please convert the illustrations to one of the following formats: EPS (or PDF), or TIFF (or JPEG) with a minimum of 300 dpi. Illustrations will be published in colour at no additional charge. Figure captions should be supplied at the end of the text. Each article should include no more than 10 figures.

References

All the references cited in the text should be given in the reference list, and vice versa. Regular research papers have a reference limit of 50 cites and short communications should not exceed 20 cites.

References should be quoted in the text as name and year within brackets. When more than two authors are referred, the name of the first author should be used, with the addendum et al. At the end of the text references should be listed alphabetically by author´s name, in the following style:

Badding, M.E., Briner, J.P., Kaufman, D.S. 2013. 10 Be ages of late Pleistocene deglaciation and Neoglaciation in the north-central Brooks Range, Arctic Alaska. *Journal of Quaternary Science* 28, 95-102. http://doi.org/10.1002/jqs.2596.

French, H.M. 2007. *The Periglacial Environmen*t. Third Edition. Wiley, Chichester, 458 pp.

Camuffo, D., Enzi, S. 1995. Reconstructing the climate of northern Italy from archive sources. In: R. Bradley, P.D. Jones P.D. (Eds.), *Climate since A.D. 1500*. Routledge, London, pp. 143-154.

IDERM 2011. Ortofoto regional del vuelo de 1981. Available at: http://cartomur.imida.es/visorcartoteca/ (last access: 20/06/2011).

The authors will provide, if possible, the DOI number at the end of each cited article.

Once the paper is accepted, a pre-print version will be available at the website of the journal with its corresponding DOI number.

One set of page proofs will be sent by e-mail to the corresponding author as a PDF file.

Each author will receive, at no cost, a PDF file of the article and one printed copy of the corresponding issue of the journal.

The publishing policy in *Cuadernos de Investigación Geográfica* makes the evaluation and publication processes free, in agreement with the policy of making accessible the advances in Physical Geography to the scientific community.

CUADERNOS DE INVESTIGACIÓN GEOGRÁFICA
GEOGRAPHICAL RESEARCH LETTERS
Normas de publicación

Cuadernos de Investigación Geográfica (*Geographical Research Letters*) publica trabajos científicos inéditos sometidos a una revisión por pares. Los artículos no deberán superar las 7500 palabras, aunque pueden publicarse trabajos de mayor dimensión si su interés así lo aconseja. También publica notas y crónicas que no deberán superar las 2500 palabras.

El envío de trabajos se realiza online a través de la página web de la revista http://publicaciones.unirioja.es/revistas/cig.

Preparación de manuscritos

Los manuscritos estarán escritos preferentemente en inglés. Aquellos autores que tengan dificultades con este idioma deberán enviar el texto a un nativo (o a una persona con excelente dominio de este idioma). Aquellos manuscritos que sean difíciles de entender debido a una redacción en inglés deficiente serán devueltos a los autores antes de ser evaluados científicamente.

Los manuscritos deben incorporar necesariamente la siguiente información:

Carta de presentación. Los autores deberán dirigir al Editor una carta de presentación del manuscrito resaltando los aspectos más sobresalientes del trabajo. En esta carta se sugerirán cinco expertos en la materia (nombre, institución y correo electrónico) -no vinculados directamente con los autores- que podrán actuar de evaluadores.
Título. Debe ser conciso e informativo del contenido del manuscrito.
Nombres de los autores y afiliaciones. Indique los nombres y apellidos de los autores, añadiendo la afiliación profesional de cada autor: institución, dirección postal, país y correo electrónico.
Autor de correspondencia. Indique el autor de contacto, su centro de trabajo, su dirección y el correo electrónico. Con este autor el equipo editorial mantendrá la correspondencia en todo el proceso de edición.
Abstract/Resumen. Es necesario incluir un resumen (entre 300 y 400 palabras) del contenido del manuscrito que incorpore información sobre los objetivos de la investigación, los resultados y las conclusiones principales. Si el artículo es publicado en español, obligatoriamente debe incorporarse un resumen en inglés.
Palabras clave. Inmediatamente después del resumen, se debe proporcionar un máximo de 5 palabras clave. Estas palabras clave son utilizadas con fines de indexación.
Agradecimientos. Incluya los agradecimientos en una sección independiente, al final del manuscrito, antes del listado de referencias bibliográficas. Si en los agradecimientos se desea incorporar a los responsables de la financiación de la investigación, debe añadir el título del proyecto (número), organización financiadora y país.

Estructura del manuscrito

La estructura del manuscrito será lo más sencilla posible. Se aconseja dividir el texto en secciones numeradas (1, 2, 3…). Las subsecciones también deben numerarse 1.1 (luego 1.1.1, 1.1.2, …), 1.2, etc. En cualquier caso, en el manuscrito es necesario incluir: Introducción, Área de Estudio, Métodos y Materiales, Resultados, Discusión y Conclusiones como secciones. Las subsecciones pueden tener un breve encabezado.

Se deberán numerar consecutivamente las ecuaciones que vayan en el texto principal.

En los textos escritos en español, los decimales estarán separados por una coma (por ej., 27,3). Se utilizará un punto para el separador de miles en números de cuatro o más cifras (por ej., 24.237). En los textos escritos en inglés, los decimales estarán separados por un punto (por ej., 27.3). Se utilizará una coma para el separador de miles en números de cuatro o más cifras (por ej., 24,237).

Tablas

Las tablas deben presentarse como texto editable y no como imágenes. Las tablas se pueden colocar en el interior del texto o en páginas separadas al final. Es necesario numerar las tablas e incorporar un encabezamiento.

Figuras

Las figuras, mapas y fotos se entregarán en archivos separados y numerados consecutivamente en relación con su posición en el texto. Dichos archivos se enviarán juntos en uno o varios archivos comprimidos (.zip, .rar) que tengan un tamaño máximo de 4 Mb. Se admiten archivos EPS (o PDF) o TIFF (o JPEG) con una resolución mínima de 300 dpi. Figuras, mapas y fotos se publicarán en color, sin coste adicional. Los pies de figura se incluirán al final del texto. Se admitirá hasta un máximo de 10 figuras por artículo.

Referencias bibliográficas

Asegúrese de que todas las referencias citadas en el texto estén presentes en la lista de referencias (y viceversa). Los trabajos de investigación regulares (artículos) tienen un límite de 50 referencias y las comunicaciones breves no deben exceder las 20 citas.

En el texto se citará el nombre del autor y el año entre paréntesis. Caso de que el trabajo citado corresponda a más de dos autores se especificará el primero, añadiendo posteriormente et al. Al final del texto se incluirá la lista de referencias por orden alfabético, siguiendo el siguiente modelo:

Badding, M.E., Briner, J.P., Kaufman, D.S. 2013. 10 Be ages of late Pleistocene deglaciation and Neoglaciation in the north-central Brooks Range, Arctic Alaska. *Journal of Quaternary Science* 28, 95-102. http://doi.org/10.1002/jqs.2596

French, H.M. 2007. *The Periglacial Environment*. Third Edition. Wiley, Chichester, 458 pp.

Camuffo, D., Enzi, S. 1995. Reconstructing the climate of northern Italy from archive sources. In: R. Bradley, P.D. Jones P.D. (Eds.), *Climate since A.D. 1500*. Routledge, London, pp. 143-154.

IDERM 2011. Ortofoto regional del vuelo de 1981. Disponible en: http://cartomur.imida.es/visorcartoteca/ (Fecha de acceso: 20/06/2011).

Los autores añadirán, cuando sea posible, el número de DOI al final de cada artículo citado.

Cuando el artículo sea aceptado, en la página web de la revista estará disponible una versión pre-print con su correspondiente DOI.

Las pruebas de imprenta se enviarán como archivo PDF y por correo electrónico al autor de contacto.

La evaluación y publicación de artículos en *Cuadernos de Investigación Geográfica* es gratuita y responde a la política de la revista de poner los avances en Geografía Física al alcance del mundo científico.

Administración / Administration

Universidad de La Rioja
Servicio de Publicaciones
Piscinas, 1, 26006 LOGROÑO (España)
Tel.: (+34) 941299187 Fax: (+34) 941299193
Correo-e: publicaciones@unirioja.es

Edición electrónica / E-Journal

EISSN: 1697-9540
http://publicaciones.unirioja.es/revistas/cig
cig@unirioja.es

Indización y Calidad / Indexation and Quality Analysis

Bases de Datos y Recursos para el análisis de la calidad de las revistas científicas /
Databases and Resources for the analysis of the Scientific Journal's Quality:

CARHUS Plus+ 2018
CIRC (EC3 Metrics)
Dialnet Métricas (Fundación Dialnet)
DOAJ (Directory of Open Access Journals)
ERIH Plus (European Science Fundation)
ESCI, Emerging Sources Citation Index (Web of Science™ , Clarivate Analytics)
Fuente Académica Plus (EBSCO)
Latindex (Catálogo)
MIAR (Matriz de Información para el Análisis de Revistas)
Periodicals Index Online (ProQuest)
SCIMAGO Journal & Country Rank (SJR)
Scopus (Elsevier)
Sello de Calidad FECYT

Cuadernos de Investigación Geográfica / *Geographical Research Letters*
A scientific journal of Physical Geography

CUADERNOS DE INVESTIGACIÓN GEOGRÁFICA
GEOGRAPHICAL RESEARCH LETTERS

TOMO 48 (1), Año 2022

UNIVERSIDAD DE LA RIOJA